FRUIT RESPONSES TO BIOTIC AND ABIOTIC STRESSORS DURING POSTHARVEST

EDITED BY: Claudia Anabel Bustamante, Isabel Lara and Natalia Marina Villarreal

PUBLISHED IN: Frontiers in Plant Science

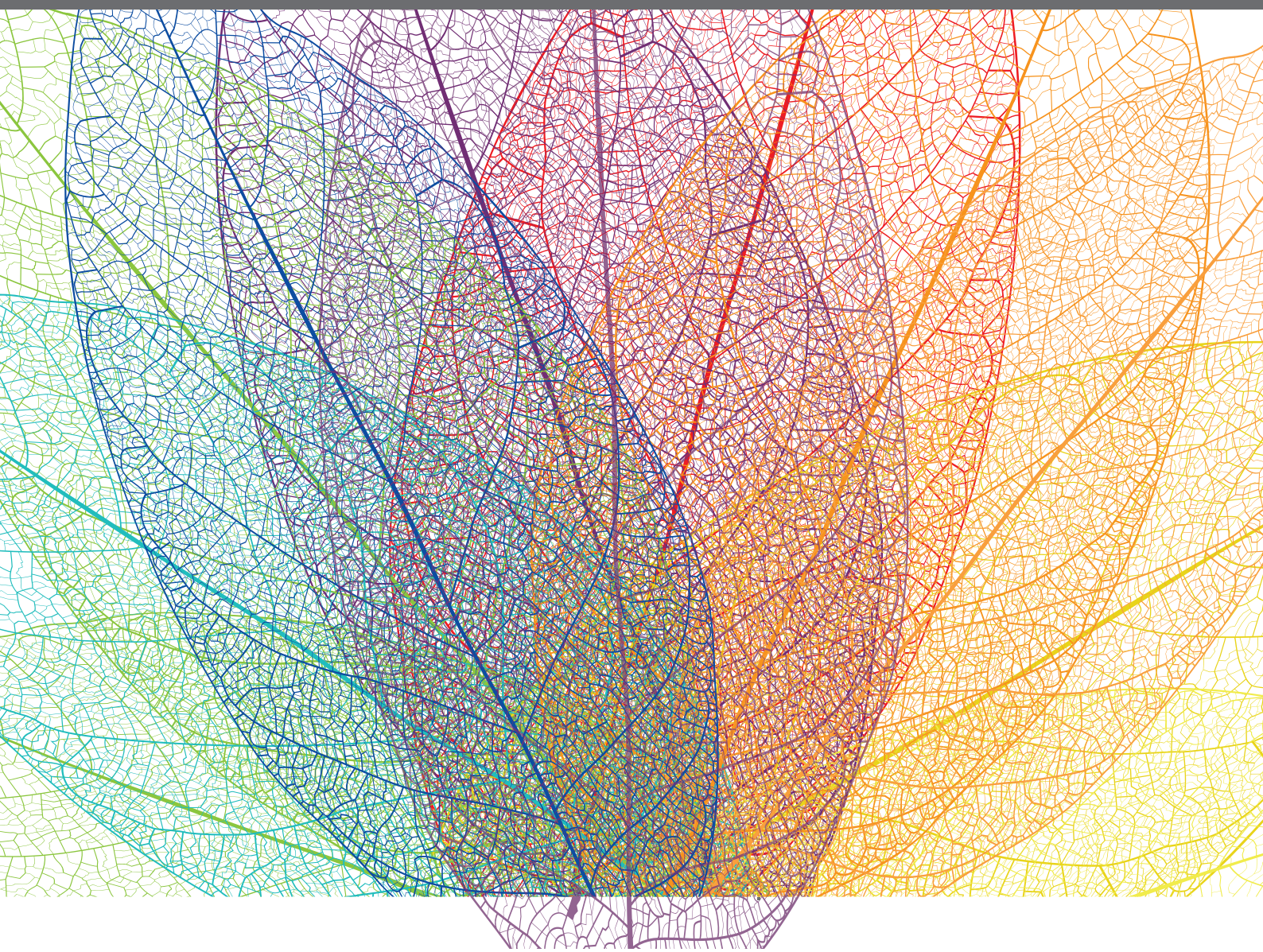

frontiers Research Topics

ISSN 1664-8714
ISBN 978-2-88976-205-7
DOI 10.3389/978-2-88976-205-7

About Frontiers

Frontiers is more than just an open-access publisher of scholarly articles: it is a pioneering approach to the world of academia, radically improving the way scholarly research is managed. The grand vision of Frontiers is a world where all people have an equal opportunity to seek, share and generate knowledge. Frontiers provides immediate and permanent online open access to all its publications, but this alone is not enough to realize our grand goals.

Frontiers Journal Series

The Frontiers Journal Series is a multi-tier and interdisciplinary set of open-access, online journals, promising a paradigm shift from the current review, selection and dissemination processes in academic publishing. All Frontiers journals are driven by researchers for researchers; therefore, they constitute a service to the scholarly community. At the same time, the Frontiers Journal Series operates on a revolutionary invention, the tiered publishing system, initially addressing specific communities of scholars, and gradually climbing up to broader public understanding, thus serving the interests of the lay society, too.

Dedication to Quality

Each Frontiers article is a landmark of the highest quality, thanks to genuinely collaborative interactions between authors and review editors, who include some of the world's best academicians. Research must be certified by peers before entering a stream of knowledge that may eventually reach the public - and shape society; therefore, Frontiers only applies the most rigorous and unbiased reviews.
Frontiers revolutionizes research publishing by freely delivering the most outstanding research, evaluated with no bias from both the academic and social point of view. By applying the most advanced information technologies, Frontiers is catapulting scholarly publishing into a new generation.

What are Frontiers Research Topics?

Frontiers Research Topics are very popular trademarks of the Frontiers Journals Series: they are collections of at least ten articles, all centered on a particular subject. With their unique mix of varied contributions from Original Research to Review Articles, Frontiers Research Topics unify the most influential researchers, the latest key findings and historical advances in a hot research area! Find out more on how to host your own Frontiers Research Topic or contribute to one as an author by contacting the Frontiers Editorial Office: frontiersin.org/about/contact

FRUIT RESPONSES TO BIOTIC AND ABIOTIC STRESSORS DURING POSTHARVEST

Topic Editors:
Claudia Anabel Bustamante, Centro de Estudios Fotosintéticos y Bioquímicos (CEFOBI), Argentina
Isabel Lara, Universitat de Lleida, Spain
Natalia Marina Villarreal, CONICET Instituto Tecnológico de Chascomús (INTECH), Argentina

Citation: Bustamante, C. A., Lara, I., Villarreal, N. M., eds. (2022). Fruit Responses to Biotic and Abiotic Stressors During Postharvest. Lausanne: Frontiers Media SA. doi: 10.3389/978-2-88976-205-7

Table of Contents

frontiers | Frontiers in Plant Science

EDITORIAL
published: 28 April 2022
doi: 10.3389/fpls.2022.914841

Editorial: Fruit Responses to Biotic and Abiotic Stressors During Postharvest

Isabel Lara[1]*, *Claudia A. Bustamante*[2] *and Natalia M. Villarreal*[3,4]

[1] Postharvest Unit, AGROTÈCNIO-CERCA Center, Universitat de Lleida, Lleida, Spain, [2] Bases bioquímicas de la calidad de frutos y exporte de fotoasimilados, Centro de Estudios Fotosintéticos y Bioquímicos (CEFOBI), Rosario, Argentina, [3] Laboratorio de Bioquímica y Fisiología de la Maduración de Frutos, Instituto Tecnológico de Chascomús (INTECH, CONICET-UNSAM), Chascomús, Pcia, Buenos Aires, Argentina, [4] Escuela de Bio y Nanotecnologías (EByN, UNSAM), Buenos Aires, Argentina

Keywords: fruit quality, postharvest, ripening, senescence, shelf life, stress

Editorial on the Research Topic

Fruit Responses to Biotic and Abiotic Stressors During Postharvest

INTRODUCTION

The ripening process encompasses many molecular, biochemical and physiological alterations in the course of which fleshy fruits acquire those sensory attributes which render them edible (Seymour et al., 2013; Kapoor et al., 2022). These modifications do not stop after harvest, and hence these produce are highly perishable commodities. Because postharvest deterioration causes important economic losses, a variety of postharvest strategies are applied in an attempt to preserve quality attributes and thus to extend storage and shelf life potential of fruits as well as other high-value horticultural produce such as cut flowers. Postharvest management needs to be tailored to each particular species, but very often involves refrigerated storage which can result in chilling injury and thus be detrimental for consumer acceptance. Other approaches for the postharvest management of horticultural commodities may also have negative effects on some quality traits and, at any rate, are not applicable in all cases.

This Research Topic was launched to gather novel information on responses to stress factors encountered during postharvest handling of horticultural produce, potentially providing hints for improved preservation of quality and marketability. The articles included in this Research Topic (a) examined the biochemical and molecular mechanisms involved in those responses, and (b) explored the efficacy of plant hormone treatments for the alleviation of stress symptoms. These studies considered a range of climacteric (apple, banana, peach, tomato) and non-climacteric (carambola, orange, pomegranate) fruit species as well as cut roses as an example of a commercially relevant floricultural crop, and are briefly presented below.

CHILLING STRESS AND CHILLING INJURY

The articles in this Research Topic illustrate the detrimental effects of cold storage on certain quality traits in some commercially important fruit crops, especially external appearance. For instance, bitter pit is an important disorder in apple affecting both fruit appearance and taste, occurring primarily during cold storage. Whereas generally considered to arise from low or unbalanced calcium levels, there is little information on the cell structure alterations involved therein. Qiu et al. observed increased amounts of amyloplasts in flesh cells of bitter pit-affected apples, and suggested this factor may disrupt calcium distribution leading to programmed cell death, imbalanced cell metabolism and bitter pit development.

OPEN ACCESS

Edited and reviewed by:
Leo Marcelis, Wageningen University and Research, Netherlands

***Correspondence:**
Isabel Lara
Isabel.lara@udl.cat

Specialty section:
This article was submitted to Crop and Product Physiology, a section of the journal Frontiers in Plant Science

Received: *07 April 2022*
Accepted: *11 April 2022*
Published: *28 April 2022*

Citation:
Lara I, Bustamante CA and Villarreal NM (2022) Editorial: Fruit Responses to Biotic and Abiotic Stressors During Postharvest. Front. Plant Sci. 13:914841. doi: 10.3389/fpls.2022.914841

Transcriptomic approaches allowed the identification of genes expressed differentially in response to chilling stress. Huang et al. identified 111 cuticle-related genes differentially regulated by chilling injury-inducing temperature in bananas, indicating a role for cuticle in chilling injury responses. Tomato fruit can also develop chilling injury symptoms upon transfer to ambient temperature, including accelerated softening and mealiness development. While such symptoms have been related to modified cell wall metabolism, results of transcriptome analysis undertaken by Hunter et al. suggest that accelerated softening was associated rather to turgor reduction. Chilling exposure also altered the expression of genes involved in protection and repair of oxidative damage, heat shock proteins and chaperonins, which could be used as molecular markers of cold response. Furthermore, epigenetic factors such as DNA methylation were apparently more relevant than gene expression for explaining differences associated to the development of mealiness in peach fruit kept under cold storage (Rothkegel et al.), and might also prove useful tools in breeding programs.

Non-climacteric fruits are also prone to chilling injury. In pomegranate, symptoms often manifest as peel browning, which could be delayed and attenuated by packaging in modified atmosphere, with or without 1-methylcyclopropene treatment (Valdenegro-Espinoza et al.). Contrarily, exogenous ethylene boosted lipid peroxidation and oxidative damage. Accordingly, 2,4-epibrassinolide applications to carambola fruit enhanced the antioxidant system, inhibited respiration rates and delayed senescence (Zhu et al.), in agreement with reports that brassinosteroids help counteracting both abiotic and biotic stress in plants (Kang and Guo, 2011).

OTHER STRESS FACTORS

Other studies compiled in this Research Topic addressed additional abiotic stress factors such as low O_2 concentrations in storage atmosphere. Postharvest storage under controlled or modified atmospheres has been the object of intense research efforts, and it is a widespread practice for the mid- to long-term postharvest preservation of some temperate fruit crops. While the reduction in respiration rates generally delays ripening- and senescence-associated changes, the concomitant decrease in oxidative phosphorylation levels causes a shift to fermentative metabolism which may lead to detrimental effects on flavor and to some physiological disorders, thus compromising sensory quality and economic returns. Even so, considerably less published research on this topic is available for tropical fruits. This information was reviewed by Benkeblia. This survey indicated that low O_2 levels can help extend the shelf life of tropical fruits, but also emphasised the wide range of metabolic processes affected, and the need to tailor these procedures on a case-by-case basis, since tropical fruits are remarkably diverse in structure, physiology and tolerance to O_2 deprivation.

Water stress is also a relevant driver of fruit quality losses. Sharp increases in relative humidity during postharvest handling often result in non-chilling peel pitting (NCPP), an important peel disorder in citrus fruit. Romero et al. found that transcriptomic responses to abrupt rehydration in NCPP-affected oranges involve membrane disorganization, cell wall modification and proteolysis.

Horticultural produce is also sensitive to wound stress induced during handling and transportation. This is particularly relevant for ornamental commodities such as flowers, which will rapidly deteriorate in response to the outburst in ethylene production caused by mechanical damage. WRKY transcription factors (TFs) are involved in plant stress, senescence and wounding responses, and are known to interact with a range of plant growth regulators (Jiang et al., 2017). Accordingly, Jing et al. examined the events involved in perception and transmission of the wound signal in cut roses. Transcriptomic analysis in response to wound, exogenous ethylene, and a combination of both, allowed the identification of many genes expressed differentially, among which *RhWRKY33*, highly expressed in senescing, wounded and ethylene-treated petals. Silencing of *RhWRKY33* delayed senescence, which suggests a role as a positive regulator of ethylene-mediated wound responses.

CONCLUSIONS

In summary, the articles in this Research Topic (a) identified differential patterns of gene expression and epigenetic regulation in response to a range of abiotic stress factors, (b) hinted at their potential as molecular markers of stress tolerance, and (c) evaluated the feasibility of plant hormone treatments for symptom relief. This Research Topic also highlighted the importance of fruit skin and overall appearance to meet consumers' expectations and ensure commercial revenues.

AUTHOR CONTRIBUTIONS

All authors listed have made a substantial, direct, and intellectual contribution to the work and approved it for publication.

FUNDING

Current work at IL's lab was funded by Grant 2017 SGR 1108 (Generalitat de Catalunya, Catalonia, Spain), CAB's lab was funded by grants from Universidad Nacional de Rosario (80020180300050UR), and NV's lab received grants from ANPCyT (PICT-2018-3412 and PICT-2018-3166).

REFERENCES

Jiang, J., Ma, S., Ye, N., Jiang, M., Cao, J., and Zhang, J. (2017). WRKY transcription factors in plant responses to stresses. *J. Integr. Plant Biol.* 59, 86–101. doi: 10.1111/jipb.12513

Kang, Y. Y., and Guo, S. R. (2011). "Role of Brassinosteroids on Horticultural Crops", in *Brassinosteroids: A Class of Plant Hormone*, eds S. Hayat, and A. Ahmad (Dordrecht, Netherlands: Springer), 269–288.

Kapoor, L., Simkin, A. J., George Priya Doss, C., and Siva, R. (2022). Fruit ripening: dynamics and integrated analysis of carotenoids and anthocyanins. *BMC Plant Biol.* 22, 1-22. doi: 10.1186/s12870-021-03411-w

Seymour, G. B., Poole, M., Giovannoni, J., and Tucker, G. A. (eds). (2013). *The Molecular Biology and Biochemistry of Fruit Ripening*. Oxford, UK: Wiley-Blackwell.

Conflict of Interest: The authors declare that the research was conducted in the absence of any commercial or financial relationships that could be construed as a potential conflict of interest.

frontiers in Plant Science

ORIGINAL RESEARCH
published: 04 June 2021
doi: 10.3389/fpls.2021.678295

Exogenous 2,4-Epibrassinolide Treatment Maintains the Quality of Carambola Fruit Associated With Enhanced Antioxidant Capacity and Alternative Respiratory Metabolism

Xiaoyang Zhu[1†], Yuxin Chen[1†], Junyi Li[1], Xiaochun Ding[1], Shuangling Xiao[2], Silin Fan[1], Zunyang Song[1], Weixin Chen[1] and Xueping Li[1]*

[1] Guangdong Provincial Key Laboratory of Postharvest Science of Fruits and Vegetables/Engineering Research Center for Postharvest Technology of Horticultural Crops in South China, College of Horticulture, South China Agricultural University, Guangzhou, China, [2] College of Land Resources and Environment, Jiangxi Agricultural University, Nanchang, China

OPEN ACCESS

Edited by:
Isabel Lara,
Universitat de Lleida, Spain

Reviewed by:
Daniel Alexandre Neuwald,
Competence Centre for Fruit Growing-Lake Constance, Germany
Asunción Amorós,
Miguel Hernandez University, Spain

***Correspondence:**
Xueping Li
lxp88@scau.edu.cn

[†] These authors have contribute equally to this work

Specialty section:
This article was submitted to Crop and Product Physiology, a section of the journal Frontiers in Plant Science

Received: 09 March 2021
Accepted: 22 April 2021
Published: 04 June 2021

Citation:
Zhu X, Chen Y, Li J, Ding X, Xiao S, Fan S, Song Z, Chen W and Li X (2021) Exogenous 2,4-Epibrassinolide Treatment Maintains the Quality of Carambola Fruit Associated With Enhanced Antioxidant Capacity and Alternative Respiratory Metabolism. Front. Plant Sci. 12:678295. doi: 10.3389/fpls.2021.678295

Brassinosteroids act by delaying fruit ripening. The effects of different concentrations of 2,4-epibrassinolide (eBL) treatments on carambola fruit ripening were investigated. The results show that treatment of 2.8 mg L^{-1}, eBL with 10 min effectively delays ripening and maintains the quality of carambola fruit. This is achieved by retarding color changes and firmness losses while maintaining high level of soluble protein content and vitamin C, and low organic acid content. eBL-delayed senescence may be due to the inhibition of respiration rate and enhanced antioxidant system. It is noteworthy that eBL treatment markedly reduces the content of fructose-6-phosphate (6-P-F) and enhances the activity of cytochrome oxidase (CCO), and the total activity of glucose-6-phosphate dehydrogenase (G-6-PDH) and 6-phosphate gluconate dehydrogenase (6-PGDH). eBL treatment induces the IAA and GA contents but reduces that of ABA. In general, senescence retardation and quality improvement by eBL treatment may be due to the enhanced antioxidant capacity and altered respiratory pathways.

Keywords: carambola fruit, brassinolide, fruit quality, respiratory metabolism, antioxidant capacity

INTRODUCTION

Carambola (*Averrhoa carambola* L.) fruit, commonly known as star fruit, is popular in Southeast Asian countries and China owing to its nutritional and pharmacological value (Gol et al., 2015). It is an economically important fruit in tropical and subtropical areas and has been cultivated for hundreds of years. The unique star shape and attractive appearance, in addition to its special flavor and nutritional and pharmacological value, provide a considerable market potential as a

Abbreviations: eBL, 2,4-epibrassinolide; BRs, brassinosteroids; 6-P-F, fructose-6-phosphate; CCO, cytochrome oxidase; G-6-PDH, glucose-6-phosphate dehydrogenase; 6-PGDH, 6-phosphate gluconate dehydrogenase; AsA, ascorbic acid; PVP, polyvinylpyrrolidone; MDA, malondialdehyde; PPO, polyphenol oxidase; POD, peroxidase; CAT, catalase; SOD, superoxide dismutase; AAO, ascorbic acid oxidase; PGI, hexose isomerase; SDH, succinate dehydrogenase; ABA, abscisic acid; GA, gibberellin acid; IAA, indole-3-acetic acid; AOS, active oxygen species.

garnish for salads and drinks. Carambola fruit is a typical non-climacteric fruit (Warren and Sargent, 2011). It is a juicy fruit that has a fragile and succulent pulp with attractive flesh and a distinctive flavor. These fruit are highly perishable and have a high moisture content and susceptibility to mechanical damage and dehydration, which cause extensive postharvest losses and limit their marketability. Thus, it is important to explore simple, effective, and inexpensive processes for its preservation. Different techniques have been reported to extend the shelf-life and maintain the quality of harvested carambola fruit, including low-temperature storage (Ali et al., 2004), 1-methylcyclopropene treatment (Warren and Sargent, 2011), edible coatings (Gol et al., 2015), polyamines (PAs) treatment (Ahmad and Ali, 2019) and methyl jasmonate treatment (Mustafa et al., 2016).

Low-temperature storage and modified atmosphere packaging are the main managements used to control carambola fruit ripening. However, low-temperature storage will cause chilling injury and affect the skin coloration and structure of carambola fruit (Ali et al., 2004). The use of a controlled atmosphere could effectively maintain fruit quality and extend the shelf life of fruits and vegetables, but these techniques are capital intensive and expensive and may cause an unpleasant flavor (Kader et al., 1989).

Plant bioregulators are natural and safe phenolic compounds that exhibit a high potential to control postharvest losses of horticultural crops. Among the different bioregulators that have been tested, gibberellic acid, 1-naphthalene acetic acid (NAA), 6-benzylamino purine, and salicylic acid, NAA effectively maintains the quality of carambola fruit, reduces postharvest losses, and prolongs fruit shelf life (Hazarika and Tariang, 2019). Brassinosteroids (BRs) are a class of natural plant hormones that play important roles in regulating plant development, growth, and stress resistance (Bajguz and Hayat, 2009). BRs have been widely used to improve plant stress resistance (Bajguz and Hayat, 2009). As plant growth regulators that have low toxicity and are ecofriendly, BRs have the potential to improve quality of postharvest horticultural products. Postharvest BR treatment effectively delayed jujube fruit senescence by reducing ethylene production, effectively inhibiting the development of blue mold rot by enhancing activities of defense-related enzymes and maintaining fruit quality (Zhu et al., 2010). Other studies showed that BRs induced fruit ripening via increasing ethylene production (Zhu T. et al., 2015). For example, treatment with BRs promoted mango fruit ripening *via* an acceleration of the ethylene production and respiration rate (Zaharah et al., 2012). BRs promoted persimmon fruit ripening by promoting ethylene production, increasing the respiration rate, and influencing cell wall-degrading enzymes and ethylene biosynthesis (He et al., 2018). Brassinolide application effectively induced tomato fruit ripening by increasing soluble sugars, ascorbic acid, lycopene contents, respiration rate, and ethylene production, as well as the expression of genes related to ethylene synthesis (Zhu T. et al., 2015).

To date, the effects of BRs on carambola fruit are not known. The aim of this study was to investigate the effects of BRs on postharvest fruit ripening and quality attributes of carambola fruit and the possible mechanisms for these effects.

MATERIALS AND METHODS

Plant Material and Treatments

Carambola fruit were collected from an orchard in Zengcheng (Guangzhou, China). The variety named "*Averrhoa carambola* Linn. cv. Xiangmi" was introduced from Singapore. Fruit at approximately 70% maturity were harvested, rapidly transported to the laboratory and precooled at 20°C. The fruit that were cleaned with water and air-dried at room temperature that lacked diseases and blemishes and were of uniform shape, weight, and maturity were selected for further treatment.

For the preliminary experiments, the selected carambola fruit were randomly divided into four groups, and each group contained 80 fruit. The 2,4-epibrassinolide (eBL) (EKEAR Biotechnology Co., Ltd., Shanghai, China) were dissolved in ethanol and then diluted in distilled water (treatment solution) as the desired concentrations. Four concentration of eBL treatment solution, including 0, 1.4, 2.8, and 9.4 mg L^{-1}, were prepared, and fruit were immersed in different eBL solutions for 10 min, and then air-dried for 2 h. The carambola fruit were placed in unsealed plastic bags (0.02 mm thick) and stored at room temperature (25 ± 1°C). Fruit ripening process were then monitored by the periodic measurement of respiration, firmness, and peel color.

Several preliminary experiment results showed that 2.8 mg L^{-1} eBL treatment exhibited the desired effects among the four concentrations tested (**Figure 1**). Then 2.8 mg L^{-1} eBL treatment was selected to further study the effects of eBL on carambola fruit ripening and quality. Fruit after pretreatment were then selected randomly and divided into two groups, and each group contained 120 fruit. Fruit in each group were soaked in a water solution with 0 and 2.8 mg L^{-1} eBL for 10 min, respectively, and then air-dried for 30 min and stored at 25 ± 1°C. The carambola fruit were placed in unsealed plastic bags (0.02 mm thick). At least 15 fruit were monitored by the periodic measurement of respiration, firmness, and peel color, respectively. Samples were collected at 0, 3, 5, 7, 9, and 11 days. The middle part of fruit without seeds was collected and diced, frozen in liquid nitrogen, and stored at −80°C for further use. All the treatments were conducted in three biological replicates.

Evaluation of Fruit Ripening

The fruit ripening was evaluated and monitored by periodic measurements of fruit respiration, firmness, and peel color. Fruit color was evaluated by manual observation and measurement with a colorimeter. Manual observations were evaluated by the fruit ripening index, which is a scale from 1 to 6 as described by Omar et al. (2012) with minor modifications: (1) Bright green in color, green-mature; (2) green with a small amount of yellowish color; (3) more green than yellow; (4) more yellow than green; (5) Yellow with a small amount of green; and (6) Completely yellow. The fruit color was also determined using a chromameter-2 reflectance colorimeter (Minolta, Osaka, Japan) equipped with a CR-300 measuring head and recorded as lightness (L), hue angle (h), or chroma (c). Five points around the equatorial region on each fruit were selected for the measurement. The fruit firmness

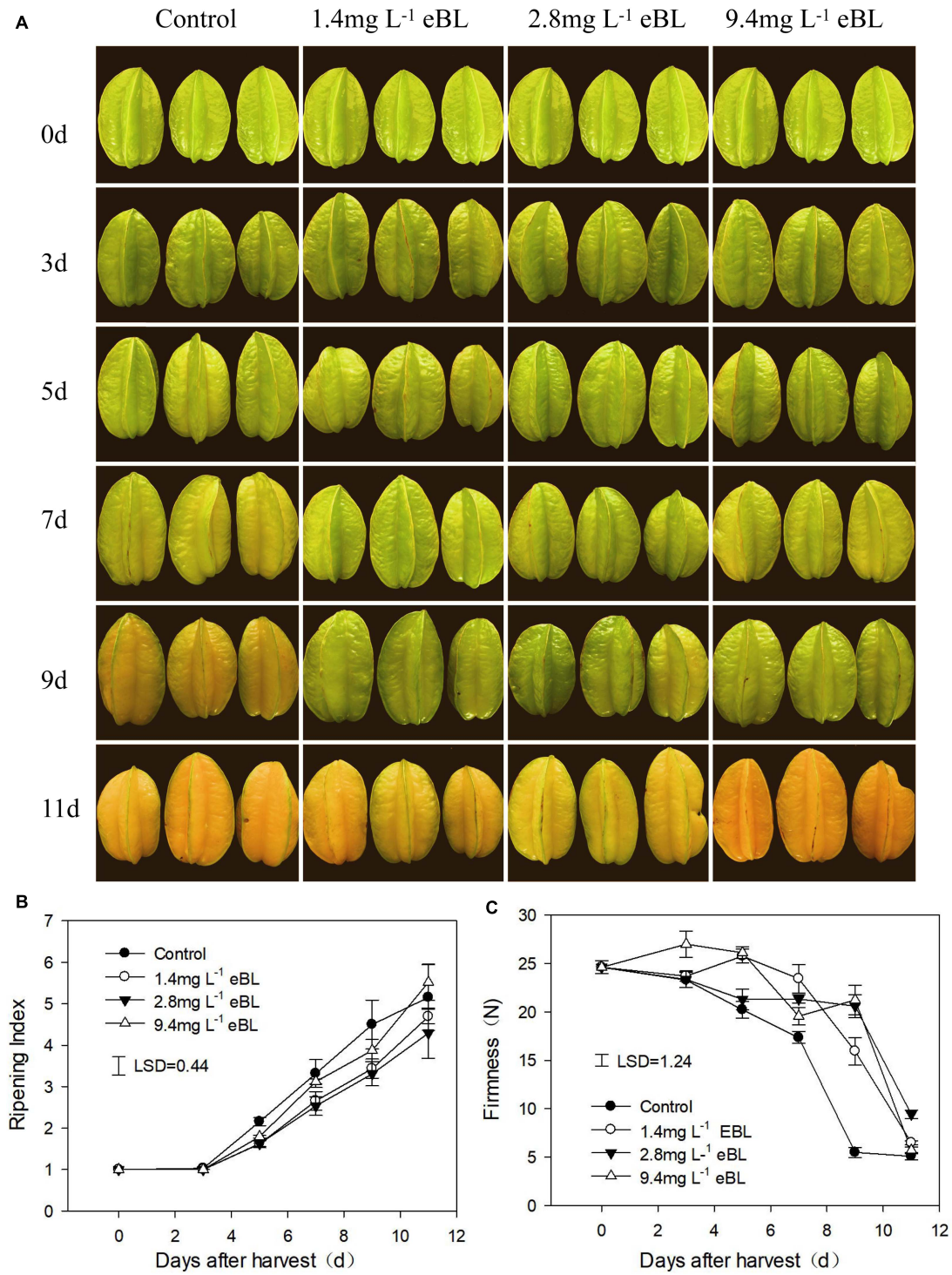

FIGURE 1 | The effects of different 2,4-epibrassinolide (eBL) concentrations on carambola fruit ripening. **(A)** Photos of carambola fruit treated with different concentration of eBL; **(B,C)** fruit ripening index **(B)** and firmness **(C)** under different treatments. Least significant differences (LSDs) were calculated to compare significant effects at the 5% level. Each data point represents the mean ± S.E. ($n = 3$).

was determined using an Instron 5,542 penetrometer (Instron, Norwood, MA, United States) equipped with a cylindrical flat-surfaced plunger (5 mm diameter). A 2-mm slice of fruit skin was removed, and the firmness of fruit was measured at a penetration depth of 2 cm on three different fruit at five different points per fruit. Fruit firmness (N) was expressed as the mean of these

50 measurements. Fruit respiration was determined using gas chromatograph as described by Zhu X. et al. (2015).

Determination of Soluble Protein and Vitamin C and Soluble Protein Contents

Fruit flesh (100 g) was cut into small pieces, homogenized, and filtered to measure the ascorbic acid (AsA) contents as described by Lu et al. (2010). The soluble protein was determined as described by Deng et al. (2012). One gram of pulp was ground with 4 ml extraction buffer [0.05 mol L^{-1} phosphate buffer,pH 7.8, containing 0.2 mmol L^{-1} EDTA and 1% polyvinylpyrrolidone (PVP)]. The mixture was centrifuged at 13,000 r min^{-1} for 20 min at 4°C. The supernatant was collected as the protein extraction. Then 1 ml of the supernatant was taken and 5 ml of Coomassie Brilliant Blue G-250 solution was added and mixed. The determination was conducted by measuring the absorbance at 595 nm.

Determination of Sugar and Organic Acid Contents

Glucose, fructose, and sucrose are the main sugar components in fruit, which were measured as described by Wang et al. (2010), with minor modifications. Briefly, 5 g of carambola pulp was ground in liquid nitrogen and then 1 g powder and 50 ml of distilled water were mixed crushed by a cell grinder (BILON96-II, Shanghai, China). The sugar compounds were extracted 60 times by ultrasonic oscillation (ultrasonic time of 3 s, gap time of 5 s, and ultrasonic power of 150 W). Then the sample mixture was filtered with 0.22 μm filter, and the filtrate was used for the determination of soluble sugars. The separations were performed on a Dionex ICS3000 Multifunctional Ion Chromatograph (Dionex, Sunnyvale, CA, United States), using a Dionex CarboPac PA1 (2 × 250 mm) column at 30°C with 40 mmol L^{-1} NaOH as the eluent at a flow rate of 0.25 ml min^{-1}.

A standard curve was drawn using the standard solution. The standard solution was prepared as follows: accurately weigh 0.5 g of fructose, glucose, and sucrose and diluted to a 100-ml volumetric flask with ultrapure water to obtain a single standard solution with each concentration of 5.0 mg ml^{-1}. At the same time, a mixed standard stock solution of fructose, glucose, and sucrose was prepared, with the concentration of fructose, glucose, and sucrose being all 5.0 mg ml^{-1}. The standard solution was gradually diluted for sampling to draw the standard curve.

The organic acid was determined using an Agilent 1200 series rapid-resolution LC system (Agilent Technologies, CA, United States). Briefly, 10 g of pulp sample was ground with a freezer grinder, then 1 g of powder was mixed with the extraction solution (8 ml of 0.015 mol L^{-1} potassium dihydrogen phosphate (pH = 3) with 1.0% HPLC purity of methanol) in a 10-ml tube. The mixture was vortex mix for 30 s and shocked at 40°C for 2 h, and then centrifuged at 11,000 × *g* for 15 min. The supernatant solution was collected and added to 10 ml volume with the extract solution. The final extraction solution was filtered with 0.45 filter, and the filtrate was used for the determination of organic acid.

The determination was conducted using an Agilent 1200 series rapid-resolution LC system plus with an Agilent Eclipse Plus C18 column. The mobile phase is the 0.015-mol L^{-1} potassium dihydrogen phosphate (pH = 3) and 1% HPLC-grade methanol mixture. The column temperature was maintained at 25°C, and the injection volume was 15 μl, with a flow rate at 0.8 ml min^{-1}.

Analysis of Malondialdehyde and H_2O_2 Contents and Antioxidant-Related Enzymatic Activities

The malondialdehyde (MDA) content was measured as described by Guo et al. (2013). MDA content was determined by adding 0.6% thiobarbituric acid (TBA) and 2 ml crude extract. The mixture was boiled in a water bath for 15 min and then quickly cooled in an ice bath. The absorbance was measured at 532 nm with UV-2450 spectrophotometer (Shimadzu Corporation, Kyoto, Japan) and corrected for non-specific absorption at 600 nm. The MDA concentration was calculated using the extinction coefficient of 155 mM cm^{-1}. H_2O_2 was determined using a Hydrogen Peroxide Assay Kit (A064, Nanjing Jiancheng Bioengineering Institute, Nanjing, China) according to the manufacturer's instructions.

For the enzyme extraction, all procedures were carried out at 4°C. The activities of polyphenol oxidase (PPO) and peroxidase (POD) were measured as described by Shi et al. (2013). Briefly, 1 g of the pulp was ground and homogenized with 4 ml of extraction buffer (0.2 mol L^{-1} sodium phosphate buffer (pH 6.5) containing 0.01 g ml^{-1} PVP for PPO, and 0.2 mol L^{-1} sodium phosphate buffer (pH 6.4) with 0.02 g ml^{-1} PVP for POD). Then the extracts were centrifuged at 12,000 × *g* for 20 min at 4°C, and the supernatants were used as crude enzyme. PPO activity was determined by measuring absorbance at 410 nm. For POD, the reaction mixtures containing 0.5 ml crude extract and 2 ml guaiacol substrate (100 mmol L^{-1} sodium phosphate (pH 6.4) and 8 mmol L^{-1} guaiacol) were incubated for 5 min at 30°C. The increase in absorbance at 460 nm was determined after 1 ml H_2O_2 (24 mmol L^{-1}) was added.

The catalase (CAT) and superoxide dismutase (SOD) activity were measured as described by You et al. (2004) with a slight modification. Crude enzyme was extracted using 1 g of pulp and 4 ml of extraction buffer containing 0.05 g of polyvinylpolypyrrolidone (PVPP) (50 mmol L^{-1} sodium borate buffer (pH 7.0, containing 5 mmol L^{-1} mercaptoethanol) for CAT, sodium phosphate buffer (100 mM, pH 6.4) was used for SOD. The reaction mixture contained 0.5 ml enzyme, 2 ml sodium phosphate buffer (50 mmol L^{-1}, pH 7.0), and 0.5 ml H_2O_2 (40 mmol L^{-1}) in a total volume of 3.0 ml. The decomposition of H_2O_2 was measured by the decline in absorbance at 240 nm.

The activity of ascorbic acid oxidase (AAO) was determined using an AAO Activity Assay Kit (Nanjing Jiancheng Bioengineering Institute) according to the manufacturer's instructions.

Determination of the Activities of Respiratory Metabolic Enzymes

Four key enzymes involved in different respiratory metabolism pathways were tested, including phosphate hexose isomerase

(PGI), succinate dehydrogenase (SDH), cytochrome oxidase (CCO), and the total activity of glucose-6-phosphate dehydrogenase (G-6-PDH) and 6-phosphate gluconate dehydrogenase (6-PGDH). The PGI activity is directly reflected by the content of substrate fructose 6-phosphate (6-P-F). The PGI activity was measured as described by Li et al. (2016). Briefly, 0.5 g of frozen samples was ground in 2.5 ml Tris-HCl buffer (0.05 mol L^{-1}, pH 7.4) on ice and then centrifuged at 5,000 × *g* at 4°C for 30 min. The supernatant was collected and stored at 4°C until use. A volume of 0.5 ml of the supernatant and 1 ml of glucose 6-phosphate (6-P-G) was mixed and incubated in a water bath for 5 min at 30°C, and then 2 ml of trichloroacetic acid was added and centrifuged at 5,000 × *g* at 4°C for 15 min. A volume of 1 ml of supernatant, 6 ml of HCl, and 2 ml of resorcinol were mixed, and the content of 6-P-F content was determined at 520 nm using 6-P-F as a standard. The content of 6-P-F was expressed as grams per kilogram.

The activity of SDH was measured as described by Li et al. (2016) with minor modifications. Briefly, 0.5 g of sample was ground with 2 ml of phosphate buffer (pH 7.2) and centrifuged at 10,000 × *g* at 4°C for 15 min. The precipitate was suspended in 5 ml of Tris-HCl buffer (0.06 mol L^{-1}) and used as the enzyme solution. The reaction solution was composed of 0.1 mL of 1.5 mol L^{-1} potassium phosphate buffer (pH 7.4), 0.1 ml of 1.2 mol L^{-1} succinic acid (pH 7.4), 0.1 ml of 0.9 mmol L^{-1} 2,6-sodium dichloroindophenol and 2.5 ml of distilled water. The reaction solution was incubated at 30°C for 10 min, and 0.1 ml of enzyme was added and gently mixed. A volume of 0.1 ml of phenazine methyl sulfate (PMS) was added to the start of the reaction in a cuvette, and the absorbance at 600 nm was recorded using a Powerwave 340 plate reader (Biotek Instruments, Winooski, VT, United States) after 15–60 s of reaction. A change in the OD_{600} per minute of 0.01 was defined as a unit of enzyme activity (U), and the enzyme activity was expressed as in Units per kilogram (FW).

The activity of CCO was determined as described by Li et al. (2016). Briefly, 0.5 g of a frozen sample was ground in 1.25 ml phosphate buffer (0.04 mol L^{-1}, pH = 2), shaken for 30 s and then centrifuged at 3,000 × *g* at 4°C for 10 min. The supernatant was collected for enzyme assay. A volume of 0.1 ml of supernatant, 0.2 ml cytochrome *c* (0.04%), and 3 ml of distilled water were preincubated at 37°C for 2 min, and then 0.1 ml of dimethyl-*p*-phenylenediamine (0.4%) was added and incubated at 37°C for 1–3 min. The pH was adjusted to 5.6∼6 using 0.1 mol L^{-1} HCl. A volume of 10 ml of the reaction solution was centrifuged at 5,000 × *g* at 4°C for 5 min, and the absorbance was recorded at 510 nm for 10 min. The CCO activity was calculated as follows: OD × dilution factor/fresh weight and expressed as OD per kilogram FW.

The total activities of G-6-PDH + 6-PGDH were assayed as described by Li et al. (2016). A total of 0.5 g of frozen samples was ground in 2.5 ml of prechilled extraction buffer (0.05 mol L^{-1} phosphate buffer, pH 6.8, 0.25 mol L^{-1} sucrose, 0.005 mol L^{-1} EDTA, and 1 g L^{-1} bovine serum albumin) on ice, centrifuged at 10,000 × *g* at 4°C for 15 min, and the supernatant was discarded. The precipitate was suspended in 2.5 ml of 0.05 mol L^{-1} Tris-HCl buffer (pH 7.4) as the enzyme solution. A volume of 0.05 ml of enzyme solution was added in 0.45 ml reaction solution [5 mmol L^{-1} 6-P-G, 5 mmol L^{-1} $MgCl_2$, 5 mmol L^{-1} Tris-HCl (pH 7.4)], and the absorbance was immediately measured at 340 nm. A volume of 0.05 ml 0.1 mol L^{-1} Tris-HCl buffer (pH = 7.4) was used as the control. The total activities of G-6-PDH + 6-PGDH were expressed as millimoles NADP per kilogram per minute.

Determination of the Content of Endogenous Hormones

Three types of hormones (indole-3-acetic acid (IAA), gibberellin acid (GA_3), and abscisic acid (ABA)) were analyzed as described by Zhang et al. (2005) with minor modifications. Briefly, 1.0 g of frozen sample was ground in liquid nitrogen, and 8-ml precooled 80% methanol (*v*/*v*) was added, mixed, and extracted at 4°C overnight. After centrifugation (10,000 × *g* at 4°C for 15 min), the supernatant was collected. The pellet was reextracted with 6 ml of prechilled 80% methanol. A total of 0.3 g PVPP was added to the combined supernatants, shaken at 100 g at 4°C for 1 h and centrifuged at 10,000 × *g* at 4°C for 15 min. The supernatants were evaporated to dryness under nitrogen gas, reconstituted in 80% methanol, and filtered (PTFE, 0.22 μm; ANPEL Laboratory Technologies, Shanghai, China) before HPLC.

The extracts were analyzed using an Agilent 1200 Series liquid chromatography system (Agilent Technologies, Santa Clara, CA, United States) equipped with an Agilent Eclipse Plus C18 column. A volume of 10 μl of sample was injected with the mobile phase (100% HPLC-grade methanol, acetonitrile, phosphate acid buffer solution (pH 6) = 20:15:65) at a flow rate of 0.8 ml min^{-1}. The column temperature was maintained at 35°C. A diode-array detector (DAD) was used for detection at 210 nm for IAA and GA_3 and 254 nm for ABA. IAA, GA3, and ABA were identified by comparing their retention volumes with those of reference standards (Sigma-Aldrich, United States).

Statistical Analysis

The experiment was arranged in a completely randomized design. Each treatment comprised three replicates. The data were analyzed using SPSS 17.0 (SPSS, Chicago, IL, United States). SigmaPlot 10.0 (Systat Software, San Jose, CA, United States) was used to create most of the figures. All the results were expressed as the mean ± S.E.

RESULTS

The Effects of eBL on Fruit Ripening

First, we screened a suitable concentration of eBL to use to delay fruit ripening. As shown in **Figure 1**, three different concentrations were tested, and we observed that low concentrations of eBL (1.4 and 2.8 mg L^{-1}) could effectively delay fruit coloring process as compared with the control, particularly for the 2.8-mg L^{-1} treatment, but there was no significant difference between a high concentration (9.4 mg L^{-1}) of eBL and the control (**Figure 1A**). The fruit firmness gradually decreased during storage and dropped rapidly from days 7 to

9. All the eBL treatments delayed the decrease in firmness, and fruit treated with 2.8 mg L^{-1} eBL were more firm compared with the others at end of storage (**Figure 1B**). These results indicated that treatment with 2.8 mg L^{-1} eBL could effectively delay fruit ripening. Thus, 2.8 mg L^{-1} eBL was selected for further study.

As shown **Figure 2**, eBL treatment (2.8 mg L^{-1}) effectively delayed the coloring process of carambola fruit by approximately 2 days (**Figures 2A,B**). Color is one of the most important indicators of fruit ripening and quality. The color was normally measured using the values of L^*, C^* and $h°$, which indicated the brightness, color saturation C^*, and chromaticity angle, respectively. L^* indicates brightness, and C^* indicates the brightly colored fruit. The larger the value, the brighter the fruit color, while $h°$ is the characteristic value of color, indicating the hue of different colors. The $h°$ of carambola from preharvest to full ripening of fruit ranged from 90 to 110°, and the value was closer to 90, indicating that the carambola was yellow. The L^* decreased during the first 2 days and then increased gradually from day 3 in control fruit. The C^* value gradually increased as the fruit ripened. Treatment with eBL delayed the increase in L^* and C^* values compared with those of the control (**Figures 2C,D**). The $h°$ decreased with fruit ripening, and the eBL treatment delayed the decrease (**Figure 2E**). All these data indicated that the eBL treatment effectively delayed changes in fruit color. The eBL treatment also maintained fruit firmness and reduced its respiration rate compared with the control (**Figures 2F,G**).

The Vc content changed in a similar manner in eBL-treated and control fruit with an increase during the first 3 days but a gradual decrease during the latter storage; however, the Vc content was much higher in eBL-treated fruit than in the control fruit (**Figure 2H**). The content of soluble protein increased during storage before slightly decreasing at the latter storage in the control group. The eBL treatment induced production of soluble protein, which increased with storage and was much higher than that in the control fruit (**Figure 2I**).

The Effect of eBL Treatment on Content of Sugars and Organic Acids

Sugar and organic acid contents are the most important indicators of fruit quality. As shown in **Figure 3**, treatment with eBL significantly altered the accumulation of sugars and organic acids, particularly for the organic acids (**Figure 3**). The three main sugars in carambola increased with fruit storage and then decreased from day 7. The eBL treatment slightly reduced the total sugar content at days 5 and 11, particularly for the content of sucrose (**Figures 3A–D**). Four main types of organic acids, including pyruvic acid, oxalic acid, citric acid, and malic acid were tested. The contents of pyruvic acid, oxalic acid, and malic acid decreased with storage, and treatment with eBL enhanced the decrease, which was much lower in the eBL-treated fruit than that of the control fruit (**Figures 3E,F,H**). Only the content of citric acid showed a sharp increase during the first 3 days before gradually decreasing during the latter storage. Treatment with eBL reduced the content of citric acid compared with that of control (**Figure 3G**).

The Effect of eBL Treatment on the Antioxidant Capacity of Fruit

MDA is the end product of cellular lipid peroxidation, and its content can indicate the extent of lipid peroxidation. As shown in **Figure 4A**, the content of MDA increased with fruit storage in the control fruit. Treatment with eBL dramatically reduced the content of MDA in carambola fruit, which increased slightly and remained stable during the latter storage period (**Figure 4A**), indicating that eBL alleviated the degree of cell membrane lipid peroxidation and reduced cell membrane damage. The content of H_2O_2 in the control fruit increased rapidly during the first 5 days and then decreased slightly during the latter storage period (**Figure 4B**). Similar changes were observed in the eBL-treated fruit, but the content was much lower in the eBL-treated fruit.

The activities of four antioxidant enzymes were tested to determine the antioxidant system. As shown in **Figure 4C**, the activity of PPO gradually increased with storage; treatment with eBL slightly reduced the activity of PPO compared with that of the control, but no significant difference was observed (**Figure 4C**). The activity of SOD increased during the first 3 days and then decreased slightly, but it increased again from day 9. Treatment with eBL dramatically induced the activity of PPO, which increased rapidly during the first 9 days and then decreased slightly. The PPO activity was significantly higher in eBL-treated fruit than that of control (**Figure 4D**). The activity of POD dropped sharply during the first 3 days and then increased slightly and remained stable during later storage. Similar changes were observed for eBL-treated fruit, but eBL significantly induced the activity of POD (**Figure 4E**). The activity of CAT in the control fruit increased sharply during the first 3 days and the decreased with storage, but it increased again at the end of storage. Following the treatment with eBL, the activity of CAT dramatically increased during the first 3 days compared with control and then remained stable during the latter storage period, resulting in much higher activity than that in the control group (**Figure 4F**). The activity of AAO decreased sharply during the first 3 days, then remained at a stable level and decreased from the days 9 to 11. There was no significant difference between the control and eBL treatment from 0 to 9 days, but the AAO activity was significantly higher during latter storage period in eBL-treated fruit compared with that in the control fruit (**Figure 4G**).

The Effect of eBL Treatment on the Activities of Respiratory Metabolic Enzymes

PGI is a key enzyme in the glycolytic [Embden-Meyerhof-Parnas (EMP)] pathway. Fructose-6-phosphate (F-6-P) is the product catalyzed by PGI in EMP respiratory pathway, which demonstrates the activities of PGI. As shown in **Figure 5A**, the content of F-6-P increased gradually as fruit ripened. Compared with the control group, treatment with eBL significantly reduced the content of F-6-P, indicating that the activity of PGI was inhibited. SDH is a key enzyme in the tricarboxylic acid (TCA) cycle. As shown in **Figure 5B**, the activity of SDH increased gradually as fruit ripened and reached its peak on day 9 before decreasing. Compared with the control, treatment with eBL

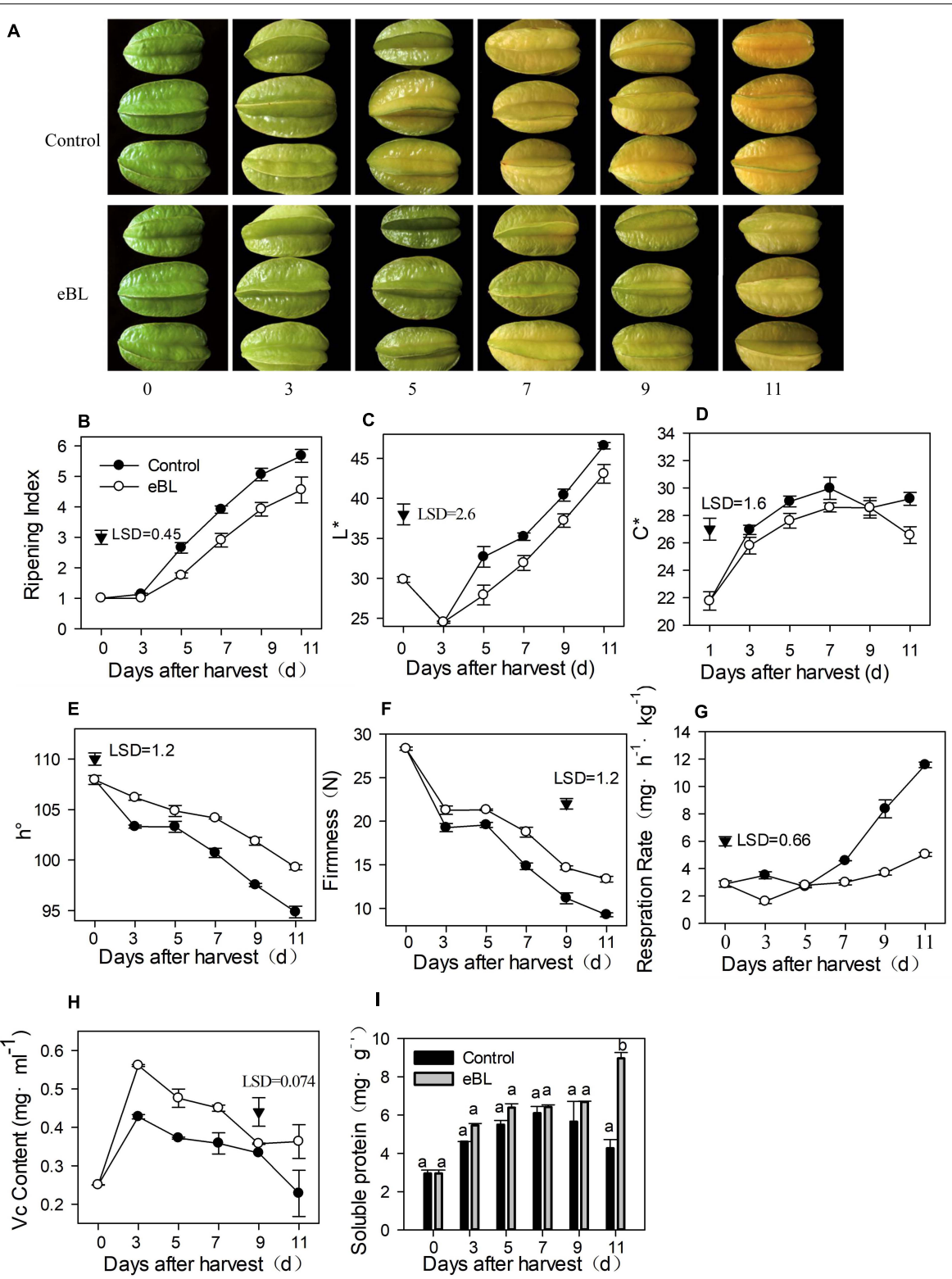

FIGURE 2 | The effects of 2,4-epibrassinolide (eBL) on carambola fruit ripening. **(A)** Photos of carambola fruit treated with or without eBL; **(B)** fruit ripening index assessment; **(C–E)** fruit color changes in L^* value **(C)**, C^* value **(D)**, and $h°$ value **(E)**; **(F)** fruit firmness changes; **(G)** fruit respiration rate; **(H,I)** the content of Vc **(H)** and soluble protein **(I)**. Carambola fruit were stored at room temperature (25 ± 1°C) after treatment. Least significant differences (LSDs) were calculated to compare significant effects at the 5% level. Each data point represents the mean ± S.E. ($n = 3$). Means within a column among different groups followed by the same letter are not significantly different at the 5% level.

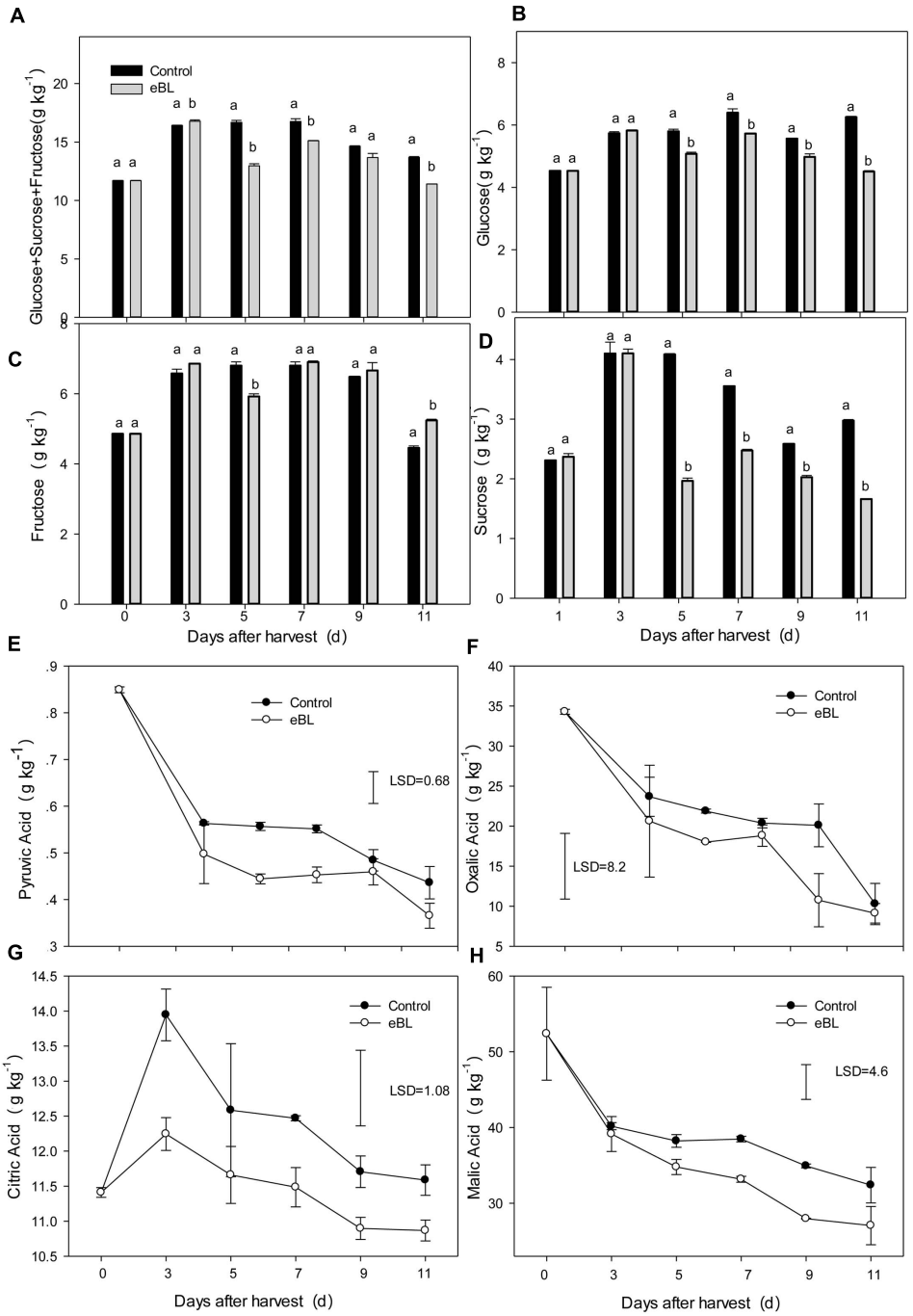

FIGURE 3 | Effects of eBL treatment on the content of sugars and organic acids. **(A)** The total content of glucose, fructose, and sucrose; **(B–D)** the total content of glucose **(B)**, fructose **(C)**, and sucrose **(D)**; **(E–H)** the total content of pyruvic acid **(E)**, oxalic acid **(F)**, citric acid **(G)**, and malic acid **(H)**. Least significant differences (LSDs) were calculated to compare significant effects at the 5% level. Each data point represents the mean ± S.E. ($n = 3$).

slightly induced the activity of SDH although the increase was not statistically significant (**Figure 5B**). CCO is a cytochrome oxidase and key enzyme in the cytochrome pathway (CCP). CCO activity decreased during the first 5 days and then increased from days 5 to 11 (**Figure 5C**). Treatment with eBL induced the activity of CCO during storage.

G-6-PDH and 6-PGDH are the key enzymes of the pentose phosphate pathway (PPP). Their activities are directly related to the PPP pathway. Compared with the control, treatment with eBL induced the activities of G-6-PDH and 6-PGDH. The activities of G-6-PDH and 6-PGDH remained relatively stable during storage, and no significant difference was identified during the first 5 days

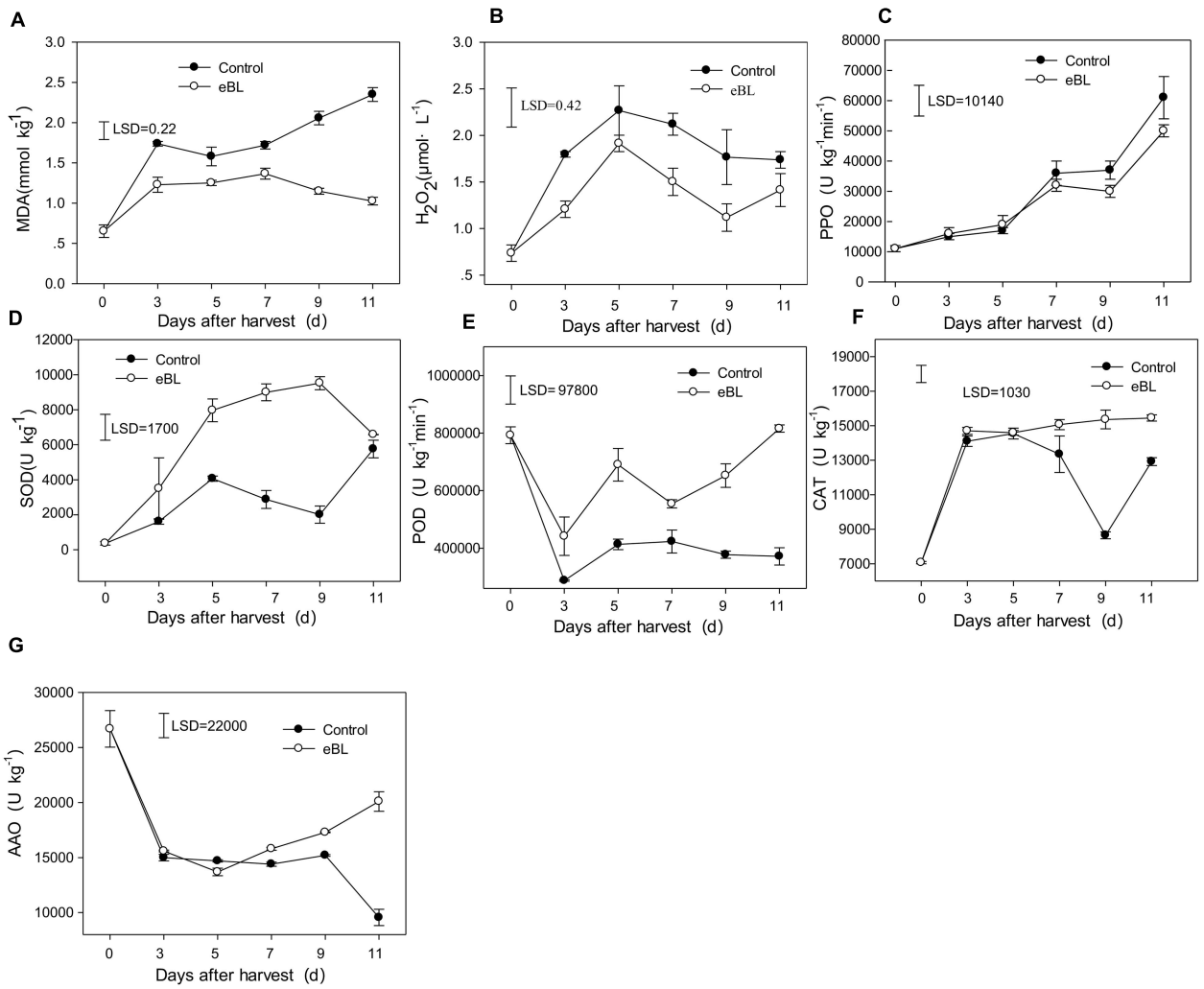

FIGURE 4 | Effects of eBL treatment on the content of reactive oxygen species and antioxidant-related enzyme activities. **(A)** The content of MDA; **(B)** the content of H_2O_2; **(C)** PPO activity; **(D)** SOD activity; **(E)** POD activity; **(F)** CAT activity; **(G)** AAO activity. Least significant differences (LSDs) were calculated to compare significant effects at the 5% level. Each data point represents the mean ± S.E. ($n = 3$).

between the control and samples treated with eBL. The enzymes in fruit treated with eBL rapidly increased from day 5 and reached their maximal levels of activity on day 7, which was significantly higher than those of the control, and then decreased (**Figure 5D**). These results showed that treatment with eBL reduced the EMP pathways and strengthened the respiratory metabolic pathway of CCO and PPP during storage of carambola fruit.

The Effect of Treatment With eBL on Contents of IAA, GA3, and ABA

As shown in **Figure 6**, the IAA content decreased during fruit storage, but treatment with eBL induced its accumulation, which increased during the first 5 days and then gradually decreased. The content of IAA in fruit treated with eBL was significantly higher than that of the control fruit (**Figure 6A**). The content of GA_3 remained at a relatively stable level for the first 3 days and then decreased gradually with fruit ripening. Similar changes in the content of GA_3 were observed for fruit treated with eBL, but the content of GA_3 in fruit treated with eBL was much higher than that of control fruit (**Figure 6B**). ABA increased with fruit ripening, and fruit treated with eBL exhibited a lower-level ABA compared with that of the control fruit (**Figure 6C**).

DISCUSSION

Extensive studies over the past three decades have revealed that BRs are important regulators for plant development, growth, and adaption to stress (Bajguz and Hayat, 2009). The potential role of BRs in regulating fruit ripening has also been investigated in recent decades. Most of these studies focus on their roles of maintaining the quality of fruit sensitive to chilling injury. For example, treatment with BRs has been proven to enhance the chilling tolerance in harvested tomato (Aghdam et al., 2012),

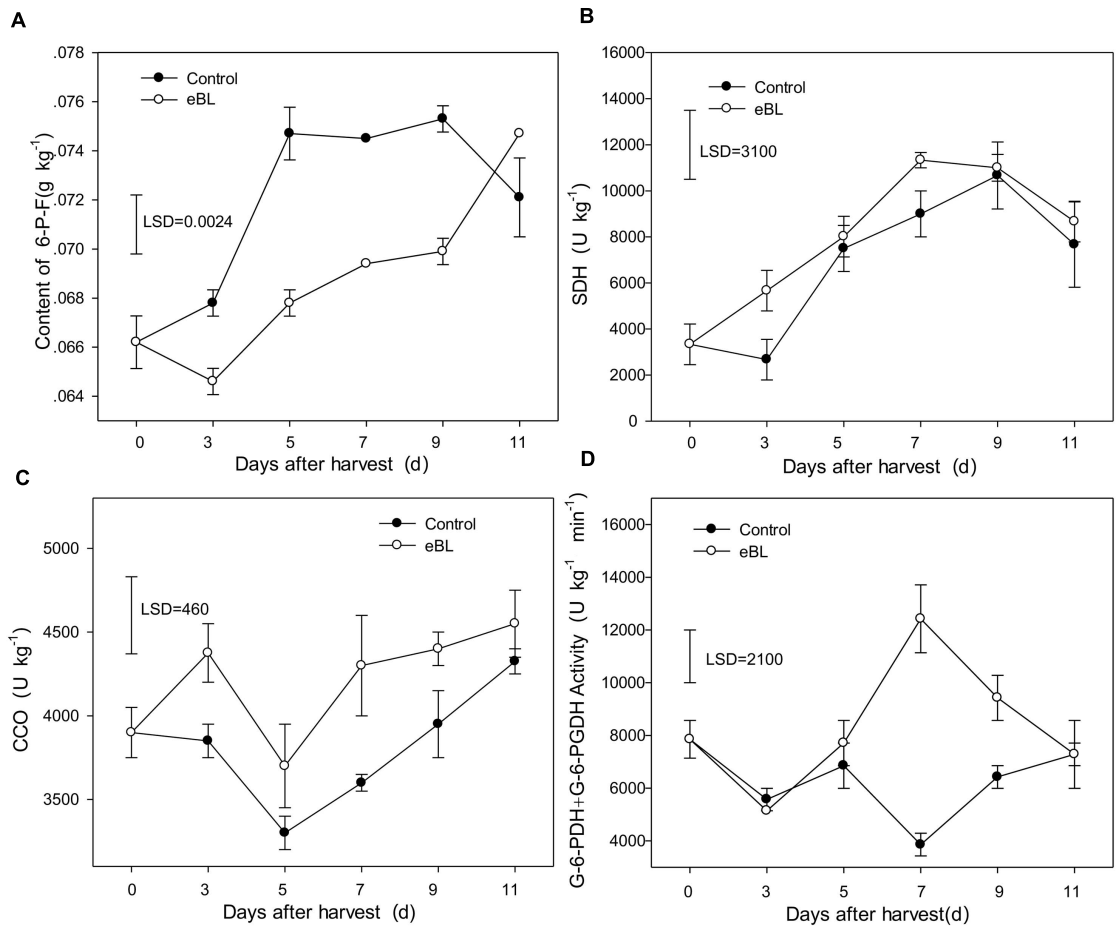

FIGURE 5 | Effects of eBL treatment on the activities of respiration-related enzymes. **(A)** The content of 6-P-F; **(B)** SDH activity; **(C)** CCO activity; **(D)** the total activities of G-6-PDH + 6-PGDH. Least significant differences (LSDs) were calculated to compare significant effects at the 5% level. Each data point represents the mean ± S.E. ($n = 3$).

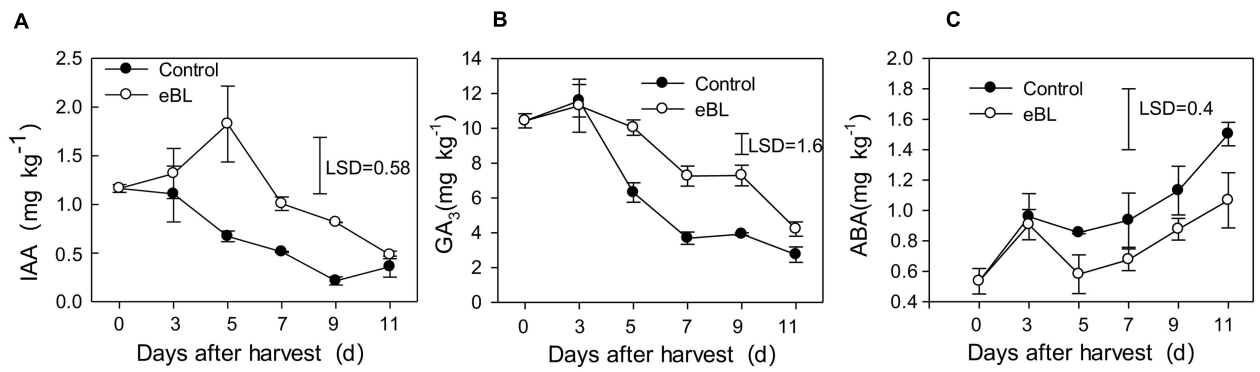

FIGURE 6 | Effects of eBL treatment on the content of endogenous hormones. **(A)** IAA; **(B)** GA3; **(C)** ABA. Least significant differences (LSDs) were calculated to compare significant effects at the 5% level. Each data point represents the mean ± S.E. ($n = 3$).

bamboo shoots (Liu et al., 2016), and mango (Li et al., 2012), which primarily act by enhancing the activities of enzymes involved in antioxidant pathways and those related to proline and energy metabolism and membrane integrity. In this study, we showed that treatment with eBL delayed the ripening of carambola by inhibiting color changes, decreasing firmness, and reducing respiration of fruit. Treatment with eBL also improved the flavor of fruit by maintaining content of vitamin C and

reducing content of organic acids. Similar results have also been reported in jujube fruit, in which treatment with BR effectively delayed the development of senescence by reducing production of ethylene (Zhu et al., 2010). BR effectively reduced the respiration of fruit and enhanced activities of antioxidant enzymes in carambola and jujube fruit. In peach fruit, BR treatment reduced fruit decay caused by *Penicillium expansum* associated with the induction of antioxidant activity. BR also delayed fruit senescence *via* reducing the decrease in flesh hardness, content of soluble solids (SSC), and titratable acid (TA) in peach fruit (Ge et al., 2016). Recent work showed that eBR treatment delay apple and pear fruit ripening by suppressing ethylene biosynthesis. BR activated the expression of PuBZR1, a key transcription factor in BR signaling pathway, which interact with PuACO1 and suppresses expression of *ACO1* and *ACS1a* and ACO1 activity, thereby reducing ethylene production during pear and apple fruit ripening (Ji et al., 2020). In strawberry, preharvest eBL treatment significantly enhanced strawberry fruit nutritional and overall quality *via* enhancing fruit total antioxidant activity, total phenolics, and total anthocyanins contents and reducing the decay extension and microbial count during storage. The effects of eBL also showed dose dependence which low concentration showed better effect than high concentration (Sun et al., 2019; Zahedipour-Sheshglani and Asghari, 2020). These results are also in line with our results that suitable low concentration of eBL showed better effect on maintaining carambola than high concentration (**Figure 1**).

However, a substantial amount of research showed that BRs play dual effects on fruit ripening, which also accelerated fruit ripening in a number of types of fruit, including tomato (Zhu T. et al., 2015), mango (Zaharah and Singh, 2012), and persimmon (He et al., 2018). Treatment with BRs promoted ripening in mango fruit *via* accelerating the production of ethylene and increasing rate of respiration (Zaharah and Singh, 2012). Treatment with BRs promoted ripening in persimmon fruit by promoting the production of ethylene, increasing respiration rate, and influencing cell wall-degrading enzymes and ethylene biosynthesis (He et al., 2018). The application of brassinolide effectively induced ripening in tomato fruit by increasing soluble sugars, ascorbic acid, contents of lycopene, respiration rate, and ethylene production, as well as the expression of genes related to ethylene synthesis (Zhu T. et al., 2015). These results indicated that BRs may play a different role in various fruit species, depending on their ripening process. Other treatments also effectively function to preserve carambola fruit. For example, treatment with polyamines (PAs) effectively maintains the quality of postharvest carambola fruit by enhancing the capacity of antioxidants and reducing the activity of cell wall-degrading enzymes, thus prolonging the shelf life of fruit (Ahmad and Ali, 2019). Treatment with methyl jasmonate improved the quality of carambola fruit and alleviated chilling injury during cold storage and transportation (Mustafa et al., 2016). Treatment with edible coatings significantly delayed the senescence of carambola fruit and maintained fruit quality (Gol et al., 2015). However, to our knowledge, this is the first report that a simple eBL treatment could effectively delay carambola fruit senescence and maintain fruit quality. BRs could be a potential commercial application in the carambola industry owing to their safe nature and simple operation.

The process of fruit ripening has been considered an oxidative phenomenon that requires a turnover of active oxygen species (AOS), including H_2O_2 and the superoxide anion (Kaushal, 2016). It has been reported that the formation of O_2^- and accumulation of H_2O_2 increased significantly during fruit ripening, as indicated by an increase in protein oxidation and lipid peroxidation products (Jimenez et al., 2002). Therefore, the antioxidant systems play an important role in both fruit ripening and senescence processes (Jimenez et al., 2002). Changes in the antioxidant systems during fruit ripening have previously been described. For example, Jiménez et al. reported that the levels of H_2O_2 and lipid peroxidation increased with fruit ripening, as well as the antioxidant components: glutathione (GSH) and AsA content and antioxidant enzyme activities of CAT, SOD, and ascorbate peroxidase (APX) in tomato (Jimenez et al., 2002). However, in blackberry fruit, it was shown that GSH, AsA, and related enzymes declined with fruit ripening (Wang and Jiao, 2001). In jujube fruit, the total antioxidant components increased with fruit ripening (Zhu et al., 2010). In this study, the H_2O_2 content increased with fruit ripening, accompanied with the lipid peroxidation level that was indicated by an increase in the content of MAD (**Figure 4**). The antioxidant component Vc increased at first and then slightly decreased with fruit ripening. The enzymatic activities of PPO, SOD, and CAT increased with fruit ripening, but those of POD and AAO declined with fruit ripening (**Figure 4**).

In this study, eBL treatment significantly reduced the contents of H_2O_2 and MDA by enhancing the activities of PPO, SOD, POD, CAT, and AAO, resulting in a lower degree of oxidative damage. Treatment with eBL can result in important roles in reducing the active oxygen species by enhancing the fruit antioxidant system in this study. Similar results have also been observed in other studies. Treatment with BRs significantly induced the Vc content and activities of CAT, PAL, PPO and SOD in jujube (Zhu et al., 2010), which is consistent with our results. The exogenous application of BRs enhanced the activity of antioxidant enzymes, including POD, CAT, and glutathione reductase ascorbate and alleviated chilling injury in pepper during storage (Wang et al., 2012). Brassinolide treatment significantly induced the enzymatic activities of PPO, POD, and SOD in cowpea leaves under salt stress, conferring tolerance to salt stress by increasing the activities of those antioxidative enzymes (Elmashad and Mohamed, 2012). Pretreatment of eBL enhanced the antioxidant capacity of wucai *via* inducing the activities of key enzymes of the AsA-GSH including APX, glutathione reductase (GR), dehydroascorbate reductase (DHAR), and monodehydroascorbate reductase (MDHAR), resulting in delayed senescence and quality deterioration (Yuan et al., 2021). All these results are consistent with our results. Other hormones such as salicylic acid and methyl jasmonate also improve fruit physicochemical properties by enhancing the antioxidant activity of mangosteen and dragon fruit during cold storage (Mustafa et al., 2018). The tolerance of plants to stress conditions may be associated with the ability to remove AOS through AOS detoxifying enzymes, such as SOD, GR, POD, CAT,

and PPO, indicating that these antioxidant enzymes play an important role in protecting fruit from oxidative damage.

Respiration plays a vital role in high plants, and respiratory metabolism is an important metabolic activity in harvested crops (Lin et al., 2019). Respiratory rate and the respiratory pathways involved are closely related to the ripening and senescence of postharvest horticultural crops (Li et al., 2016). Respiration is one main measurable indicator of the metabolic activity of postharvest crops, with a high respiration rate accelerating ripening or senescence and shortening the storability of fruits and vegetables (Li et al., 2016; Lin et al., 2019). Respiratory metabolic pathways include the EMP, phospho pentose pathway (HMP or PPP), TCA, and CCP (Fernie et al., 2004). The respiratory pathway and respiratory intensity depend on crop varieties, the external environment or different treatment, which are closely related to the changes in activities of respiratory metabolic enzymes (Lin et al., 2018). SDH is the crucial enzyme of TCA pathway, which participates in the reversible oxidation of succinic acid into fumaric acid (Lin et al., 2018). CCO is the key enzyme of CCP, which catalyzes the transfer of electrons from ferrocytochrome *c* to molecular oxygen and plays a key role in aerobic metabolism and energy production during oxidative phosphorylation (Lin et al., 2018). PGI is thought to be the crucial enzyme of EMP, while G-6-PDH and 6-PGDH are the key enzymes involved in PPP (Li et al., 2016). Glucose-6-phosphate (G-6-P) can be transformed to fructose-6-phosphate (F-6-P) through catalysis by PGI in the EMP respiratory pathway. In this study, the four key factors involved in four respiratory metabolic pathways were determined. The content of F-6-P, product of PGI, increased with fruit senescence. Treatment with eBL significantly reduced the production of F-6-P, indicating an inhibition of the EMP pathway. However, treatment with eBL induced the activities of CCO, G-6-PDH, and 6-PGDH compared with the control, indicating that the eBL treatment enhanced PPP and CCP pathways (**Figure 5**). These results indicated that the decreased activity of EMP respiratory pathway, but the increased ratio of PPP and CCP respiratory pathways, played an important role in delaying carambola fruit senescence following treatment with eBL. It is hypothesized that the treatment with eBL delayed fruit senescence and respiration, which was linked to the inhibition of activities of crucial enzymes in EMP-TCA cycle and the enhancement pf activity of key enzymes in respiratory pathway of PPP and CCP, such as G-6-PDH and 6-PGDH.

These findings were consistent with a previous study that the controlled atmosphere (CA) treatment of 30% O_2 + 70% CO_2 accelerated the senescence of broccoli, which was primarily owing to the inhibition in total activities of G-6-PDH, 6-PGDH, CCO, and SDH. However, CA treatment of 50% O_2 + 50% CO_2 delayed the senescence of broccoli, which was primarily related to the increased levels of G-6-PDH and 6-PGDH activities and reduced activities of SDH and CCO (Li et al., 2017). In longan fruit, H_2O_2 stimulated pulp breakdown owing to a decreased proportion of PPP pathway, the increased proportions of EMP pathway, TCA cycle, and CCP in total respiratory pathways, which primarily regulate the activities of key enzymes, including PGI, SDH, CCO, G-6-PDH, and 6-PGDH (Lin et al., 2020). Salicylic acid (SA) treatment effectively reduced the fruit disease index and respiration rate by decreasing the activities of PGI, SDH, and CCO but boosting the activities of G-6-PDH + 6-PGDH (Chen et al., 2020). This indicated that treatment with SA retards the development of disease *via* decreasing the respiratory pathways of EMP-TCA cycle and CCP but increasing PPP respiratory pathway (Chen et al., 2020). In nectarine fruit, treatment with chitosan delayed fruit senescence, which was primarily owing to the inhibition of the respiration rate and an enhancement of the antioxidant system (Zhang et al., 2019), which is consistent with our results. Additionally, treatment with chitosan significantly suppressed the activity of SDH enzyme and increased total activity of G-6-PDH and 6-PGDH. All of these results showed that the enhancement of PPP and reduction of EMP respiratory pathway aid in the preservation and quality of harvested horticultural crops.

Fruit ripening is a complex process regulated by various factors and coordinated by plant hormones. Hormone cross-talk is critical for the fruit ripening process. There is a close relationship between BR and GA and IAA signaling during many developmental processes in plants (Wang and Yang, 2008). Auxin is a critical hormone in fruit development and IAA is the key regulator of fruit development in non-climacteric and climacteric fruit (Sam et al., 2014). In grape, the highest content of IAA has been detected in flowers and young berries, and it gradually decreases to low levels throughout the ripening period. IAA play a negative role in anthocyanin and sugar accumulation, which associated with delayed ripening of grapeberry (Böttcher et al., 2011; Ziliotto et al., 2012). The auxin contents are usually kept in variant or tend to decrease during the fruit postharvest period. Postharvest exogenous IAA treatments could delay ripening in some fruits (Chen et al., 2016; Moro et al., 2017), thus suggesting auxin also plays an important role in the control of postharvest fruit ripening.

It was reported that exogenous brassinosteroid treatments increased growth and endogenous brassinosteroid, auxin, as well as gibberellin levels of apple nursery trees (Zheng et al., 2019). However, brassinosteroids and gibberellic acid (GA3) play different roles in cherry fruit coloring process, and brassinosteroids promoted fruit coloring but GA3 sprays significantly delayed maturation time and the development of skin color (Li et al., 2020). ABA play an important role in fruit ripening, especially for non-climacteric fruit. Studies have found that BRs and ABA interact to regulate many biological processes in plants (Zhang et al., 2009). ABA is important for seed dormancy during embryo maturation and inhibits seed germination, but BRs promote seed germination, which tend to antagonize the effect of ABA (Finkelstein et al., 2008). A study also found that BR treatment promoted the production of ethylene and IAA in squash hypocotyls but reduced the ABA content (Jong-Seon et al., 1989).

For the non-climacteric fruit such as grape and strawberry, the content of IAA and GA decreased with fruit ripening. In addition, the content of ABA and ethylene increased with fruit ripening (Fuentes et al., 2019). This results also observed in carambola fruit in present work. Our results showed that the contents of IAA and GA3 decreased with fruit ripening in carambola fruit, but eBL treatment delayed fruit ripening and

increased the content of IAA and GA3. ABA content increased with fruit ripening but reduced by eBL treatment. All these results seem that IAA and GA are negatively related to fruit ripening of carambola fruit and ABA is positively related to carambola fruit ripening. BRs interact with these hormones and affects their synthesis and coregulates carambola fruit ripening process. However, the underline cross-talk regulation needs further investigation.

CONCLUSION

This study showed that treatment with eBL delayed the ripening of carambola fruit and improved its taste by reducing content of organic acids. Treatment with eBL inhibited the respiration rate of fruit and enhanced antioxidant system by increasing the activities of POD, SOD, CAT, and AAO and decreasing the accumulation of H_2O_2 and MDA. eBL alters the respiratory metabolic pathway by inhibiting activity of PGI but increasing activity of G-6-PDH and 6-PGDH and CCO. The endogenous hormone contents of fruit were altered by application of eBL. The contents of IAA and GA were induced, but that of ABA was reduced. In general, treatment with eBL primarily maintains the quality of carambola fruit by enhancing the antioxidant capacity of fruit and altering its respiratory metabolism. The increased PPP and CCP respiratory pathway and decreased EMP pathway may aid in the preservation of carambola fruit.

DATA AVAILABILITY STATEMENT

The original contributions presented in the study are included in the article/supplementary material, further inquiries can be directed to the corresponding author/s.

AUTHOR CONTRIBUTIONS

XZ: conceptualization, funding acquisition, resources, and writing—original draft. YC: investigation, data curation, formal analysis, and methodology. JL: software, investigation, and methodology. XD: resources and validation. SX: software and methodology. SF: software, methodology, and validation. ZS: methodology and validation. WC: supervision, resources, and writing—review and editing. XL: conceptualization, funding acquisition, project administration, resources, supervision, and writing—review and editing. All the authors read and approved the final manuscript.

FUNDING

This work was supported by the Special Fund for Agro-scientific Research in the Public Interest (201303077-1) and Pearl River Talent Program for Young Talent (Grant No. 2017GC010321).

REFERENCES

Aghdam, M. S., Asghari, M., Farmani, B., Mohayeji, M., and Moradbeygi, H. (2012). Impact of postharvest brassinosteroids treatment on PAL activity in tomato fruit in response to chilling stress. *Sci. Hortic.* 144, 116–120.

Ahmad, A., and Ali, A. (2019). Improvement of postharvest quality, regulation of antioxidants capacity and softening enzymes activity of cold-stored carambola in response to polyamines application. *Postharvest Biol. Technol.* 148, 208–217.

Ali, Z. M., Chin, L.-H., Marimuthu, M., and Lazan, H. (2004). Low temperature storage and modified atmosphere packaging of *Carambola fruit* and their effects on ripening related texture changes, wall modification and chilling injury symptoms. *Postharvest Biol. Technol.* 33, 181–192.

Bajguz, A., and Hayat, S. (2009). Effects of brassinosteroids on the plant responses to environmental stresses. *Plant Physiol. Biochem.* 47, 1–8.

Böttcher, C., Boss, P. K., and Davies, C. (2011). Acyl substrate preferences of an IAA-amido synthetase account for variations in grape (*Vitis vinifera* L.) berry ripening caused by different auxinic compounds indicating the importance of auxin conjugation in plant development. *J. Exp. Bot.* 62, 4267–4280. doi: 10.1093/jxb/err134

Chen, J., Mao, L., Lu, W., Ying, T., and Luo, Z. (2016). Transcriptome profiling of postharvest strawberry fruit in response to exogenous auxin and abscisic acid. *Planta* 243, 183–197. doi: 10.1007/s00425-015-2402-5

Chen, Y., Sun, J., Lin, H., Lin, M., Lin, Y., Wang, H., et al. (2020). Salicylic acid reduces the incidence of Phomopsis longanae Chi infection in harvested longan fruit by affecting the energy status and respiratory metabolism. *Postharvest Biol. Technol.* 160:111035.

Deng, L. L., Pan, X. Q., Sheng, J. P., and Lin, S. (2012). Optimization of experimental conditions for the determination of water soluble protein in apple pulp using coomassie brilliant blue method. *Food Sci.* 10, 809–819.

Elmashad, A. A. A., and Mohamed, H. I. (2012). Brassinolide alleviates salt stress and increases antioxidant activity of cowpea plants (*Vigna sinensis*). *Protoplasma* 249, 625–635. doi: 10.1007/s00709-011-0300-7

Fernie, A. R., Carrari, F., and Sweetlove, L. J. (2004). Respiratory metabolism: glycolysis, the TCA cycle and mitochondrial electron transport. *Curr. Opin. Plant Biol.* 7, 254–261.

Finkelstein, R., Reeves, W., Ariizumi, T., and Steber, C. (2008). Molecular aspects of seed dormancy. *Annu. Rev. Plant Biol.* 59, 387–415.

Fuentes, L., Figueroa, C. R., and Valdenegro, M. (2019). Recent advances in hormonal regulation and cross-talk during non-climacteric fruit development and ripening. *Horticulturae* 5:45.

Ge, Y. H., Li, C. Y., Tang, R. X., Sun, R. H., and Li, J. R. (2016). Effects of postharvest brassinolide dipping on quality parameters and antioxidant activity in Peach fruit. *Acta Horticulturae* 1144, 377–384. doi: 10.17660/ActaHortic.2016.1144.56

Gol, N. B., Chaudhari, M. L., and Rao, T. V. R. (2015). Effect of edible coatings on quality and shelf life of carambola (*Averrhoa carambola* L.) fruit during storage. *J. Food Sci. Technol.* 52, 78–91.

Guo, Q., Lv, X., Xu, F., Zhang, Y., Wang, J., Lin, H., et al. (2013). Chlorine dioxide treatment decreases respiration and ethylene synthesis in fresh-cut "Hami" melon fruit. *Int. J. Food Sci. Technol.* 48, 1775–1782.

Hazarika, T. K., and Tariang, K. (2019). Plant bio-regulators for enhancing quality and storability of Carambola (*Averrhoa carambola*) fruits. *Indian J. Agric. Sci.* 89, 1323–1327.

He, Y., Li, J., Ban, Q., Han, S., and Rao, J. (2018). Role of brassinosteroids in persimmon (*Diospyros kaki* L.) Fruit Ripening. *J. Agric. Food Chem.* 66, 2637–2644. doi: 10.1021/acs.jafc.7b06117

Ji, Y., Qu, Y., Jiang, Z., Su, X., Yue, P., Li, X., et al. (2020). Brassinosteroids suppress ethylene biosynthesis via transcription factor BZR1 in pear and apple fruit. *bioRxiv [Preprint]* doi: 10.1101/2020.02.27.968800

Jimenez, A., Creissen, G., Kular, B., Firmin, J., Robinson, S., Verhoeyen, M., et al. (2002). Changes in oxidative processes and components of the antioxidant system during tomato fruit ripening. *Planta* 214, 751–758. doi: 10.1007/s004250100667

Jong-Seon, E., Susumu, K., and Naoki, S. (1989). Changes in levels of auxin and abscisic acid and the evolution of ethylene in squash hypocotyls after treatment with brassinolide. *Plant Cell Physiol.* 30, 807–810.

Kader, A. A., Zagory, D., and Kerbel, E. L. (1989). Modified atmosphere packaging of fruits and vegetables. *Crit. Rev. Food Sci. Nutr.* 28, 1–30.

Kaushal, S. (2016). Reactive oxygen species (ROS) and associated scavenging mechanisms during fruit ripening. *Botany* 66, 176–186. doi: 10.1104/pp.109.138107

Li, B., Zhang, C., Cao, B., Qin, G., Wang, W., and Tian, S. (2012). Brassinolide enhances cold stress tolerance of fruit by regulating plasma membrane proteins and lipids. *Amino Acids* 43, 2469–2480. doi: 10.1007/s00726-012-1327-6

Li, L., Kitazawa, H., Wang, X., and Sun, H. (2017). Regulation of respiratory pathway and electron transport chain in relation to senescence of postharvest white mushroom (*Agaricus bisporus*) under High O2/CO2 controlled atmospheres. *J. Agric. Food Chem.* 65, 3351–3359. doi: 10.1021/acs.jafc.6b05738

Li, L., Lv, F., Guo, Y., and Wang, Z. (2016). Respiratory pathway metabolism and energy metabolism associated with senescence in postharvest Broccoli (*Brassica oleracea* L. var. italica) florets in response to O2/CO2 controlled atmospheres. *Postharvest Biol. Technol.* 111, 330–336.

Li, M., Cheng, S., Wang, Y., and Dong, Y. (2020). Improving fruit coloration, quality attributes, and phenolics content in "Rainier" and "Bing" cherries by gibberellic acid combined with homobrassinolide. *J. Plant Growth Regul.* 39, 1130–1139.

Lin, L., Lin, Y., Lin, H., Lin, M., Ritenour, M. A., Chen, Y., et al. (2019). Comparison between "Fuyan" and "Dongbi" longans in aril breakdown and respiration metabolism. *Postharvest Biol. Technol.* 153, 176–182.

Lin, Y., Lin, H., Chen, Y., Wang, H., Lin, M., Ritenour, M. A., et al. (2020). The role of ROS-induced change of respiratory metabolism in pulp breakdown development of longan fruit during storage. *Food Chem.* 305:125439. doi: 10.1016/j.foodchem.2019.125439

Lin, Y., Lin, Y., Lin, H., Chen, Y., Wang, H., and Shi, J. (2018). Application of propyl gallate alleviates pericarp browning in harvested longan fruit by modulating metabolisms of respiration and energy. *Food Chem.* 240, 863–869. doi: 10.1016/j.foodchem.2017.07.118

Liu, Z., Li, L., Luo, Z., Zeng, F., Jiang, L., and Tang, K. (2016). Effect of brassinolide on energy status and proline metabolism in postharvest bamboo shoot during chilling stress. *Postharvest Biol. Technol.* 111, 240–246.

Lu, X. H., Sun, D. Q., Mo, Y. W., Xi, J. G., and Sun, G. M. (2010). Effects of post-harvest salicylic acid treatment on fruit quality and anti-oxidant metabolism in pineapple during cold storage. *J. Hortic. Sci. Biotechnol.* 85, 454–458.

Moro, L., Hassimotto, N., and Purgatto, E. (2017). Postharvest auxin and methyl jasmonate effect on anthocyanin biosynthesis in red raspberry (*Rubus idaeus* L.). *J. Plant Growth Regul.* 36, 773–782.

Mustafa, M. A., Ali, A., Seymour, G. B., and Tucker, G. A. (2016). Enhancing the antioxidant content of carambola (*Averrhoa carambola*) during cold storage and methyl jasmonate treatments. *Postharvest Biol. Technol.* 118, 79–86.

Mustafa, M. A., Ali, A., Seymour, G., and Tucker, G. (2018). Treatment of dragonfruit (*Hylocereus polyrhizus*) with salicylic acid and methyl jasmonate improves postharvest physico-chemical properties and antioxidant activity during cold storage. *Sci. Hortic.* 231, 89–96.

Omar, A. F., Atan, H., and MatJafri, M. Z. (2012). Visible spectral linearisation, gradient shift and normalisation in quantifying carambola acidity. *Food Biophys.* 7, 289–295. doi: 10.3390/s130404876

Sam, C., Figueroa, C. R., and Helen, N. (2014). Movers and shakers in the regulation of fruit ripening: a cross-dissection of climacteric versus non-climacteric fruit. *J. Exp. Bot.* 65, 4705–4722. doi: 10.1093/jxb/eru280

Shi, J., Liu, A., Li, X., and Chen, W. (2013). Control of P*hytophthora nicotianae* disease, induction of defense responses and genes expression of papaya fruits treated with *Pseudomonas putida* MGP1. *J. Sci. Food Agric.* 93, 568–574. doi: 10.1002/jsfa.5831

Sun, Y., Asghari, M., and Zahedipour-Sheshgelani, P. (2019). Foliar spray with 24-epibrassinolide enhanced strawberry fruit quality, phytochemical content, and postharvest life. *J. Plant Growth Regul.* 39, 920–929.

Wang, H., Li, X., and Chen, W. (2010). Determination of organic acids in pineapple fruits during storage by ion chromatography. *J. Trop. Crop* 31, 1720–1725.

Wang, Q., Ding, T., Gao, L., Pang, J., and Yang, N. (2012). Effect of brassinolide on chilling injury of green bell pepper in storage. *Sci. Hortic.* 144, 195–200.

Wang, S. Y., and Jiao, H. (2001). Changes in oxygen-scavenging systems and membrane lipid peroxidation during maturation and ripening in blackberry. *J. Agric. Food Chem.* 49, 1612–1619. doi: 10.1021/jf0013757

Wang, T. Q., and Yang, X. (2008). Effects of brassinolide on contents of nucleic acid and endogenous hormones in stem apex of Broccoli. *Acta Hortic. Sin.* 35, 661–666.

Warren, O., and Sargent, S. A. (2011). "Carambola (*Averrhoa carambola* L.)," in *Postharvest Biology Technology Tropical Subtropical Fruits*, ed. E. Yahia (Amsterdam: Elsevier).

You, S. W., Shi, P. T., Yong, X., Guo, Z. Q., and Yao, H. (2004). Changes in the activities of pro- and anti-oxidant enzymes in peach fruit inoculated with Cryptococcus laurentii or *Penicillium expansum* at 0 or 20 °C. *Postharvest Biol. Technol.* 34, 21–28.

Yuan, L., Nie, L., Ji, Q., Zheng, Y., Zhang, L., Zhu, S., et al. (2021). The effect of exogenous 24-epibrassinolide pretreatment on the quality, antioxidant capacity, and postharvest life of wucai (*Brassica campestris* L.). *Food Sci. Nutr.* 9, 1323–1335. doi: 10.1002/fsn3.2075

Zaharah, S. S., and Singh, Z. (2012). Role of brassinosteroids in mango fruit ripening. *Acta Horticulturae* 934, 929–935. doi: 10.17660/ActaHortic.2012.934.124

Zaharah, S. S., Singh, Z., Symons, G. M., and Reid, J. B. (2012). Role of Brassinosteroids, Ethylene, abscisic acid, and Indole-3-acetic acid in mango fruit ripening. *J. Plant Growth Regul.* 31, 363–372.

Zahedipour-Sheshglani, P., and Asghari, M. (2020). Impact of foliar spray with 24-epibrassinolide on yield, quality, ripening physiology and productivity of the strawberry. *Sci. Hortic.* 268:109376.

Zhang, S., Cai, Z., and Wang, X. (2009). The primary signaling outputs of brassinosteroids are regulated by abscisic acid signaling. *Proc. Natl. Acad. Sci.* 106, 4543–4548. doi: 10.1073/pnas.0900349106

Zhang, W., Zhao, H., Zhang, J., Sheng, Z., Cao, J., and Jiang, W. (2019). Different molecular weights chitosan coatings delay the senescence of postharvest nectarine fruit in relation to changes of redox state and respiratory pathway metabolism. *Food Chem.* 289, 160–168. doi: 10.1016/j.foodchem.2019.03.047

Zhang, Y. L., Dang, Y., Jing, Z., and Xiao-Ping, L. I. (2005). Simultaneous Determination of gibberellin (GA_3) and abscisic acid (ABA) in peach tissue by high performance liquid chromatography. *Acta Bot. Boreali-occidentalia Sin.* 25, 1467–1471.

Zheng, L., Gao, C., Zhao, C., Zhang, L., Han, M., An, N., et al. (2019). Effects of brassinosteroid associated with auxin and gibberellin on apple tree growth and gene expression patterns. *Hortic. Plant J.* 5, 93–108.

Zhu, T., Tan, W., Deng, X., Zheng, T., Zhang, D., and Lin, H. (2015). Effects of brassinosteroids on quality attributes and ethylene synthesis in postharvest tomato fruit. *Postharvest Biol. Technol.* 100, 196–204.

Zhu, X., Shen, L., Fu, D., Si, Z., Wu, B., Chen, W., et al. (2015). Effects of the combination treatment of 1-MCP and ethylene on the ripening of harvested banana fruit. *Postharvest Biol. Technol.* 107, 23–32. doi: 10.1093/jxb/ers178

Zhu, Z., Zhang, Z., Qin, G., and Tian, S. (2010). Effects of brassinosteroids on postharvest disease and senescence of jujube fruit in storage. *Postharvest Biol. Technol.* 56, 50–55.

Ziliotto, F., Corso, M., Rizzini, F. M., Rasori, A., Botton, A., and Bonghi, C. (2012). Grape berry ripening delay induced by a pre-véraison NAA treatment is paralleled by a shift in the expression pattern of auxin- and ethylene-related genes. *BMC Plant Biol.* 12:185. doi: 10.1186/1471-2229-12-185

Conflict of Interest: The authors declare that the research was conducted in the absence of any commercial or financial relationships that could be construed as a potential conflict of interest.

frontiers in Plant Science

ORIGINAL RESEARCH
published: 10 June 2021
doi: 10.3389/fpls.2021.684130

Identification of DNA Methylation and Transcriptomic Profiles Associated With Fruit Mealiness in *Prunus persica* (L.) Batsch

*Karin Rothkegel[1], Alonso Espinoza[1], Dayan Sanhueza[1], Victoria Lillo-Carmona[1], Aníbal Riveros[1], Reinaldo Campos-Vargas[2] and Claudio Meneses[1,3]**

[1] Facultad Ciencias de la Vida, Centro de Biotecnología Vegetal, Universidad Andrés Bello, Santiago, Chile, [2] Departamento de Producción Agrícola, Facultad de Ciencias Agronómicas, Centro de Estudios Postcosecha, Universidad de Chile, Santiago, Chile, [3] FONDAP Center for Genome Regulation, Santiago, Chile

OPEN ACCESS

Edited by:
Claudia Anabel Bustamante, Centro de Estudios Fotosintéticos y Bioquímicos (CEFOBI), Argentina

Reviewed by:
Pedro Martinez-Gomez, Center for Edaphology and Applied Biology of Segura, Spanish National Research Council, Spain
George Manganaris, Cyprus University of Technology, Cyprus
Diep R. Ganguly, Australian National University, Australia

***Correspondence:**
Claudio Meneses
claudio.meneses@unab.cl

Specialty section:
This article was submitted to Plant Abiotic Stress, a section of the journal Frontiers in Plant Science

Received: *22 March 2021*
Accepted: *17 May 2021*
Published: *10 June 2021*

Citation:
Rothkegel K, Espinoza A, Sanhueza D, Lillo-Carmona V, Riveros A, Campos-Vargas R and Meneses C (2021) Identification of DNA Methylation and Transcriptomic Profiles Associated With Fruit Mealiness in Prunus persica (L.) Batsch. Front. Plant Sci. 12:684130. doi: 10.3389/fpls.2021.684130

Peach (*Prunus persica*) fruits have a fast ripening process and a shelf-life of days, presenting a challenge for long-distance consuming markets. To prolong shelf-life, peach fruits are stored at low temperatures (0 to 7 °C) for at least two weeks, which can lead to the development of mealiness, a physiological disorder that reduces fruit quality and decreases consumer acceptance. Several studies have been made to understand this disorder, however, the molecular mechanisms underlying mealiness are not fully understood. Epigenetic factors, such as DNA methylation, modulate gene expression according to the genetic background and environmental conditions. In this sense, the aim of this work was to identify differentially methylated regions (DMRs) that could affect gene expression in contrasting individuals for mealiness. Peach flesh was studied at harvest time (E1 stage) and after cold storage (E3 stage) for 30 days. The distribution of DNA methylations within the eight chromosomes of *P. persica* showed higher methylation levels in pericentromeric regions and most differences between mealy and normal fruits were at Chr1, Chr4, and Chr8. Notably, differences in Chr4 co-localized with previous QTLs associated with mealiness. Additionally, the number of DMRs was higher in CHH cytosines of normal and mealy fruits at E3; however, most DMRs were attributed to mealy fruits from E1, increasing at E3. From RNA-Seq data, we observed that differentially expressed genes (DEGs) between normal and mealy fruits were associated with ethylene signaling, cell wall modification, lipid metabolism, oxidative stress and iron homeostasis. When integrating the annotation of DMRs and DEGs, we identified a *CYP450 82A* and an *UDP-ARABINOSE 4 EPIMERASE 1* gene that were downregulated and hypermethylated in mealy fruits, coinciding with the co-localization of a transposable element (TE). Altogether, this study indicates that genetic differences between tolerant and susceptible individuals is predominantly affecting epigenetic regulation over gene expression, which could contribute to a metabolic alteration from earlier stages of development, resulting in mealiness at later stages. Finally, this epigenetic mark should be further studied for the development of new molecular tools in support of breeding programs.

Keywords: peach, chilling injury, Rosaceae, epigenetics, cytosine methylation

INTRODUCTION

Peaches [*Prunus persica* (L.) Batsch] and nectarines [*Prunus persica* (L.) Batsch var. nectarina] are climacteric stone fruits that belong to the Rosaceae family. Once harvested, *P. persica* fruits ripen fast within days at room temperature in spring and summer. To slow down the ripening process and prolong postharvest life, a cold storage is usually used at 0 °C for at least two weeks. However, this method can trigger a physiological disorder known as chilling injury (CI), which is manifested during ripening (Lurie and Crisosto, 2005). The symptoms of CI include mealy texture, flesh browning and/or bleeding, and leatheriness. The main cause of mealiness has been attributed to the metabolism of cell wall pectins, where mealy fruits are associated with an altered pectin methylesterase (PME) and endo-polygalacturonase (PG) activity (Brummell et al., 2004). Concomitantly, it has been suggested that mealiness is caused by the accumulation of insoluble calcium-pectate gel complexes in the middle lamella, trapping free water (Ben-Arie and Lavee, 1971). Another reported effect of CI on *P. Persica* is a reduced cell-to-cell adhesion, resulting in cell separation instead of cell rupture when chewing (King et al., 1989). More recently, studies have also suggested an alteration in reactive oxygen species (ROS) metabolism, mitochondrial respiration, sugar catabolism, amino acid usage, proteomic reprogramming and the importance of jasmonic acid signals in reducing CI via ethylene and sugars (Kan et al., 2011; Monti et al., 2019; Zhao et al., 2021).

Mealiness is genetically influenced and is also related with maturity date, since early cultivars have a lower susceptibility than later cultivars (Crisosto et al., 1999). In 2015, Nuñez-Lillo et al. (2015) studied an F2 Venus × Venus population, detecting one QTLs (Quantitative Trait Loci) for mealiness on linkage group 4 (LG4), explaining 34% of phenotypic variation. Within those QTLs, nine candidate genes related to cell wall synthesis, ethylene signaling and cold stress were identified. Later in 2019, Nuñez-Lillo et al. (2019) studied an F1 O' Henry x NR-053 population, identifying an additional QTL in LG5, and an endo-1,3-beta-glucosidase as one of the candidate genes associated with mealiness.

At the transcriptomic level, Pons et al. (2014) studied a population (Pop-DG) segregating for CI, indicating that the transcriptome of peach fruits was changing during cold storage and was concomitant with the development of CI, highlighting that genes associated with cold response were differentially regulated between sensitive and resistant individuals. Afterward, Pons et al. (2016), analyzed the transcript profiles of the same population, but with different cold storage treatments and subsequent ripening. The results showed that during cold storage, the ripening program involving ethylene, auxin, and cell wall metabolism became desynchronized in susceptible fruits. Another study using a tolerant "Oded" and a relatively tolerant "Hermoza" peach cultivars identified that genes related to oxidative stress and biosynthesis of metabolites with antioxidant activity were positively correlated with CI tolerance (Puig et al., 2015). Moreover, the results suggested that ethylene signaling is related to CI tolerance, but also that auxins may play a role.

To better understand the molecular mechanisms modulating gene expression during plant development and adaptation, epigenomic approaches are an important layer of information. Epigenetic modifications involve histone changes, non-coding RNAs and DNA methylation, which influence chromatin structure and accessibility to genetic information (Zhang et al., 2018). In particular, cytosine DNA methylation has a key role in development, imprinting, silencing of transposable elements, abiotic and biotic responses (Law and Jacobsen, 2010). DNA methylation can be present under three different cytosine contexts: CpG, CHG, and CHH, where the H can be C, T, or A. An example of changes in DNA methylation during fruit ripening is the Colorless non-ripening (*Cnr*) mutant in tomato (*Solanum lycopersicum*), where colorless fruits loss cell-to-cell adhesion and have a mealy pericarp (Manning et al., 2006). This natural mutation involves high levels of cytosine methylation in a 286-bp region upstream of an SBP-box transcription factor, inhibiting fruit ripening and gene expression. A more recent study in tomato also showed that cytosine demethylation by a DNA glycosylase *SIDML2/ROS1* is necessary for the activation of ripening-induced genes and inhibition of ripening-repressed genes, revealing a critical role for DNA methylation during fruit ripening (Lang et al., 2017). In addition, changes in DNA methylation can be further used for the identification of novel markers, which will consider the genetic background, together with changing environmental conditions, as recently studied in *Prunus* (Prudencio et al., 2018; Rothkegel et al., 2020). In this sense, molecular approaches associated with agronomical traits should be implemented together with classical genetics in order to support breeding programs (García-Gómez et al., 2021).

Mealiness is a well-studied disorder, however, the molecular mechanisms leading to this phenotype are not entirely known. In order to elucidate if changes in DNA methylation levels are involved with susceptibility to cold storage, the aim of this work was to identify differentially methylated regions (DMRs) that could affect gene expression in contrasting individuals for mealiness at harvest time and after cold storage. This work will contribute with the first epigenomic study on mealiness, novel DMRs and additional differentially expressed genes (DEGs) that could be further studied as potential markers to differentiate susceptible peach fruits from tolerant fruits at harvest time.

MATERIALS AND METHODS

Plant Material and Phenotyping

A previously characterized F2 V × V population of 151 individuals [*Prunus persica* (L.) Batsch] was used for fruit quality characters obtained from the self-pollination variety "Venus" (Nuñez-Lillo et al., 2015; Lillo-Carmona et al., 2020). This population located at Institute of Agricultural Research (INIA), Rayentué, Región de O'Higgins, Chile (34°32′14″ S, 70°83′44″ W), corresponds to six-year-old trees grown on

G × N rootstock that segregates for mealiness, soluble solids content and maturity date. These fruits are freestone, with yellow and melting flesh. For season 2016–2017, peach fruits were harvested and at least five fruits were evaluated considering one individual with tolerance to cold and another individual with susceptibility to develop mealiness as determined in previous seasons (2012, 2013, and 2014) by our laboratory (Nuñez-Lillo et al., 2015; Lillo-Carmona et al., 2020). Fruits were harvested (E1 stage) and stored at −80 °C considering flesh firmness of 53 N and 0.8–1.2 values (average of each peach cheek measurement) of chlorophyll absorbance index (I_{AD}) with a portable Vis/NIR DA-Meter. Flesh firmness was determined using a Fruit Pressure Tester (Effigi, Alfonsine, Italy) on both peach cheeks.

A second pool of harvested fruits was stored at 0 °C for 30 days, corresponding to E3 stage (**Figure 1A**). After cold storage, fruits were stored at −80 °C until further use, while another group of fruits was stored at 20 °C for 7 days until flesh firmness was approximately 7 N, corresponding to E4 stage (ready to eat). Fruits from each pool and condition were evaluated for juiciness considering at least five biological replicates (**Figure 1A**). For E4 stage, firmness and juiciness were evaluated, while for E3 stage only firmness was measured. Juiciness was determined through a protocol described by Infante et al. (2009), where fruits with a value lower than 30% of juice were referred as mealy fruits, whereas fruits with higher values were considered as normal fruits. These juiciness values were compared using a mean separation test (ANOVA) and post-hoc Tukey-HSD test ($P < 0.05$). Finally, three fruits per individual (normal and mealy) were used at E1 and E3 stages for MethylC-Seq and RNA-Seq.

MethylC-Seq

Bisulfite treatment was carried out from genomic DNA obtained from frozen peach flesh at harvest time (E1) and after cold storage (E3). Three fruits from a tolerant individual and additional three fruits from a sensitive individual were used as biological replicates. Genomic DNA was extracted using a DNeasy Plant mini kit (QIAGEN, Germantown, MD, United States) according to manufacturer's instructions. The integrity of DNA was assessed in a 1.5% (p/v) agarose gel and concentration was determined with Qubit Fluorometer (Thermo Fisher Scientific, Waltham, MA, United States). Afterward, 100 ng of DNA was used for bisulfite treatment with the EZ DNA methylation gold kit (Zymo, Irvine, CA, United States) as previously described (Rothkegel et al., 2017). Twelve bisulfite treated libraries were generated considering two individuals (normal and mealy), two sampling points (E1 and E3) and three biological replicates. Libraries were generated with the TruSeq DNA Methylation kit (Illumina, San Diego, CA, United States) according to manufacturer's instructions. All libraries were validated with Qubit Fluorometer and Fragment Analyzer (Advanced Analytical Technologies, Ankeny, IA, United States) and later sequenced in HiSeq 4000, 2 × 100 bp Paired-end mode (Illumina, San Diego, CA, United States). Raw data is available in NCBI sequence read archives (PRJNA705001).

Processing of MethylC-Seq Reads and Identification of Differentially Methylated Regions

Initially, raw reads were filtered and adapters removed using Trim Galore[1]. Filtered reads were mapped against the reference genome of *P. persica* v.2.0.a1 using Bismark with no mismatches to obtain the methylation state of CpG, CHG, and CHH cytosine contexts (Krueger and Andrews, 2011; Verde et al., 2017). At the same time, reads were aligned to the plastid genome of *P. persica*, which is unmethylated, in order to obtain the bisulfite conversion rate. The bisulfite conversion rate was obtained by dividing the number of methylated cytosines and total cytosines of the chloroplast genome. For the identification of DMRs we used methylPipe considering cytosines covered with at least five reads and a *P*-value of 0.05 or less, a binsize of 10 and at least ten consecutives methylated cytosines using the find DMR function (Kishore et al., 2015). Comparisons were made for: (1) E3 vs. E1 in normal and mealy fruits; and (2) mealy vs. normal fruits at E1 and E3. A Kruskal-Wallis test was performed and regions with changes in methylation of at least two-fold were considered as DMR. Genes that overlapped with a DMR, including 2,000 bp upstream and downstream, were annotated as differentially methylated and used to perform a Gene Ontology (GO) analysis (FDR < 0.01) using AgriGO and REVIGO to decrease redundancy[2].

RNA-Seq

Total RNA from 4 gr of frozen peach mesocarp was isolated using the sodium borate decahydrate method described by Meisel et al. (2005). RNA integrity was assessed using Fragment Analyzer electrophoresis and Qubit Fluorometer. Twelve strand-specific libraries (2 individuals × 2 conditions × 3 biological replicates), were generated from 1 μg of total RNA using TruSeq Stranded mRNA kit (Illumina, San Diego, CA, United States). Validated libraries were sequenced in HiSeq 4000, 2 × 100 bp Paired-end mode and raw data is available in NCBI sequence read archive (PRJNA705416).

Processing of RNA-Seq Reads and Identification of Differentially Expressed Genes

Sequenced reads were trimmed with Trim Galore and mapped to the reference genome of *P. persica* v.2.0.a1 using Spliced Transcripts Alignment to a Reference (STAR; Dobin et al., 2013). Uniquely mapped reads were normalized as trimmed mean of M-values (TMM) and used for DEG analysis with EdgeR considering a False Discovery Rate (FDR) < 0.01 and a fold-change of 1 or more (Robinson et al., 2010). Differentially

[1]https://www.bioinformatics.babraham.ac.uk/projects/trim_galore/

[2]http://bioinfo.cau.edu.cn/agriGO/analysis.php

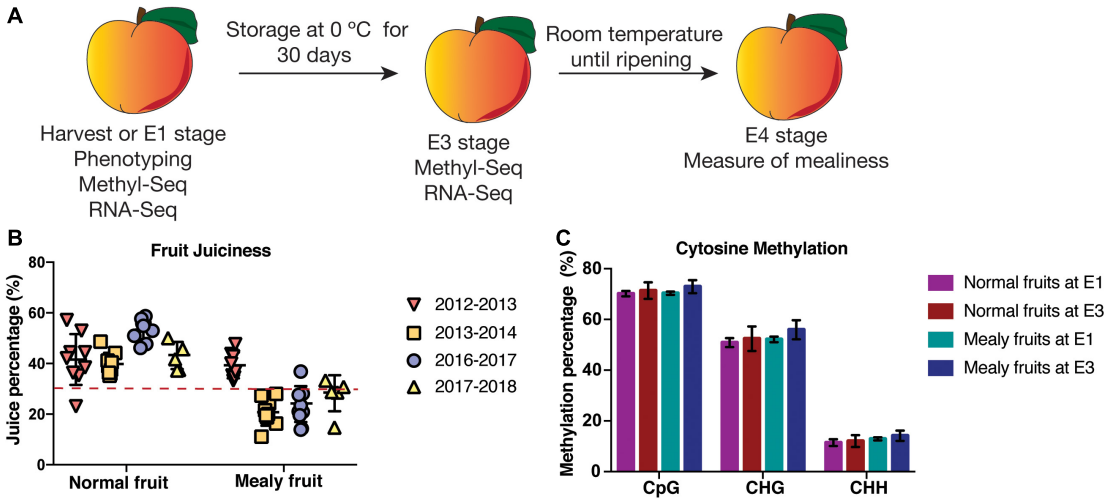

FIGURE 1 | Phenotyping and global levels of DNA methylation in *P. persica* fruits susceptible and resistant to mealiness. **(A)** Experimental design for one resistant and one susceptible individual for mealiness. At harvest (E1), three fruits per tree were used for MethylC-Seq and RNA-Seq analysis, while another pool of fruits was stored in a cold chamber at 0 °C to promote mealiness. After 30 days of cold treatment (E3 stage), three fruits were used for MethylC-Seq and RNA-Seq analysis. At E4 stage, at least five fruits were ripened at room temperature and used for the measure of juice content. **(B)** Juice content (%) during four seasons in at least five fruits of an individual resistant and susceptible to mealiness, respectively. The dotted line represents a 30% threshold to consider fruits as mealy or normal. The same trees were evaluated in all seasons. **(C)** Absolute methylation levels (%) for cytosine contexts CpG, CHG and CHH (H = C, T or A) in normal and mealy fruits at E1 and E3.

expressed genes were obtained by comparing (1) E3 vs. E1 in normal and mealy fruits; and (2) mealy vs. normal fruits at E1 and E3. Variability in gene expression between mealy and normal fruits at E1 and E3 was considered to rank the top50 genes whose expression level was affected the most, represented as a heatmap. Additionally, DEGs that overlapped with DMRs, including 2,000 bp upstream and downstream of gene annotation, were considered as differentially methylated. Hypermethylated regions associated with downregulated genes and vice-versa were represented as heatmaps considering expression levels.

Real Time qPCR Analysis

From total RNA, one microgram was treated with DNase I (Thermo Fisher Scientific), followed by the synthesis of cDNA using the SuperScript™ first-strand synthesis system and oligo dT primers (Thermo Fisher Scientific), according to the standard protocol. Before use, each cDNA sample was diluted 1:10 with nuclease free water. The RT-qPCR assay was performed in an AriaMx real-time PCR system (Agilent Technologies, Santa Clara, CA, United States) with a master mix of KAPA SYBR®FAST qPCR master mix (Kapa Biosystems, Wilmington, MA, United States), 10 μM of forward and reverse primers (**Supplementary Table 1**), ROX dye, template cDNA and PCR-grade water for a final volume of 10 μL. All RT-qPCR assays were performed using three biological and three technical replicates. The expression profiles of *PpeSAUR50* (Prupe.3G035000), *PpeERF4* (Prupe.4G176200), *PpeERF5* (Prupe.5G062000), and *PpeXET* (Prupe.3G172000) were normalized to *PpeTEF2* (EST TC3544) (Tong et al., 2009).

RESULTS

Methylome Sequencing of Nectarine Fruits Contrasting for Mealiness

In order to determine the phenotypic parameters of mealiness, initially we used a V × V population of 151 siblings that was previously phenotyped during 2012, 2013, and 2014 for firmness, soluble solids contents, titratable acidity, weight and I_{AD} at E1 stage (Nuñez-Lillo et al., 2015). During these seasons, the average juiciness was 32.6%, ranging between 15 and 51% and obtaining a unimodal distribution. Afterward, during season 2016–2017, the same phenotypic parameters were measured, showing no significant differences for firmness, I_{AD} and soluble solids content (Lillo-Carmona et al., 2020). Moreover, juiciness ranged from 21,56% in mealy fruits, to 52.68% in normal fruits.

For the present study, we used the same two contrasting siblings from season 2016 to 2017 phenotyped by Lillo-Carmona et al. (2020) since they showed a consistent phenotype for mealiness during at least two seasons. For flesh juiciness, fruits showing a 30% or less of juice content were considered as mealy, obtaining fruits with a normal juice content (∼44.5%) during four seasons (2012–2013; 2013–2014; 2016–2017, and 2017–2018) and mealy fruits during three seasons (2013–2014; 2016–2017, and 2017–2018), showing a variable phenotype (**Figure 1B**).

Afterward, normal and mealy fruits were sequenced at E1 and E3 stages to analyze the methylation profiles that could be associated with the phenotype (**Table 1**). From total bisulfite reads, at least a 53.4% mapped uniquely to the *Prunus persica* v2.0 genome, whereas 17.2% reads showed no alignment. From uniquely mapped reads, approximately a 71.2% of cytosines were

methylated in the CpG context, followed by a 52.8% in the CHG context and a 12.6% in the CHH context, with no significant differences between conditions (**Figure 1C**; **Supplementary Table 2**). At the same time, to analyze the bisulfite conversion rate, we mapped bisulfite reads to the chloroplast genome of peach, obtaining at least a 99.3% of conversion rate (**Supplementary Table 3**). To analyze the variability of global methylations, we conducted a PCA (**Supplementary Figure 2**). Despite PCA explains only a 25% of variability in DNA methylations, normal fruits at E1 and E3 are well separated from mealy fruits at the same conditions.

When studying the methylation level within the eight chromosomes of peach, we observed that highest levels of methylation are associated with the average location of centromeres. Differences between mealy and normal fruits were present in Chr1 with increased methylation in mealy fruits and Chr2 with increased methylation at 6,081,175 bp in normal fruits. Additionally, Chr4 showed higher methylation levels in mealy fruits, whereas Chr8 possess regions with higher methylation in mealy fruits and others with higher methylation in normal fruits (**Figure 2A**). Furthermore, methylation differences within Chr4 were mostly contributed to CHG and CHH cytosine contexts, which also co-localized with previously reported QTLs for mealiness (**Figure 2B**) (Cantín et al., 2010; Nuñez-Lillo et al., 2015, 2019).

The candidate genes contained within these QTLs located in Chr4 and Chr5 are shown in **Table 2**. From these genes, those that presented DMRs between mealy and normal fruits at E1 are associated with gibberellin biosynthesis, with an increase of 45.9% in the methylation level of mealy fruits, signal transduction with an increase of 9.9%, protein transport with an increase of 4.9% and cell wall modification with a decrease of −13.7%. At E3, differences in methylation levels includes a gene related with carbohydrate transport, showing an increase of 46.6% in mealy fruits, genes related with protein phosphorylation (−24.8%) and iron ion binding (−10.8%) (**Table 2**).

Annotation and Identification of Differentially Methylated Regions in Normal and Mealy Fruits at E1 and E3 Stages

To evaluate the distribution of methylations in all the annotated genes of *P. persica* (n = 26,873 genes), we obtained the methylation pattern within coding regions, including 2-kb upstream and 2-kb downstream (**Figures 3A,B**). For the CG context, methylation levels are higher upstream and downstream the transcribed regions, but with lower levels within TSS (transcription start site) and TES (transcription end site). Normal fruits showed a higher level of methylation than mealy fruits, however, all samples decreased their methylation when exposed to cold (E3 stage). On the contrary, for transposable elements (TE), CG methylations are higher within the TE rather than upstream and/or downstream. In the CHG context, methylation level is higher in upstream and downstream regions, maintaining low levels within transcribed regions. In the same context, TEs showed high levels of methylation, with a similar profile than CG methylations. In the CHH context, low levels of methylation are observed within the transcribed regions of genes, while high levels are present upstream and downstream. Regarding TEs, high levels of CHH methylation are observed within TE, but higher levels are present in mealy fruits at E1 and E3 stages when compared to normal fruits.

For the identification of DMRs, we considered the bisulfite conversion rate of each sample and a p-value < 0.05 for binominal test. When studying normal fruits at E3 vs. E1, we observed a similar amount of hypermethylated and hypomethylated regions, with most DMRs occurring in CHH context (**Figure 3C**). However, in mealy fruits at E3 vs. E1, CHH methylation showed higher number of hypermethylations (n = 218 DMRs) when compared to hypomethylations (n = 119 DMRs). When comparing mealy fruits vs. normal fruits at E1, we observed that differences in methylation mainly occurred in the CHH context with 274 hypermethylations and 167

TABLE 1 | Parameters of *Prunus persica* whole genome bisulfite sequencing and mapping of each sample and condition.

Sample	Sequence pairs analyzed	Uniquely mapped reads	Multiple mapped reads	Reads with no alignments	Genome coverage
Normal fruit at E1 R1	29,593,511	15,855,721	8,087,885	5,649,905	7X
Normal fruit at E1 R2	27,418,488	14,642,251	8,066,107	4,710,130	7X
Normal fruit at E1 R3	32,698,148	17,503,344	9,179,958	6,014,846	8X
Normal fruit at E3 R1	29,572,246	15,849,712	8,165,217	5,557,317	7X
Normal fruit at E3 R2	37,201,194	19,621,951	11,453,156	6,126,087	9X
Normal fruit at E3 R3	39,364,014	20,005,394	13,327,321	6,031,299	9X
Mealy fruit at E1 R1	30,242,762	15,788,636	8,575,159	5,878,967	7X
Mealy fruit at E1 R2	29,659,178	15,381,741	8,749,903	5,527,534	7X
Mealy fruit at E1 R3	32,770,016	15,350,153	11,278,650	6,141,213	7X
Mealy fruit at E3 R1	43,879,328	24,399,996	13,014,693	6,464,639	11X
Mealy fruit at E3 R2	36,227,923	19,872,745	10,317,302	6,037,876	9X
Mealy fruit at E3 R3	35,383,415	18,463,308	11,327,215	5,592,892	8X

From the total sequence pairs analyzed, the number of uniquely mapped reads, multiple mapped reads and reads with no alignment was obtained. Genome coverage was estimated using a genome size of 225.7 Mb and considering only the uniquely mapped reads. Three biological replicates (R1, R2, and R3) were considered as three independent fruits per condition.

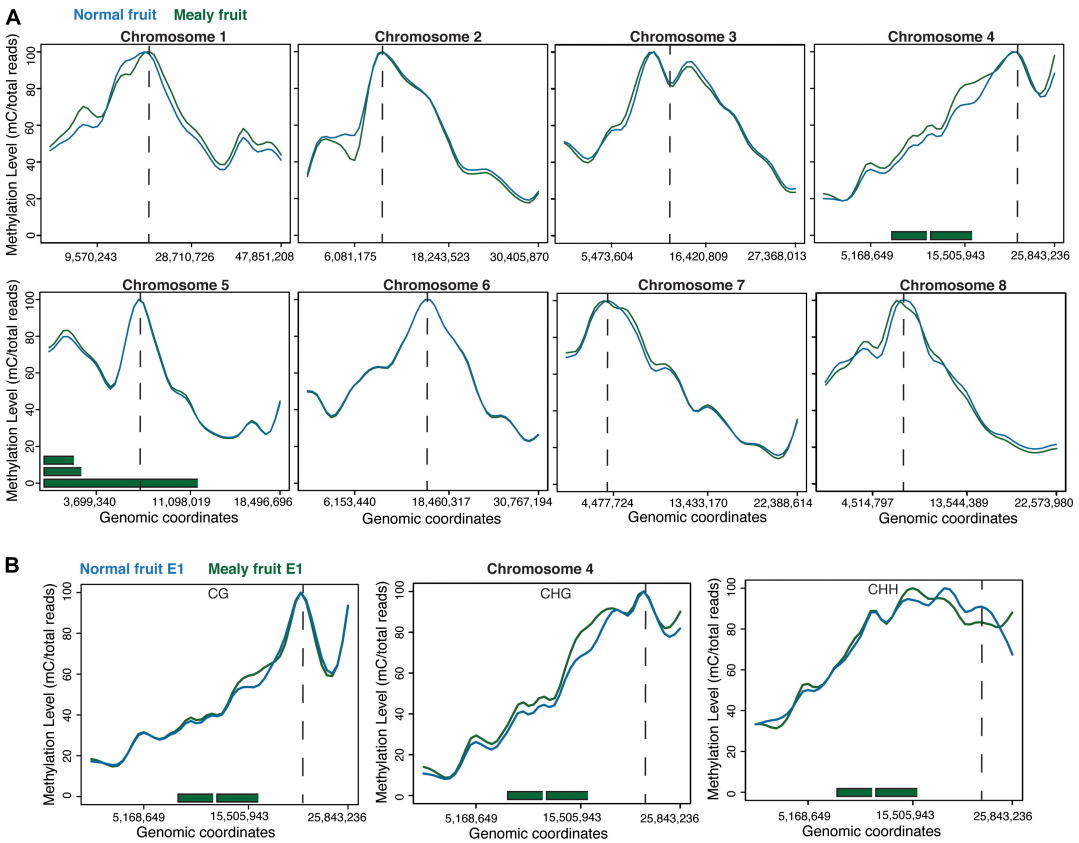

FIGURE 2 | DNA methylation levels across the eight pseudomolecules of *P. Persica.* **(A)** Methylation levels considering all cytosine contexts in normal fruits (blue line) and mealy fruits (green line). Horizontal green bars represent the location of previously identified QTLs for mealiness, while dashed vertical lines indicates the approximate location of centromeres. **(B)** Methylation levels in CpG, CHG, and CHH contexts within chromosome 4, the main candidate associated with mealiness phenotype based on QTL studies.

TABLE 2 | Genes that co-localized with QTLs for mealiness within chromosomes 4 and 5 and presented differentially methylated regions (DMRs) between mealy and normal fruits at E1 and E3 stages.

Stage	Gene ID	Description	Pathway	Methylation difference (%)	Location
E1	Prupe.4G128700	*ENT-KAURENE SYNTHASE*	Gibberellin biosynthesis	45.9	Intron
	Prupe.4G241500	*Mitochondrial import inner membrane translocase TIM50*	Protein transport	4.9	Downstream
	Prupe.5G074600	*Disease resistance protein-related*	Signal transduction	9.9	Upstream
	Prupe.5G069600	*PECTINESTERASE 68-RELATED*	Cell wall modification	−13.7	Intron
E3	Prupe.4G155700	*Bidirectional sugar transporter SWEET2*	Carbohydrate transport	46.6	Upstream
	Prupe.4G195300	*G-type lectin S-receptor-like serine*	Protein phosphorylation	−24.8	3′ UTR
	Prupe.5G077800	*CYTOCHROME P450-LIKE PROTEIN RELATED*	Iron ion binding	−10.8	Intron

The methylation difference indicates an increase (positive) or decrease (negative) of methylation percentage in mealy fruits regarding to normal fruits.

hypomethylations in mealy fruits. Additionally, at E3, the number of hypermethylations in mealy fruits increased to 335 DMRs, while hypomethylations are maintained in 164 DMRs (**Figure 3C**). The annotation, methylation differences and description of each DMR in all cytosine contexts from normal fruits at E3 vs. E1, mealy fruits at E3 vs. E1, mealy fruits vs. normal fruits at E1 and E3 are detailed in **Supplementary Tables 4–7**, respectively.

From annotated DMRs, our interest was focused on which locations are more susceptible to change their methylation level. We observed that in normal fruits at E3, differences in methylation occurred upstream ($n =$ 11 DMRs) of genes (**Figure 4A**), while in mealy fruits the number of DMRs is higher upstream ($n =$ 16 DMRs) and downstream ($n =$ 22 DMRs) of genes (**Figure 4B**). On the other hand, in mealy fruits vs. normal fruits, the number of DMRs located upstream of genes increased from 37 DMRs at E1, to 46 DMRs at E3 (**Figures 4C,D**).

To better understand which pathways may be affected by these changes in DNA methylation, we performed a GO analysis of the annotated DMRs between mealy and normal fruits

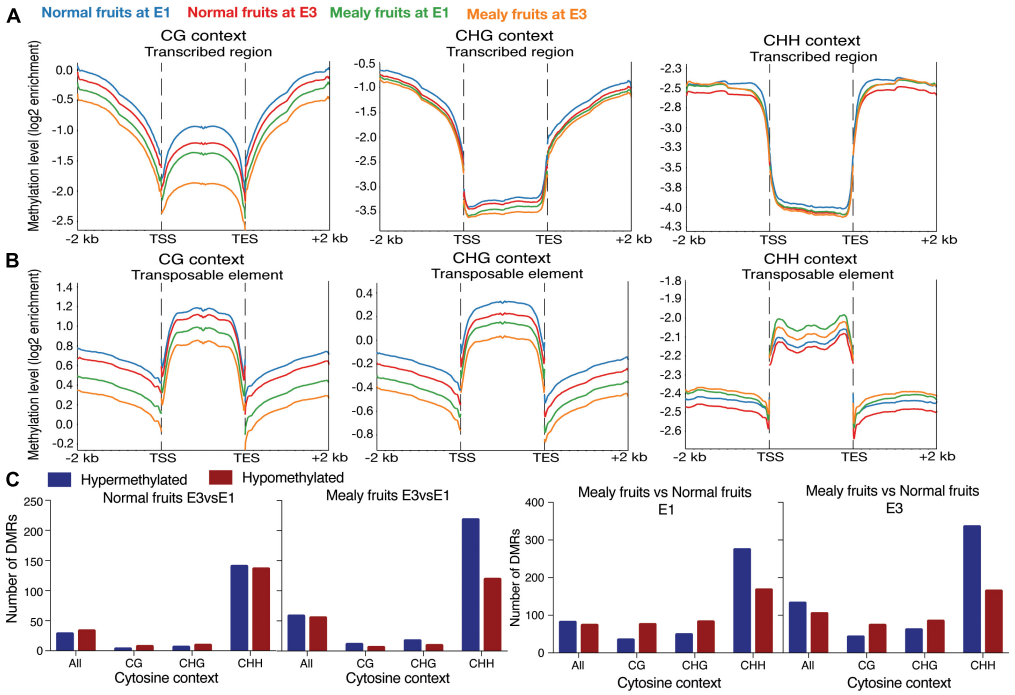

FIGURE 3 | Average distribution of global DNA methylation throughout coding regions and number of differentially methylated regions. **(A)** DNA methylation level in annotated genes, including 2 kb upstream and downstream of the transcription start site (TSS) and transcription end site (TES), respectively. Each color represents a different condition. **(B)** DNA methylation level in annotated transposable elements (TE), including 2 kb upstream and downstream of TSS and TES. **(C)** Number of Differentially Methylated Regions (DMRs) close to annotated genes (up to 2 kb upstream and downstream) in normal fruits at E3 vs. E1 stages, mealy fruits at E3 vs. E1, mealy fruits vs. normal fruits at E1 and mealy fruits vs. normal fruits at E3. Blue bars indicate hypermethylated regions and red bars hypomethylated regions. DMRs where considered in all cytosine contexts and individual contexts (CpG, CHG, and CHH). Three biological replicates, a log2 enrichment difference >1 and a *p*-value < 0.05 were considered to identify a DMR.

(**Table 3**), where overrepresented molecular functions affected in mealy fruits corresponded to "ATP binding" and "purine nucleotide binding" at E1. At E3 stage, we observed an increase in overrepresented terms, where a higher frequency was obtained in "catalytic activity" with a 65.83%, "ATP binding" with 14.13% and "purine nucleotide binding" with 16.11%.

Transcriptome Sequencing and Identification of Differentially Expressed Genes in Normal and Mealy Fruits

In order to elucidate the transcriptional changes associated with the pattern of DNA methylations in response to chilling injury or mealiness, we analyzed RNA-Seq libraries from the same samples as MethylC-Seq (**Table 4**). Using samples from normal and mealy fruits at E1 and E3 stages, we obtained a 78–95% of uniquely mapped reads, 1.5–5.5% of reads that aligned in multiple regions and 1.5–19.6% of reads that did not align to the reference of *P. persica* genome v2.0. Considering only the reads that aligned uniquely, we followed further analysis.

To visualize the distribution of global transcriptomic data, we used a PCA (**Figure 5A**). In this case, all the conditions (normal fruit at E1, normal fruit at E3, mealy fruit at E1, and mealy fruit at E3) are well separated, while biological replicates grouped together, explaining a 92% of variability. For the identification of DEGs, we first considered normal and mealy fruits at E3 regarding to E1, and additionally compared mealy fruits vs. normal fruits at E1 and E3 (**Figure 5B**). For the first comparison, we obtained a higher number of downregulated genes ($n =$ 3,436 DEGs) in normal fruits and in mealy fruits ($n =$ 3,704 DEGs) at E3. However, when comparing mealy fruits vs. normal fruits, we observed a decreased number of DEGs, where most of them are overexpressed in mealy fruits at E1 ($n =$ 966 DEGs), increasing toward E3 ($n =$ 1,276 DEGs). The annotation and transcript level of each DEG is detailed in **Supplementary Tables 8–11**.

Afterward, we ranked the top 50 DEGs with higher variance between normal and mealy fruits (**Figure 5C**). Genes that showed an increased expression in mealy fruits at E1 includes *ETHYLENE-RESPONSIVE TRANSCRIPTION FACTORS* (*ERFs*) 109 and 017, a cold acclimation gene *DREB1D*, defense genes *BON1* and *WRKY70*, and a cell wall gene *GALACTURONOSYLTRANSFERASE-like 10.* Another group of genes that showed an increased expression only in mealy fruits at E3 considers a lipid transport gene *LTPG1,* cell wall genes *XYLOGLUCAN XTH8* and a probable *POLYGALACTURONASE,* whereas a ROS scavenging gene *L-ASCORBATE PEROXIDASE APX2* was highly expressed both at E1 and E3 in mealy fruits. Genes that showed a decreased expression only in mealy fruits at E1 and E3 are *ERF1B,* a *CELL WALL-ASSOCIATED RECEPTOR*

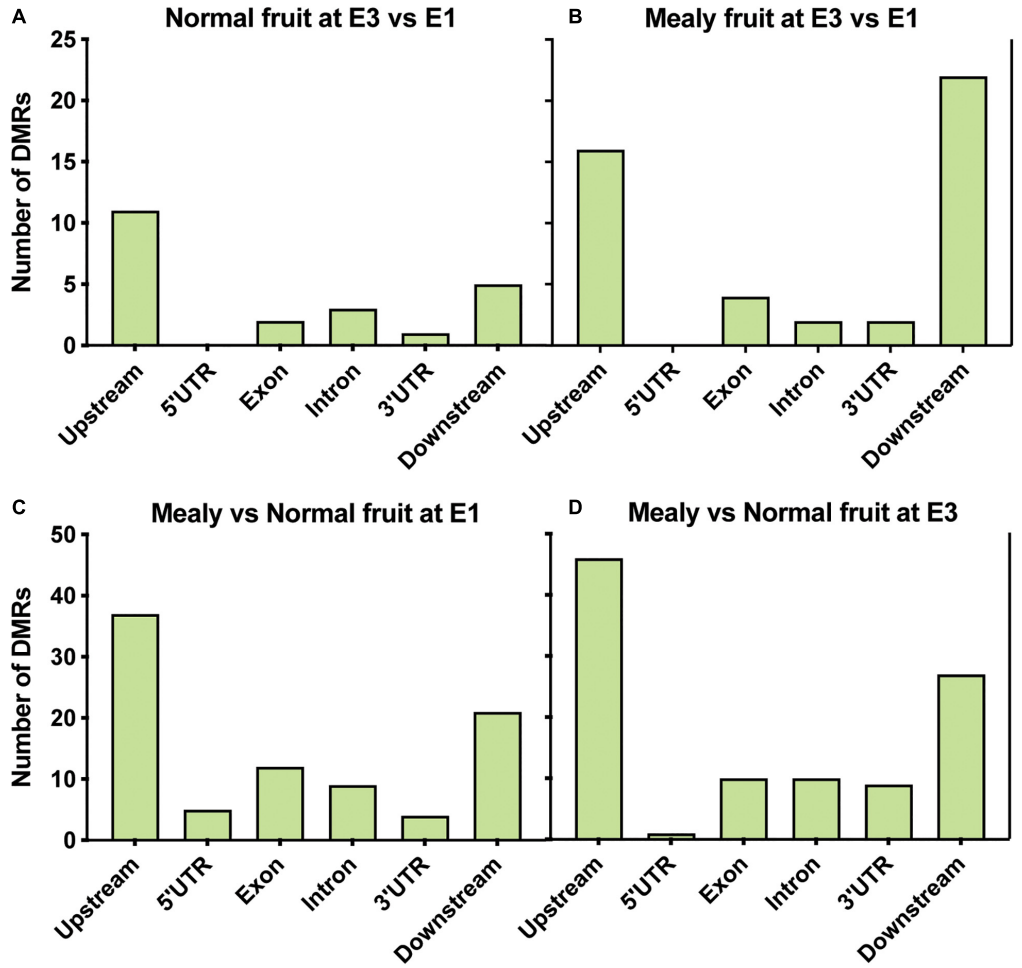

FIGURE 4 | Location of DMRs within annotated genes of *P. persica*. Number of DMRs located upstream (up to 2 kb), 5' UTR, exons, introns, 3′ UTR, and downstream (up to 2 kb) of annotated genes in samples from **(A)** normal fruits at E3 vs. E1 **(B)** mealy fruits at E3 vs. E1 **(C)** mealy vs. normal fruits at E1, and **(D)** mealy vs. normal fruits at E3.

KINASE 2 WAK2, a *UDP-GLYCOSYLTRANSFERASE*, a *GDSL esterase/lipase* and a *O-ACYLTRANSFERASE WSD1* gene from the lipid metabolism, an *ARG7-like* gene associated with auxin and cold response, and a *CYTOCHROME P450 82A3* (*CYP82A3*) gene involved in sideretin biosynthesis in response to iron deficiency.

Additionally, in order to validate RNA-Seq data, we studied with real-time qPCR analysis the expression level of *PpeSAUR50*, *PpeERF5, PpeERF4*, and *PpeXET*, which were differentially expressed from RNA-Seq data between normal and mealy fruits (**Supplementary Figure 2**). The expression level of the four genes was similar between RNA-Seq and qPCR, showing differences between normal and mealy fruits.

Integration of Methylomic and Transcriptomic Data

For the integration of both methylation and transcriptomic data, we further studied only DMRs that co-localized with DEGs between normal and mealy fruits. At E1, hypermethylated genes that decreased their expression in mealy fruits correspond to a *THREONINE-tRNA LIGASE* and the recently mentioned *CYP82A3* (**Figure 6A**). On the contrary, hypomethylated genes

TABLE 3 | Gene Ontology (GO) analysis of annotated genes associated with DMRs from mealy fruits vs. normal fruits at E1 and E3 stages.

Stage	Molecular function	Frequency	Term ID
E1	ATP binding	14.13%	GO:0005524
	Purine nucleotide binding	16.11%	GO:0017076
E3	Structural constituent of ribosome	2.68%	GO:0003735
	Catalytic activity	65.83%	GO:0003824
	Structural molecule activity	3.27%	GO:0005198
	ATP binding	14.13%	GO:0005524
	Ligase activity	3.54%	GO:0016874
	Purine nucleotide binding	16.11%	GO:0017076

The columns show the overrepresented molecular functions, their frequency in each stage and the associated identity.

that increased their expression in mealy fruits involves a *CELLULOSE SYNTHASE-LIKE PROTEIN E6* and a probable *GLUCOSE TRANSPORTER 3*. Regarding to *CYP82A3*, the gene viewer of DNA methylations in mealy fruits at E1 and E3 revealed an hypermethylation across the entire gene located within the anti-sense strand. Furthermore, this hypermethylation is associated with the silencing of *CYP82A3* and with the presence of a TE within the sense strand (**Figure 6B**). Additional hypermethylated genes at E3 that decreased their expression in mealy fruits includes an *UDP-ARABINOSE 4-EPIMERASE 1*, *FRIGIDA-like PROTEIN 3*, a *REGULATOR OF TELOMERE ELONGATION HELICASE 1*, and a *TMV RESISTANCE PROTEIN N* (**Figure 6C**). The methylation profile of *UDP-ARABINOSE 4-EPIMERASE 1* also shows an hypermethylation upstream the gene, only in mealy fruits, which co-localized with a TE that may affect this pattern (**Figure 6D**).

Regarding to the higher methylation levels observed in mealy fruits, we further wanted to know if DNA methyltransferases and DNA demethylases changed their expression level in fruits susceptible to mealiness. For this, we searched for *Arabidopsis thaliana* orthologous genes within the *P. Persica* genome. Four putative DNA methyltransferases were identified in peach, one *METHYLTRANSFERASE 1* (*MET1*), one *CHROMOMETHYLTRANSFERASE 3* (*CMT3*) and two *DOMAINS REARRANGED METHYLTRANSFERASE 2* (*DRM2*). Regarding to DNA demethylases, we identified one *REPRESSOR OF SILENCING 1* (*ROS1*), one *TRANSCRIPTIONAL ACTIVATOR DEMETER* (*DME*) and one *DEMETER-like 2* (*DML2*). The expression profile of each gene is shown in **Figure 7**. For the expression level of DNA methyltransferases, in general all of them decrease their expression after cold storage, however, only *DRM2.2* shows significant differences between mealy and normal fruits, where mealy fruits presented a lower expression of *DRM2.2* (**Figure 7A**). On the other hand, DNA demethylases *ROS1* and *DME* showed a significant downregulation in mealy fruits at E3 (**Figure 7B**).

DISCUSSION

The Methylome of *P. persica* Fruits Reveals Epigenomic Differences Between Normal and Mealy Fruits Associated With Genetic Variance

Mealiness is a texture disorder characterized by the lack of juice from the flesh. In this study, we used samples from season 2016 to 2017, where no significant differences were obtained in firmness, I_{AD} and soluble solids (Lillo-Carmona et al., 2020). However, for fruit juiciness mealy fruits presented a 21.56% of juice and normal fruits a 52.68%, coincident with this textural disorder. Although mealiness is mostly influenced by the genetic background and maturation stage of the fruit, there is also an environmental factor that causes seasonal variability within the phenotype (Campos-Vargas et al., 2006), reason why a tree can produce mealy or normal fruits according to the season, as observed in **Figure 1B**. In fact, the contribution of the environmental effect over mealiness variance has been estimated between 36.5 and 57.5% in biparental populations of peach, coinciding with correlation values between seasons (Peace et al., 2005; Cantín et al., 2010; Nuñez-Lillo et al., 2015). Together with this, PCA results explained a 25% of variability in DNA methylations between normal and mealy fruits, indicating that most differences in global DNA methylation are due to genetic differences between siblings and to a lesser extend due to cold temperatures.

The methylome of nectarine fruits, obtained from two individuals with contrasting susceptibility to mealiness, was studied through MethylC-Seq before cold storage (E1 stage) and after 30 days at 0 °C (E3 stage). From methylome results, both in normal and mealy fruits, cytosine methylation was higher in the CpG context, followed by CHG and CHH, coinciding with previous methylome studies of *Arabidopsis thaliana*, apple (*Malus domestica borkh.*), *Populus euphratica* and sweet cherry (*Prunus avium* L.), showing that different pathways regulate DNA methylation (Lister et al., 2008; Daccord et al., 2017; Su et al., 2018; Rothkegel et al., 2020).

TABLE 4 | Parameters of *Prunus persica* transcriptome sequencing (RNA-Seq) and mapping of each sample and condition.

Sample	Processed reads	Uniquely mapped reads	Multiple mapped reads	Reads with no alignments	GC (%)
Normal fruit at E1 R1	26,432,188	22,634,900	703,271	3,094,017	47
Normal fruit at E1 R2	36,943,878	28,957,820	726,711	7,259,347	48
Normal fruit at E1 R3	32,478,417	26,966,410	635,225	4,876,782	48
Normal fruit at E3 R1	26,658,213	24,597,488	1,145,517	915,208	47
Normal fruit at E3 R2	20,609,623	19,335,278	840,540	433,805	46
Normal fruit at E3 R3	29,430,088	26,858,876	1,277,757	1,293,455	47
Mealy fruit at E1 R1	24,835,025	20,663,761	381,677	3,789,587	48
Mealy fruit at E1 R2	30,053,367	28,573,366	572,053	907,948	47
Mealy fruit at E1 R3	29,446,889	27,909,819	526,394	1,010,676	47
Mealy fruit at E3 R1	76,758,936	70,198,217	3,842,565	2,718,154	46
Mealy fruit at E3 R2	83,076,369	77,232,835	4,515,452	1,328,082	46
Mealy fruit at E3 R3	104,224,838	92,005,533	5,829,593	6,389,712	47

Three biological replicates were considered as three independent fruits.

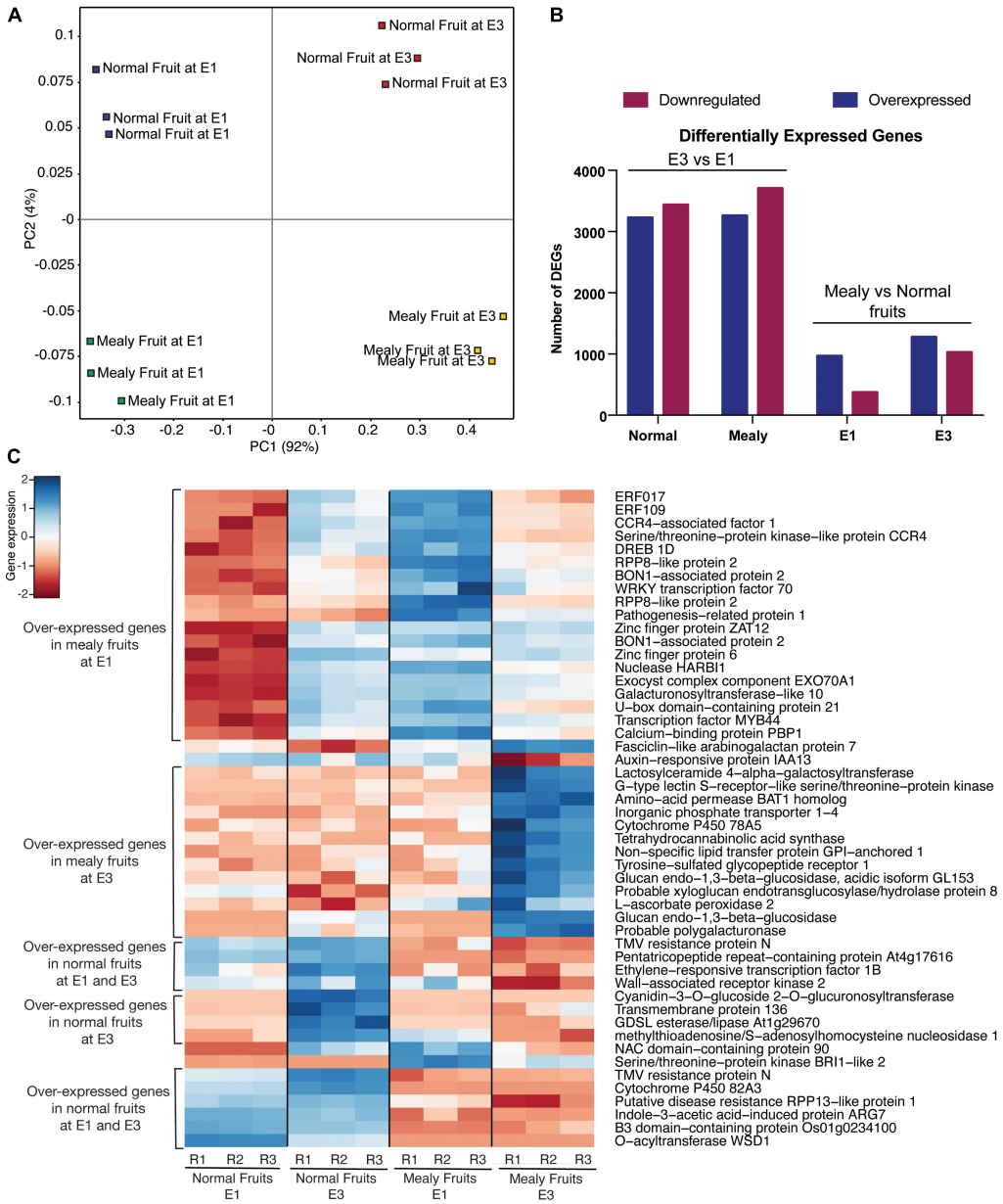

FIGURE 5 | Transcriptomic profile of *P.persica* fruits susceptible and resistant to mealiness. **(A)** Principal Component Analysis (PCA) of global gene expression in normal (resistant) and susceptible fruits at E1 and E3. **(B)** Number of differentially expressed genes (DEGs) at E3 vs. E1, and in mealy vs. normal fruits. **(C)** Heatmap of the top 50 DEGs with higher variance in their transcript level between normal fruits and mealy fruits. Color key indicates the median log2 TMM-normalized values, where red to blue represents low to high levels of transcript, respectively.

At the chromosome level, regions with higher methylation indicate the approximate location of centromeres, which are mainly comprised by TEs and repetitive elements (Verde et al., 2013). Therefore, methylation in all cytosine context is higher in pericentromeric heterochromatin (Lister et al., 2008). Additionally, differences in methylation between mealy and normal fruits within Chr1, Chr2, Ch4, and Chr8 could be attributed to the genetic variance and polymorphisms between individuals, affecting the methylation pattern. For instance, higher methylation levels within Chr4 of mealy fruits are close to pericentromeric heterochromatin and also co-localized with previously identified QTLs for mealiness, confirming genetic variability (Nuñez-Lillo et al., 2015).

Candidate genes for mealiness comprised within QTLs (Nuñez-Lillo et al., 2015; Nuñez-Lillo et al., 2019), also presented DMRs between mealy and normal fruits. At E1 stage, an increase in methylation of mealy fruits was observed in *ENT-KAURENE SYNTHASE*, a gene involved in gibberellin biosynthesis, a plant growth phytohormone suggested to reduce mealiness in nectarine fruits when applied exogenously

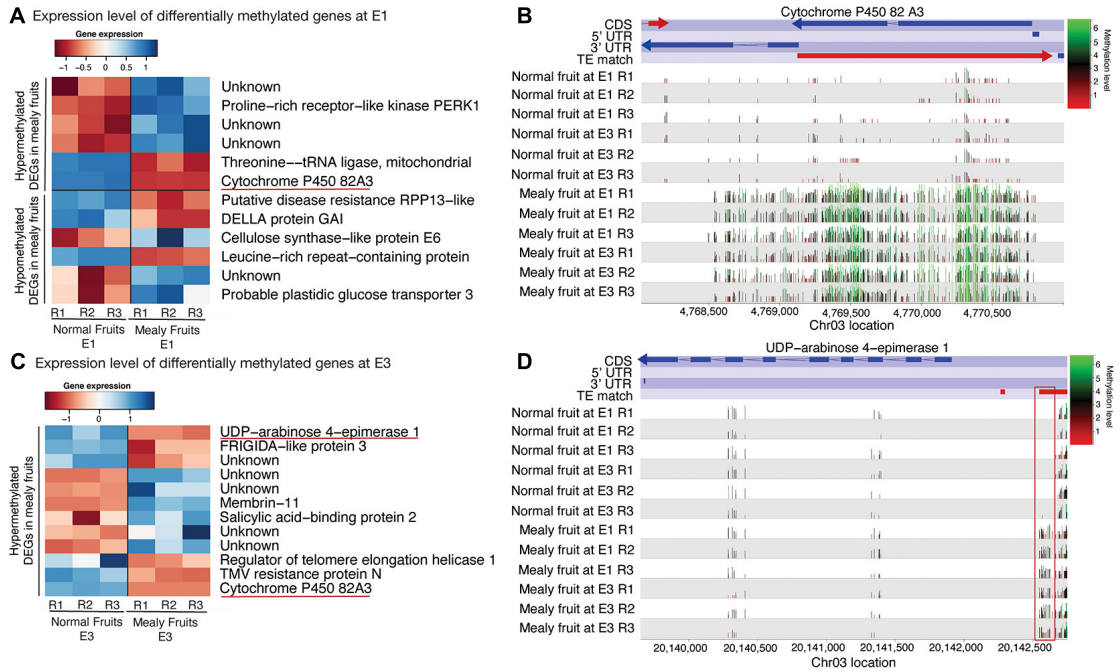

FIGURE 6 | Differentially expressed genes between normal and mealy fruits associated with changes in DNA methylation. **(A)** Expression levels of DEGs overlapping with DMRs between normal and mealy fruits at E1. DEGs are grouped as hypermethylated and hypomethylated. **(B)** Cytosine methylation level of a hypermethylated region in mealy fruits compared to normal fruits. The DMR of approximately 2.500 bp is located within the coding region of a *CYP450* 82A3 (Prupe.3G066200) gene. Color key indicates methylation levels where green represents high levels and red, low levels. **(C)** Expression levels of DEGs overlapping with hypermethylated regions between normal and mealy fruits at E3. **(D)** DNA methylation level of a hypermethylated region in mealy fruits compared to normal fruits. The DMR of approximately 120 bp is located in the promoter region of an *UDP-ARABINOSE 4-EPIMERASE1* (Prupe.3G187800) gene.

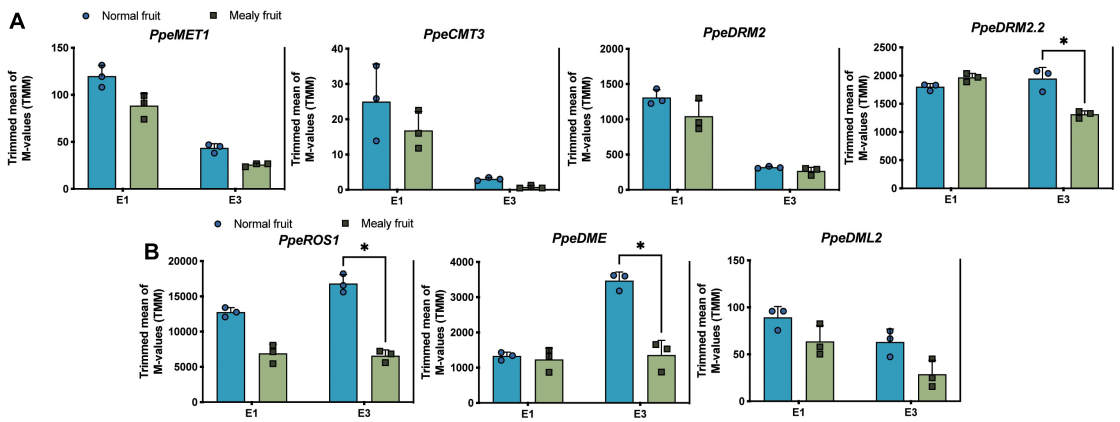

FIGURE 7 | Expression levels of four putative DNA methyltransferases and three 5-mC glycosylases in normal and mealy *P.persica* fruits. Transcript levels of **(A)** methyltransferases *MET1* (Prupe.7G183100), *CMT3* (Prupe.6G011600), *DRM2* (Prupe.8G038800), and *DRM2.2* (Prupe.6G322700). **(B)** Transcript levels of 5-mC glycosylases *ROS1* (Prupe.7G118000), *DME* (Prupe.7G005000), and *DML2* (Prupe.6G119100). Transcripts were analyzed by RNA-Seq using three biological replicates. Asterisks represent significant differences (p-value ≤ 0.05) between normal and mealy fruits using a Two-Way ANOVA test. Error bars represent standard deviation (SD).

(Lurie and Crisosto, 2005; Pegoraro et al., 2015). On the other hand, a gene showing a decrease of methylation in mealy fruits is *PECTINESTERASE 68*, a gene involved with cell wall metabolism. In this case, an alteration in the activity of polygalacturonases and pectinesterases can lead to the accumulation of gel-forming pectic compounds in the apoplast, retaining free water and resulting in mealy texture (Lurie et al., 2003; Brummell et al., 2004).

At E3 stage, the sugar transporter *SWEET2* presented increased methylation levels in mealy fruits, which could be associated with cold storage. Although the accumulation of sugars in peach fruits is an important trait for consumers, they

also play an important role for cold tolerance by acting as osmolytes and protecting cell membranes (Ding et al., 2019).

Distribution of Global DNA Methylation Patterns Is Related to Transposable Elements and Genetic Variance

The distribution and level of DNA methylation patterns are important factors for gene regulation and to avoid proliferation of TEs. For instance, gene body methylation is associated with CpG context and usually occurs within exons, but not in TSS and TES (Takuno and Gaut, 2013). According to the same study, methylated genes within their exons at CpG context, are constitutively expressed, however, CHG and CHH methylation tend to be lower within transcribed regions. Coincident with this, the methylation levels at CHG and CHH were lower within genes of peach, while methylation at CpG in transcribed regions was higher.

On the other hand, DNA methylation at gene promoters is associated with silencing by inhibiting the binding of transcription factors (Zhang et al., 2018). DNA methylation in non-coding regions can be consequence of nearby transposons and other repeats, which might be the case of peach, where methylation levels within TEs and neighbor regions is variable. Moreover, TEs respond to environmental stimuli. For example, in *A. thaliana* the repression of *VERNALIZATION INSENSITIVE 3* (*VIN3*) in the absence of cold is contributed by a TE located at the promoter region (Kim et al., 2010). In our study, the presence of TEs in mealy and normal fruits may generate a dynamic profile of DNA methylations between siblings, which in turn could alter gene regulation nearby. In fact, TEs represent a 29.6% of the peach genome, whereas a 7.54% of the genome are uncharacterized repeats (Verde et al., 2013).

The identification of DMRs between E3 and E1 stages in normal and mealy fruits showed that differences in the methylation level in response to cold storage occur mainly upstream and downstream of genes in CHH cytosines, being hypermethylated at E3 in both siblings, but with an increased number of DMRs in mealy fruits (**Figure 3C**). Several studies have indicated CHH methylation as a response to abiotic stress, suggesting a role for transient CHH methylation in response to environmental stimuli. For instance, during chilling accumulation in sweet cherry (*Prunus avium*), floral buds showed an increase in CHH methylation in genes associated with cold signaling, oxidation-reduction process, phenylpropanoid, and lipid metabolism (Rothkegel et al., 2020).

On the other hand, comparisons between mealy and normal fruits also showed hypermethylations of the CHH context in mealy fruits even before cold storage at E1, suggesting that genetic variance between siblings could result in increased DNA methylations in susceptible fruits. A GO analysis to identify which processes may be related with these DMRs in mealy fruits revealed molecular functions coincident with a metabolic response that is different in mealy fruits regarding to normal fruits. Regarding this, a previous proteomic analysis of peach fruits has showed that processes like ROS metabolism and cellular homeostasis are affected after cold storage (Nilo et al., 2010). In the same study, a decreased accumulation of catalases and ferritins was observed in cold stored fruits, suggesting an interaction between iron homeostasis and ROS levels.

Genes Associated With Ethylene Signaling, Cell Wall Modification, Lipid Metabolism, Oxidative Stress, and Iron Homeostasis Are Differentially Expressed in Mealy Fruits

Responses to low temperatures involve transcriptomic and metabolic reprogramming. At the transcriptomic level, PCA and the number of DEGs showed that gene expression is affected not only by the genotype of each individual, but also by the fruit condition (E1 and E3). Moreover, most DEGs were obtained between E1 and E3 rather than in mealy vs. normal fruits as observed in methylome data. This difference in gene expression may be due to an energetic reprogramming in order to establish a new metabolic homeostasis for acclimation under cold conditions, which is regulated by several factors, such as signaling pathways and transcription factors (Fürtauer et al., 2019).

Regarding overrepresented pathways, ethylene signaling is essential for a series of developmental processes, such as growth and senescence, and responses to abiotic and biotic stress. In peach, we identify the ethylene response factors *ERF109*, *ERF017*, and *DREB1D* with higher expression in mealy fruits at E1 stage when compared to E3, while *ERF1B* was downregulated at E1 and E3 (**Figure 8**), coincident with previous studies that suggested that CI is associated with a decreased ethylene production (Wang et al., 2017; Nilo-Poyanco et al., 2018).

Another determinant factor for the development of mealiness is the cell wall, where initial studies have found an association between mealiness and the altered activity of pectin methylesterases (PME) and endo-polygalacturonases during cold storage, resulting in higher levels of soluble pectins and mealy texture (Buescher and Furmanski, 1978; Ben-Arie and Sonego, 1980; Lurie et al., 1994). Concomitantly, in mealy fruits at E1 we identify a *GALACTURONOSYLTRANSFERASE-like 10* (*GAUT10*) showing higher expression (**Figure 8**). Afterward at E3, *XYLOGLUCAN XTH8* and a probable *POLYGALACTURONASE* (*PG*) presented an increased expression, while a *CELL WALL-ASSOCIATED RECEPTOR KINASE 2 WAK2* was downregulated, suggesting an altered cell wall metabolism during cold storage.

As one of the first barriers to the environment, the cell membrane is important to integrate the environmental signal into the cell. In the case of low temperatures, a decrease in membrane fluidity correlates with the proportion of desaturated fatty acids, affecting the metabolism of lipids (Martiniere et al., 2011). Moreover, in *A. thaliana*, the levels of polyunsaturated fatty acids are pivotal for survival to low temperatures (<12°C) (Miquel et al., 1993). In peach, we have found that *LTPG1*, associated with lipid transport, is overexpressed in mealy fruits after cold storage (**Figure 8**). While a *GDSL esterase/lipase* and a *O-ACYLTRANSFERASE WSD1* are downregulated in mealy fruits in both conditions, indicating that the lipid metabolism is differentially regulated probably due to the genetic background

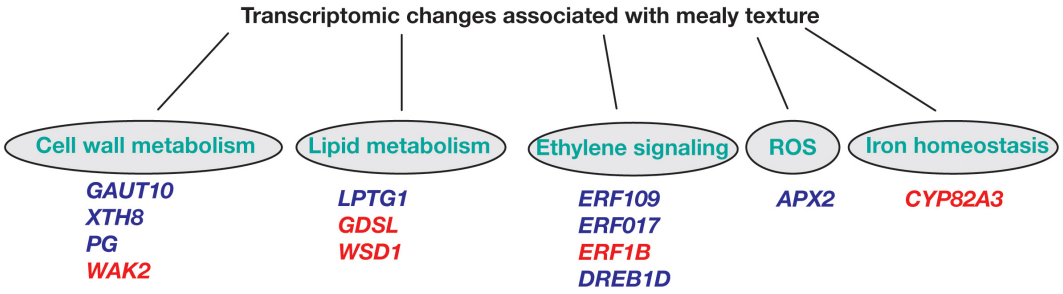

FIGURE 8 | Hypothetical scheme of differentially expressed genes between mealy and normal fruits associated to metabolic pathways leading to mealiness in *P. persica* fruits. Biological processes of cell wall metabolism, lipid metabolism, ethylene signaling, ROS (reactive oxygen species) and iron homeostasis are represented. Genes highlighted in blue are overexpressed, while red colored genes are downregulated in mealy fruits. *GAUT10: GALACTURONOSYLTRANSFERASE-like 10; XTH8: XYLOGLUCAN ENDOTRANSGLUCOSYLASE/HYDROLASE PROTEIN 8; PG: POLYGALACTURONASE; WAK2: WALL-ASSOCIATED RECEPTOR KINASE 2; LPTG1: NON-SPECIFIC LIPID TRANSFER PROTEIN GPI-ANCHORED 1; GDSL esterase/lipase; WSD1: O-ACYLTRANSFERASE; ERF: ETHYLENE-RESPONSIVE FACTOR; DREB1D: DEHYDRATION-RESPONSIVE ELEMENT BINDING 1D; APX2: L-ASCORBATE PEROXIDASE 2; CYP82A3: CYTOCHROME P450 82 A3.*

of each individual since these changes occurred before cold storage. In fact, a recent study using the same peach individuals has identified 119 metabolites and 189 lipids with significant differences in abundance between juicy and mealy fruits, where lipids were proposed as biomarkers for mealiness at E1 and E3 stages (Lillo-Carmona et al., 2020).

Regarding oxidative stress, the signaling of ROS is associated with biotic and abiotic responses. Usually, an abiotic stress like low temperatures increase the levels of ROS because of a lower stability of scavenging enzymes (Ding et al., 2019). Some of these scavenging enzymes correspond to superoxide dismutase, ascorbate peroxidase, catalase, and glutathione peroxidase (Müller and Munné-Bosch, 2015). In this study, we identify a *PEROXIDASE APX2* that is highly expressed in mealy fruits before and after cold storage (**Figure 8**), indicating that susceptible fruits might generate lower ROS levels and thus, a lower signal to induce a cold response.

The connection between ROS and iron homeostasis has also been reported, where hydrogen peroxide (H_2O_2) molecules react with Fe^{2+} to generate hydroxyl radicals, which attack pectin polysaccharides, decreasing mealiness susceptibility (Airianah et al., 2016; Choudhury et al., 2016). Furthermore, we have found that a *CYP82A3* gene associated with iron deficiency is silenced in mealy fruits (**Figure 8**) and thus, we hypothesize that low levels of Fe^{2+} due to *CYP82A3* silencing and low levels of ROS due to high *APX2* expression, could result in lower hydroxyl radicals, promoting a favorable environment for pectin accumulation and mealiness development.

The Downregulation of *CYP82A3* and *UDP-ARABINOSE 4* in Mealy Fruits Is Accompanied by Higher Methylation Levels and the Presence of a TE

The superfamily of CYTOCHROME P450 has an important role in promoting plant growth, development, and stress responses with detoxification pathways (Xu et al., 2015). Regarding development, CYP 450s are involved in several metabolic pathways, such as cytokinin and flavonoid biosynthesis, and iron deficiency (Kruse et al., 2008; Berim and Gang, 2013). As previously mentioned, we have found that a putative *CYP82A3* is not expressed in mealy fruits, which is associated with its hypermethylation. Moreover, this hypermethylation coincides with the localization of a TE in the opposite strand, suggesting that the presence of the TE might be responsible for an increase in methylation levels, affecting gene expression.

Another downregulated gene in mealy fruits is *UDP-ARABINODE 4*. L-arabinose (Ara) in plants is an important component of glycoproteins, flavonoids, signaling peptides and cell wall polysaccharides, participating in cell wall biosynthesis (Rautengarten et al., 2017). In this sense, an imbalance of Ara affects directly the composition of the cell wall and may also be involved in mealiness texture, where a decreased cell-to-cell adhesion causes cell separation instead of cell rupture during chewing (Brummell et al., 2004). In our study, the downregulation of *UDP-ARABINOSE 4 EPIMERASE 1* is associated with an increase in the methylation level upstream. The encoded protein catalyzes the 4-epimerization of UDP-$_D$-Xyl to UDP-$_L$-Ara (Burget et al., 2003), suggesting that the levels of xylose could also be affected in mealy fruits. Interestingly, this hypermethylation co-localized with a TE match, which may affect gene expression in a similar way than *CYP82A3*. Altogether, these results highlight that genetic variability due to TEs and repetitive elements results in increased DNA methylation levels in mealy fruits before cold storage, which could affect gene expression and tolerance during cold storage.

DNA Glycosylases Are Downregulated in Mealy Fruits, Contributing With an Increase in DNA Methylations

DNA methyltransferases and glycosylases are key factors for the establishment and maintenance of methylation patterns. Methylation in the CpG context is the most abundant and is maintained during DNA replication by DNA METHYLTRANSFERASE 1 (MET1) (Finnegan et al., 1996).

While methylation in the CHG context is maintained by a reinforcing loop involving CHROMOMETHYLASE 3 (CMT3) and histone marks (H3K9) (Du et al., 2012). Methylation in CHH occurs *de novo* and is maintained by DOMAINS REARRANGED METHYLTRANSFERASE 2 (DRM2), together with non-coding RNAs in a pathway known as RNA-directed DNA Methylation (RdDM) (Law and Jacobsen, 2010). In peach we have found four homologous to these DNA methyltransferases, *PpeMET1*, *PpeCMT3*, *PpeDRM2*, and *PpeDRM2.2*. The transcript levels for all these genes have shown a decrease in expression at E3 stage in normal and mealy fruits, indicating that the regulation of these genes is affected by low temperatures in peach fruits.

On the other hand, DNA demethylation involves the participation of glycosylases REPRESSOR OF SILENCING 1 (ROS1), DEMETER (DME) and DEMETER-like (DML), which act during DNA reparation through a process of base excision, removing methylated cytosines (Gong et al., 2002; Choi et al., 2002; Ortega-Galisteo et al., 2008). In peach, we have identified *PpeROS1, PpeDME*, and *PpeDML2*, whose expression increased after cold storage only in normal fruits, indicating a higher control of DNA methylations. On the contrary, mealy fruits were associated with higher levels of DNA methylations, possibly due to a lower expression of DNA glycosylases. These results are concomitant with the key role described for DNA demethylation during fruit ripening by Lang et al. (2017), where mutant tomato plants for a *ROS1* homolog gene failed to ripen because ripening genes were silenced by DNA methylations.

CONCLUSION

In conclusion, in this study we obtained different DNA methylation patterns between normal and mealy fruits, showing higher methylation levels in mealy fruits, particularly in the CHH context. Moreover, these differences in methylation appears to be mostly influenced by genetic differences between siblings (e.g., TEs and repetitive elements), coinciding with previous QTL studies. When integrating RNA-Seq data, we found that *CYP82A3* and *UDP-ARABINOSE 4 EPIMERASE 1* are downregulated in mealy fruits, coinciding with the presence of TEs, possibly affecting iron homeostasis and cell wall metabolism. From gene expression data, a lower expression of DNA glycosylases during cold storage could contribute with higher methylation levels in mealy fruits. Taken together, this study provides an additional layer of information to better understand the complex phenotype of mealiness. Moreover, the patterns of DNA methylation and expression levels of *CYP82A3* and *UDP-ARABINOSE 4* could be further studied as novel markers for their use, together with molecular markers, in order to support peach breeding programs.

DATA AVAILABILITY STATEMENT

The datasets presented in this study can be found in online repositories. The names of the repository/repositories and accession number(s) can be found below: https://www.ncbi.nlm.nih.gov/genbank/, PRJNA705001; PRJNA705416.

AUTHOR CONTRIBUTIONS

CM, RC-V, and KR designed the research. AE, AR, and VL-C conducted field work and phenotyping. KR generated MethylC-Seq libraries. AE and KR contributed with bioinformatic analysis of MethylC-Seq. DS contributed with RNA-seq and qPCR experiments, while AR, AE, and KR performed bioinformatic analysis of RNA-seq. CM conducted statistical analysis and KR wrote the original manuscript. KR, CM, VL-C, DS, and RC-V edited and reviewed the original manuscript. All authors read and approved the submitted version.

FUNDING

This study was funded by Fondo Nacional de Desarrollo Científico y Tecnológico (ANID-FONDECYT 1200804), a Ph.D. national grant (ANID-PFCHA/Doctorado Nacional 2017-21170365), and ANID-FONDECYT POSTDOCTORADO 2018-3180306.

ACKNOWLEDGMENTS

We want to thank INIA Rayentué for giving us access to the V x V segregant population from their fields.

SUPPLEMENTARY MATERIAL

The Supplementary Material for this article can be found online at: https://www.frontiersin.org/articles/10.3389/fpls.2021.684130/full#supplementary-material

REFERENCES

Airianah, O. B., Vreeburg, R. A. M., and Fry, S. C. (2016). Pectic polysaccharides are attacked by hydroxyl radicals in ripening fruit: evidence from a fluorescent fingerprinting method. *Ann. Bot.* 117, 441–455. doi: 10.1093/aob/mcv192

Ben-Arie, R., and Lavee, S. (1971). Pectic changes occurring in Elberta peaches suffering from woolly breakdown. *Phytochemistry* 10, 531–538. doi: 10.1016/S0031-9422(00)94693-4

Ben-Arie, R., and Sonego, L. (1980). Pectolytic enzyme activity involved in woolly breakdown of stored peaches. *Phytochemistry* 19, 2553–2555. doi: 10.1016/S0031-9422(00)83917-5

Berim, A., and Gang, D. R. (2013). The roles of a flavone-6-hydroxylase and 7-O-demethylation in the flavone biosynthetic network of sweet basil. *J. Biol. Chem.* 288, 1795–1805. doi: 10.1074/jbc.M112.420448

Brummell, D. A., Dal Cin, V., Lurie, S., Crisosto, C. H., and Labavitch, J. M. (2004). Cell wall metabolism during the development of chilling injury in cold-stored peach fruit: association of mealiness with arrested disassembly of cell wall pectins. *J. Exp. Bot.* 55, 2041–2052. doi: 10.1093/jxb/erh228

Buescher, R. W., and Furmanski, R. J. (1978). Role of pectinesterase and polygalacturonase in the formation of woolliness in peaches. *J. Food Sci.* 43, 264–266. doi: 10.1111/j.1365-2621.1978.tb09788.x

Burget, E. G., Verma, R., Mølhøj, M., and Reiter, W. D. (2003). The biosynthesis of L-Arabinose in plants. *Plant Cell* 15, 523–531. doi: 10.1105/tpc.008425

Campos-Vargas, R., Becerra, O., Baeza-Yates, R., Cambiazo, V., González, M., Meisel, L., et al. (2006). Seasonal variation in the development of chilling injury in 'O'Henry' peaches. *Sci. Hortic.* 110, 79–83. doi: 10.1016/j.scienta.2006.06.019

Cantín, C. M., Crisosto, C. H., Ogundiwin, E. A., Gradziel, T., Torrents, J., Moreno, M. A., et al. (2010). Chilling injury susceptibility in an intra-specific peach [*Prunus persica* (L.) Bastch] progeny. *Postharvest Biol. Technol.* 58, 79–87. doi: 10.1016/j.postharvbio.2010.06.002

Choi, Y., Gehring, M., Johnson, L., Hannon, M., Harada, J. J., Goldberg, R. B., et al. (2002). DEMETER, a DNA glycosylase domain protein, is required for endosperm gene imprinting and seed viability in *Arabidopsis*. *Cell* 110, 33–42. doi: 10.1016/s0092-8674(02)00807-3

Choudhury, F. K., Rivero, R. M., Blumwald, E., and Mittler, R. (2016). Reactive oxygen species, abiotic stress and stress combination. *Plant J.* 90, 856–867. doi: 10.1111/tpj.13299

Crisosto, C. H., Mitchell, F. G., and Ju, Z. G. (1999). Susceptibility to chilling injury of peach, nectarine, and plum cultivars grown in California. *HortScience* 34, 1116–1118. doi: 10.21273/HORTSCI.34.6.1116

Daccord, N., Celton, J. M., Linsmith, G., Becker, C., Choisne, N., Schijlen, E., et al. (2017). High-quality de novo assembly of the apple genome and methylome dynamics of early fruit development. *Nat. Genet.* 49, 1099–1106. doi: 10.1038/ng.3886

Ding, Y., Shi, Y., and Yang, S. (2019). Advances and challenges in uncovering cold tolerance regulatory mechanisms in plants. *New Phytol.* 222, 1690–1704. doi: 10.1111/nph.15696

Dobin, A., Davis, C. A., Schlesinger, F., Drenkow, J., Zaleski, C., Jha, S., et al. (2013). STAR: ultrafast universal RNA-seq aligner. *Bioinformatics* 29, 15–21. doi: 10.1093/bioinformatics/bts635

Du, J., Zhong, X., Bernatavichute, Y. V., Stroud, H., Feng, S., Caro, E., et al. (2012). Dual binding of chromomethylase domains to H3K9me2-containing nucleosomes directs DNA methylation in plants. *Cell* 151, 167–180. doi: 10.1016/j.cell.2012.07.034

Finnegan, E. J., Peacock, W. J., and Dennis, E. S. (1996). Reduced DNA methylation in *Arabidopsis thaliana* results in abnormal plant development. *Proc. Natl. Acad. Sci. U.S.A.* 93, 8449–8454. doi: 10.1073/pnas.93.16.8449

Fürtauer, L., Weiszmann, J., Weckwerth, W., and Nägele, T. (2019). Dynamics of plant metabolism during cold acclimation. *Int. J. Mol. Sci.* 20:5411. doi: 10.3390/ijms20215411

García-Gómez, B. E., Salazar, J. A., Nicolás-Almansa, M., Razi, M., Rubio, M., Ruiz, D., et al. (2021). Molecular bases of fruit quality in *Prunus* species: an integrated genomic, transcriptomic, and metabolic review with a breeding perspective. *Int. J. Mol. Sci.* 22, 333. doi: 10.3390/ijms22010333

Gong, Z., Morales-Ruiz, T., Ariza, R. R., Roldán-Arjona, T., David, L., and Zhu, J. K. (2002). ROS1, a repressor of transcriptional gene silencing in *Arabidopsis*, encodes a DNA glycosylase/lyase. *Cell* 111, 803–814. doi: 10.1016/S0092-8674(02)01133-9

Infante, R., Meneses, C., and Crisosto, C. H. (2009). Preconditioning treatment maintains taste characteristic perception of ripe 'September Sun' peach following cold storage. *Int. J. Food Sci. Technol.* 44, 1011–1016. doi: 10.1111/j.1365-2621.2008.01864.x

Kan, J., Wang, H., and Jin, C. (2011). Changes of reactive oxygen species and related enzymes in mitochondrial respiration during storage of harvested peach fruits. *Agric. Sci. China* 10, 149–158. doi: 10.1016/S1671-2927(11)60317-9

Kim, D. H., Zografos, B. R., and Sung, S. (2010). Vernalization-mediated VIN3 induction overcomes the LIKE-HETEROCHROMATIN PROTEIN1/POLYCOMB REPRESSION COMPLEX2-mediated epigenetic repression. *Plant Physiol.* 154, 949–957. doi: 10.1104/pp.110.161083

King, G. A., Henderson, K. G., and Lill, R. E. (1989). Ultrastructural changes in the nectarine cell wall accompanying ripening and storage in a chilling-resistant and chilling-sensitive cultivar. *N. Z. J. Crop Hortic. Sci.* 17, 337–344. doi: 10.1080/01140671.1989.10428054

Kishore, K., de Pretis, S., Lister, R., Morelli, M. J., Bianchi, V., Amati, B., et al. (2015). MethylPipe and compEpiTools: a suite of R packages for the integrative analysis of epigenomics data. *BMC Bioinformatics* 16:313. doi: 10.1186/s12859-015-0742-6

Krueger, F., and Andrews, S. R. (2011). Bismark: a flexible aligner and methylation caller for bisulfite-seq applications. *Bioinformatics* 27, 1571–1572. doi: 10.1093/bioinformatics/btr167

Kruse, T., Ho, K., Yoo, H. D., Johnson, T., Hippely, M., Park, J. H., et al. (2008). In planta biocatalysis screen of P450s identifies 8-methoxypsoralen as a substrate for the CYP82C subfamily, yielding original chemical structures. *Chem. Biol.* 15, 149–156. doi: 10.1016/j.chembiol.2008.01.008

Lang, Z., Wang, Y., Tang, K., Tang, D., Datsenka, T., Cheng, J., et al. (2017). Critical roles of DNA demethylation in the activation of ripening-induced genes and inhibition of ripening-repressed genes in tomato fruits. *Proc. Natl. Acad. Sci. U.S.A.* 114, E4511–E4519. doi: 10.1073/pnas.1705233114

Law, J. A., and Jacobsen, S. E. (2010). Establishing, maintaining and modifying DNA methylation patterns in plants and animals. *Nat. Rev. Genet.* 11, 204–220. doi: 10.1038/nrg2719

Lillo-Carmona, V., Espinoza, A., Rothkegel, K., Rubilar, M., Nilo-Poyanco, R., Pedreschi, R., et al. (2020). Identification of metabolite and lipid profiles in a segregating peach population associated with mealiness in *Prunus persica* (L.) Batsch. *Metabolites* 10:154. doi: 10.3390/metabo10040154

Lister, R., O'Malley, R. C., Tonti-Filippini, J., Gregory, B. D., Berry, C. C., Millar, A. H., et al. (2008). Highly integrated single-base resolution maps of the epigenome in *Arabidopsis*. *Cell* 133, 523–536. doi: 10.1016/j.cell.2008.03.029

Lurie, S., and Crisosto, C. H. (2005). Chilling injury in peach and nectarine. *Postharvest Biol. Technol.* 37, 195–208. doi: 10.1016/j.postharvbio.2005.04.012

Lurie, S., Levin, A., Greve, L. C., and Labavitch, J. M. (1994). Pectic polymer changes in nectarines during normal and abnormal ripening. *Phytochemistry* 36, 11–17. doi: 10.1016/S0031-9422(00)97003-1

Lurie, S., Zhou, H. W., Lers, A., Sonego, L., Alexandrov, S., and Shomer, I. (2003). Study of pectin esterase and changes in pectin methylation during normal and abnormal peach ripening. *Physiol. Plant* 119, 287–294. doi: 10.1034/j.1399-3054.2003.00178.x

Manning, K., Tör, M., Poole, M., Hong, Y., Thompson, A. J., King, G. J., et al. (2006). A naturally occurring epigenetic mutation in a gene encoding an SBP-box transcription factor inhibits tomato fruit ripening. *Nat. Genet.* 38, 948–952. doi: 10.1038/ng1841

Martiniere, A., Shvedunova, M., Thomson, A. J., Evans, N. H., Penfield, S., Runions, J., et al. (2011). Homeostasis of plasma membrane viscosity in fluctuating temperatures. *New Phytol.* 192, 328–337. doi: 10.1111/j.1469-8137.2011.03821.x

Meisel, L., Fonseca, B., González, S., Baeza-Yates, R., Cambiazo, V., Campos, R., et al. (2005). A rapid and efficient method for purifying high quality total RNA from peaches (*Prunus persica*) for functional genomics analyses. *Biol. Res.* 38, 83–88. doi: 10.4067/s0716-97602005000100010

Miquel, M., James, D. Jr., Dooner, H., and Browse, J. (1993). *Arabidopsis* requires polyunsaturated lipids for low-temperature survival. *Proc. Natl. Acad. Sci. U.S.A.* 90, 6208–6212. doi: 10.1073/pnas.90.13.6208

Monti, L. L., Bustamante, C. A., Budde, C. O., Gabilondo, J., Müller, G. L., Lara, M. V., et al. (2019). Metabolomic and proteomic profiling of Spring Lady peach fruit with contrasting woolliness phenotype reveals carbon oxidative processes and proteome reconfiguration in chilling-injured fruit. *Postharvest Biol. Technol.* 151, 142–151. doi: 10.1016/j.postharvbio.2019.02.007

Müller, M., and Munné-Bosch, S. (2015). Ethylene response factors: a key regulatory hub in hormone and stress signaling. *Plant Physiol.* 169, 32–41. doi: 10.1104/pp.15.00677

Nilo, R., Saffie, C., Lilley, K., Baeza-Yates, R., Cambiazo, V., Campos-Vargas, R., et al. (2010). Proteomic analysis of peach fruit mesocarp softening and chilling injury using difference gel electrophoresis (DIGE). *BMC Genomics* 11:43. doi: 10.1186/1471-2164-11-43

Nilo-Poyanco, R., Vizoso, P., Sanhueza, D., Balic, I., Meneses, C., Orellana, L. A., et al. (2018). A *Prunus persica* genome-wide RNA-seq approach uncovers major differences in the transcriptome among chilling injury sensitive and non-sensitive varieties. *Physiol. Plant.* 166, 772–793. doi: 10.1111/ppl.12831

Nuñez-Lillo, G., Balladares, C., Pavez, C., Urra, C., Sanhueza, D., Vendramin, E., et al. (2019). High-density genetic map and QTL analysis of soluble solid

content, maturity date, and mealiness in peach using genotyping by sequencing. *Sci. Hortic.* 257:108734. doi: 10.1016/j.scienta.2019.108734

Nuñez-Lillo, G., Cifuentes-Esquivel, A., Troggio, M., Micheletti, D., Infante, R., Campos-Vargas, R., et al. (2015). Identification of candidate genes associated with mealiness and maturity date in peach [*Prunus persica* (L.) Batsch] using QTL analysis and deep sequencing. *Tree Genet. Genomes* 11:86. doi: 10.1007/s11295-015-0911-9

Ortega-Galisteo, A. P., Morales-Ruiz, T., Ariza, R. R., and Roldán-Arjona, T. (2008). *Arabidopsis* DEMETER-LIKE proteins DML2 and DML3 are required for appropriate distribution of DNA methylation marks. *Plant Mol. Biol.* 67, 671–681. doi: 10.1007/s11103-008-9346-0

Peace, C. P., Crisosto, C. H., and Gradziel, T. M. (2005). Endopolygalacturonase: a candidate gene for freestone and melting flesh in peach. *Mol. Breed.* 16, 21–31. doi: 10.1007/s11032-005-0828-3

Pegoraro, C., Tadiello, A., Girardi, C. L., Chaves, F. C., Quecini, V., Costa de Oliveira, A., et al. (2015). Transcriptional regulatory networks controlling woolliness in peach in response to preharvest gibberellin application and cold storage. *BMC Plant Biol.* 15:279. doi: 10.1186/s12870-015-0659-2

Pons, C., Marti, C., Forment, J., Crisosto, C. H., Dandekar, A. M., and Granell, A. (2014). A bulk segregant gene expression analysis of a peach population reveals components of the underlysing mechanism of the fruit cold response. *PLoS One* 9:e90706. doi: 10.1371/journal.pone.0090706

Pons, C., Marti, C., Forment, J., Crisosto, C. H., Dandekar, A. M., and Granell, A. (2016). A genetic genomics-expression approach reveals components of the molecular mechanisms beyond the cell wall that underlie peach fruit woolliness due to cold storage. *Plant Mol. Biol.* 92, 483–503. doi: 10.1007/s11103-016-0526-z

Prudencio, A. S., Werner, O., Martínez-García, P. J., Dicenta, F., Ros, R. M., and Martínez-Gómez, P. (2018). DNA methylation analysis of dormancy release in almond (*Prunus dulcis*) flower buds using epi-genotyping by sequencing. *Int. J. Mol. Sci.* 19:3542. doi: 10.3390/ijms19113542

Puig, C. P., Dagar, A., Ibanez, C. M., Singh, V., Crisosto, C. H., Friedman, H., et al. (2015). Pre-symptomatic transcriptome changes during cold storage of chilling sensitive and resistant peach cultivars to elucidate chilling injury mechanisms. *BMC Genomics* 16:245. doi: 10.1186/s12864-015-1395-6

Rautengarten, C., Birdseye, D., Pattathil, S., McFarlane, H. E., Saez-Aguayo, S., Orellana, A., et al. (2017). The elaborate route for UDP-arabinose delivery into the Golgi of plants. *Proc. Natl. Acad. Sci. U.S.A.* 114, 4261–4266. doi: 10.1073/pnas.1701894114

Robinson, M. D., McCarthy, D. J., and Smyth, G. K. (2010). EdgeR: a Bioconductor package for differential expression analysis of digital gene expression data. *Bioinformatics* 26, 139–140. doi: 10.1093/bioinformatics/btp616

Rothkegel, K., Sánchez, E., Montes, C., Greve, M., Tapia, S., Bravo, S., et al. (2017). DNA methylation and small interference RNAs participate in the regulation of MADS-box genes involved in dormancy in sweet cherry (*Prunus avium* L.). *Tree Physiol.* 37, 1739–1751. doi: 10.1093/treephys/tpx055

Rothkegel, K., Sandoval, P., Soto, E., Lissette, U., Riveros, A., Lillo, V., et al. (2020). Dormant but active: chilling accumulation modulates the epigenome and transcriptome of *Prunus avium* during bud dormancy. *Front. Plant Sci.* 11:1115. doi: 10.3389/fpls.2020.01115

Su, Y., Bai, X., Yang, W., Wang, W., Chen, Z., Ma, J., et al. (2018). Single-base-resolution methylomes of *Populus euphratica* reveal the association between DNA methylation and salt stress. *Tree Genet. Genomes* 14:86. https://link.springer.com/article/10.1007/s11295-018-1298-1

Takuno, S., and Gaut, B. S. (2013). Gene body methylation is conserved between plant orthologs and is of evolutionary consequence. *Proc. Natl. Acad. Sci. U.S.A.* 110, 1797–1802. doi: 10.1073/pnas.1215380110

Tong, Z., Gao, Z., Wang, F., Zhou, J., and Zhang, Z. (2009). Selection of reliable reference genes for gene expression studies in peach using real-time PCR. *BMC Mol. Biol.* 10:71. doi: 10.1186/1471-2199-10-71

Verde, I., Abbot, A., Scalabrn, S., Jung, S., Shu, S., Marroni, F., et al. (2013). The high-quality draft genome of peach (*Prunus persica*) identifies unique patterns of genetic diversity, domestication and genome evolution. *Nat. Genet.* 45, 487–494. doi: 10.1038/ng.2586

Verde, I., Jenkins, J., Dondini, L., Micali, S., Pagliarani, G., Vendramin, E., et al. (2017). The Peach v2.0 release: high-resolution linkage mapping and deep resequencing improve chromosome-scale assembly and contiguity. *BMC Genomics* 18:225. doi: 10.1186/s12864-017-3606-9

Wang, K., Yin, X. R., Zhang, B., Grierson, D., Xu, C. J., and Chen, K. S. (2017). Transcriptomic and metabolic analyses provide new insights into chilling injury in peach fruit. *Plant Cell Environ.* 40, 1531–1551. doi: 10.1111/pce.12951

Xu, J., Wang, X., and Guo, W. (2015). The cytochrome P450 superfamily: key players in plant development and defense. *J. Integr. Agric.* 14, 1673–1686. doi: 10.1016/s2095-3119(14)60980-1

Zhang, H., Lang, Z., and Zhu, J. K. (2018). Dynamics and function of DNA methylation in plants. *Nat. Rev. Mol. Cell Biol.* 19, 489–506. doi: 10.1038/s41580-018-0016-z

Zhao, Y., Song, C., Brummel, D. A., Qi, S., Lin, Q., and Duan, Y. (2021). Jasmonic acid treatment alleviates chilling injury in peach fruit by promoting sugar and ethylene metabolism. *Food Chem.* 338:128005. doi: 10.1016/j.foodchem.2020.128005

Conflict of Interest: The authors declare that the research was conducted in the absence of any commercial or financial relationships that could be construed as a potential conflict of interest.

frontiers in Plant Science

REVIEW
published: 16 July 2021
doi: 10.3389/fpls.2021.670803

Physiological and Biochemical Response of Tropical Fruits to Hypoxia/Anoxia

*Noureddine Benkeblia**

Department of Life Sciences, The Biotechnology Centre, The University of the West Indies, Kingston, Jamaica

Aerobic respiration and oxygen consumption are indicators of routine metabolic rate, and dissolved oxygen in plant tissues is one of the most important environmental factors affecting their survival. The reduction of available O_2 leads to hypoxia which causes a limitation of the oxidative phosphorylation; when O_2 is absent, tissues generate ATP by activating the fermentative glycolysis to sustain glycolysis in the absence of mitochondrial respiration, which results in the production of lactate. Overall, hypoxia was reported to often decrease the respiration rate (O_2 uptake) and delay the climacteric rise of ethylene in climacteric fruits by inhibiting action, thus delaying their ripening. Much research has been done on the application of postharvest hypoxia and anoxia treatment to temperate fresh crops (controlled or modified atmosphere), however, very few reported on tropical commodities. Indeed, the physiological mode of action of low or absence of oxygen in fresh crops is not well understood; and the physiological and biochemical bases of the effects low or absence of O_2 are also yet to be clarified. Recent investigations using omics technologies, however, have provided useful information on the response of fresh fruits and vegetables to this abiotic stress. The aims of this review are to (i) report on the oxygen exchange in the crops tissue, (ii) discuss the metabolic responses to hypoxia and anoxia, and (iii) report the physiological and biochemical responses of crops tissues to these abiotic stresses and the potential benefits of these environmental conditions.

Keywords: tropical fruits, physiology, biochemistry, hypoxia, anoxia

OPEN ACCESS

Edited by:
Natalia Marina Villarreal, CONICET Instituto Tecnológico de Chascomús (INTECH), Argentina

Reviewed by:
Yueming Jiang, South China Botanical Garden, Chinese Academy of Sciences, China
Qing-gang Zhu, Northwest A&F University, China

***Correspondence:**
Noureddine Benkeblia
noureddine.benkeblia@uwimona.edu.jm

Specialty section:
This article was submitted to Crop and Product Physiology, a section of the journal Frontiers in Plant Science

Received: *22 February 2021*
Accepted: *23 June 2021*
Published: *16 July 2021*

Citation:
Benkeblia N (2021) Physiological and Biochemical Response of Tropical Fruits to Hypoxia/Anoxia. Front. Plant Sci. 12:670803. doi: 10.3389/fpls.2021.670803

INTRODUCTION

From the botanical point of view, tropical fruits are a diverse group of commodities native to tropical regions which are geographically defined as regions between the latitudes 23° North and South of the equator, with temperatures averaging around 27°C and little variation in photoperiod (Samson, 1986). Tropical fruits present a large biodiversity varying in structure, characteristics, and physiology (Wongs-Areea and Noichinda, 2014). Although the variations of tropical fruits are not well established, banana, pineapples, papaya, and avocado fall within the category of major tropical fruits, while others such as lychee, durian, rambutan, guava, passionfruit, mangosteen, tamarind, and some others are considered minor tropical fruits (FAO, 2003; Paull and Duarte, 2011, 2012).

Atmosphere composition consists of 78% nitrogen (N_2), 21% oxygen (O_2), 0.04% carbon dioxide (CO_2), 0.93% argon, small amounts of other gases, and variable amount of water vapor at 20°C

and absolute pressure of 1 atm. Oxygen depletion or hypoxia occurs when the partial pressure of oxygen is low enough to limit the production of ATP by mitochondria, whereas anoxia (absence of O_2) is attained when ATP mitochondrial production is insignificant compared to that generated by glycolysis and fermentation. Under normal condition of oxygen level (*normoxia*) cells run aerobic respiration and energy in the form of ATP is produced by oxidative phosphorylation. However, a reduction in oxygen (*hypoxia*) reduces the oxidative phosphorylation, while the absence of oxygen (*anoxia*) stops the phosphorylation process (Wongs-Aree and Noichinda, 2018; Salvatierra et al., 2020). This diverts the production of energy to the fermentation pathway producing fermentative by-products that accumulate in the cells (Boersig et al., 1988; Pfister-Sieber and Brändle, 1994; Cho et al., 2021).

In plant cells, oxygen partial pressure between organs of plant, for example in shoots O_2 concentration is much higher in comparison with roots (Kotula et al., 2015; van Dongen and Licausi, 2015). On the other hand, oxygen availability also varies significantly in time and space, and the distribution of active O_2 depends on its diffusion and convection, and the conductivity of gas transport in specific tissues (Armstrong et al., 2006; Ho et al., 2011; Licausi, 2011; Wang et al., 2017).

Intrinsically, the oxygen status of cells is variable and depends to a great extent on the concentration or partial pressure of atmospheric oxygen supply. This status differentiates between hypoxia and anoxia. Tissues are under hypoxic conditions when the oxygen partial pressure is the limiting factor of ATP production; anoxic conditions are characterized by a limited production of ATP by oxidative phosphorylation, which is mainly produced by fermentation (Drew, 1997; Atwell et al., 2015).

Under unfavorable conditions of oxygen deprivation, plants develop different structural and metabolic adaptations that are genetically controlled, however, the form of adaptation and shift in metabolism depend on the specific response of each species and its tolerance (**Figure 1**; Beaudry, 2000; Huang et al., 2008; Ioannidi et al., 2009; Toro and Pinto, 2015; Boecx, 2018). This response causes the molecular mechanisms to react to the low or absence of oxygen (Davies et al., 1974; Jackson et al., 1991; Kennedy et al., 1992; Perata and Alpi, 1993; Ricard et al., 1994; Ratcliffe, 1995; Schmidt et al., 2018), as well as an acclimatization where ethylene was found to play a role (**Figure 1**; Hartman et al., 2021).

In plants, it has been established that anaerobic metabolic pathways other than ethanol production exist (Perata and Alpi, 1993; Ricard et al., 1994; Kolb and Joly, 2010; Ventura et al., 2020). First, plants respond to hypoxia/anoxia by producing lactate and the reaction consists of reducing pyruvate by the lactate dehydrogenase (LDH) (Mithran et al., 2010). Under prolonged exposure to hypoxia/anoxia, pyruvate is converted to acetaldehyde by pyruvate decarboxylase (PDC), and then the acetaldehyde is converted to ethanol by the acetaldehyde dehydrogenase (LDH). The lactate-ethanol transition pathway depends on the initial pH of the cytoplasmic compartment (Felle, 2005, 2010; Hossain and Uddin, 2011), and the lower the pH, the faster this transition occurs because LDH has an optimal alkaline pH of 8.0 while PDC has an optimal acidic pH of 5.8 (Davies et al., 1974; Davies, 1980; Morrell et al., 1990; Fox et al., 1994; Kato-Noguchi and Morokum, 2007; Cukrov et al., 2016).

Since tolerance of fresh crops to hypoxia/anoxia is of great economic importance in postharvest science and modified atmosphere packaging (MAP) technology, numerous investigations have been carried out to elucidate the mechanisms underlying the effect of oxygen deprivation on the physiological, biochemical, and organoleptic parameters of crops and their shelf-life. This review aims to describe the effects of low oxygen availability -hypoxia/anoxia- on the physiology, the biochemistry and the quality attributes of tropical fruits in order to determine the optimal condition of MAP application in postharvest handling and storage of these commodities.

ANOXIA/HYPOXIA AND CELL METABOLIC CHANGES

Under hypoxic/anoxic conditions, the electron transport chain in the mitochondria leads to the progressive suppression and the inhibition of ATP synthesis. To compensate this lack of aerobic energy, the cell switches to produce ATP by anaerobic glycolysis. Basically, hypoxia/anoxia causes a decrease in ATP production, but this decrease is more significant in the anoxia-intolerant plants; this suggests that the ability of the anoxia-tolerant species to sustain their energy supply might be the key factor for survival under anoxia/hypoxia (**Figure 2**; Crawford, 1992; Hanhijärvi and Fagerstedt, 1994, 1995; Nakamura and Noguchi, 2020; Zahra et al., 2021). Nevertheless, response to oxygen deprivation is more complex than it seems and requires further investigation at different plants levels. Tolerance to hypoxia/anoxia, however, appears to depend on a dual morphological and metabolic adaptations which are specific to species and tissue types (Kennedy et al., 1992; Perata et al., 1993; Ratcliffe, 1995; Mariani and Ferrante, 2017; Nakamura and Noguchi, 2020; Zahra et al., 2021).

Although no fundamental metabolic differences have been observed between anoxia tolerant and intolerant plant species (Pfister-Sieber and Brändle, 1994), sugar availability is important since some tissues (e.g., roots) suffer more from sugar starvation under anoxia (Saglio, 1985). Indeed, when O_2 becomes less available starch is rapidly hydrolyzed and channeled to the fermentative pathway for ATP production in order to compensate the lack of oxidative phosphorylation (Perata and Alpi, 1993). Although it was noted that starch reserve mobilization is affected by anoxia, anoxia-tolerant plants have been shown to break down starch much easier than anoxia-intolerant species (Perata et al., 1992).

From the metabolic point of view, oxygen unavailability and the production of ATP by fermentative glycolysis cause the acidification of the cytoplasm (Summers et al., 2000; Gout et al., 2001; Greenway and Gibbs, 2003) and, depending on the tolerance to low oxygen partial pressure, the cellular pH remains stable but drops when energy becomes short (Felle, 2005, 2010). This drop in the pH leads to the accumulation of lactate which in turn inhibits LDH and activates PDC producing acetaldehyde, which is converted to ethanol by alcohol dehydrogenase (ADH).

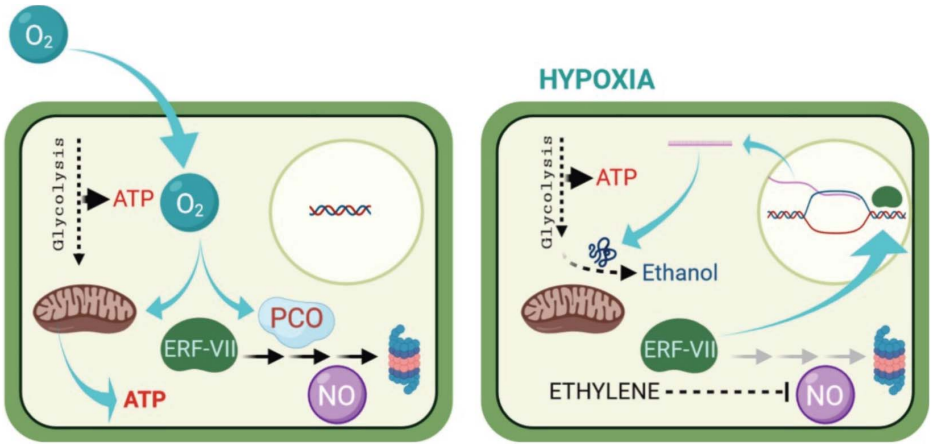

FIGURE 1 | How plants sense oxygen. Under aerobic conditions (left), aerobic respiration in the mitochondria provides most off the energy (ATP) required for the cell metabolism. The ERF—VIII transcription factor genes are constitutively expressed, but their stability is compromised by the activity pf PCOs. Which is a process requiring oxygen, oxidize the N-terminal Cys residue, channeling the ERF-VII proteins to the proteasome, in a process also requiring nitric oxide (NO). Under hypoxia (right), the respiration in the mitochondria is drastically reduced, and AT production can only occur because of enhanced glycolytic activity. The ERF-VII proteins are stabilized because of the absence of oxygen and also thank to ethylene production, which dampers the presence of NO in the cell. The stable ERF-VII proteins migrate to the nucleus where they activate the transcription of Hypoxia-Responsive Genes (HRGs), including genes encoding proteins required for the alcoholic fermentation. (From Loreti and Perata, 2020, published under an open access Creative Common CC BY license).

However, cytoplasm acidification is not caused solely by lactate accumulation, but also by the possible passive H^+ and potassium (K^+) leakage from the vacuole and the protoplasm under limited ATP availability and inhibition of vacuolar H^+-ATPase (Ratcliffe, 1995; Gout et al., 2001; Kulichikhin et al., 2007; Yemelyanov et al., 2020). Indeed, ethanol is the primary end product of fermentation in tissues of higher plants under to low oxygen, even though its catalysis and regulation involve components that will be identified in the future (Bui et al., 2019). However, other studies suggest that other fermentation pathways exist, such as the alanine pathway which is quantitatively minor (Davies et al., 1974; Nover, 1989; Jackson et al., 1991; Ricard et al., 1994). Under anaerobic fermentation, pyruvate can therefore be converted into products other than ethanol such as alanine, malate, and succinate which have been detected under early anoxic conditions. Although these diversified glycolytic pathways are recommended for enhancing the tolerance of plants to anoxia using molecular engineering (Lee et al., 2014; Diab and Limami, 2016), this physiological mechanism is not fully clear (Pfister-Sieber and Brändle, 1994).

Indeed, the effects of hypoxia/anoxia do not solely depend on the quantity of oxygen availability for ATP production, but also on the exposure time. Under prolonged anoxia, ethanol was found to be the most abundant end product of fermentation, but interestingly some plants showed their ability to release it into their surrounding environment, thereby increasing their tolerance to anoxia (Crawford and Zochowski, 1984; Kato-Noguchi and Morokum, 2007). Another metabolic consequence under anoxia is the alteration of the cellular redox state of the cell, and the ability of the plant to survive under hypoxia/anoxia consists of their capacity to maintain the cell redox (i.e., $NADH/NAD^+$-ratio), since a decrease in $NADH/NAD^+$ was noted in anoxia-intolerant plants (Chirkova et al., 1992; Nakamura and Noguchi, 2020). However, under oxygen deprivation anoxia-tolerant plants have higher ability to oxidize NADPH to $NADP^+$ *via* glycolysis and fermentation, and this oxidation leads to less accumulation of reducing equivalents (Guglielminetti et al., 1995, 1999). Furthermore, prolonged hypoxia/anoxia, ATP needs also triggers the fermentation pathway and LDH and ADH generate NAD^+.

From the molecular point of view, the mechanisms signaling the response to anoxia still remain unclear and not well elucidated, and the sensors of hypoxia/anoxia in plants are not clearly understood (Geigenberger, 2003; Gibbs and Greenway, 2003). Molecular responses to oxygen deprivation have focused on the regulation of genes expression and activation of enzymes involved in acclimation of metabolism such amylases (Bailey-Serres and Chang, 2005). So far, a direct oxygen sensor has not been established in plants, but some studies have demonstrated that increased ADH gene expression and fermentative metabolism are triggered under hypoxia/anoxia (Koch et al., 2000). Other mechanisms which use different sets of transcription factors (TFs) and ethylene responsive factor family (ERF) to perceive low-oxygen derived signals have been reported to play a primordial role in the determination of survival with reduced oxygen availability (Licausi et al., 2010b; Licausi, 2011).

Cytosolic calcium patterns $(Ca^{2+})_{cyt}$ have also been recognized as important elements in signaling, and there has been increased interest in identifying the calcium fate involved in $(Ca^{2+})_{cyt}$ changes in specific signaling pathways (Bush, 1995; Subbaiah et al., 1998; Yemelyanov et al., 2011; Lindberg et al., 2012; Hironari and Takashi, 2014). In this regard, one of the suggested hypotheses is the role of Ca^{2+} as a messenger. This hypothesis is supported by the work of Subbaiah et al. (1998) who observed an increase of Ca^{2+} in the cytosol suggesting its possible participation in anoxic signaling

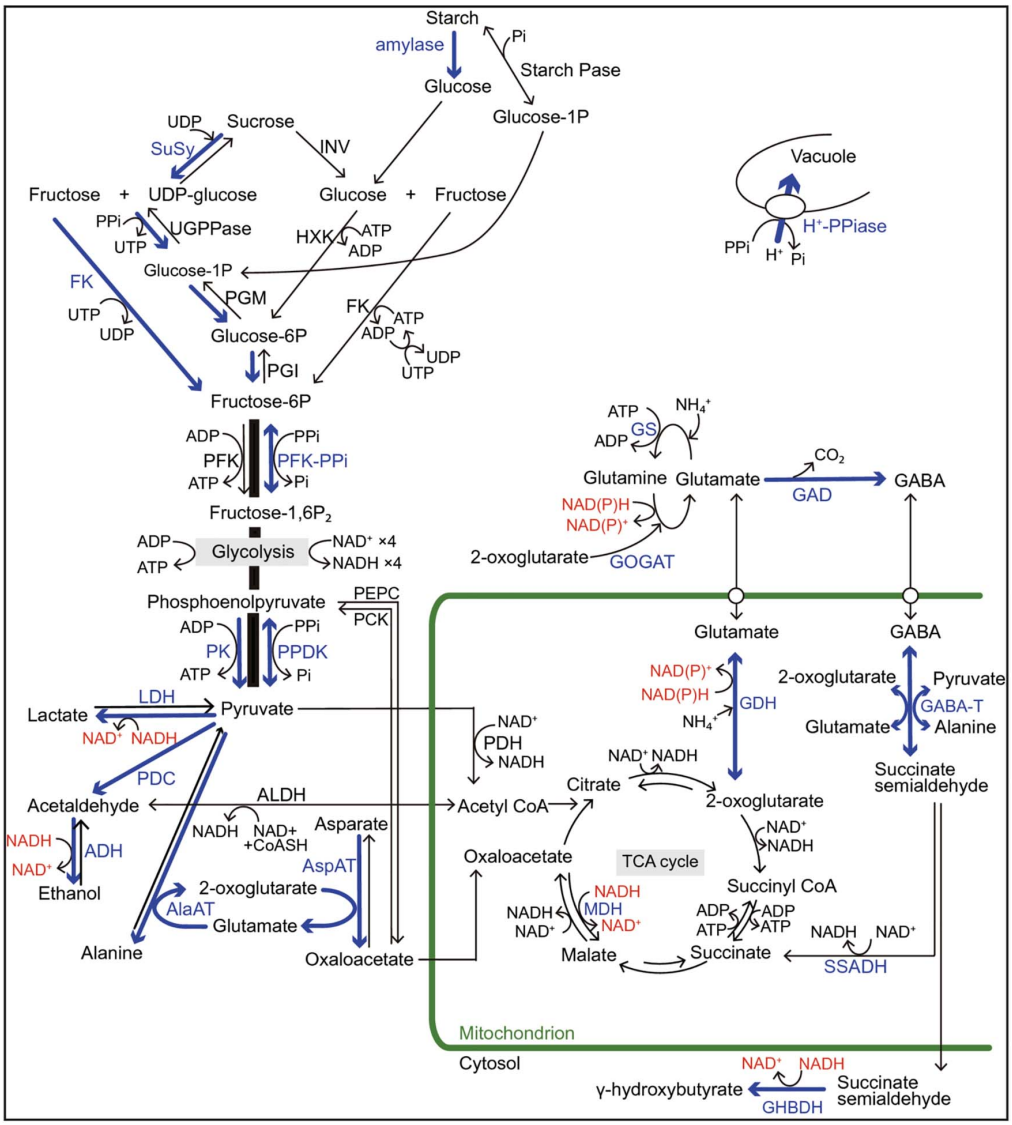

FIGURE 2 | Regulations of sugar catabolism, fermentation, glycolysis, and major amino acid metabolism associated with NAD(P) + regeneration and ATP production in terrestrial and wetland plants under O_2-deficient conditions. Blue arrows and letters indicate the reactions and enzymes in the up-regulated pathways when the mitochondrial electron transport and the TCA-cycle flux decrease under O_2-deficient conditions. Red letters indicate the regeneration of NAD(P)+ from NAD(P)H. In rice plants, the blue pathways contribute to their tolerance to long-term O_2 deficiency compared with the terrestrial plants. Some wetland plants such as rice also have a high ability to optimally regulate the pyruvate level by activation of pyrophosphate (PPi)-dependent phosphofructokinase (PFK-PPi) and pyruvate phosphate dikinase (PPDK) that consume PPi instead of ATP for energy conservation. Besides glycolysis, PPi is consumed to regulate the cytosolic pH by the tonoplast H+-pumping pyrophosphatase (H+-PPiase) instead of H+-ATPase in wetland plants. Although two independent pathways for sucrose degradation contribute to the regulation of glycolytic flux in both terrestrial and wetland plants, the UDP-dependent sucrose synthase (SuSy) pathway is regarded as energetically more advantageous for survival under O_2-deficient conditions than the invertase (INV) pathway because here, PPi is utilized instead of ATP. Sugar supply to glycolysis through starch mobilization is observed in species with developed storage organs such as tuber, rhizome, and endosperm. In NAD(P)H regeneration during the metabolisms of 2-oxoglutarate and glutamate associated with γ-aminobutyric acid (GABA) production, the glutamate dehydrogenase (GDH) pathway without ATP consumption is more efficient in energy consumption than the NAD(P)H-dependent glutamine: 2-oxoglutarate aminotransferase (GOGAT) pathway with ATP consumption. The accumulation of some amino acids such as GABA, alanine, and glutamate play an important role in avoiding carbohydrate loss not only during O_2-deficient conditions but also during the recovery phase of re-oxygenation after hypoxia/anoxia. Alanine accumulation by alanine aminotransferase (AlaAT) can operate non-circular TCA-cycle and gluconeogenesis under O_2 deficiency and re-oxygenation. ADH, alcohol dehydrogenase; AlaAT, alanine aminotransferase; ALDH, acetaldehyde dehydrogenase; AspAT, aspartate aminotransferase; CoASH, coenzyme A; FK, fructokinase; GABA-T, GABA transaminase; GAD, glutamate decarboxylase; GHBDH, γ-aminobutyrate dehydrogenase; Glucose-1-P, glucose-1-phosphate; GS, glutamine synthetase; HXK, hexokinase; LDH lactate dehydrogenase; MDH, malate dehydrogenase; PCK, phosphoenolpyruvate carboxykinase; PDC, pyruvate decarboxylase; PDH; pyruvate dehydrogenase; PEPC, phosphoenolpyruvate carboxylase; PFK, ATP-dependent phosphofructokinase; PFK-PPi, PPi-dependent phosphofructokinase; PGI, phosphoglucoisomerase; PGM, phosphoglucomutase; Pi, phosphate; PK, pyruvate kinase; PPDK, pyruvate Pi dikinase; SSADH, succinate semialdehyde dehydrogenase; Starch Pase, starch phosphorylase; TCA, tricarboxylic acid; UDP, uridine diphosphate; UGPPase, UDP-glucose pyrophosphorylase; UTP, uridine triphosphate. (From Nakamura and Noguchi, 2020; an open access article distributed under the terms of the Creative Commons CC BY license).

(Sedbrook et al., 1996; Bose et al., 2011). In a recent study, Igamberdiev and Hill (2018) suggested the possible release of Ca^{2+} from cell compartments to the cytosol under the decrease of ATP concentration resulting in the suppression of ATPases and activation of calcium ion channels.

EFFECTS OF HYPOXIA/ANOXIA ON THE RESPIRATION RATE AND ETHYLENE PRODUCTION

Unlike animal products, crops are living organisms and they continue to respire and are metabolically active during, either, before or after harvest. This respiration is the chemical process of energy production by converting glucose to carbon dioxide, water and heat. The respiration rate (*RR*) of a fresh crop is therefore determined by the speed at which this chemical process occurs, and a high *RR* leads to a faster depletion of glucose and loss of freshness. Indeed, under aerobic condition oxygen exchange in fruit depends greatly on its physiology (type of fruit and vegetable) (Platenius, 1942; Brady et al., 1970; Varoquaux et al., 1992; Kader, 1994) and it relies on O_2 diffusion from the atmosphere to the fruit following Fick's law (Palmes and Lindenboom, 1979; Kader and Saltveit, 2003).

However, as a dynamic process resulting from a chemical reaction, following van't Hoff's law (van't Hoff, 1884; Kemp, 1987), *RR* is influenced by different factors mainly temperature (Waghmare et al., 2013). Atmospheric oxygen concentration also significantly affects *RR* depending on CO_2 accumulation during respiration, regulation of the respiratory metabolism in addition to O_2 diffusion limitation and availability which reduces significantly *RR* (Gupta et al., 2009; Ho et al., 2018). However, at low temperatures it was observed that *RR* was likely reduced by a specific response to a signal generated by a plant oxygen sensor (Ho et al., 2018).

From the metabolic point of view, more information is readily available on the effects of O_2 than on CO_2 (Watkins, 2000). Atmospheric carbon dioxide also influences the *RR* of crop commodities, however, the mechanisms on how CO_2 affect *RR* are still not well understood, and CO_2 might increase or decrease *RR* depending on the type of fruit (Mathooko, 1996). Overall, the *RR* of commodities decreases with the decrease in oxygen partial pressure below 21 kPa, and the effect of hypoxia becomes more significant below 10 kPa oxygen partial pressure (Chervin et al., 1996).

Practically, extensive literature has reported on the effects of hypoxia/anoxia on numerous temperate fruits (Ho et al., 2014; Boeckx et al., 2019), while limited references are readily available on tropical fruits in comparison. When exposed to low oxygen concentration, hypoxia/anoxia significantly reduced the *RR* of avocado (El-Mir et al., 2001), banana (Wade, 1974; Yi et al., 2006), Japanese persimmon (Imahori et al., 1998), mango (Yahia and Vazquez-Moreno, 1993), kiwi (Botondi et al., 2012; Huang et al., 2014), pear (Ho et al., 2018), and dragon fruit (Ho et al., 2021), while the absence of oxygen increased the *RR* of lychee (Liu et al., 2015).

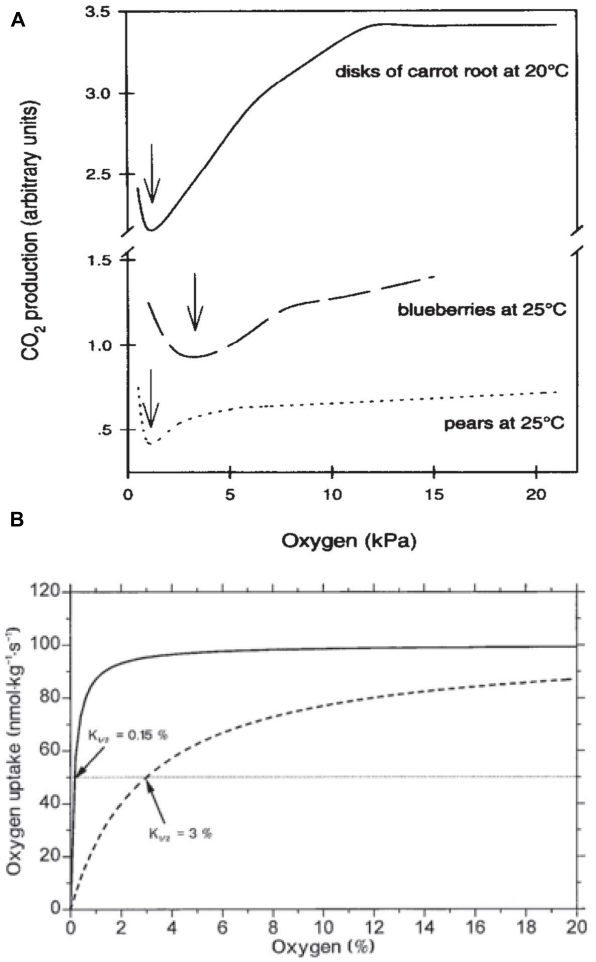

FIGURE 3 | (A) Plant CO_2 production in response to oxygen depletion. Data on carrot are from Leshuk and Saltveit (1990), on blueberries from Beaudry et al. (1992) and on pears from Boersig et al. (1988). Arrows indicate ACPs (Chervin et al., 1996, with permission of Elsevier). **(B)** Hypothetical respiratory responses to O_2 for a respiratory system of low diffusive resistance exhibiting a $K_{1/2}$ of about 0.15% O_2, representative of single cells or tissues, and a tissue with significant diffusive resistance to gas exchange with an $K_{1/2}$ of 3% O_2 (with open permission).

On the other hand, oxygen is closely linked to the rate of respiration of fresh crops and is required for the biosynthesis of ethylene, and ERFs have been shown to play a role under hypoxia/anoxia (Licausi et al., 2010a,b; Licausi, 2011). In an interesting study, Sanders and de Wild (2003) modelized *in vivo* ethylene production rate in relation to O_2 partial pressure using tomato, and their findings are in agreement with the molecular findings since they noted that ethylene biosynthesis and perception was positively related to O_2 partial pressure (Mustroph et al., 2010). Thus, similar to the effects on *RR*, hypoxia/anoxia reduced levels of oxygen uptake and slowed down ethylene production in avocado (Zhang et al., 2011), saskatoon fruit (Rogiers and Knowles, 1998), banana (Imahori et al., 2013), and kiwi fruit (Botondi et al., 2012).

Nevertheless, a decrease in the *RR* does not change the respiratory quotient (RQ = CO_2/O_2) –which is a good indicator of the trigger of the fermentation pathway– until O_2 partial pressure reaches the compensation point c.a. 2 kPa (**Figures 3A,B**; Beaudry et al., 1992; Banks et al., 1993; Peppenlenbos et al., 1996). Therefore, this suggests that commodities are not significantly stressed by oxygen depletion since carbohydrates are still completely oxidized to CO_2 and the end products of anoxia, namely lactate and acetaldehyde, do not accumulate until the oxygen partial pressure falls below 2 kPa (Beaudry et al., 1992).

HYPOXIA/ANOXIA AND FRESH CROPS RIPENING, QUALITY, AND STORABILITY

As described above, hypoxia/anoxia may have beneficial effects, such as slowing down the *RR*, ethylene production, and even reducing the incidence of some physiological disorders (Mojević and Tešanović, 2011; Lurie and Tonutti, 2014; Kongpatjirak et al., 2016) such as delaying ripening (Pesis et al., 1994; Pegoraro et al., 2012), softening (Wu et al., 2020), deastringency (Zhu et al., 2018), browning (Phonyiam et al., 2016), internal breakdown (Lizada and Rumbaoa, 2017), and also diseases (Fallik et al., 2003). However, it is important to note that following exposure of the fruit to anoxic conditions, the accumulation of the ethanol fermentation metabolites -acetaldehyde and ethanol- may be enhanced to extreme levels. The occurrence of anaerobic conditions in the internal atmospheres of fruit and vegetables, and their tendency to develop off-flavors also depend on their anatomical structure and morphology (Porat and Falik, 2008).

The modification of atmosphere was first developed by Kidd and West (1927a,b), and a general consensus was reached on hypoxia/anoxia and the effects in reducing rate of respiration, ethylene synthesis and sensitivity, and lipid catabolism and other oxidative reactions (Burton, 1974; Knee, 1991). Hypoxic/anoxic conditions have shown to delay ripening and senescence of many fruits and these effects were behind the development of MAP and controlled atmosphere (CA) postharvest storage technologies. Extensive literature is readily available on the effects of hypoxia/anoxia on crops, but little on tropical fruits. Green banana fruit stored under low (2%) and absence (0%) of oxygen for 7 days showed high ADH activity and accumulated more ethanol under total anoxia (0% O_2), while low oxygen showed a delayed onset of the climacteric peak and extended the shelf-life of banana but reduced remarkably the production of ester volatiles, i.e., ethyl acetate, isoamyl acetate, and isobutyl acetate (Imahori et al., 2013). Similar results on banana were obtained and the application of pure nitrous oxide (100% N_2O) or combined to low O_2 levels delayed ripening and extended the shelf-life of the fruit (Palomer et al., 2005; Yi et al., 2006).

Short anoxic treatment of pineapple maintained flesh and pulp color; delayed the increase in total sugar content and enhanced total ascorbic acid content during storage; and maintained overall postharvest quality of the fruit stored at ambient temperature (Techavuthiporn et al., 2017). When hypoxically pre-treated (3% O_2 for 24 h) or exposed to low oxygen (1 and 0.25% O_2 for 1–3 days), avocado fruit increased their tolerance to hypoxia (El-Mir et al., 2001). Litchi is known to have a very short shelf-life, and its short exposure to anoxia (0% O_2) markedly delayed skin browning and reduced rotting while maintaining the physical quality of the fruit during storage (Jiang et al., 2004; Liu et al., 2007). Mango is also one of the most widely consumed but perishable tropical fruit. Interestingly, anoxic treatment for 24 h prior to storage showed to be effective in retarding ripening, maintaining firmness, and delaying color change (Kongpatjirak et al., 2016). In a study on cherimoya, Palma et al. (1993) noted that hypoxia (5% O_2) delayed ripening and the edible condition differed with oxygen treatment and was inversely proportional to O_2 concentration. In a recent study, Ho et al. (2021) investigated the effect of different hypoxic treatments on dragon fruit (*Hylocereus undatus*) and their results showed that 2 kPa O_2 + 5 kPa CO_2 was the optimal hypoxic treatment in maintaining the shelf-life of the fruit during storage.

TABLE 1 | Effects of hypoxia/anoxia on some tropical fruits.

Fruit	Hypoxia/anoxia	Benefits	References
Avocado	2–5% O_2	Reduce respiration rate Ethylene production Delay ripening	El-Mir et al., 2001
Banana	2–5% O_2	Delay ripening	Palomer et al., 2005; Yi et al., 2006; Imahori et al., 2013
Cherimoya	5%	Reduce respiration rate Reduce ethylene production Delay ripening Delay ripening Firmness retention	Palma et al., 1993; Escribano et al., 1997
Durian	3–5% O_2	Reduce CO_2 production Reduce ethylene production Delay ripening	Minh, 2017
Litchi	5%	Reduce skin browning	Jiang et al., 2004; Liu et al., 2007
Mango	3–5% O_2	Delay ripening	Kongpatjirak et al., 2016
Papaya	2–8% O_2	Delay ripening Degreening and softening Enhanced quality	Rohani et al., 1997; González-Aguilar et al., 2003
Pineapple	2–5% O_2	Reduce respiration rate Delay senescence	Techavuthiporn et al., 2017
Rambutan	3% O_2	Reduce respiration rate Delay senescence	O'Hare et al., 1994
Sweetsop	3–5 O_2	Reduce respiration rate Reduce ethylene production Delay ripening	Broughton and Guat, 1979; Venkatram et al., 2016
Dragon	2% O_2	Delay senescence	Ho et al., 2021
Persimmon	95% CO_2	Removal of astringency	Min et al., 2014; Salvador et al., 2008

Another benefit of hypoxia/anoxia is the improvement of the quality attributes of some fruits. Hypoxia was shown to be a beneficial treatment for the removal of astringency from persimmon to improve the fruit quality after harvest. Although the longer the fruit is stored, the less effective is the treatment (Salvador et al., 2008), the application of hypoxic treatment with high CO_2 (95%) effectively reduced high soluble tannins (SCTs) content which is one of the most important causes of persimmon fruit astringency (Min et al., 2014). **Table 1** summarizes the main findings of hypoxia/anoxia treatments effects on tropical fruits.

CONCLUSION AND FUTURE DIRECTIONS

In postharvest science, hypoxia/anoxia treatments combined with packaging technology have been used as one of the most inexpensive non-chemical technology to prevent physiological disorders, reduce diseases incidence, delay ripening, extending shelf-life, and even improving some quality attributes of a large number of temperate fresh commodities during transportation and storage. Nevertheless, few studies have been focusing on how oxygen deprivation affects tropical fruits. These atmospheric conditions and treatments with low or total absence of oxygen have shown different efficacy levels which depend on composition of the atmosphere, the treatment and storage duration, and the type of commodity treated and their tolerance and response to total or partial absence of oxygen. Overall, on several tropical fruits low or absence of oxygen has shown its involvement in reducing the *RR* and ethylene biosynthesis, prolonging therefore the shelf-life of these commodities and maintaining some quality attributes and freshness. However, data showed that changes in oxygen availability and ethylene emission rates in reaction to the surrounding hypoxic or anoxic atmosphere varies with different intrinsic and extrinsic factors particularly oxygen levels and temperatures. On the other hand and from the fundamental point of view, the timing of the converging pathways to acetaldehyde and ethanol production and the distinct energy-dependent signaling pathways operating during hypoxia/anoxia are still unclear and not fully understood since most tropical fruits are known to have higher *RR*s and many of them are climacteric fruits. Besides the progress and advances in plant physiology and hypoxia/anoxia effects on plant tissues, fruits admittedly react differently to extremely low or total absence of oxygen conditions during exposure and storage in terms of tolerance, *RR*, ethylene production, volatiles biosynthesis, and acetaldehyde, alanine, and ethanol production and accumulation. In order to decipher the effects of hypoxia/anoxia mechanisms on tissues in general, it is first crucial to elucidate the different oxygen sensing mechanisms involved, the specific molecular and metabolic changes occurring at the earliest stages of the hypoxic/anoxic conditions, and establish whether these changes are a sort of adaptation response to oxygen deprivation. Another direction in understanding hypoxia/anoxia effects on plants is to elucidate whether the different oxygen-sensing mechanisms have different activation thresholds, and how these sophisticated sensing and signaling networks likely enable plants to tailor their adaptive responses to face the severity and duration of hypoxic/anoxic conditions. Elucidating these mechanisms will be of great importance and applications in enhancing our understanding of crop physiology in these extreme conditions. It will also a key step in determining which low oxygen atmospheric conditions may be worth testing on tropical fruits to determine the optimal postharvest handling and storage conditions of these sensitive commodities and maintaining longer their freshness and quality attributes. Indeed, anoxia/hypoxia should be further investigated for its potential application to extend the shelf-life and preserve the quality attributes of numerous less known tropical fruits by setting optimal O_2 concentration either as a pre-treatment for a very short time span prior to storage or in MAP or CA storage technologies.

AUTHOR CONTRIBUTIONS

The author confirms being the sole contributor of this work and has approved it for publication.

ACKNOWLEDGMENTS

I thank Suchetta Stephenson for her critical reading and editing of the manuscript.

REFERENCES

Armstrong, J., Jones, R. E., and Armstrong, W. (2006). Rhizome phyllosphere oxygenation in Phragmites and other species in relation to redox potential, convective gas flow, submergence and aeration pathways. *New Phytol.* 172, 719–731. doi: 10.1111/j.1469-8137.2006.01878.x

Atwell, B. J., Greenway, H., and Colmer, T. D. (2015). Efficient use of energy in anoxia-tolerant plants with focus on germinating rice seedlings. *New Phytol.* 206, 35–56. doi: 10.1111/nph.13173

Bailey-Serres, J., and Chang, R. (2005). Sensing and signalling in response to oxygen deprivation in plants and other organisms. *Ann. Bot.* 96, 507–518. doi: 10.1093/aob/mci206

Banks, N. H., Dadzie, B. K., and Cleland, D. J. (1993). Reducing gas exchange of fruits with surface coatings. *Postharvest Biol. Technol.* 3, 269–284. doi: 10.1016/0925-5214(93)90062-8

Beaudry, R. M. (2000). Responses of horticultural commodities to low oxygen: Limits to the expanded use of modified atmosphere packaging. *HortTechnology* 10, 491–500. doi: 10.21273/HORTTECH.10.3.491

Beaudry, R. M., Cameron, A. C., Shirazi, A., and Dostal-Lange, D. L. (1992). Modified-atmosphere packaging of blueberry fruit: effect of temperature on package O_2 and CO_2. *J. Am. Soc. Hortic. Sci.* 117, 436–441. doi: 10.21273/JASHS.117.3.436

Boecx, J. (2018). *Regulation of the Respiratory Metabolism of Apple During (dynamic) Controlled Atmosphere Storage*. Ph.D. thesis. Belgium: Katholieke Universiteit Leuven.

Boeckx, J., Pols, S., Hertog, M. L. A. T. M., and Nicolaï, B. M. (2019). Regulation of the central carbon metabolism in apple fruit exposed to postharvest low-oxygen stress. *Front. Plant Sci.* 10:1384. doi: 10.3389/fpls.2019.01384

Boersig, M. R., Kader, A. A., and Romani, R. J. (1988). Aerobic-anaerobic respiratory transition in pear fruit and cultured pear fruit cells. *J. Am. Soc. Hortic. Sci*. 113, 869–873.

Bose, B., Pottosin, I. I., Shabala, S. S., Palmgren, M. G., and Shabala, S. (2011). Calcium efflux systems in stress signaling and adaptation in plants. *Front. Plant Sci*. 02:85. doi: 10.3389/fpls.2011.00085

Botondi, R., Russo, V., and Mencarelli, F. (2012). Anaerobic metabolism during short and long term storage of kiwifruit. *Postharvest Biol. Technol*. 64, 83–90. doi: 10.1016/j.postharvbio.2011.09.017

Brady, C. J., O'connell, P. B. H., Smydzuk, J., and Wade, N. L. (1970). Permeability, sugar accumulation, and respiration rate in ripening banana fruits. *Aust. J. Biol. Sci*. 23, 1143–1152. doi: 10.1071/BI9701143

Broughton, W. J., and Guat, T. (1979). Storage conditions and ripening of the custard apple *Annona squamosa* L. *Sci. Hortic*. 10, 73–82. doi: 10.1016/0304-4238(79)90071-2

Bui, L. T., Novi, G., Lombardi, L., Iannuzzi, C., Rossi, J., Santaniello, A., et al. (2019). Conservation of ethanol fermentation and its regulation in land plants. *J. Exp. Bot*. 70, 1815–1827. doi: 10.1093/jxb/erz052

Burton, W. G. (1974). Some biophysical principles underlying the controlled atmosphere storage of plant material. *Ann. Appl. Biol*. 78, 149–168. doi: 10.1111/j.1744-7348.1974.tb01494.x

Bush, D. S. (1995). Calcium regulation in plant cells and its role in signaling. *Annu. Rev. Plant Physiol. Plant Mol. Biol*. 46, 95–122. doi: 10.1146/annurev.pp.46.060195.000523

Chervin, C., Brady, C. J., Patterson, B. D., and Faragher, J. D. (1996). Could studies on cell responses to low oxygen levels provide improved options for fruit storage and disinfestation? *Postharvest Biol. Technol*. 7, 289–299. doi: 10.1016/0925-5214(95)00048-8

Chirkova, T. V., Zhukova, T. M., and Bugrova, M. P. (1992). Redox reactions of plant cells in response to short-term anaerobiosis. *Vestnik SPBGU* 3, 82–86.

Cho, H. Y., Loreti, E., Shih, M. C., and Perata, P. (2021). Energy and sugar signaling during hypoxia. *New Phytol*. 229, 57–63. doi: 10.1111/nph.16326

Cukrov, D., Zermiani, M., Brizzolara, S., Cestaro, A., Licausi, F., Luchinat, C., et al. (2016). Extreme hypoxic conditions induce selective molecular responses and metabolic reset in detached apple fruit. *Front. Plant Sci*. 7:146. doi: 10.3389/fpls.2016.00146

Crawford, R. M. M. (1992). Oxygen availability as an ecological limit to plant distribution. *Adv. Ecol. Res*. 23, 93–185. doi: 10.1016/S0065-2504(08)60147-6

Crawford, R. M. M., and Zochowski, Z. M. (1984). Tolerance of anoxia and ethanol toxicity in chickpea seedlings (*Cicer arietinum* L.). *J. Exp. Bot*. 35, 1472–1480. doi: 10.1093/jxb/35.10.1472

Davies, D. D. (1980). *Biochemistry of Plants. A Comprehensive Treatise. Vol. 2: Metabolism and Respiration*. New York, NY: Academic Press.

Davies, D. D., Grego, S., and Kenworthy, P. (1974). The control of the production of lactate and ethanol by higher plants. *Planta* 118, 297–310. doi: 10.1007/BF00385580

Diab, H., and Limami, A. M. (2016). Reconfiguration of N metabolism upon hypoxia stress and recovery: Roles of alaninea aminotransferase (AlaAT) and glutamate dehydrogenase (GDH). *Plants* 5:25. doi: 10.3390/plants5020025

Drew, M. C. (1997). Oxygen deficiency and root metabolism: Injury and acclimation under hypoxia and anoxia. *Annu. Rev. Plant Physiol. Plant Mol. Biol*. 48, 223–250. doi: 10.1146/annurev.arplant.48.1.223

El-Mir, M., Gerasopoulos, D., Metzidakis, I., and Kanellis, A. K. (2001). Hypoxic acclimation prevents avocado mesocarp injury caused by subsequent exposure to extreme low oxygen atmospheres. *Postharvest Biol. Technol*. 23, 215–226. doi: 10.1016/S0925-5214(01)00124-7

Escribano, M. I., Del Cura, B., Munõz, T., and Merodio, C. (1997). The effect of high carbon dioxide at low temperature on ribulose 1,5-biphosphate carboxylase and polygalacturonase protein levels in cherimoya fruit. *J. Amer. Soc. Hort. Sci*. 122, 258–262. doi: 10.21273/JASHS.122.2.258

Fallik, E., Polevaya, Y., Tuvia-Alkalai, S., Shalom, Y., and Zuckermann, H. (2003). A 24-h anoxia treatment reduces decay development while maintaining tomato fruit quality. *Postharvest Biol. Technol*. 29, 233–236. doi: 10.1016/S0925-5214(03)00109-1

FAO (2003). *Medium-Term Prospects for Agricultural Commodities. Projections for the year 2010*. Rome: Food and Agriculture Organization.

Felle, H. H. (2010). "pH signaling during anoxia," in *Waterlogging Signalling and Tolerance in Plants*, eds S. Mancuso and S. Shabala (Berlin: Springer), 79–96. doi: 10.1007/978-3-642-10305-6_5

Felle, H. H. (2005). pH regulation in anoxic plants. *Ann. Bot*. 96, 519–532. doi: 10.1093/aob/mci207

Fox, G. G., McCallan, N. R., Ratcliffe, R. G. (1994). Manipulating cytoplasmic pH under anoxia: a critical test of the role of pH in the switch from aerobic to anaerobic metabolism. *Planta* 190, 210–217. doi: 10.1007/BF00202588

Geigenberger, P. (2003). Response of plant metabolism to too little oxygen. *Curr. Opin. Plant Biol*. 6, 247–256. doi: 10.1016/s1369-5266(03)00038-4

Gibbs, J., and Greenway, H. (2003). Mechanisms of anoxia tolerance in plants. I. Growth, survival and anaerobic catabolism. *Funct. Plant Biol*. 30, 1–37. doi: 10.1071/PP98095_ER

González-Aguilar, G. A., Buta, J. G., and Wang, C. Y. (2003). Methyl jasmonate and modified atmosphere packaging (MAP) reduce decay and maintain postharvest quality of papaya "Sunrise. *Postharvest Biol. Technol*. 28, 361–370. doi: 10.1016/S0925-5214(02)00200-4nb

Gout, E., Boisson, A. M., Aubert, S., Douce, R., and Bligny, R. (2001). Origin of the cytoplasmic pH changes during anaerobic stress in higher plant cells. Carbon-13 and phosphorous-31 nuclear magnetic resonance studies. *Plant Physiol*. 125, 912–925. doi: 10.1104/pp.125.2.912

Greenway, H., and Gibbs, J. (2003). Mechanisms of anoxia tolerance in plants. II. Energy requirements for maintenance and energy distribution to essential processes. *Funct. Plant Biol*. 30, 999–1036. doi: 10.1071/PP98096

Guglielminetti, L., Yamaguchi, J., Perata, P., and Alpi, A. (1995). Amylolytic activities in cereal seeds under aerobic and anaerobic conditions. *Plant Physiol*. 109, 1069–1076. doi: 10.1104/pp.109.3.1069

Guglielminetti, L., Loreti, E., Perata, P., and Alpi, A. (1999). Sucrose synthesis in cereal grains under oxygen deprivation. *J. Plant Res*. 112, 353–359. doi: 10.1007/PL00013889

Gupta, K. J., Zabalza, A., and Van Dongen, J. T. (2009). Regulation of respiration when the oxygen availability changes. *Physiol. Plant*. 137, 383–391. doi: 10.1111/j.1399-3054.2009.01253.x

Hanhijärvi, A. M., and Fagerstedt, K. V. (1994). Comparison of the effect of natural and experimental anoxia on carbohydrate and energy metabolism in *Iris pseudacorus* rhizomes. *Physiol. Plant*. 90, 437–444. doi: 10.1111/j.1399-3054.1994.tb08799.x

Hanhijärvi, A. M., and Fagerstedt, K. V. (1995). Comparison of carbohydrate utilization and energy charge in the yellow flag iris (*Iris pseudacorus*) and garden iris (*Iris germanica*) under anoxia. *Physiol. Plant*. 93, 493–497. doi: 10.1111/j.1399-3054.1995.tb06848.x

Hartman, S., Sasidharan, R., and Voesenek, L. A. C. J. (2021). The role of ethylene in metabolic acclimations to low oxygen. *New Phytol*. 229, 64–70. doi: 10.1111/nph.16378

Hironari, H., and Takashi, S. (2014). Calcium signaling in plant endosymbiotic organelles: Mechanism and role in physiology. *Mol. Plant* 7, 1094–1104. doi: 10.1093/mp/ssu020

Ho, P. L., Tran, D. T., Hertog, M. L. A. T. M., and Nicolaï, B. M. (2021). Effect of controlled atmosphere storage on the quality attributes and volatile organic compounds profile of dragon fruit (*Hylocereus undatus*). *Postharvest Biol. Technol*. 173:111406. doi: 10.1016/j.postharvbio.2020.111406

Ho, Q. T., Hertog, M. L. A. T. M., Verboven, P., Ambaw, A., Rogge, S., Verlinden, B. E., et al. (2018). Down-regulation of respiration in pear fruit depends on temperature. *J. Exp. Bot*. 69, 2049–2060. doi: 10.1093/jxb/ery031

Ho, Q. T., Buts, K., Herremans, E., Hertog, M. L. A. T. M., Verboven, P., and Nicolai, B. M. (2014). "Hypoxic storage of fruit"," in *Low-Oxygen Stress in Plants*, eds J. T. van Dongen and F. Licausi (Wien: Springer-Verlag), 353–369. doi: 10.1007/978-3-7091-1254-0_18

Ho, Q. T., Verboven, P., Verlinden, B. E., Herremans, E., Wevers, M., Carmeliet, J., et al. (2011). A three-dimensional multiscale model for gas exchange in fruit. *Plant Physiol*. 155, 1158–1168. doi: 10.1104/pp.110.169391

Hossain, M. A., and Uddin, S. N. (2011). Mechanisms of waterlogging tolerance in wheat: Morphological and metabolic adaptations under hypoxia or anoxia. *Aust. J. Crop Sci*. 5, 1094–1101. doi: 10.3316/informit.044652841339657

Huang, Z., Guo, L., Wang, H., Qu, H., Ma, S., Liu, Y., et al. (2014). Energy status of kiwifruit stored under different temperatures or exposed to long-term anaerobic conditions or pure oxygen. *Postharvest Biol. Technol*. 98, 56–64. doi: 10.1016/j.postharvbio.2014.07.008

Huang, S., Colmer, T. D., and Millar, A. H. (2008). Does anoxia tolerance involve altering the energy currency towards PPi? *Trends Plant Sci*. 13, 221–227. doi: 10.1016/j.tplants.2008.02.007

Igamberdiev, A. U., and Hill, R. D. (2018). Elevation of cytosolic Ca^{2+} in response to energy deficiency in plants: the general mechanism of adaptation to low oxygen stress. *Biochem. J.* 475, 1411–1425. doi: 10.1042/BCJ20180169

Imahori, Y., Kohei Yamamoto, K., Tanaka, H., and Bai, J. (2013). Residual effects of low oxygen storage of mature green fruit on ripening processes and ester biosynthesis during ripening in bananas. *Postharvest Biol. Technol.* 77, 19–27. doi: 10.1016/j.postharvbio.2012.11.004

Imahori, Y., Kota, M., Ueda, Y., Yoshioka, H., and Chachin, K. (1998). Relationship between low-oxygen induced injury and respiration in several fruits under hypoxia. *J. JPN. Food Stor. Sci. Soc.* 5, 303–308. doi: 10.5891/jafps.24.303

Ioannidi, E., Kalamaki, M. S., Engineer, C., Pateraki, I., Alexandrou, D., Mellidou, I., et al. (2009). Expression profiling of ascorbic acid-related genes during tomato fruit development and ripening and in response to stress conditions. *J. Exp. Bot.* 60, 663–678. doi: 10.1093/jxb/ern322

Jackson, M. B., Davis, D. D., and Lambers, H. (1991). *Plant Life Under Oxygen Deprivation: Ecology, Physiology and Biochemistry*. The Hague: SAB Academic Publishing.

Jiang, Y., Su, X., Duan, X., Lin, W., and Li, W. (2004). Anoxia treatment for delaying skin browning, inhibiting disease development and maintaining the quality of litchi fruit. *Food Technol. Biotechnol.* 42, 131–134.

Kader, A. A. (1994). "Modified and controlled atmosphere storage of tropical fruits," in *Postharvest Handling of Tropical Fruits*, eds B. R. Champ, E. Highley, and J. I. Johnson (Australia: ACIAR Proceedings), 239–249.

Kader, A. A., and Saltveit, M. E. (2003). "Respiration and gas exchange," in *Postharvest Physiology and Pathology of Vegetables*, eds J. A. Bartz and J. K. Brecht (New York: Marcel Dekker), 7–29.

Kato-Noguchi, H., and Morokum, M. (2007). Ethanolic fermentation and anoxia tolerance in four rice cultivars. *J. Plant Physiol.* 164, 168–173. doi: 10.1016/j.jplph.2005.09.017

Kemp, H. R. (1987). The effect of temperature and pressure on equilibria: A derivation of the van't Hoff rules. *J. Chem. Educ.* 64, 482–484. doi: 10.1021/ed064p482

Kennedy, R. A., Rumpho, M. E., and Fox, T. C. (1992). Anaerobic metabolism in plants. *Plant Physiol.* 100, 1–6. doi: 10.1104/pp.100.1.1

Kidd, F., and West, C. (1927a). *Relation Between the Respiratory Activity and the Keeping Quality of Apples*. Report of the Food Investigation Board for 1925. London, UK: DSIR.

Kidd, F., and West, C. (1927b). *A Relation between the Concentration of Oxygen and Carbon Dioxide in the Atmosphere, Rate of Respiration, and Length of Storage Life of Apples. Report of the Food Investigation Board for 1925, 1926*. London, UK: DSIR.

Koch, K. E., Ying, Z., Wu, Y., and Avigne, W. (2000). Multiple paths of sugar-sensing and a sugar/oxygen overlap for genes of sucrose and ethanol metabolism. *J. Exp. Bot.* 51, 417–427. doi: 10.1093/jexbot/51.suppl_1.417

Knee, M. (1991). "Fruit metabolism and practical problems of fruit storage under hypoxia and anoxia," in *Plant Life under Oxygen Deprivation: Ecology, Physiology and Biochemistry*, eds M. B. Jackson, D. D. Davies, and H. Lamberts (The Hague: SPB Academic Publishing), 229–243.

Kolb, R. M., and Joly, C. A. (2010). Germination and anaerobic metabolism of seeds of *Tabebuia cassinoides* (Lam.) DC subjected to flooding and anoxia. *Flora Morphol. Dist. Func. Ecol. Plants* 205, 112–117. doi: 10.1016/j.flora.2009.01.001

Kongpatjirak, P., Safitri, A. A., and Setha, S. (2016). Pre-storage anoxia treatment affects fruit quality, antioxidant properties, and shelf life of mango. *J. Food Sci. Agric. Technol.* 2, 1–5.

Kotula, L., Clode, P. L., Striker, G. G., Pedersen, O., Lauchli, A., Shabala, S., et al. (2015). Oxygen deficiency and salinity affect cell-specific ion concentrations in adventitious roots of barley (*Hordeum vulgare*). *New Phytol.* 208, 1114–1125. doi: 10.1111/nph.13535

Kulichikhin, K. Y., Aitio, O., Chirkova, T. V., and Fagerstedt, K. V. (2007). Effect of oxygen concentration on intracellular pH, glucose-6-phosphate and NTP content in rice (Oryza sativa) and wheat (*Triticum aestivum*) root tips: In vivo 31P-NMR study. *Physiol. Plant.* 129, 507–518. doi: 10.1111/j.1399-3054.2006.00819.x

Lee, D. J., Chi, Y. T., Kim, D. M., Choi, S. H., Lee, J. Y., and Choi, G. W. (2014). Ectopic expression of CaRLK1 enhances hypoxia tolerance with increasing alanine production in Nicotiana spp. *Plant Mol. Biol.* 86, 255–270. doi: 10.1007/s11103-014-0227-4

Leshuk, J. A., and Saltveit, M. E. Jr. (1990). A simple system for the rapid determination of the anaerobic compensation point of plant tissue. *HortScience* 25, 480–482. doi: 10.21273/HORTSCI.25.4.480

Licausi, F. (2011). Regulation of the molecular response to oxygen limitations in plants. *New Phytol.* 190, 550–555. doi: 10.1111/j.1469-8137.2010.03562.x

Licausi, F., Weits, D. A., Pant, B. D., Scheible, W. R., Geigenberger, P., and van Dongen, J. T. (2010b). Hypoxia responsive gene expression is mediated by various subsets of transcription factors and miRNAs that are determined by the actual oxygen availability. *New Phytol.* 190, 442–456. doi: 10.1111/j.1469-8137.2010.03451.x

Licausi, F., Van Dongen, J. T., Giuntoli, B., Novi, G., Santaniello, A., Geigenberger, P., et al. (2010a). HRE1 and HRE2, two hypoxia−inducible ethylene response factors, affect anaerobic responses in Arabidopsis thaliana. *Plant J.* 62, 302–305. doi: 10.1111/j.1365-313X.2010.04149.x

Lindberg, S., Kader, M. A., and Yemelyanov, V. (2012). "Calcium signalling in plant cells under environmental stress," in *Environmental Adaptations and Stress Tolerance of Plants in the Era of Climate Change*, eds P. Ahmad and M. Prasad (New York, NY: Springer), 325–360. doi: 10.1007/978-1-4614-0815-4_15

Liu, T., Wang, H., Kuang, J., Sun, C., Shi, J., Duan, X., et al. (2015). Short-term anaerobic, pure oxygen and refrigerated storage conditions affect the energy status and selective gene expression in litchi fruit. *LWT Food Sci. Technol.* 60, 1254–1261. doi: 10.1016/j.lwt.2014.09.003

Liu, H., Song, L. L., Jiang, Y. M., Joyce, D. C., Zhao, M. M., You, Y., et al. (2007). Short-term anoxia treatment maintains tissue energy levels and membrane integrity and inhibits browning of harvested litchi fruit. *J. Sci. Food Agric.* 87, 1767–1771. doi: 10.1002/jsfa.2920

Lizada, M. C. C., and Rumbaoa, R. A. (2017). Ethylene and the adaptive response of mango to hypoxia. *Acta Hortic.* 1178, 143–146. doi: 10.17660/ActaHortic.2017.1178.25

Loreti, E., and Perata, P. (2020). The many facets of hypoxia in plants. *Plants* 9:745. doi: 10.3390/plants9060745

Lurie, S., and Tonutti, P. (2014). Heat and hypoxia stress and their effects on stored fruits. *Stewart Postharvest Rev.* 3, 1–7.

Mariani, L., and Ferrante, A. (2017). Agronomic management for enhancing plant tolerance to abiotic stresses–drought, salinity, hypoxia, and lodging. *Horticulturae* 3:52. doi: 10.3390/horticulturae3040052

Mathooko, F. M. (1996). Regulation of ethylene biosynthesis in higher plants by carbon dioxide. *Postharvest Biol. Technol.* 7, 1–26. doi: 10.1016/0925-5214(95)00026-7

Min, T., Fang, F., Ge, H., Shi, Y. N., Luo, Z. R., Yao, Y. C., et al. (2014). Two novel anoxia-induced ethylene response factors that interact with promoters of deastringency-related genes from persimmon. *PLoS One* 9:e97043. doi: 10.1371/journal.pone.0097043

Minh, N. T. (2017). Investigation of MAP for durian preservation. *Int. J. Appl. Eng. Res.* 24, 15298–15303.

Mithran, M., Paparelli, E., Novi, G., Perata, P., and Loreti, E. (2010). Analysis of the role of the pyruvate decarboxylase gene family in *Arabidopsis thaliana* under low-oxygen conditions. *Plant Biol.* 16, 28–34. doi: 10.1111/plb.12005

Mojeviæ, M. V., and Tešanoviæ, D. B. (2011). Influence of short anoxia treatment and maturation on quality and storage of tomatoes. *J. Agric. Sci.* 56, 121–131. doi: 10.2298/JAS1102121M

Morrell, S., Greenway, H., and Davis, D. D. (1990). Regulation of pyruvate decarboxylase in vitro and in vivo. *J. Exp. Bot.* 41, 131–139. doi: 10.1093/jxb/41.2.131

Mustroph, A., Lee, S. C., Oosumi, T., Zanetti, M. E., Yang, H., Ma, K., et al. (2010). Cross-kingdom comparison of transcriptomic adjustments to low-oxygen stress highlights conserved and plant-speci?c responses. *Plant Physiol.* 152, 1484–1500. doi: 10.1104/pp.109.151845

Nakamura, M., and Noguchi, K. (2020). Tolerant mechanisms to O_2 deficiency under submergence conditions in plants. *J. Plant Res.* 133, 343–371. doi: 10.1007/s10265-020-01176-1

Nover, L. (1989). "Anaerobic stress," in *Heat Shock and Other Stress Responses Systems of Plants*, eds L. Nover, D. Neumann, and D. D. Scharf (New York: Springer Verlag), 69–90.

O'Hare, T. J., Prasad, A., and Cooke, A. W. (1994). Low temperature and controlled atmosphere storage of rambutan. *Postharvest Biol. Technol*. 4, 147–157. doi: 10.1016/0925-5214(94)90016-7

Palma, T., Stanley, D. W., Aguillera, J. M., and Zoffoli, J. P. (1993). Respiratory behavior of cherimoya (*Annona cherimola* Mill.) under controlled atmospheres. *HortScience* 8, 647–549. doi: 10.21273/HORTSCI.28.6.647

Palmes, E. D., and Lindenboom, R. H. (1979). Ohm's law, Fick's law, and diffusion samplers for gases. *Anal. Chem*. 51, 2400–2401. doi: 10.1021/ac50050a026

Palomer, X., Roig-Villanova, I., Grima-Calvo, D., and Vendrell, M. (2005). Effects of nitrous oxide (N_2O) treatment on the postharvest ripening of banana fruit. *Postharvest Biol. Technol*. 36, 167–175. doi: 10.1016/j.postharvbio.2004.12.008

Paull, R. E., and Duarte, O. (2011). *Tropical Fruits*. Vol. 1. Wallingford, UK: CABI Publisher.

Paull, R. E., and Duarte, O. (2012). *Tropical Fruits*. Vol. 2. Wallingford, UK: CABI Publisher.

Pegoraro, P., Schreinert dos Santos, R., Krüger, M. M., Tieche, A., Carlos da Maia, L., Rombaldi, C. V., et al. (2012). Effects of hypoxia storage on gene transcript accumulation during tomato fruit ripening. *Braz. J. Plant Physiol*. 24, 141–148. doi: 10.1590/S1677-04202012000200007

Peppenlenbos, H. W., Tijskens, L. M. M., Vant'Leven, J., and Wilkinson, E. C. (1996). Modelling oxidative and fermentation carbon dioxide production of fruits and vegetables. *Postharvest Biol. Technol*. 9, 283–295. doi: 10.1016/S0925-5214(96)00029-4

Perata, P., and Alpi, A. (1993). Plant responses to anaerobiosis. *Plant Sci*. 93, 1–17. doi: 10.1016/0168-9452(93)90029-Y

Perata, P., Geshi, N., Akazawa, T., and Yamaguchi, J. (1993). Effect of anoxia on the induction of α-amylase in cereal seeds. *Planta* 191, 402–408. doi: 10.1007/BF00195699

Perata, P., Pozueta-Romero, J., Akazawa, T., and Yamaguchi, J. (1992). Effect of anoxia on starch breakdown in rice and wheat seeds. *Planta* 188, 611–618. doi: 10.1007/BF00197056

Pesis, E., Marinansky, R., Zauberman, G., and Fuchs, Y. (1994). Prestorage low-oxygen atmosphere treatment reduces chilling injury symptoms in 'Fuerte' avocado fruit. *HortScience* 29, 1042–1046. doi: 10.21273/HORTSCI.29.9.1042

Pfister-Sieber, M., and Brändle, R. (1994). Aspects of plant behaviour under anoxia and post-anoxia. *P. Roy. Soc. Edinb. B* 102B, 313–324. doi: 10.1017/S0269727000014305

Phonyiam, O., Kongsuwan, A., and Setha, S. (2016). Effect of short-term anoxic treatment on internal browning and antioxidant ability in pineapple cv. *Phulae. Int. Food Res. J*. 23, 521–527.

Platenius, H. (1942). The effects of respiration rate and respiratory quotient of some vegetables. *Plant Physiol*. 17, 179–197. doi: 10.1104/pp.17.2.179

Porat, R., and Falik, E. (2008). "Production of off-flavours in fruit and vegetables under fermentative conditions," in *Fruit and Vegetable Flavour. Recent Advances and Future Prospects*, eds B. Brückner and S. G. Wyllie (Cambridge: Woodhead Publishing), 150–164. doi: 10.1533/9781845694296.2.150

Ratcliffe, R. G. (1995). "Metabolic aspects of the anoxic response in plant tissue," in *Environment and Plant Metabolism*, ed. N. Smirnoff (London: Bios Scientific Publishers), 111–127.

Ricard, B., Couee, I., Raymon, P., Saglio, P. H., Stanet-Ges, V., and Pradet, A. (1994). Plant metabolism under anoxia. *Plant Physiol. Biochem*. 32, 1–10.

Rogiers, S. Y., and Knowles, N. R. (1998). Effects of storage temperature and atmosphere on saskatoon (*Amelanchier alnifolia* Nutt.) fruit quality, respiration and ethylene production. *Postharvest Biol. Technol*. 13, 183–190. doi: 10.1016/S0925-5214(98)00012-X

Rohani, M. Y., Zaipun, M. Z., and Norhayati, M. (1997). Effect of modified atmosphere on the storage life and quality of Eksotika papaya. *J. Trop. Agric. Food Sci*. 25, 103–113.

Saglio, P. H. (1985). Effect of path or sink anoxia on sugar translocation in roots of maize seedlings. *Plant Physiol*. 77, 285–290. doi: 10.1104/pp.77.2.285

Salvador, A., Arnal, L., Besada, C., Larrea, V., Hernando, I., and Pérez-Munuera, I. (2008). Reduced effectiveness of the treatment for removing astringency in persimmon fruit when stored at 15°C: Physiological and microstructural study. *Postharvest Biol. Technol*. 49, 340–347. doi: 10.1016/j.postharvbio.2008.01.015

Salvatierra, A., Toro, G., Mateluna, P., Opazo, I., Ortiz, M., and Pimentel, P. (2020). Keep calm and survive: Adaptation strategies to energy crisis in fruit trees under root hypoxia. *Plants* 9:1108. doi: 10.3390/plants9091108

Samson, J. A. (1986). *Trop Fruits*. New York, NY: Longman.

Sanders, M. G., and de Wild, H. P. J. (2003). The relation between in vivo ethylene production and oxygen partial pressure. *Postharvest Biol. Technol*. 30, 143–151. doi: 10.1016/S0925-5214(03)00102-9

Schmidt, R. S., Fulda, M., Paul, M. V., Anders, M., Plum, F., Weits, D. A., et al. (2018). Low-oxygen response is triggered by an ATP-dependent shift in oleoyl-CoA in Arabidopsis. *Proc. Natl. Acad. Sci. U. S. A*. 115, E12101–E12110. doi: 10.1073/pnas.1809429115

Sedbrook, J. C., Kronebusch, P. J., Borisy, G. G., Trewavas, A. J., and Masson, P. H. (1996). Transgenic AEQUORIN reveals organ-specific cytosolic Ca^{2+} responses to anoxia in *Arabidopsis thaliana* seedlings. *Plant Physiol*. 111, 243–257. doi: 10.1104/pp.111.1.243

Subbaiah, C. C., Bush, D. S., and Sachs, M. M. (1998). Mitochondrial contribution to the anoxic Ca^{2+} signal in maize suspension-cultured cells. *Plant Physiol*. 118, 759–771. doi: 10.1104/pp.118.3.759

Summers, J. E., Ratcliffe, R. G., and Jackson, M. B. (2000). Anoxia tolerance in the aquatic monocot *Potamogeton pectinatus*: absence of oxygen stimulates elongation in association with an unusually large Pasteur effect. *J. Exp. Bot*. 51, 1413–1422. doi: 10.1093/jexbot/51.349.1413

Techavuthiporn, C., Boonyaritthongchai, P., and Supabvanich, S. (2017). Physicochemical changes of "Phulae" pineapple fruit treated with short-term anoxia during ambient storage. *Food Chem*. 228, 388–393. doi: 10.1016/j.foodchem.2017.02.028

Toro, G., and Pinto, M. (2015). Plant respiration under low oxygen. *Chil. J. Agric. Res*. 75, 57–70. doi: 10.4067/S0718-58392015000300007

van Dongen, J. T., and Licausi, F. (2015). Oxygen sensing and signaling. *Annu. Rev. Plant Biol*. 66, 345–367. doi: 10.1146/annurev-arplant-043014-114813

van't Hoff, M. J. H. (1884). Etudes de dynamique chimique. *Rec. Trav. Chim. Pays Bas* 3, 333–336. doi: 10.1002/recl.18840031003

Varoquaux, P., Gouble, B., Baron, C., and Yildiz, F. (1992). Respiratory parameters and sugar catabolism of mushroom (*Agaricus bisporus* Lange). *Postharvest Biol. Technol*. 16, 51–61. doi: 10.1016/S0925-5214(99)00004-6

Venkatram, A., Bhagwan, A., Pratap, M., and Reddy, D. V. V. (2016). Effect of modified atmosphere package on physicochemical characteristics of 'Balanagar" custard apple (*Annona squamosa* L.) fruits stored at 15 ±1 °C. *Int. J. Sci. Nat*. 7, 332–338.

Ventura, I., Brunello, L., Iacopino, S., Valeri, M. C., Novi, G., Dornbusch, T., et al. (2020). Arabidopsis phenotyping reveals the importance of alcohol dehydrogenase and pyruvate decarboxylase for aerobic plant growth. *Sci. Rep*. 10:16669. doi: 10.1038/s41598-020-73704-x

Wade, N. L. (1974). Effects of oxygen concentration and ethephon upon the respiration and ripening of banana fruits. *J. Exp. Bot*. 25, 955–964. doi: 10.1093/jxb/25.5.955

Waghmare, R. B., Mahajan, P. V., and Annapure, U. S. (2013). Modelling the effect of time and temperature on respiration rate of selected fresh-cut produce. *Postharvest Biol. Technol*. 80, 25–30. doi: 10.1016/j.postharvbio.2013.01.012

Watkins, C. B. (2000). Responses of horticultural commodities to high carbon dioxide as related to modified atmosphere packaging. *HortTechnol* 10, 502–506. doi: 10.21273/HORTTECH.10.3.501

Wang, F., Chen, Z. H., and Shabala, S. (2017). Hypoxia sensing in plants: On a quest for ion channels as putative oxygen sensors. *Plant Cell Physiol*. 58, 1126–1142. doi: 10.1093/pcp/pcx079

Wongs-Aree, C., and Noichinda, S. (2018). "Glycolysis fermentative by-products and secondary metabolites involved in plant adaptation under hypoxia during pre- and postharvest," in *Hypoxia and Anoxia*, eds K. Das and M. S. Biradar (London: IntechOpen Publisher), 59–72. doi: 10.5772/intechopen.80226

Wongs-Areea, C., and Noichinda, S. (2014). ""Postharvest physiology and quality maintenance of tropical fruits"," in *Postharvest Handling. A System Approach*, eds W. J. Florowski, R. L. Shewfelt, S. E. Prussia, and N. Banks (Amsterdam: Academic Press), 275–312.

Wu, W., Wang, M. M., Gong, H., Liu, X. F., Guo, D. L., Sun, N. J., et al. (2020). High CO_2/hypoxia-induced softening of persimmon fruit is modulated by DkERF8/16 and DkNAC9 complexes. *J. Exp. Bot*. 71, 2690–2700. doi: 10.1093/jxb/eraa009

Yahia, E. M., and Vazquez-Moreno, L. (1993). Responses of mango to insecticidal oxygen and carbon dioxide atmospheres. *LWT Food Sci. Technol*. 26, 42–48. doi: 10.1006/fstl.1993.1008

Yemelyanov, V. V., Chirkova, T. V., Shishova, M. F., and Lindberg, S. M. (2020). Potassium efflux and cytosol acidification as primary anoxia-induced events in wheat and rice seedlings. *Plants* 9:1216. doi: 10.3390/plants9091216

Yemelyanov, V. V., Shishova, M. F., Chirkova, T. V., and Lindberg, S. M. (2011). Anoxia-induced elevation of cytosolic Ca^{2+} concentration depends on different Ca2+ sources in rice and wheat protoplasts. *Planta* 234, 271–280. doi: 10.1007/s00425-011-1396-x

Yi, C., Jiang, Y. M., Sun, J., Luo, Y. B., Jiang, W. B., and Macnish, A. (2006). Effects of short-term N_2 treatments on ripening of banana fruit. *J. Hortic. Sci. Biotechnol.* 81, 1025–1028. doi: 10.1080/14620316.2006.11512166

Zahra, N., Hafeez, M. B., Shaukat, K., Wahid, A., Hussain, S., Naseer, R., et al. (2021). Hypoxia and Anoxia Stress: Plant responses and tolerance mechanisms. *J. Agro. Crop Sci.* 207, 249–284. doi: 10.1111/jac.12471

Zhang, Z., Huber, D. J., and Rao, J. (2011). Ripening delay of mid-climacteric avocado fruit in response to elevated doses of 1-methylcyclopropene and hypoxia-mediated reduction in internal ethylene concentration. *Postharvest Biol. Technol.* 60, 83–91. doi: 10.1016/j.postharvbio.2011.01.001

Zhu, Q. G., Gong, Z. Y., Wang, M. M., Li, X., Grierson, D., Yin, X. R., et al. (2018). A transcription factor network responsive to high CO2/hypoxia is involved in deastringency in persimmon fruit. *J. Exp. Bot.* 69, 2061–2070. doi: 10.1093/jxb/ery028

Conflict of Interest: The author declares that the research was conducted in the absence of any commercial or financial relationships that could be construed as a potential conflict of interest.

frontiers in Plant Science

ORIGINAL RESEARCH
published: 16 July 2021
doi: 10.3389/fpls.2021.685416

Transcriptome Responses of Ripe Cherry Tomato Fruit Exposed to Chilling and Rewarming Identify Reversible and Irreversible Gene Expression Changes

Donald A. Hunter[1], Nathanael J. Napier[1], Zoe A. Erridge[1], Ali Saei[1†], Ronan K. Y. Chen[1], Marian J. McKenzie[1], Erin M. O'Donoghue[1], Martin Hunt[1], Laurie Favre[1,2], Ross E. Lill[1] and David A. Brummell[1]*

[1] The New Zealand Institute for Plant & Food Research Limited, Food Industry Science Centre, Palmerston North, New Zealand, [2] Centre for Postharvest and Refrigeration Research, Massey University, Palmerston North, New Zealand

OPEN ACCESS

Edited by:
Claudio Bonghi,
University of Padua, Italy

Reviewed by:
De-Mei Meng,
Tianjin University of Science and Technology, China
Shifeng Cao,
Zhejiang Wanli University, China
Nicola Busatto,
Fondazione Edmund Mach, Italy

***Correspondence:**
David A. Brummell
david.brummell@plantandfood.co.nz

†Present address:
Ali Saei,
BioLumic Ltd., Palmerston North, New Zealand

Specialty section:
This article was submitted to Crop and Product Physiology, a section of the journal Frontiers in Plant Science

Received: 25 March 2021
Accepted: 21 June 2021
Published: 16 July 2021

Citation:
Hunter DA, Napier NJ, Erridge ZA, Saei A, Chen RKY, McKenzie MJ, O'Donoghue EM, Hunt M, Favre L, Lill RE and Brummell DA (2021) Transcriptome Responses of Ripe Cherry Tomato Fruit Exposed to Chilling and Rewarming Identify Reversible and Irreversible Gene Expression Changes. Front. Plant Sci. 12:685416. doi: 10.3389/fpls.2021.685416

Tomato fruit stored below 12°C lose quality and can develop chilling injury upon subsequent transfer to a shelf temperature of 20°C. The more severe symptoms of altered fruit softening, uneven ripening and susceptibility to rots can cause postharvest losses. We compared the effects of exposure to mild (10°C) and severe chilling (4°C) on the fruit quality and transcriptome of 'Angelle', a cherry-type tomato, harvested at the red ripe stage. Storage at 4°C (but not at 10°C) for 27 days plus an additional 6 days at 20°C caused accelerated softening and the development of mealiness, both of which are commonly related to cell wall metabolism. Transcriptome analysis using RNA-Seq identified a range of transcripts encoding enzymes putatively involved in cell wall disassembly whose expression was strongly down-regulated at both 10 and 4°C, suggesting that accelerated softening at 4°C was due to factors unrelated to cell wall disassembly, such as reductions in turgor. In fruit exposed to severe chilling, the reduced transcript abundances of genes related to cell wall modification were predominantly irreversible and only partially restored upon rewarming of the fruit. Within 1 day of exposure to 4°C, large increases occurred in the expression of alternative oxidase, superoxide dismutase and several glutathione S-transferases, enzymes that protect cell contents from oxidative damage. Numerous heat shock proteins and chaperonins also showed large increases in expression, with genes showing peak transcript accumulation after different times of chilling exposure. These changes in transcript abundance were not induced at 10°C, and were reversible upon transfer of the fruit from 4 to 20°C. The data show that genes involved in cell wall modification and cellular protection have differential sensitivity to chilling temperatures, and exhibit different capacities for recovery upon rewarming of the fruit.

Keywords: tomato (*Solanum lycopersicum*), chilling injury, fruit softening, cell wall modifying genes, heat shock protein genes

INTRODUCTION

Tomato is an originally tropical fruit that requires postharvest storage above 12°C to avoid deleterious effects on flavor (Maul et al., 2000). Storage at lower temperatures is used to prolong storage life and enable shipping to more distant markets, but can result in severe chilling injuries including surface pitting, uneven or partial ripening, reduced softening, accelerated softening, mealiness, water-soaking, and susceptibility to rots (Cheng and Shewfelt, 1988; Jackman et al., 1992; Lurie and Sabehat, 1997; Devaux et al., 2005; Vega-Garcia et al., 2010; Rugkong et al., 2011; Biswas et al., 2012; Albornoz et al., 2019). Chilling injuries are thought to result initially from phase transitions of cell membranes and increases in reactive oxygen species (ROS) such as superoxide radical, hydrogen peroxide and hydroxyl radical, which if not detoxified cause inactivation of enzymes, degradation of proteins and DNA, and lipid peroxidation that compromises membrane function (Sevillano et al., 2009). Membrane deterioration can lead to impaired ATP biosynthesis, reduced respiration, and leakage of ions, metabolites and water between cell compartments or out of the cell, and even cell rupture.

Tomato is a well-established model system for understanding ripening, but less is known about its responses to stress. The susceptibility of tomato fruit to chilling injury varies with cultivar and ripening stage. Frequently the most severe symptoms appear when green or breaker fruit are transferred to shelf temperatures of 20–22°C for ripening, after storage below approximately 6°C for 2 weeks or more (Biswas et al., 2016). If ripening is already advanced prior to cold storage, fruit are more resistant to chilling stress, display fewer chilling injury symptoms, and can be stored at lower temperatures and for longer periods than mature green or breaker fruit (Hobson, 1987; Gómez et al., 2009). Previous studies of transcriptome responses to chilling stress in tomato have used fruit harvested and stored at the mature-green or breaker stages, where ripening processes form a major part of transcriptional activity (Cruz-Mendívil et al., 2015; Albornoz et al., 2019; Zhang et al., 2019; Tang et al., 2020). The transcriptome responses to chilling stress of cherry tomato fruit that have already achieved full ripeness prior to cold storage are currently unknown.

Ripening in tomato involves changes in gene expression controlling accumulation of the carotenoid lycopene, alterations to sugar and organic acid composition, production of aroma volatiles, and changes to fruit firmness and textural properties. Chilling injury affects the gene expression of many of these aspects of the ripening program (Zhang et al., 2019; Tang et al., 2020), as well as the ethylene signaling and response pathway (Rugkong et al., 2011). Fruit softening during normal ripening is caused by reductions in cell turgor (Shackel et al., 1991) and by a range of modifications to the cell wall and middle lamella brought about by enzymes secreted from the symplast into the apoplast (Brummell and Harpster, 2001). Cell wall changes include depolymerization of homogalacturonan and hemicelluloses, demethylesterification of homogalacturonan, solubilization of pectins and hemicelluloses, and loss of pectic β-galactan and α-arabinan side chains (Brummell, 2006). Together, these changes alter polysaccharide structure and the bonding between polymers in the wall, causing wall swelling and reducing wall strength and intercellular adhesion. The enzymes involved are encoded by ripening-related members of gene families including polygalacturonase (PG), pectate lyase (PL), pectin methylesterase (PME), expansin (EXP), endo-1,4-β-glucanase ("cellulase," Cel), xyloglucan endo-transglycosylase/hydrolase (XTH), β-galactosidase and α-arabinofuranosidase.

An extended storage life enables produce to be shipped by sea rather than by air, but after cold storage fruit need to possess an acceptable shelf-life at 20°C. In this study, we examined the effects of long-term mild and severe chilling on ripe fruit of a relatively chilling-resistant cultivar, 'Angelle', of the cherry tomato type. This cultivar is commercially harvested at the red ripe stage and shows extensive postharvest storage life, even at 20°C. Two storage temperatures, 10 and 4°C, were chosen as a way to separate gene expression responses to mild and severe cold stress, and to investigate which gene expression changes were reversible upon rewarming of the fruit. Since fruit were already ripe at harvest and exhibiting full color, genes related to fruit softening and responses to oxidative and abiotic stress, rather than carotenoid accumulation or ripening transcription factors, were chosen for examination during cold storage.

MATERIALS AND METHODS

Fruit Material

Fruit of cherry tomato (*Solanum lycopersicum* var. *cerasiforme* L.) 'Angelle' were obtained from a packhouse at commercial ripeness during the middle of the production season in 2018 and 2019. Plastic clamshell punnets each containing 20–23 fruit arrived at the research facility the day after packing, and were stored overnight at 20°C to ensure evaporation of surface condensation moisture.

In each of the two experiments, one set of replicates was processed after the overnight storage at 20°C (termed Day 0). In the first experiment (year 2018, total of 30 punnets), storage at three different temperatures was compared. One set of punnets was maintained at 20°C for 6 days to study development at a typical shelf temperature. Half the remaining punnets were placed in cold storage at 10°C and the other half at 4°C, representing mild and severe chilled storage conditions, respectively. Samples were removed at 6 and 27 days, with further sets of replicates stored for 27 days plus an additional 1 and 6 days at 20°C. In the second experiment (year 2019, total of 21 punnets), the focus was on earlier molecular responses to chilling temperature. Punnets were stored at 4°C, with replicates removed after 1, 4, 12, and 19 days. Additional replicates were removed at 12 and 19 days and transferred to 20°C for 7 days. A schematic representation of the experimental design is shown in **Supplementary Figure 1**. At each temperature/time

point, analysis was carried out using three biological replicates (punnets of fruit).

Physiological Measurements

Firmness was measured on a TA.XT Plus Texture Analyser (Stable Micro Systems, Godalming, United Kingdom) with a 75-mm compression plate attachment. The force required for compression of 0.5 mm was measured at a test speed of 0.5 mm s^{-1}, with a trigger force of 10 g. Three biological replicates were analyzed at each time point, comprising eight fruit per biological replicate punnet. Three independent firmness measurements were taken at different locations on each fruit, avoiding the locule wall ($n = 72$).

Free juice was measured using a modification of the method developed for peach by Lill and van der Mespel (1988). Free juice was estimated in fruit stored at 20°C for 6 days (never exposed to cold), and for fruit stored for 27 days at 4 or 10°C plus 20°C for 6 days. For each fruit, a shallow cut was made in the skin in the shape of a 1-cm square, the peel carefully removed and the underlying pericarp excised. An identical piece of pericarp was excised from the opposite side of the same fruit. The two pericarp pieces were blotted dry of surface juice and locule gel then both placed in a 5-mL disposable syringe (Terumo, Somerset, NJ, United States) with luer taper (aperture ∼1.5 mm) but without a needle. The tissue (∼0.9–1.4 g) was pushed through the syringe into a weighed microfuge tube, which was re-weighed then the homogenate was centrifuged at 13,000*g* for 5 min. The supernatant was transferred to a new weighed tube, and the weight of the supernatant calculated as a percentage of the weight of the homogenate. Six fruit per treatment were assessed, two from each of three different replicate punnets.

RNA Isolation, RNA-Seq Library Construction and Sequencing

Fruit pericarp tissue was separated from locule walls and seeds, then the pericarp was snap frozen in liquid nitrogen. For each temperature/time point there were three biological replicates (punnets), each consisting of four pooled fruit. The tissue was ground to a fine powder under liquid nitrogen conditions using an analytical grinding mill. RNA was isolated using a modified CTAB method (Gambino et al., 2008), using aliquots of 300 mg of ground tissue in 900 μL of CTAB buffer. Final RNA pellets were washed with 70% ethanol and resuspended in 33 μL of sterile water. RNA samples were quantified using a NanoDrop 1000 Spectrophotometer (Thermo Fisher Scientific, Auckland, New Zealand) and RNA integrity assessed using a Standard Sensitivity RNA Analysis Kit (DNF-471) on a Fragment Analyzer 5300 System (Agilent Technologies, Santa Clara, CA, United States). All samples had an $A_{260/280}$ ≥1.8 and an RNA Integrity Number ≥8. Samples for Experiment 1 were sent to the Australian Genome Research Facility (Melbourne, Australia) for library preparation and 100 bp paired end sequencing on a NovaSeq platform. Samples for Experiment 2 were sent via Custom Science (Auckland, New Zealand) to a sequencing center for stranded RNA library preparation and 150 bp paired end sequencing on a HiSeq platform.

RNA-Seq Analysis

Raw read quality was assessed using FastQC software[1]. SortMeRNA (Kopylova et al., 2012) was used to filter rRNA from the raw reads. Trimmomatic (Bolger et al., 2014) with settings "HEADCROP:10 SLIDINGWINDOW:5:20 MINLEN:50" was used to trim the low quality reads and sequencing adapters. The trimmed reads were mapped to the *S. lycopersicum* build_3.00 genome using STAR (Dobin et al., 2013) with default parameters. HTSeq-count supplied with ITAG3.2 gene models was used to compute the number of raw reads mapped to each gene.

For differential expression analysis, input genes were initially filtered to remove genes with mean counts of less than 200 across all samples. Gene counts of filtered reads were normalized using the Relative Log Expression method of DESeq2 with default parameters (Love et al., 2014).

The pairwise gene selection method was used to select the top 50 most variable genes per pairwise comparison, and principal component analysis (PCA) performed using the FactoMineR package[2]. Genes for cluster analysis (displayed in the expression pattern figures) were first identified as having a fold change of >3-fold up or down and P-value < 0.01. They then underwent variance stabilizing transformation and hierarchical clustering using the "complete" clustering and "euclidean" distance methods. For heat maps, coloration was performed in Excel (Microsoft, Seattle, WA, United States) using conditional formatting and the red, yellow, green color scale with red for the highest transcript abundance. The conditional formatting was performed on each row separately so that the highest and lowest values for each transcript were colored red and green, respectively.

Enriched biological themes and KEGG pathways were identified using the DAVID Gene Functional Classification Tool[3] (Huang et al., 2009) with a >2-fold change criteria for the gene lists. Gene stable IDs in the gene list were first converted to UniProtKB/TrEMBL IDs at Biomart[4] and used as input into DAVID where they were converted to Entrez IDs for annotation enrichment analysis. The analysis identified enrichment in the gene sets of KEGG pathways[5], and Functional Annotational Clustering was used to identify further enriched biological themes within the gene sets.

RESULTS

Characterization of Chilling Effects

Ripe tomato fruit were exposed to either 10°C or 4°C chilled storage conditions for various times to discover the effects of mild and severe temperature stress on gene expression and chilling injury. Fruit were fully ripe at harvest, as shown by measurements of fruit color, which did not increase in redness relative to Day 0 during storage at either 20 or 10°C (**Supplementary Figure 2**).

[1]http://www.bioinformatics.babraham.ac.uk/projects/fastqc/

[2]http://factominer.free.fr/citation.html

[3]https://david.ncifcrf.gov/tools.jsp

[4]https://plants.ensembl.org/biomart/martview/

[5]https://www.genome.jp/kegg/pathway.html

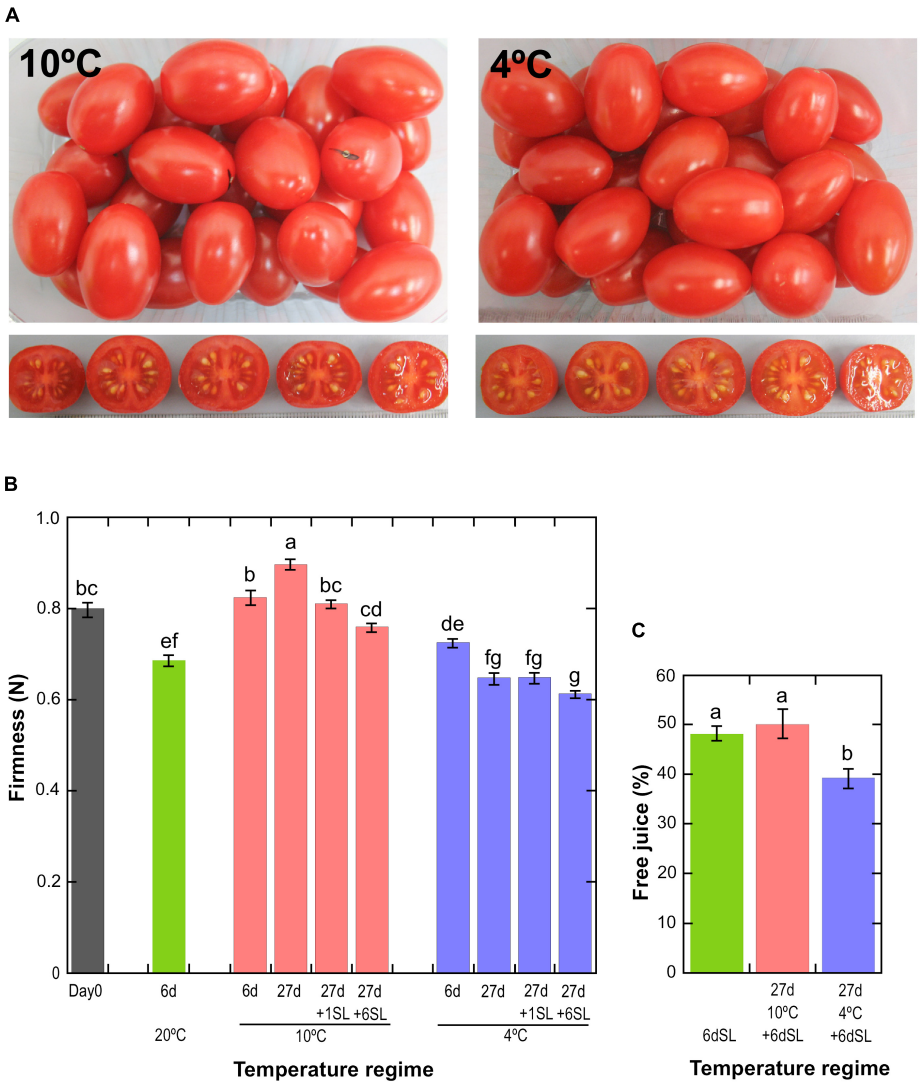

FIGURE 1 | Physiological effects of storage at different temperatures. **(A)** Fruit appearance after storage at 10 or 4°C for 27 days, followed by an additional 6 days at a shelf temperature of 20°C. **(B)** Mean fruit firmness ± SE (n = 72) measured by compression. Storage at 20°C for 6 days, or 10 or 4°C for up to 27 days with or without an additional shelf-life (SL) period of 1 or 6 days. Means not sharing a common letter are significantly different between groups at P = 0.05 as determined by LSD after a one-way ANOVA. **(C)** Mean pericarp free juice ± SD (n = 6) as determined using a homogenate and centrifugation method. Fruit were stored for 6 days at 20°C, without or with prior storage for 27 days at 10 or 4°C. Means not sharing a common letter are significantly different between groups at P = 0.001 as determined by LSD after a one-way ANOVA.

The slight reduction in the redness of fruit stored at 4°C is a mild chilling injury (**Supplementary Figure 2**). Even after storage for 27 days at 10 or 4°C followed by an additional 6 days at shelf-life conditions of 20°C, ripe 'Angelle' fruit did not display the visible symptoms of chilling injury often seen in unripe cold-stored fruit such as pitting, shriveling, soft patches or rots (**Figure 1A**). However, textural deterioration in the form of differential softening and mealiness in response to storage at different temperatures was observed. Storage of fruit for 6 days at three different temperatures showed that fruit stored at 10°C did not soften significantly relative to Day 0, whereas fruit stored at 20 or 4°C did soften (**Figure 1B**). Fruit stored at 10°C for 27 days actually tended to increase in firmness, before softening after transfer to shelf-life conditions of 20°C. Fruit stored at 4°C for 27 days softened considerably in comparison to fruit stored at 10°C, and this accelerated softening is a well-known chilling damage (Jackman et al., 1992). Transition of fruit stored at 4°C to a shelf temperature of 20°C induced little additional loss of firmness, suggesting that ripening-related softening barely resumed upon transfer to warmer temperatures.

A common symptom of chilling injury in fleshy fruit is the development of mealiness, which is caused by alterations in cell wall metabolism that affect the properties of pectin, resulting in the binding of free water and a higher degree of cell separation that causes reduced cell breakage upon biting and chewing (Lurie and Crisosto, 2005). The condition is characterized by a dry

texture and lack of free juice, but is not due to whole-fruit water loss. Mealiness is the major chilling injury symptom in cold-stored peaches (Lurie and Crisosto, 2005) but tomatoes are also susceptible (Jackman et al., 1992), and the condition can be assessed by measuring free juice (**Figure 1C**). Fruit stored for 6 d at 20°C (never exposed to cold) or stored for 27 days at 10°C followed by 6 days at 20°C yielded approximately 50% free juice, but this was reduced to 40% if fruit had been stored at 4°C. This shows that a degree of mealiness had developed during storage at severe chilling temperature. There were no significant differences in whole-fruit weight loss between the different storage regimes (**Supplementary Figure 3**).

Expression Patterns in Response to Mild or Severe Chilling Stress

Transcriptome profiling by RNA-Seq was performed after various periods of exposure to mild or severe chilling temperature, followed in some cases by a recovery period at 20°C. Sequencing depth was good, with an average of 18.5 million uniquely mapped reads per sample in Experiment 1 and 13.9 million in Experiment 2 (**Supplementary Table 1**).

i) Transcriptional dynamics during mild and severe chilling

In the first experiment, tomato fruit were exposed to 20°C for 6 days, or 10°C or 4°C for 6 or 27 days. PCA of the 720 most variable genes (derived from the 50 most variable genes in each of the pairwise comparisons) showed that the three replicates of each treatment clustered closely together (**Figure 2A**). This indicated that the transcriptome response of the biological replicates was consistent for each of the treatments. The majority of the dataset variance was explained by Component 1 (45.09% of the variance) and was associated with the temperature response, with increasing storage time and decreasing temperature shifting the samples further from the Day 0 control. Conversely, returning the stored fruit to 20°C shifted the cold-stored samples closer to the Day 0 samples, suggesting that the transcriptome response to temperature was in part reversible. Less of the variance (28.18%) was explained by Component 2, and this appeared to be associated with the progression of development, since the samples held at 20°C for 6 days were further away from Day 0 samples on this axis, but not on the Component 1 axis.

Comparisons at 6 days among the three different storage temperatures found that, relative to 20°C, fewer genes were up-regulated by exposure to 4°C than were down-regulated (291 versus 478 using a >3-fold change criterion, **Figure 2B**). Of the 291 genes that were up-regulated, 153 were chilling-specific and showed altered expression only at 4°C. Of the 478 genes that were down-regulated at 4°C, 260 were chilling-specific. The number of genes specifically up- or down-regulated at 4 vs 20°C far exceeded the numbers with altered expression specifically at 4 vs 10°C or 10 vs 20°C. Only 15 genes (six up-regulated and nine down-regulated, 1.67% of the total) showed altered gene expression in all three temperature comparisons.

The 291 genes up-regulated and 478 genes down-regulated at 4°C were categorized into four up-regulated and four down-regulated expression patterns by hierarchical clustering (**Figures 2C,D**). The number of genes in the clusters ranged from 1 to 215, and the genes comprising each cluster are listed in **Supplementary Table 2**. Relative to storage for an equivalent time at 20°C, the largest increase in transcript abundance specifically in response to chilling temperature was the single gene in Cluster 1 (**Figure 2C**), encoding a Small Auxin Up-Regulated (SAUR)-like auxin-responsive family protein (Solyc06g053260.1.1), whose transcript abundance was 190-fold higher at 4°C but only four-fold higher at 10°C. Genes with a similar but less extreme expression pattern in Cluster 3 included an alternative oxidase (Solyc08g075540.4.1), a glutathione S-transferase (Solyc12g011310.2.1) and two Dicer-like ribonucleases (Solyc11g008530.2.1, Solyc11g008540.2.1). The 45 genes in Cluster 2 had similar transcript abundances at both 4 and 10°C, and showed an increase partly because transcript abundance at 20°C had declined. Cluster 4 contained genes with only a moderate increase at 4°C. In contrast, the transcript abundance of many genes was negatively affected by chilling temperatures (**Figure 2D**). In Cluster 5, expression of 16 genes was dramatically down-regulated (some by >1000-fold) at 4°C, but were also significantly down-regulated at 10°C. This group included the ripening-related cell wall-modifying genes *EXP1*, *XTH5* and *Cel2*. Genes in Cluster 7 were affected similarly by 4 and 10°C, and included *PME2*. The vast majority of down-regulated genes were in Clusters 6 and 8, showing moderate reduction in transcript abundance at 4°C and also some reduction at 10°C. Cluster 8 included β-galactosidase *TBG4* and *XYL1*.

ii) Rapidity and reversibility of severe chilling-induced expression changes

In Experiment 2, 'Angelle' fruit were exposed to 4°C for 1, 4, 12, and 19 days, with an additional storage period of 7 days at 20°C after the latter two times. This experiment focused on the rapidity of transcriptome responses to chilling and the potential for recovery at a shelf temperature of 20°C. PCA analysis confirmed that all replicates grouped together, and that exposure to chilling temperature caused substantial shifts to the left in Component 1 (representing 64.55% of the variance) (**Figure 3A**). Movement was relatively large at 1 and 4 days, less so at 12 days and no further shift to the left occurred at 19 days. Between 1 and 19 days there was a shift down in Component 2 (representing 17.78% of the variance). An additional 7 days at shelf temperature after cold storage for 12 or 19 days caused a shift to the right in Component 1, almost back to the equivalent position of Day 0 prior to cold exposure, but still separated from Day 0 in Component 2. PCA analysis of the combined data from both seasons showed largely harmonious agreement between the two experiments (**Supplementary Figure 4**).

Differentially expressed genes were determined at 4 and 12 days of storage at chilling temperature, relative to expression at Day 0. Some genes were differentially expressed at only one of the two times and these were eliminated to concentrate on the 373 genes up-regulated and 415 genes down-regulated at both times (**Figure 3B**). The expression patterns of these gene sets were again split into four up-regulated and four down-regulated groups based on hierarchical clustering (**Figures 3C,D** and **Supplementary Table 3**). For up-regulated

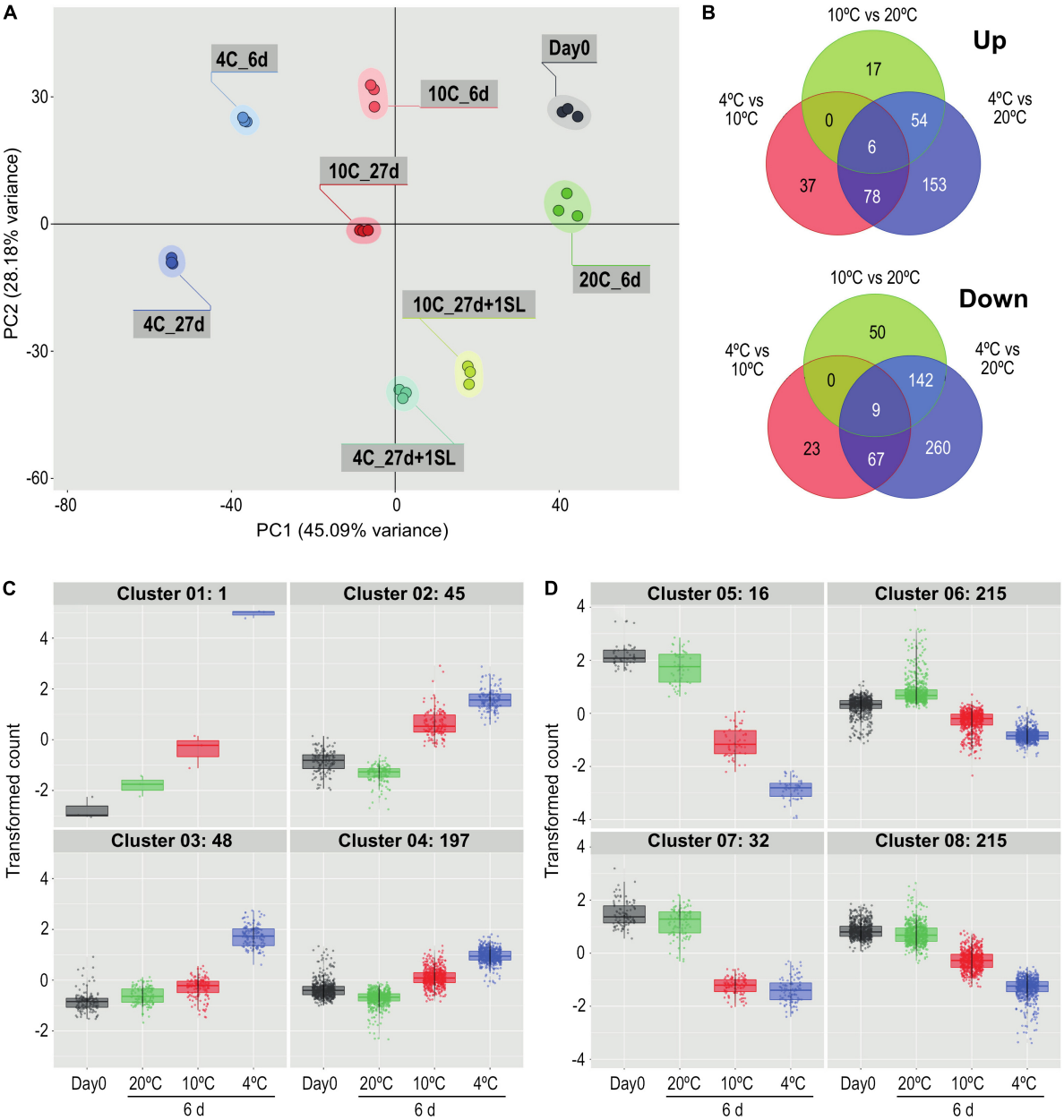

FIGURE 2 | Comparison of the effects of storage at different temperatures on the ripe tomato fruit transcriptome. **(A)** Principal component analysis of transcriptome profiles based on the 50 most variable genes in each pairwise comparison (total of 720 most variable genes), showing changes during storage at 4, 10, or 20°C. An additional 1-day period at a shelf-life (SL) temperature of 20°C was also included after 27 days. **(B)** Venn diagrams showing numbers of genes differentially expressed at 4, 10, and 20°C at 6 days of storage. For each pairwise comparison, the count values in the lower temperature treatment were compared with those in the higher temperature treatment. **(C,D)** Hierarchical cluster analysis of the gene sets that were up-regulated (291) and down-regulated (478) from the entire blue circles of **(B)** obtained from the 4°C versus 20°C comparison. Expression patterns were clustered into four groups each for up-regulated **(C)** and down-regulated **(D)** genes. Genes were considered differentially expressed if they had a mean count in all compared samples of 200 or more, an adjusted *P*-value of 0.01 and >3-fold increase or decrease.

genes, the number of genes in the clusters varied between 4 and 330 (**Figure 3C**). Cluster 1 contained the genes that showed the most rapid and largest increase in transcript abundance at 4°C, and whose transcript abundance returned to close to pre-exposure values upon rewarming. This cluster included the SAUR-like auxin-responsive family protein (Solyc06g053260.1.1) highlighted in Experiment 1. Clusters 2–4 contained genes with a similar expression profile to Cluster 1, but were less dramatically increased or were not able to return to Day 0 values after rewarming. Cluster 4 contained numerous genes involved in amelioration of stress, including an alternative oxidase (Solyc08g075540.4.1), a superoxide

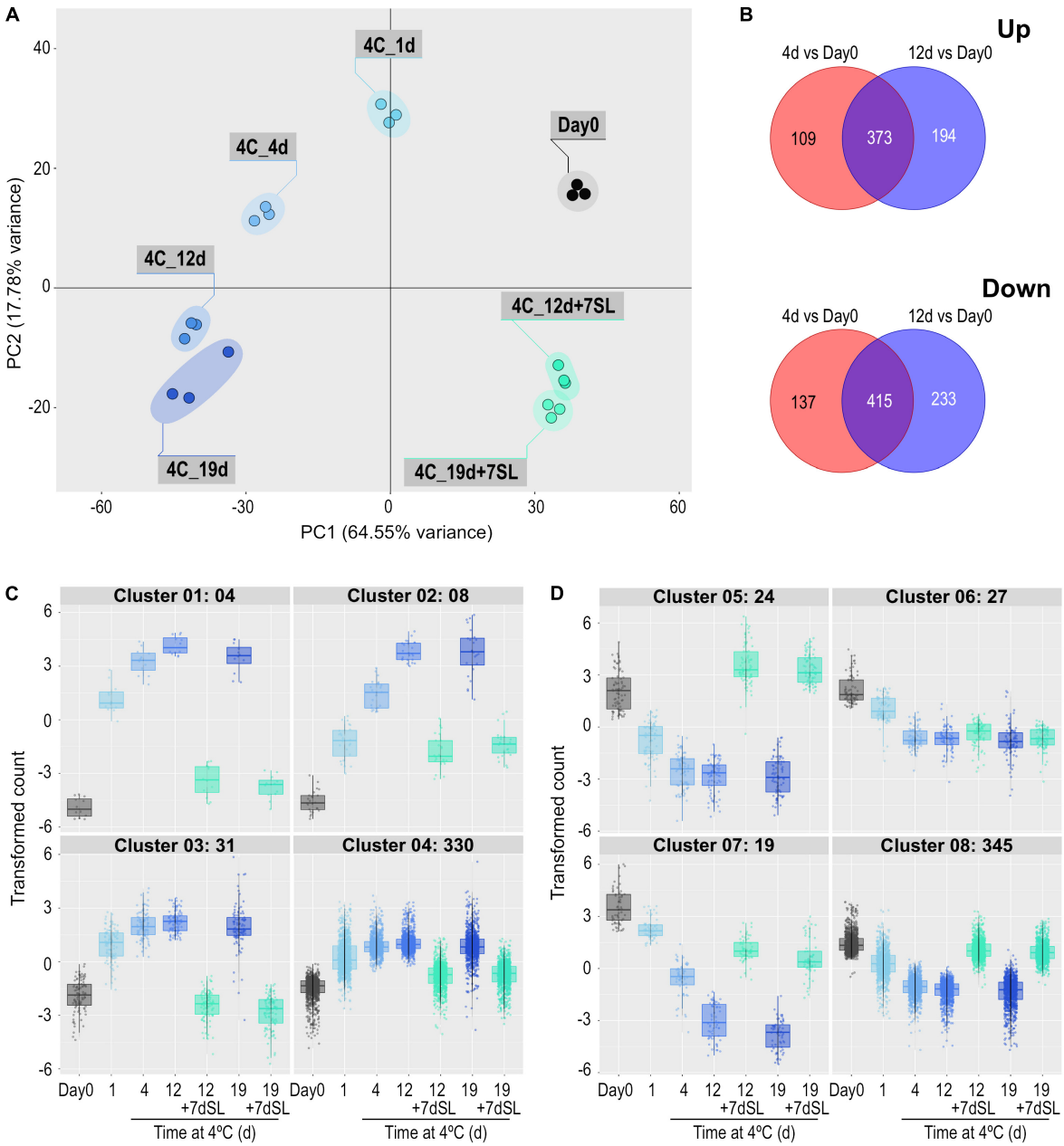

FIGURE 3 | Effect of storage at 4°C for various times on the ripe tomato fruit transcriptome. An additional 7-day period at a shelf-life (SL) temperature of 20°C was also included after 12 and 19 days. **(A)** Principal component analysis of transcriptome profiles based on the 50 most variable genes in each pairwise comparison (total of 617 most variable genes). **(B)** Venn diagrams showing numbers of genes differentially expressed at 4 and 12 days of exposure to 4°C, relative to Day 0. **(C,D)** Hierarchical cluster analysis of the gene sets that were up-regulated (373) and down-regulated (415) at both time points compared with Day 0. Expression patterns were clustered into four groups each for up-regulated **(C)** and down-regulated **(D)** genes. Genes were considered differentially expressed if they had a mean count in all compared samples of 200 or more, an adjusted *P*-value of 0.01 and >3-fold increase or decrease.

dismutase (Solyc09g082690.3.1), four glutathione S-transferases, and numerous heat shock proteins (HSPs) and chaperonin proteins. Relative to Day 0, a large number of genes were progressively down-regulated during chilling (**Figure 3D**). Those in Cluster 5 increased to above the Day 0 value upon subsequent transfer to shelf temperature, those in Clusters 7 and 8 were able to return partially or almost completely to pre-exposure mRNA abundances upon rewarming, while those in Cluster 6 remained mostly depressed. Several genes putatively involved in ripening-related cell wall modification were in these clusters: *XTH5* was in Cluster 5, pectate lyase *PL* in Cluster 6, *EXP1*, *Cel2*, and *PME2* in Cluster 7, and *TBG4* and *PME1.9* in Cluster 8. The ripening-related transcription factor *COLORLESS NON-RIPENING* (*CNR*) was also in Cluster 8.

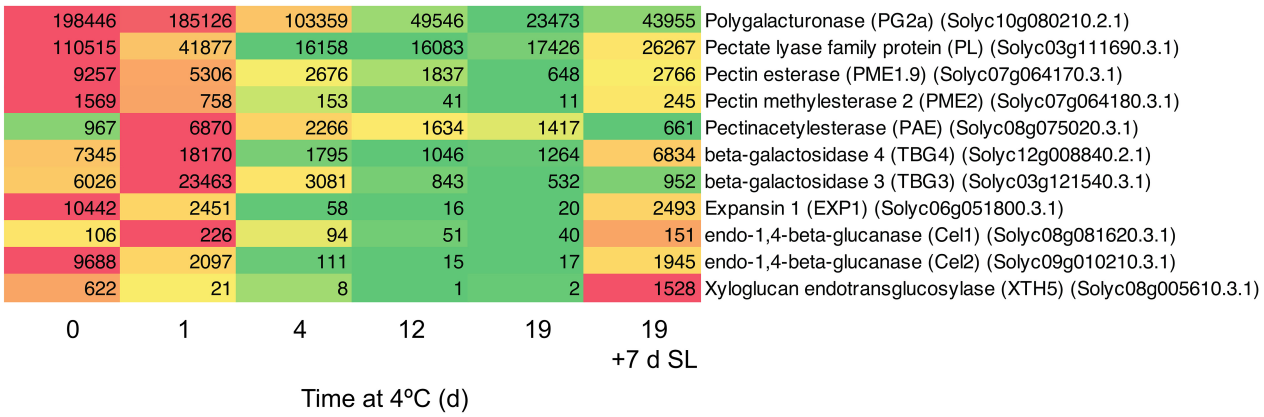

FIGURE 4 | Heat map showing cell wall modification-related genes differentially expressed in response to storage at 4°C. An additional 7-day period at a shelf-life (SL) temperature of 20°C was also included after 19 days. Red and green colors represent high and low mRNA abundance, respectively, within each transcript. Numbers in the boxes are DESeq2 mean normalized counts using the median of ratios method.

Effects of Chilling on Transcripts Encoding Genes Related to Cell Wall Modification

Since both accelerated softening and the development of mealiness may be related to cell wall metabolism, the expression of genes encoding enzymes involved in cell wall modification was examined in detail. In general, genes involved in cell wall modification were down-regulated in response to chilling (**Figure 4**). After 1 day of exposure to 4°C, some genes were slow to change in mRNA abundance (*PG2a*), some declined substantially (including *PL, EXP1, Cel2*), while others transiently increased (including *PAE, TBG3, TBG4*). However, with the exception of *PAE* which showed the opposite trend, by 4 days of exposure all were substantially lower than at Day 0 and remained so until 19 days. Upon the fruit returning to 20°C for 7 days, all of the genes with reduced mRNA abundance showed some increase, but only *TBG4*, *Cel1*, and *XTH5* achieved values close to or above the values at Day 0. This suggests that the ripening-related cell wall-modification program only partially resumed during rewarming to 20°C.

Effects of Chilling on Transcripts Encoding Genes Related to Stress Amelioration

A number of genes known to be involved in combating abiotic stress were up-regulated in response to chilling exposure. These included several genes encoding enzymes involved in scavenging ROS (**Figure 5A**). Within 1 day, the transcript abundance of an alternative oxidase increased by 49-fold, a superoxide dismutase by 15-fold and a major glutathione S-transferase by eight-fold. Expression remained elevated relative to Day 0 throughout 19 days of exposure to chilling, then declined substantially after 7 days of rewarming at 20°C. Interestingly, a catalase did not show this trend and was down-regulated during cold storage. Genes encoding a large number of heat shock, DNAJ and molecular chaperone proteins were also up-regulated (**Figure 5B**). Some of these increased to a maximum mRNA abundance after 1 day, others peaking at later times, but most remained at elevated abundance throughout the 19 days of chilling. A smaller number of similar proteins were down-regulated during exposure to chilling, suggesting that these were not directly involved in abiotic stress response. Upon transfer of the fruit to 20°C for 7 days, almost all the genes reverted to a transcript abundance similar to that prior to chilling exposure.

Transcripts Encoding Genes Related to Cell Wall Modification and Stress Amelioration Respond Differently to Mild and Severe Chilling

By comparing transcript abundance with that at Day 0 (rather than comparing 20, 10, and 4°C together at 6 days as shown in **Figure 2B**), the large number of genes up- or down-regulated at 4°C could be contrasted with the smaller number up- or down-regulated at 10°C (**Supplementary Table 4**). This showed that the antioxidant-related, HSP and chaperonin genes that were up-regulated at 4°C were not substantially up-regulated at 10°C (**Figure 6A**). In contrast, this comparison also showed that the majority of cell wall-related genes that were down-regulated at 4°C were also strongly down-regulated at 10°C (**Figure 6B**). Thus, cell wall-related gene expression (part of ripening) was sensitive to mild chilling temperatures of 10°C, but stress responses were not activated until a lower temperature was reached, such as 4°C.

Transcripts Showing Large Responses to Chilling Stress

The above two experiments have used different comparisons to identify cold-responsive genes, comparing the transcriptome of chilled fruit with that of fruit held for an equivalent time at a shelf temperature of 20°C, or to the transcriptome at Day 0 prior to cold exposure. In both cases, the genes

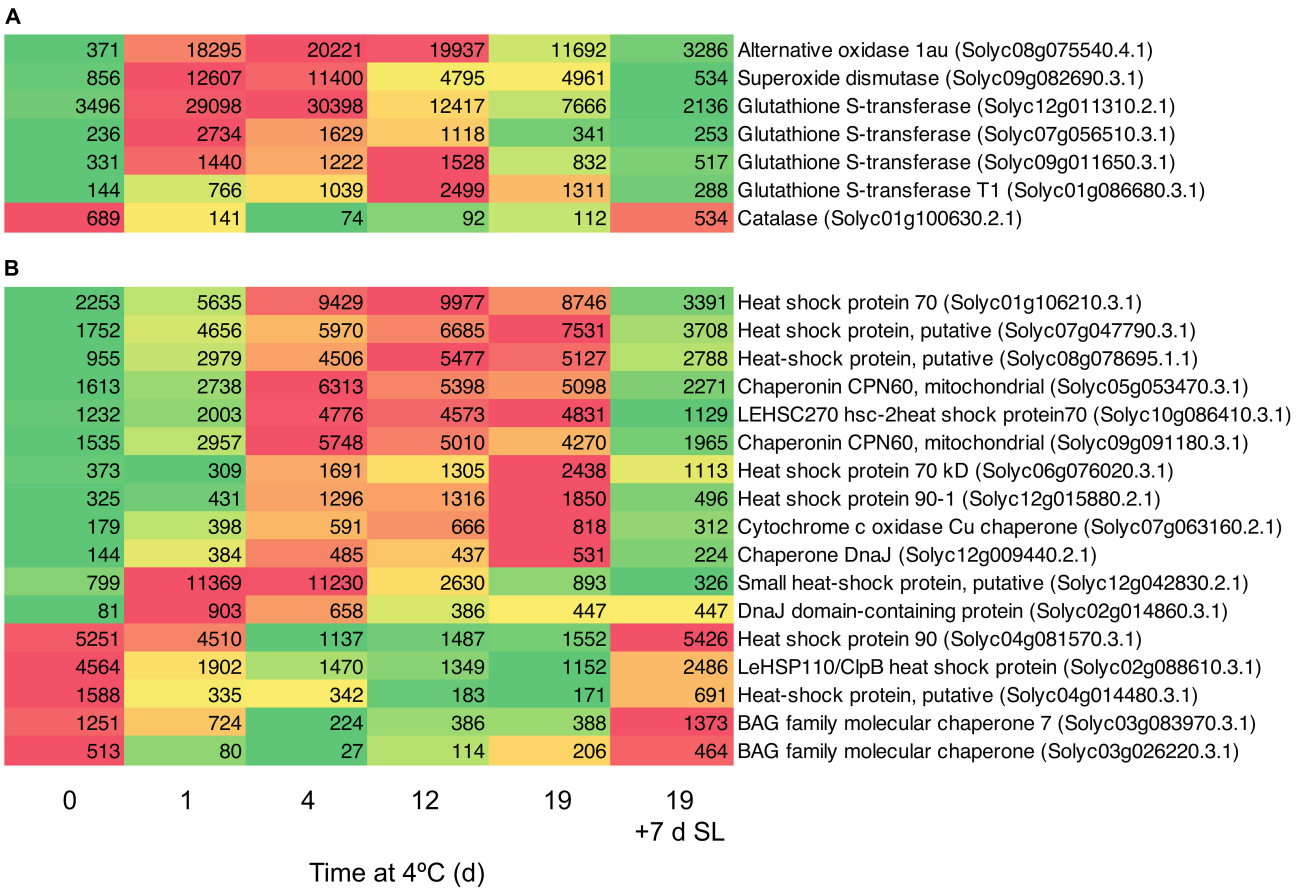

FIGURE 5 | Heat maps showing stress-related genes differentially expressed in response to storage at 4°C. An additional 7-day period at a shelf-life (SL) temperature of 20°C was also included after 19 days. **(A)** Genes encoding enzymes involved in oxidative stress. **(B)** Genes encoding heat shock and molecular chaperone proteins. Red and green colors represent high and low mRNA abundance, respectively, within each transcript. Numbers in the boxes are DESeq2 mean normalized counts using the median of ratios method.

identified as differentially expressed in response to cold were largely similar. The DAVID Gene Functional Classification Tool (Huang et al., 2009) was used to identify metabolic pathways highly enriched by exposure to chilling. The two most highly enriched pathways were "Proteasome" and "Ribosome biogenesis in eukaryotes" (**Figure 7** and **Supplementary Table 5**). The enrichment of pathways in protein degradation and biosynthesis suggests a strong metabolic re-alignment towards altering the protein composition of the cells in order to alleviate the abiotic stress.

Based on a comparison between Day 0 and 4 days of exposure to chilling, a number of genes showing the greatest fold increases (**Figure 8A**) or decreases (**Figure 8B**) were identified. Among the genes showing the greatest fold increases were a SAUR auxin-responsive family protein (increasing >1000-fold between 0 and 12 days), an alternative oxidase, two Dicer-like ribonucleases and the ripening-related transcription factor *TAG1*. The most down-regulated genes included *ECERIFERUM1*, a *ROX1* homolog (a transcription factor thought to act as a repressor of genes involved in hypoxia), and *EXP1* and *Cel2*. The data show that the expression of some genes is very highly responsive to chilling temperatures, and provide interesting avenues for further research.

Validation of Transcript Abundance Determinations

Validation of transcript abundances was performed by repeating each RNA-Seq experiment on a different tomato cultivar. Transcript abundance data for eight target genes described in this study and four reference genes is presented in **Supplementary Figure 6**. These data show that trends and transcript abundances were repeatable in different RNA-Seq experiments, across two years, in three different cultivars, each with three biological replicates.

DISCUSSION

The manifestation of chilling injury symptoms varies depending on cultivar, developmental stage and the temperatures experienced by the fruit during chilled storage. Cherry tomatoes harvested at the breaker stage and stored at 4 or

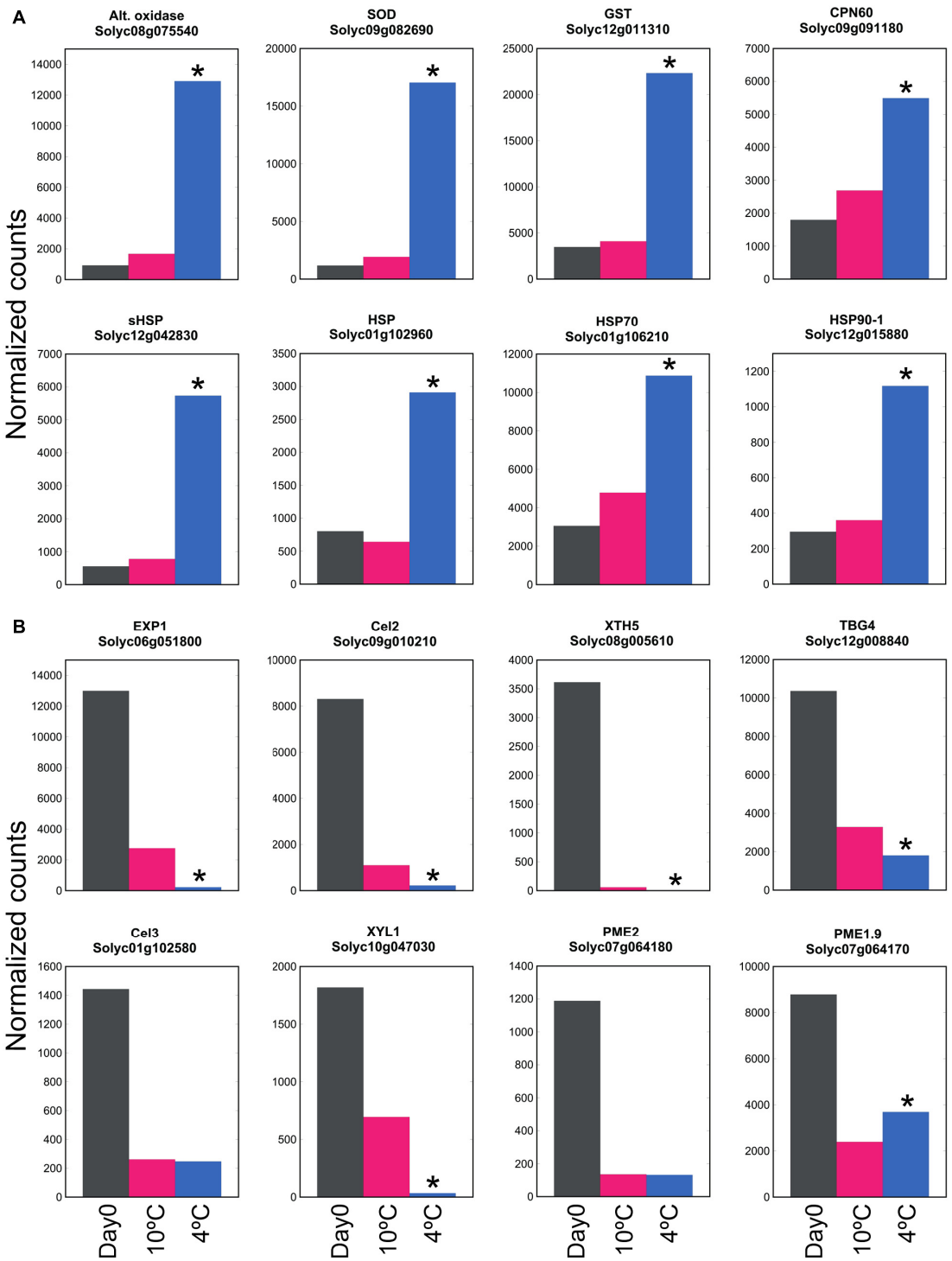

FIGURE 6 | Effect of exposure to mild or severe chilling temperature on transcript abundance of genes related to stress and ripening. **(A)** Oxidative and temperature stress. Genes encoding antioxidant enzymes, chaperonins and HSPs. **(B)** Genes related to cell wall modification. Fruit were exposed to 10 or 4°C for 6 days, and transcript abundance determined using RNA-Seq. Asterisks denote that transcript abundance at 4°C was significantly different to that at 10°C at $P < 0.05$.

5°C for 28 days displayed surface pitting and strongly impaired color development (and by inference ripening), which could not be reversed by an additional period of rewarming at 20°C (Albornoz et al., 2019; Zhang et al., 2019). In our experiments we subjected fruit which were already fully ripe to extended times at chilling temperature, with only slight effects on color

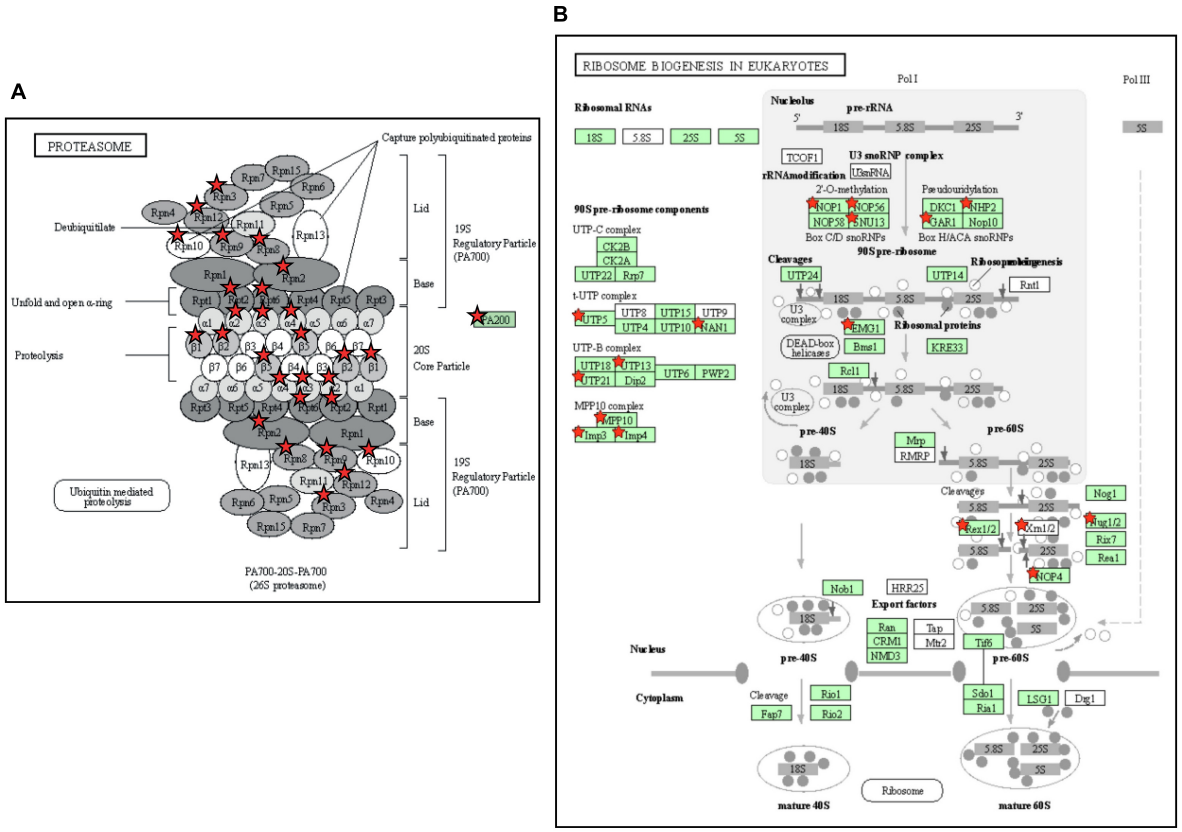

FIGURE 7 | Enrichment of pathways related to protein turnover in tomato fruit stored at 4°C. **(A)** The Proteasome pathway. The pathway was 10.3-fold enriched, with a *P*-value of 1.0e-11 and a False Discovery Rate of 7.4e-10. **(B)** The Ribosome Biogenesis in Eukaryotes pathway. The pathway was 6.2-fold enriched, with a *P*-value of 6.8e-9 and False Discovery Rate of 2.5e-7. Enriched KEGG pathways were identified using DAVID with 804 genes that exhibited a >2-fold increase in expression at both 4 and 12 days of storage relative to Day 0. Genes present in the gene set are highlighted with a red star. The gene set can be found in **Supplementary Table 5**. (To save space, panel A has been edited by moving the red stars from a separate table onto the proteasome cartoon. The original figure is shown in **Supplementary Figure 5**).

and no observable surface pitting. However, textural failure is one of the symptoms of chilling injury in tomato fruit, and can include reduced softening, accelerated softening and the development of mealiness (Jackman et al., 1992; Marangoni et al., 1995; Devaux et al., 2005). We found that ripe 'Angelle' fruit stored at 4°C softened more than fruit stored at 10°C (**Figure 1B**) and developed a degree of mealiness after transfer to 20°C (**Figure 1C**).

In contrast, mature green 'Caruso' fruit (a large loose cultivar) stored at 5°C for 28 days were firmer than non-chilled fruit (Jackman et al., 1992), although Marangoni et al. (1995) found that they became softer than non-chilled controls if at 15 days the cold-stored fruit were transferred to 22°C for 10 days. This group also found that the middle lamella of chilled fruit was swollen and less defined, and it was suggested that water moving from the symplast to the apoplast was absorbed by the swollen middle lamella, reducing cell turgor and contributing to chilling-induced softening (Marangoni et al., 1995). From a study comparing storage at two chilling temperatures, Biswas et al. (2014) concluded that storage at 6°C mainly induced loss of turgor, whereas storage at 2.5°C caused loss of both turgor and tissue integrity. An interesting observation was that fruit stored at 10°C became slightly firmer during storage (**Figure 1B**), although the fruit subsequently softened when transferred to 20°C. In cranberries stored under controlled atmosphere and in blueberries, firmness was also reported to increase during storage in still air (Gunes et al., 2002; Paniagua et al., 2013), possibly related to firming of the outer cell layers due to localized dehydration during low water loss, while high water loss was associated with softening (Paniagua et al., 2013).

Mealiness is associated with a lack of juiciness, and a soft, grainy, dry unpleasant taste that is lacking in aroma. In stonefruit, it cannot be detected from outside the fruit by measuring firmness (Lurie and Crisosto, 2005). In peach and apple, mealiness was correlated with reduced intercellular adhesion and water-soluble pectin, and with reduced activity or expression of many enzymes including PG and PME (Brummell et al., 2004; Billy et al., 2008; Segonne et al., 2014). Expression of genes encoding both of these enzymes was reduced by chilling in tomato (**Figure 4**). Since we found chilling of the fruit was accompanied by greater softening, it seemed surprising that within 4 days many of

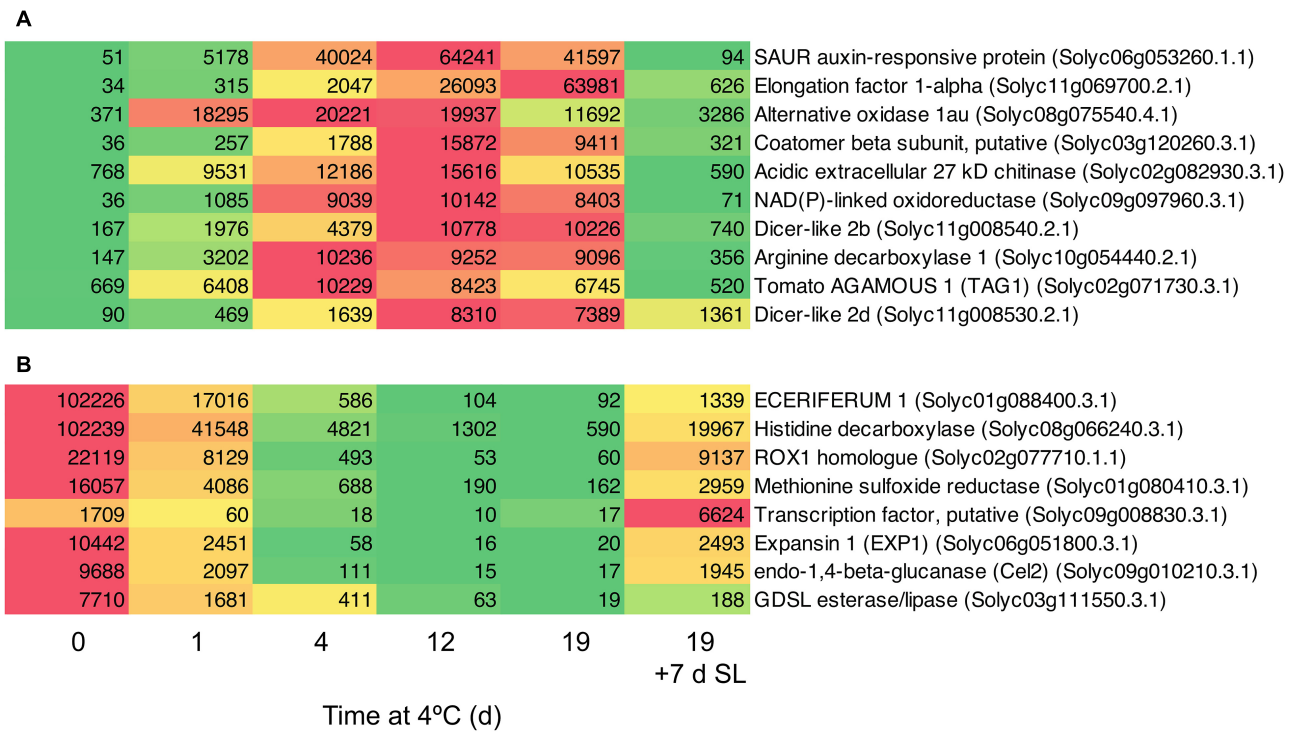

FIGURE 8 | Heat maps showing genes strongly differentially expressed in response to storage at 4°C. An additional 7-day period at a shelf-life (SL) temperature of 20°C was also included after 19 days. **(A)** Transcripts showing very large fold changes up in response to temperature. **(B)** Transcripts showing very large fold changes down in response to temperature. Red and green colors represent high and low mRNA abundance, respectively, within each transcript. Numbers in the boxes are DESeq2 mean normalized counts using the median of ratios method.

the genes associated with softening were down-regulated by chilling stress. However, since storage at 10 or 4°C caused a similar down-regulation of expression of genes involved in cell wall modification (**Figure 6B**) but had different effects on fruit softening (**Figure 1B**), this is consistent with severe chilling conditions also affecting factors other than cell wall modification, such as turgor.

Of 11 cell wall-related genes showing altered expression during chilling, 10 were down-regulated and exhibited some degree of up-regulation when the fruit were transferred to shelf temperature (**Figure 4**). For the majority of these genes the effects of chilling were only partially reversible, and transcript abundances after rewarming of the fruit were only a fraction of the Day 0 value. This suggests that any softening occurring during rewarming is due to a very limited resumption of cell wall disassembly caused by increased cell wall-related gene expression. In the cases of *PG2a, PL, EXP1, TBG3*, and *Cel2*, this was to less than 25% of the Day 0 value. Comparing mRNA abundance after an additional 7 days at 20°C with that at 19 days under chilling temperature conditions, the largest increases in fold terms were in *XTH5* (764-fold), *EXP1* (125-fold) and *Cel2* (114-fold). However, these increases were from a very low base and mRNA abundances of *EXP1* and *Cel2* were still only 25% that of the Day 0 value. Of these three genes, so far only *EXP1* has been shown to have a measurable effect on fruit softening (Brummell et al., 1999a,b; Saladié et al., 2006). More recent work has shown that the *PL* gene product is important in tomato fruit softening (Uluisik et al., 2016; Yang et al., 2017). *PL* mRNA abundance was high in ripe fruit at Day 0, and declined by ∼7-fold to a relatively constant abundance during 4–19 days of storage at 4°C (**Figure 4**). Upon transfer of the fruit to 20°C, *PL* mRNA abundance increased but by less than two-fold and also to only one-quarter of the Day 0 value.

Comparisons between studies using different cultivars, developmental stages and temperature regimes can be problematic, but using an *S. pennellii* – *S. lycopersicum* introgression line harvested at breaker and stored at 3°C for 14 days, Rugkong et al. (2011) observed limited recovery of mRNA abundance during subsequent rewarming for *PG2a*, *TBG4*, and *EXP1*, but not for *XTH5* or *PE1*. In mature green 'Micro-Tom' fruit, storage at 4°C for 7 days reduced mRNA abundances of *PME1, Cel1, EXP1*, *TBG4*, and *XTH5*, and expression of all of these recovered to some extent after transfer to 20°C for 2 days (Müller et al., 2013). However, 7 days at 4°C may not be sufficient to induce permanent chilling injury.

One of the earliest responses to chilling was a large increase in the transcript abundance of enzymes involved in combating oxidative stress. Within 1 day of exposure to 4°C, substantial increases in the transcript abundance of an alternative oxidase, superoxide dismutase, and several glutathione S-transferases were observed (**Figure 5A**). The

induction of a robust antioxidant system (Malacrida et al., 2006; Gómez et al., 2009; Vega-Garcia et al., 2010) and particularly alternative oxidase have been correlated with resistance to chilling injury in tomato as well as in pepper and banana (Fung et al., 2004, 2006; Albornoz et al., 2019; Hao et al., 2019). Upon rewarming of the fruit after severe chilling, transcript abundance changes in oxidative stress genes were almost entirely reversible (**Figure 5A**).

The small HSP Solyc12g042830.2.1 and the DNAJ domain-containing protein Solyc02g014860.3.1 were also up-regulated >10-fold within 1 day (**Figure 5B**). This was followed by slower increases in transcripts encoding a number of other HSPs and molecular chaperones, which remained elevated throughout chilling exposure. Upon rewarming of the fruit after severe chilling, transcript abundance changes in chaperonin-type genes were almost entirely reversible (**Figure 5B**). Strong cold-induced up-regulation of genes encoding numerous glutathione S-transferases and HSPs was also observed in 'Micro-Tom' (Cruz-Mendívil et al., 2015), a relatively chilling-tolerant cherry tomato line used for experimental studies (Luengwilai et al., 2012). A relationship between accumulation of small HSPs and resistance to chilling injury has been established in tomato (Sabehat et al., 1996, 1998), and appears to be common to many other species (Aghdam et al., 2013; Kashash et al., 2019). Small HSPs are believed to have a molecular chaperone function, stabilizing membranes and preventing proteins from mis-folding during heat, cold or oxidative stress (Sun et al., 2002). Comparisons of lines differing in chilling tolerance found that up-regulation of specific protein isoforms or transcripts occurred in chilling-tolerant cultivars, showing that only a few small HSPs contribute to better chilling resistance (Page et al., 2010; Ré et al., 2017). Similarly, in cold-stressed ripe tomato fruit that were analyzed prior to the symptoms of chilling injury becoming apparent, only certain HSPs and a single glutathione S-transferase showed increased protein abundance (Sanchez-Bel et al., 2012).

Cold storage of green or breaker tomato fruit down-regulates many pathways including those related to the ripening process (Rugkong et al., 2011; Zhang et al., 2019; Tang et al., 2020), but in the ripe fruit cold-affected transcriptome we detected two pathways that were strongly up-regulated. These were both related to protein metabolism: a proteasome pathway involved in protein degradation and a ribosome biogenesis pathway (**Figure 7**). In chilling-sensitive 'Heinz-722' mature-green fruit stored at 5°C, observations by electron microscopy showed that after 7 days the endoplasmic reticulum became dilated and ribosomes were lost, while membranes appeared degraded (Marangoni et al., 1989). In ripe 'p73', an early effect of cold stress (prior to symptoms becoming evident) was a down-regulation of the protein degradation machinery (Sanchez-Bel et al., 2012). These observations suggest that protein metabolism is an early casualty of cold stress. The subsequent up-regulation of pathways involved in ribosome biogenesis and protein degradation could be responses by the cell to counteract these chilling-induced degenerative processes.

Genes in Clusters 1 and 5 (**Figures 3C,D**) were highly responsive to temperature. In 'Micro-Tom', the rapid up-regulation of a dehydrin transcript has been proposed as a molecular marker of cold stress (Weiss and Egea-Cortines, 2009). The accumulation of HSPs has been proposed as a biochemical marker of chilling stress (Aghdam et al., 2013), and increased abundance of the corresponding *HSP* transcripts could also be used as molecular markers. However, we have identified genes with much greater increases in response to chilling stress than HSPs, particularly genes encoding a SAUR auxin-responsive protein, elongation factor 1-alpha, alternative oxidase, and a putative coatamer beta-subunit (**Figure 8A**). These showed massive increases in transcript abundance relative to Day 0 (the first two >1000-fold), with maxima at different times of chilling exposure. It may be possible to use these highly temperature-responsive transcripts for screening tomato lines for the timing and extent of responses to chilling stress. There may also be biochemical insights to be gained from the strong up-regulation of the *SAUR* gene in response to cold. The functions of SAUR proteins remain mainly elusive, but *SAUR* genes are responsive to abiotic stress and the proteins can interact with other hormonal pathways (Ren and Gray, 2015). In Arabidopsis, up-regulation of *AtSAUR32* regulates ABA-mediated responses to drought stress (He et al., 2021), and in chilled tomato fruit up-regulation of a *SAUR* may indicate the involvement of auxin pathways in cold response or chilling injury onset, which have previously been associated mainly with ethylene.

In conclusion, chilling injury in ripe 'Angelle' fruit was relatively modest even after extended storage at 4°C, consisting of slight color loss, accelerated softening and the development of mealiness. Decreases in the transcript abundance of many genes involved in cell wall disassembly, and the expected low activities of enzymes operating at 4°C, suggest that accelerated softening at such chilling temperatures was due to factors other than cell wall metabolism, such as reductions in turgor. Chilling-induced decreases in the expression of cell wall disassembly-related genes were only partially reversible upon rewarming of the fruit. Responses to cold stress included a rapid increase in the transcript abundance of several antioxidant-related genes involved in protection of the cell from oxidative damage, followed by large increases in HSPs and molecular chaperones. These increases were specific to 4°C, not being observed at 10°C, and were reversible when the fruit were rewarmed to a 20°C shelf temperature. Expression of pathways of genes involved in protein synthesis and degradation were also increased at 4°C, probably as the fruit responded to chilling-induced damage to the proteome.

DATA AVAILABILITY STATEMENT

The datasets presented in this study can be found in online repositories. The names of the repository/repositories and accession number(s) are: SRA NCBI, accession: PRJNA736844.

AUTHOR CONTRIBUTIONS

DH, RL, and DB conceived and planned the study. DH and NN carried out RNA-Seq data analysis and prepared the

figures. ZE and NN isolated RNA, AS created RNA-Seq analysis software. DH, NN, ZE, RC, MM, EO'D, MH, RL, and DB carried out fruit physiology measurements. LF carried out RNA-Seq data analysis. DB wrote the manuscript. All authors contributed to the article and approved the submitted version.

ACKNOWLEDGMENTS

We thank Jason Johnston for comments on the manuscript, Sheryl Somerfield for technical assistance, Duncan Hedderley for statistical analysis, T&G Global for gifting some of the fruit and Tony Corbett for assistance with the figures.

FUNDING

This project was funded by The New Zealand Institute for Plant and Food Research Limited's Strategic Science Investment Fund.

SUPPLEMENTARY MATERIAL

The Supplementary Material for this article can be found online at: https://www.frontiersin.org/articles/10.3389/fpls.2021.685416/full#supplementary-material

REFERENCES

Aghdam, M. S., Sevillano, L., Flores, F. B., and Bodbodak, S. (2013). Heat shock proteins as biochemical markers for postharvest chilling stress in fruits and vegetables. *Sci. Hort.* 160, 54–64. doi: 10.1016/j.scienta.2013.05.020

Albornoz, K., Cantwell, M. I., Zhang, L., and Beckles, D. M. (2019). Integrative analysis of postharvest chilling injury in cherry tomato fruit reveals contrapuntal spatio-temporal responses to ripening and cold stress. *Sci. Rep.* 9:2795. doi: 10.1038/s41598-019-38877-0

Billy, L., Mehanagic, E., Royer, G., Renard, C. M. G. C., Arvisenet, G., Prost, C., et al. (2008). Relationship between texture and pectin composition of two apple cultivars during storage. *Postharvest Biol. Technol.* 47, 315–324. doi: 10.1016/j.postharvbio.2007.07.011

Biswas, P., East, A. R., Brecht, J. K., Hewett, E. W., and Heyes, J. A. (2012). Intermittent warming during low temperature storage reduces tomato chilling injury. *Postharvest Biol. Technol.* 74, 71–78. doi: 10.1016/j.postharvbio.2012.07.002

Biswas, P., East, A. R., Hewett, E. W., and Heyes, J. A. (2014). Interpreting textural changes in low temperature stored tomatoes. *Postharvest Biol. Technol.* 87, 140–143. doi: 10.1016/j.postharvbio.2013.08.018

Biswas, P., East, A. R., Hewett, E. W., and Heyes, J. A. (2016). Chilling injury in tomato fruit. *Hortic. Rev.* 44, 229–278. doi: 10.1002/9781119281269.ch5

Bolger, A. M., Lohse, M., and Usadel, B. (2014). Trimmomatic: a flexible trimmer for Illumina sequence data. *Bioinformatics* 30, 2114–2120. doi: 10.1093/bioinformatics/btu170

Brummell, D. A. (2006). Cell wall disassembly in ripening fruit. *Funct. Plant Biol.* 33, 103–119. doi: 10.1071/fp05234

Brummell, D. A., Dal Cin, V., Lurie, S., Crisosto, C. H., and Labavitch, J. M. (2004). Cell wall metabolism during the development of chilling injury in cold-stored peach fruit: association of mealiness with arrested disassembly of cell wall pectins. *J. Exp. Bot.* 55, 2041–2052. doi: 10.1093/jxb/erh228

Brummell, D. A., Hall, B. D., and Bennett, A. B. (1999a). Antisense suppression of tomato endo-1,4-β-glucanase Cel2 mRNA accumulation increases the force required to break fruit abscission zones but does not affect fruit softening. *Plant Mol. Biol.* 40, 615–622. doi: 10.1023/A:1006269031452

Brummell, D. A., and Harpster, M. H. (2001). Cell wall metabolism in fruit softening and quality and its manipulation in transgenic plants. *Plant Mol. Biol.* 47, 311–340. doi: 10.1007/978-94-010-0668-2_18

Brummell, D. A., Harpster, M. H., Civello, P. M., Palys, J. M., Bennett, A. B., and Dunsmuir, P. (1999b). Modification of expansin protein abundance in tomato fruit alters softening and cell wall polymer metabolism during ripening. *Plant Cell* 11, 2203–2216. doi: 10.2307/3871019

Cheng, T. S., and Shewfelt, R. L. (1988). Effect of chilling exposure of tomatoes during subsequent ripening. *J. Food Sci.* 53, 1160–1162. doi: 10.1111/j.1365-2621.1988.tb13552.x

Cruz-Mendívil, A., López-Valenzuela, J. A., Calderón-Vázquez, C. L., Vega-García, M. O., Reyes-Moreno, C., and Valdez-Ortiz, A. (2015). Transcriptional changes associated with chilling tolerance and susceptibility in 'Micro-Tom' tomato fruit using RNA-Seq. *Postharvest Biol. Technol.* 99, 141–151. doi: 10.1016/j.postharvbio.2014.08.009

Devaux, M. F., Barakat, A., Robert, P., Bouchet, B., Guillon, F., Navez, B., et al. (2005). Mechanical breakdown and cell wall structure of mealy tomato pericarp tissue. *Postharvest Biol. Technol.* 37, 209–221. doi: 10.1016/j.postharvbio.2005.04.013

Dobin, A., Davis, C. A., Schlesinger, F., Drenkow, J., Zaleski, C., Jha, S., et al. (2013). STAR: ultrafast universal RNA-seq aligner. *Bioinformatics* 29, 15–21. doi: 10.1093/bioinformatics/bts635

Fung, R. W. M., Wang, C. Y., Smith, D. L., Gross, K. C., Tao, Y., and Tian, M. (2006). Characterization of alternative oxidase (AOX) gene expression in response to methyl salicylate and methyl jasmonate pre-treatment and low temperature in tomatoes. *J. Plant Physiol.* 163, 1049–1060. doi: 10.1016/j.jplph.2005.11.003

Fung, R. W. M., Wang, C. Y., Smith, D. L., Gross, K. C., and Tian, M. (2004). MeSA and MeJA increase steady-state transcript levels of alternative oxidase and resistance against chilling injury in sweet peppers (*Capsicum annuum* L.). *Plant Science* 166, 711–719. doi: 10.1016/j.plantsci.2003.11.009

Gambino, G., Perrone, I., and Gribaudo, I. (2008). A rapid and effective method for RNA extraction from different tissues of grapevine and other woody plants. *Phytochem. Anal.* 19, 520–525. doi: 10.1002/pca.1078

Gómez, P., Ferrer, M. A., Fernández-Trujillo, J. P., Calderón, A., Artés, F., Egea-Cortines, M., et al. (2009). Structural changes, chemical composition and antioxidant activity of cherry tomato fruits (cv. Micro-Tom) stored under optimal and chilling conditions. *J. Sci. Food Agric.* 89, 1543–1551. doi: 10.1002/jsfa.3622

Gunes, G., Liu, R. H., and Watkins, C. B. (2002). Controlled-atmosphere effects on postharvest quality and antioxidant activity of cranberry fruits. *J. Agric. Food Chem.* 50, 5932–5938. doi: 10.1021/jf025572c

Hao, J., Li, X., Xu, G., Huo, Y., and Yang, H. (2019). Exogenous progesterone treatment alleviates chilling injury in postharvest banana fruit associated with induction of alternative oxidase and antioxidant defense. *Food Chem.* 286, 329–337. doi: 10.1016/j.foodchem.2019.02.027

He, Y., Liu, Y., Li, M., Lamin-Samu, A. T., Yang, D., Yu, X., et al. (2021). The *Arabidopsis* SMALL AUXIN UP RNA32 protein regulates ABA-mediated responses to drought stress. *Front. Plant Sci.* 12:625493. doi: 10.3389/fpls.2021.625493

Hobson, G. E. (1987). Low temperature injury and the storage of ripening tomatoes. *J. Hort. Sci.* 62, 55–62. doi: 10.1080/14620316.1987.11515748

Huang, D. W., Sherman, B. T., and Lempicki, R. A. (2009). Systematic and integrative analysis of large gene lists using DAVID bioinformatics resources. *Nat. Protoc.* 4, 44–57. doi: 10.1038/nprot.2008.211

Jackman, R. L., Gibson, H. J., and Stanley, D. W. (1992). Effects of chilling on tomato fruit texture. *Physiol. Plant.* 86, 600–608. doi: 10.1034/j.1399-3054.1992.860415.x

Kashash, Y., Holland, D., and Porat, R. (2019). Molecular mechanisms involved in postharvest chilling tolerance of pomegranate fruit. *J. Sci. Food Agric.* 99, 5617–5623. doi: 10.1002/jsfa.9933

Kopylova, E., Noé, L., and Touzet, H. (2012). SortMeRNA: fast and accurate filtering of ribosomal RNAs in metatranscriptomic data. *Bioinformatics* 28, 3211–3217. doi: 10.1093/bioinformatics/bts611

Lill, R. E., and van der Mespel, G. J. (1988). A method for measuring the juice content of mealy nectarines. *Sci. Hort.* 36, 267–271. doi: 10.1016/0304-4238(88)90061-1

Love, M. I., Huber, W., and Anders, S. (2014). Moderated estimation of fold change and dispersion for RNA-seq data with DESeq2. *Genome Biol.* 15:550. doi: 10.1186/s13059-014-0550-8

Luengwilai, K., Beckles, D. M., and Saltveit, M. E. (2012). Chilling-injury of harvested tomato (*Solanum lycopersicum* L.) cv. Micro-Tom fruit is reduced by temperature pre-treatments. *Postharvest Biol. Technol.* 63, 123–128. doi: 10.1016/j.postharvbio.2011.06.017

Lurie, S., and Crisosto, C. H. (2005). Chilling injury in peach and nectarine. *Postharvest Biol. Technol.* 37, 195–208. doi: 10.1016/j.postharvbio.2005.04.012

Lurie, S., and Sabehat, A. (1997). Prestorage temperature manipulations to reduce chilling injury in tomatoes. *Postharvest Biol. Technol.* 11, 57–62. doi: 10.1016/s0925-5214(97)01411-7

Malacrida, C., Valle, E. M., and Boggio, S. B. (2006). Postharvest chilling induces oxidative stress response in the dwarf tomato cultivar Micro-Tom. *Physiol. Plant.* 127, 10–18. doi: 10.1111/j.1399-3054.2005.00636.x

Marangoni, A. G., Jackman, R. L., and Stanley, D. W. (1995). Chilling-associated softening of tomato fruit is related to increased pectinmethylesterase activity. *J. Food Sci.* 60, 1277–1281. doi: 10.1111/j.1365-2621.1995.tb04572.x

Marangoni, A. G., Smith, A. K., Yada, R. Y., and Stanley, D. W. (1989). Ultrastructural changes associated with chilling injury in mature-green tomato fruit. *J. Amer. Soc. Hort. Sci* 114, 958–962.

Maul, F., Sargent, S. A., Sims, C. A., Baldwin, E. A., Balaban, M. O., and Huber, D. J. (2000). Tomato flavor and aroma quality as affected by storage temperature. *J. Food Sci.* 65, 1228–1237. doi: 10.1111/j.1365-2621.2000.tb10270.x

Müller, G. L., Budde, C. O., Lauxmann, M. A., Triassi, A., Andreo, C. S., Drincovich, M. F., et al. (2013). Expression profile of transcripts encoding cell wall remodelling proteins in tomato fruit cv. Micro-Tom subjected to 15°C storage. *Funct. Plant Biol.* 40, 449–458. doi: 10.1071/fp12272

Page, D., Gouble, B., Valot, B., Bouchet, J. P., Callot, C., Kretzschmar, A., et al. (2010). Protective proteins are differentially expressed in tomato genotypes differing for their tolerance to low-temperature storage. *Planta* 232, 483–500. doi: 10.1007/s00425-010-1184-z

Paniagua, A. C., East, A. R., Hindmarsh, J. P., and Heyes, J. A. (2013). Moisture loss is the major cause of firmness change during postharvest storage of blueberry. *Postharvest Biol. Technol.* 79, 13–19. doi: 10.1016/j.postharvbio.2012.12.016

Ré, M. D., Gonzalez, C., Escobar, M. R., Sossi, M. L., Valle, E. M., and Boggio, S. B. (2017). Small heat shock proteins and the postharvest chilling tolerance of tomato fruit. *Physiol. Plant.* 159, 148–160. doi: 10.1111/ppl.12491

Ren, H., and Gray, W. M. (2015). SAUR proteins as effectors of hormonal and environmental signals in plant growth. *Mol. Plant* 8, 1153–1164. doi: 10.1016/j.molp.2015.05.003

Rugkong, A., McQuinn, R., Giovannoni, J. J., Rose, J. K. C., and Watkins, C. B. (2011). Expression of ripening-related genes in cold-stored tomato fruit. *Postharvest Biol. Technol.* 61, 1–14. doi: 10.1016/j.postharvbio.2011.02.009

Sabehat, A., Lurie, S., and Weiss, D. (1998). Expression of small heat-shock proteins at low temperatures. *Plant Physiol.* 117, 651–658. doi: 10.1104/pp.117.2.651

Sabehat, A., Weiss, D., and Lurie, S. (1996). The correlation between heat-shock protein accumulation and persistence and chilling tolerance in tomato fruit. *Plant Physiol.* 110, 531–537. doi: 10.1104/pp.110.2.531

Saladié, M., Rose, J. K. C., Cosgrove, D. J., and Catalá, C. (2006). Characterization of a new xyloglucan endotransglucosylase/hydrolase (XTH) from ripening tomato fruit and implications for the diverse modes of enzymic action. *Plant J.* 47, 282–295. doi: 10.1111/j.1365-313x.2006.02784.x

Sanchez-Bel, P., Egea, I., Sanchez-Ballesta, M. T., Sevillano, L., Bolarin, M. C., and Flores, F. B. (2012). Proteome changes in tomato fruits prior to visible symptoms of chilling injury are linked to defensive mechanisms, uncoupling of photosynthetic processes and protein degradation machinery. *Plant Cell Physiol.* 53, 470–484. doi: 10.1093/pcp/pcr191

Segonne, S. M., Bruneau, M., Celton, J. M., Le Gall, S., Francin-Allami, M., Juchaux, M., et al. (2014). Multiscale investigation of mealiness in apple: an atypical role for a pectin methylesterase during fruit maturation. *BMC Plant Biol.* 14:375. doi: 10.1186/s12870-014-0375-3

Sevillano, L., Sanchez-Ballesta, M. T., Romojaro, F., and Flores, F. B. (2009). Physiological, hormonal and molecular mechanisms regulating chilling injury in horticultural species. Postharvest technologies applied to reduce its impact. *J. Sci. Food Agric.* 89, 555–573. doi: 10.1002/jsfa.3468

Shackel, K. A., Greve, C., Labavitch, J. M., and Ahmadi, H. (1991). Cell turgor changes associated with ripening in tomato pericarp tissue. *Plant Physiol.* 97, 814–816. doi: 10.1104/pp.97.2.814

Sun, W. N., Van Montague, M., and Verbruggen, N. (2002). Small heat shock proteins and stress tolerance in plants. *Biochim. Biophys. Acta* 1577, 1–9. doi: 10.1016/s0167-4781(02)00417-7

Tang, N., An, J., Deng, W., Gao, Y., Chen, Z., and Li, Z. (2020). Metabolic and transcriptional regulatory mechanism associated with postharvest fruit ripening and senescence in cherry tomatoes. *Postharvest Biol. Technol.* 168:111274. doi: 10.1016/j.postharvbio.2020.111274

Uluisik, S., Chapman, N. H., Smith, R., Poole, M., Adams, G., Gillis, R. B., et al. (2016). Genetic improvement of tomato by targeted control of fruit softening. *Nat. Biotechnol.* 34, 950–952. doi: 10.1038/nbt.3602

Vega-Garcia, M. O., Lopez-Espinoza, G., Chavez Ontiveros, J., Caro-Corrales, J. J., Delgado Vargas, F., and Lopez-Valenzuela, J. A. (2010). Changes in protein expression associated with chilling injury in tomato fruit. *J. Amer. Soc. Hort. Sci.* 135, 83–89. doi: 10.21273/jashs.135.1.83

Weiss, J., and Egea-Cortines, M. (2009). Transcriptomic analysis of cold response in tomato fruits identifies dehydrin as a marker of cold stress. *J. Appl. Genet.* 50, 311–319. doi: 10.1007/bf03195689

Yang, L., Huang, W., Xiong, F., Xian, Z., Su, D., Ren, M., et al. (2017). Silencing of *SlPL*, which encodes a pectate lyase in tomato, confers enhanced fruit firmness, prolonged shelf-life and reduced susceptibility to grey mould. *Plant Biotechnol. J.* 15, 1544–1555. doi: 10.1111/pbi.12737

Zhang, W. F., Gong, Z. H., Wu, M. B., Chan, H., Yuan, Y. J., Tang, N., et al. (2019). Integrative comparative analyses of metabolite and transcript profiles uncovers complex regulatory network in tomato (*Solanum lycopersicum* L.) fruit undergoing chilling injury. *Sci. Rep.* 9:4470. doi: 10.1038/s41598-019-41065-9

Conflict of Interest: The authors declare that the research was conducted in the absence of any commercial or financial relationships that could be construed as a potential conflict of interest.

frontiers in Plant Science

ORIGINAL RESEARCH
published: 31 August 2021
doi: 10.3389/fpls.2021.732821

Differential Transcriptomic Regulation in Sweet Orange Fruit (*Citrus sinensis* L. Osbeck) Following Dehydration and Rehydration Conditions Leading to Peel Damage

Paco Romero[1], *Maria Teresa Lafuente*[1] *and Fernando Alferez*[1,2]*

[1] *Department of Food Biotechnology, Institute of Agrochemistry and Food Technology-Consejo Superior de Investigaciones Cientificas (IATA-CSIC), Valencia, Spain,* [2] *Horticultural Sciences Department, Southwest Florida Research and Education Center, University of Florida, Institute of Food and Agricultural Sciences, Immokalee, FL, United States*

Water stress is the most important environmental agent that contributes to the crop productivity and quality losses globally. In citrus, water stress is the main driver of the fruit peel disorders that impact the quality and market ability. An increasingly present post-harvest peel disorder is non-chilling peel pitting (NCPP). Non-chilling peel pitting is manifested as collapsed areas of flavedo randomly scattered on the fruit and its incidence increases due to abrupt increases in the environmental relative humidity (RH) during post-harvest fruit manipulation. In this study, we have used a custom-made cDNA microarray containing 44k unigenes from *Citrus sinensis* (L. Osbeck), covering for the first time the whole genome from this species, to study transcriptomic responses of mature citrus fruit to water stress. In the study, the global gene expression profiles of flavedo from Navelate oranges subjected to severe water stress are compared with those fruits subjected to rehydration stress provoked by changes in the RH during post-harvest, which enhances the development of NCPP. The study results show that NCPP is a complex physiological process that shares molecular responses with those from prolonged dehydration in fruit, but the damage associated with NCPP may be explained by unique features of rehydration stress at the molecular level, such as membrane disorganization, cell wall modification, and proteolysis.

Keywords: citrus, fruit quality, non-chilling peel pitting, peel disorders, water stress

OPEN ACCESS

Edited by:
Isabel Lara,
Universitat de Lleida, Spain

Reviewed by:
Juan Luis Valenzuela,
University of Almeria, Spain
Karin Albornoz,
University of Concepcion, Chile

***Correspondence:**
Fernando Alferez
alferez@ufl.edu

Specialty section:
This article was submitted to Crop and Product Physiology, a section of the journal Frontiers in Plant Science

Received: *29 June 2021*
Accepted: *28 July 2021*
Published: *31 August 2021*

Citation:
Romero P, Lafuente MT and Alferez F (2021) Differential Transcriptomic Regulation in Sweet Orange Fruit (Citrus sinensis L. Osbeck) Following Dehydration and Rehydration Conditions Leading to Peel Damage. Front. Plant Sci. 12:732821. doi: 10.3389/fpls.2021.732821

INTRODUCTION

Water stress is the most important environmental agent causing crop productivity and quality losses (Boyer, 1982; Bray, 1997; Seki et al., 2007; Deluc et al., 2009; Rizzini et al., 2009; Alferez et al., 2020) and its relevance is increasing as the global climate is changing (MacCrackken, 2008). Indeed, changes in the precipitation patterns, runoff, and evapotranspiration fluxes, among other effects of climate change, have been already observed, and their incidence on crop yield and quality is expected to increase (Mancosu et al., 2015). In citrus fruits, water stress in the orchard and during fruit manipulation is the main cause not only of yield losses due to physiological alterations, such as pre-harvest fruit drop and leaf abscission (Gomez-Cadenas et al., 1996; Iglesias et al., 2007)

but also of fruit peel disorders that impact the quality and marketability as well. The latter include stem-end rind breakdown (SERB) and post-harvest non-chilling peel pitting (NCPP). The SERB is due to prolonged dehydration (Albrigo, 1972) and manifests as collapsed areas of flavedo around fruit Calix, whereas NCPP is manifested as collapsed areas of flavedo randomly scattered on the fruit, and its incidence increases due to abrupt increases in the environmental relative humidity (RH) during post-harvest fruit manipulation (Alférez et al., 2003). This disorder may also occur in the harvested citrus fruits exposed to mild dehydration (Alferez et al., 2005; Romero et al., 2012), and in the harvested fruits held under saturated RH (Establés-Ortiz et al., 2016; Romero et al., 2020a), although the peel damage severity is lower than that occurring following rehydration of dehydrated fruit. These problems are becoming increasingly important in the past years, due to a combination of factors, such as the deficit of water resources in most of the citrus growing regions, the distance from orchards to packinghouses, and the increased time of fruit standby before packing line processing due to the production needs and market constraints (Cronje et al., 2017). Indeed, although the general climate conditions may vary among the citrus growing regions, there are common environmental factors during the harvesting seasons that affect water status in fruits leading to stress and peel disorders. Those show a similar pattern in RH that includes sharp variations in RH during the harvest season of susceptible varieties or periods of prolonged dehydration prior to post-harvest handling. For example, in Valencia (Spain), NCPP is likely to develop in Navelate and Navelina oranges after several days of sustained dry winds followed by humid winds from the Mediterranean (Agusti et al., 2001; Alférez et al., 2003); Navelate oranges grown in the Mediterranean climatic areas of South Africa are more prone to develop NCPP (Dr. P. Cronje, personal communication); finally, the pronounced fluctuations in RH are observed daily in early winter in Florida coincident with the harvesting season of the highly susceptible to NCPP Fallglo tangerine (Alferez et al., 2005). All these conditions have in common a rehydration stress event after tissue dehydration. Furthermore, rehydration of fruits dehydrated in the field is a common feature during post-harvest handling because of washing or the application of treatments to reduce decay, and also because of fruit storage at high RH.

Drought stress induces various molecular, biochemical, and physiological responses in plants (Yamaguchi-Shinozaki and Shinozaki, 2006; Seki et al., 2007; Oliver et al., 2020) and fruits (Deluc et al., 2009; Rizzini et al., 2009; Romero et al., 2012; Alferez et al., 2020). The major effects of water stress in plants are stomatal closure, inhibition of thylakoid mediated electron transport, membrane damage (Bohnert and Sheveleva, 1998), activation of antioxidant enzymes (Yuqing et al., 2021), and other diverse molecular responses, such as activation of signal transduction, lipid, and sugar metabolism, wax synthesis, cell wall regulation, and osmotic adjustment (Chen et al., 2020). In citrus plants, drought likewise induces the expression of key genes for amino acid metabolism, osmotic stress response proteins, reduction of reactive oxygen species, and transcription regulation (Gimeno et al., 2009). Previous study in our labs has shown that in citrus, the severity of water stress differentially affects the expression of phospholipase (PL)-encoding genes and the abscisic acid (ABA) regulation and/or response in both the fruit and the whole tree (Romero et al., 2013a, 2014; Alferez et al., 2020). Also, response to mild water stress in the fruit involves processes such as di, tri-valent inorganic cation transport, and molecular response to water deprivation which include both ABA-dependent and independent genes, as well as a non-impaired carbohydrate biosynthetic machinery (Romero et al., 2012). In addition, the deregulation of the ABA-signalosome components under mild water stress conditions has been linked with a higher susceptibility to NCPP development (Romero et al., 2013b). When considered together, available data up to date point out that the response and tolerance to water stress in citrus plants involve inhibition of proteolysis, activation of ABA signaling pathway and biosynthesis, phospholipid metabolism and signaling, and reinforcement of ribosomal structure (Romero et al., 2020a).

The dehydration and rehydration stresses involve disparate mechanisms at the biophysical level, for example, different evolution of turgor potential and its components across the anatomically different flavedo (the outer colored part of the fruit peel), external and internal albedo (the spongy white mesocarp) (Alférez et al., 2010), as well as different biochemical response (Alférez et al., 2008). Therefore, molecular responses to rehydration in fruit suffering previous dehydration or water stress should differ from those triggered by dehydration alone.

Previous research has shown that even slight variations in water potential may alter the synthesis of membrane lipids in different plant systems among other effects (Quartacci et al., 2002). Most of the research concerning dehydration and rehydration processes has been performed in leaves from desiccation-tolerant (resurrection) plants, with physiology adapted to withstand the sharp variations in water potential (Navari-Izzo et al., 2000; Benadjaoud et al., 2013). Some studies have been also performed in other crops such as papaya seedlings, showing changes in ABA levels in the roots and leaves during rewatering (Mahouachi et al., 2007). In the case of citrus plants, research on leaf abscission following rehydration after water stress has shown activation of several processes, such as cell wall modification (Agusti et al., 2012); it is also well-established that ABA accumulates in the roots in response to water deprivation and subsequent stress and that rewatering reduces ABA content (Gomez-Cadenas et al., 1996), illustrating the involvement of this hormone in the signaling of dehydration-rehydration processes. However, the regulatory networks involved in modulating the response to rehydration stress in citrus fruit are unknown.

Large-scale microarray analysis has been demonstrated to be a powerful tool to unravel complex regulatory networks involved in stress responses for years. In fruit, it can serve as a means to identify genes involved in the tolerance to the stresses that subsequently can be selected by breeding or used by the transformation approaches to obtain novel varieties with improved characteristics. In this study, we have used a custom-made cDNA microarray containing 44k unigenes from *Citrus sinensis* (L. Osbeck), which covers, for the first time, the whole genome from this species (Romero et al., 2020a). The main objective of the current study is to produce valuable information

on the transcriptomic response of mature citrus fruit to water stress conditions by comparing global gene expression profiles of flavedo from Navelate oranges subjected to severe water stress (dehydration) with those fruits subjected to rehydration stress provoked by changes in RH during post-harvest, which enhances the development of NCPP, the main post-harvest peel disorder related to abiotic stress. The experimental conditions used in this study are not standard post-harvest practices for citrus fruit but intended to promote NCPP in controlled conditions that allow detailed study of this disorder, as shown in previous studies (Alférez et al., 2003). The data show unique features of rehydration stress that make it different from severe dehydration and suggest new mechanisms involved in the loss of fruit quality and marketability during post-harvest.

MATERIALS AND METHODS

Plant Material and Post-harvest Treatments

Full mature Navelate [*Citrus sinensis* (L. Osbeck)] sweet oranges were harvested from the adult trees grown in commercial groves in Lliria (Valencia, Spain). The fruits were immediately delivered to the laboratory, so they were not subjected to pre-harvest water stress before treatments and divided into three lots after selecting those fruits uniform in size and without visual defects or damages. One lot was stored continuously at low RH (30% RH) for 10 days; a second lot was stored at high RH (90% RH) for the same period (non-dehydrated fruits kept at constant RH); and the third lot was stored at 30% RH for 4 days prior to being transferred to 90% RH for 6 additional days (10 days from harvest) as the condition for studying the rehydration stress (**Figure 1**). All the treatment lots were stored at 20°C to effectively induce NCPP as previously described (Alférez et al., 2003). At each sampling period, flavedo samples were collected, frozen, and homogenized in liquid nitrogen, and kept at −80°C for later analysis. The four biological replicates per treatment, each consisting of five fruits, were collected at each sampling period and used for molecular analyses as described below.

For peel damage estimation, three biological replicates of 10 fruits each per treatment were used. The peel of the fruit was inspected for the intensity and extension of NCPP symptoms to rate on a scale from 0 (no pitting/damage) to 4 (severe pitting/damage). The severity index was calculated by adding up the products of the number of fruits in each category multiplied by its score and then dividing the total obtained by the number of fruits evaluated, as described by Lafuente et al. (1997). The same fruits were used at the various evaluation dates for each treatment.

RNA Isolation and cDNA Synthesis

Total RNA was extracted from frozen flavedo samples as previously described by Romero et al. (2019). To remove genomic DNA contaminations, total RNA was treated with Ribonuclease-free DNase (Invitrogen) following the instructions of manufacturer. RNA integrity was evaluated by agarose gel electrophoresis and its concentration was determined spectrophotometrically with a NanoDrop ND-1000 spectrophotometer (Thermo Scientific, Wilmington, DE, USA). RNA quality was further verified with a Model 2100 Total RNA BioAnalyzer by using the Eukaryote Total RNA Nano kit (Agilent Technologies, Santa Clara, CA, USA). cDNAs from all the replicates and conditions were synthesized from 2 μg of RNA by using SuperScript III RT (Invitrogen, Waltham, MA, USA) in presence of Oligo(dT) 20-mer (Invitrogen) and Ribonuclease Inhibitor (Invitrogen), according to instructions from the manufacturer.

cDNA Labeling, Microarray Hybridization, and Data Acquisition and Analysis

The transcriptomic changes occurring in the flavedo of Navelate oranges stored at 20°C and different RH conditions were determined. The four biological replicate samples per treatment and sampling period were analyzed with a custom-made *Citrus* cDNA microarray previously described by Romero et al. (2020a). This microarray was developed using the Agilent technology, contained 44k unigenes, and covered the whole *C. sinensis* genome.

cDNA labeling and microarray hybridizations were performed by following the recommended protocols of Agilent Technologies, as described in Romero et al. (2020a). The microarray hybridizations were performed according to the two-color protocol (Two-Color Microarray-Based Gene Expression Analysis v. 6.5, Agilent Technologies) and hybridized microarrays were scanned using a DNA Microarray Scanner (Model G2505C, Agilent Technologies, Santa Clara, CA, USA). Feature data were extracted with the Feature Extraction Software (Agilent Technologies) using the default settings. Under the R environment, bioconductor and Limma packages were used, respectively, for data preprocessing and analysis and for differential expression analysis. Data normalization within- and among-arrays was performed by following the Loess and Aquantile algorithms, respectively. The differential expressed genes (DEG) were identified by applying a false discovery rate (FDR) below 1% and a cutoff of Log_2 Fold Change $\geq$1. Gene Ontology (GO) analysis was performed on the groups of DEG by using the GOStats package (Falcon and Gentleman, 2006), which allowed to identify of biological processes (BP), molecular functions (MF), and cellular components (CC) significantly (p-value < 0.01) under- or over-represented respect to the reference sample. In these analyses, only DEG showing at least a two-fold change in expression (Log_2 Fold Change $\geq$ 1) were considered. Venn diagrams showing the DEG distribution were plotted by using Venny 2.1 tool (https://bioinfogp.cnb.csic.es/tools/venny). The repeatability and distribution of the experimental samples were verified in a principal component analysis (PCA) considering those DEG satisfying an ANOVA analysis ($P < 0.01$) for all the conditions represented in Venn diagrams by using the STHDA tools (http://www.sthda.com). Hierarchical clustering analysis (HCA) and heatmap representation were performed by using the Instant Clue software (Nolte et al., 2018). For HCA, Euclidian distance and complete linkage were applied to rows (genes) and columns (samples). To visualize transcriptomic changes on a metabolic map, gene expression data for specific

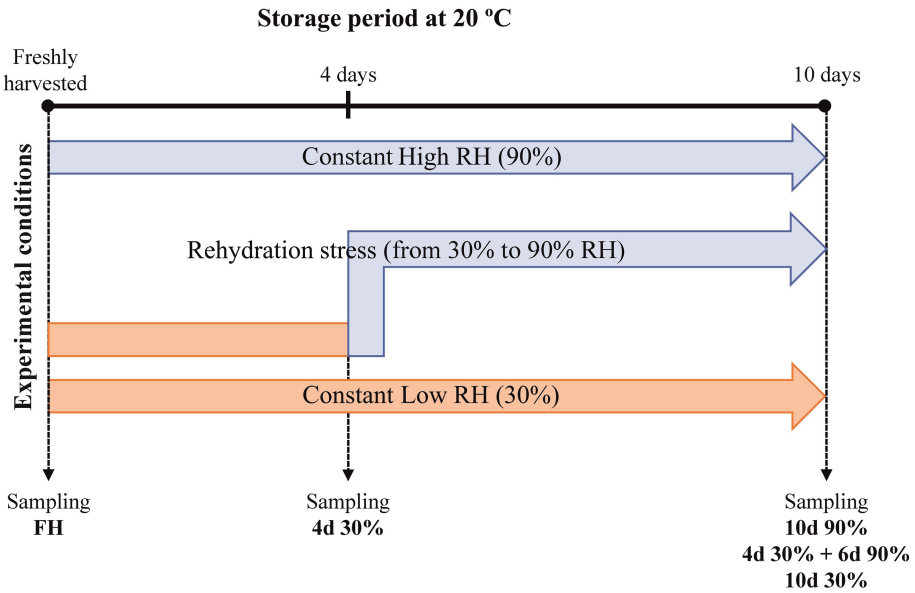

FIGURE 1 | Schematic representation of the experimental design.

comparisons were loaded into the MapMan tool (Thimm et al., 2004).

Statistical Analyses

The significant differences between means of the NCPP incidence for each treatment were established after *post-hoc* Tukey's test ($P \leq 0.05$) using Statgraphics (http://www.statpoint.net) webpage. Data are provided as the mean values ± SE of the different biological samples used in each treatment, as indicated in the figure legends.

RESULTS

NCPP Development

The incidence and development of NCPP were determined in full mature Navelate oranges stored for 10 days at 20°C under three different RH conditions: (1) constant low (30%) RH, (2) high (90%) RH, and (3) the abrupt changes in storage RH (from 30 to 90% RH). Under constant RH conditions, the development of NCPP was low (NCPP index of 0.6 in a rating scale from 0 to 4 by day 10), independently of the exposure of the fruits to low or high RH. In contrast, changing RH conditions by 4 days from low to high RH sharply increased NCPP severity during the following 6 days of storage at constant high RH. Thus, by 10 days, the NCPP index multiplied by 2.3 with respect to either constant low or high RH (**Figure 2**).

Transcriptional Analysis of NCPP Development in Response to Rehydration Stress

The fruits from Navelate orange stored at constant high (10 days at 90% RH) or low (4 and 10 days at 30% RH) RH, as well as those being transferred from low to high RH (4 days at 30% + 6 days at 90% RH) were selected to compare changes in transcriptomic profiles with those occurring at freshly harvested (FH) fruits to identify the molecular mechanisms associated with the rehydration stress in citrus fruits and NCPP development.

The DEGs obtained when comparing each condition vs. the FH fruit are listed in **Supplementary Table 1**. Venn diagrams in **Figure 3A** indicated that major changes in the number of DEG (FDR < 0.01, cutoff $Log_2FC \geq \pm 1$) occurred in fruit stored at high RH (10 days 90%, 4,632 DEG), followed by the fruit stored for a short (4 days 30%, 2,750 DEG) and long (10 days 30%, 2.507 DEG) period under low RH, and by the rehydration-stressed fruit (4 days 30% + 6 days 90%, 2,479 DEG). The number of upregulated genes was higher than that of downregulated in all conditions. Interestingly, the number of induced genes was about two-fold higher than that of repressed in fruit stored for 10 days under severe dehydration and in rehydration-stressed fruit; while in fruit stored for a shorter period (4 days) under 30% RH and in constant high RH fruit (10 days 90% RH), the number of up- and downregulated genes was similar.

The distribution of DEG in the Venn diagrams allows discriminating specific and common responses among all the conditions in the experimental design (**Figure 3A**). Fruit subjected to severe dehydration (30%) specifically upregulated 327 and 527 genes while repressed 357 and 309 genes, when stored for short (4 days) and long (10 days) periods, respectively. The number of DEG specifically regulated by transferring the fruit from low to high RH (rehydration stress) notably diminished (215 induced + 201 repressed), whereas it was more than three-fold higher (980 induced + 1,519 repressed) when fruit was held under constant high RH (10 days 90%). The number of commonly regulated DEGs between the rehydrated fruit and the rest of the conditions in the experimental design was the highest when compared with the long-term severe

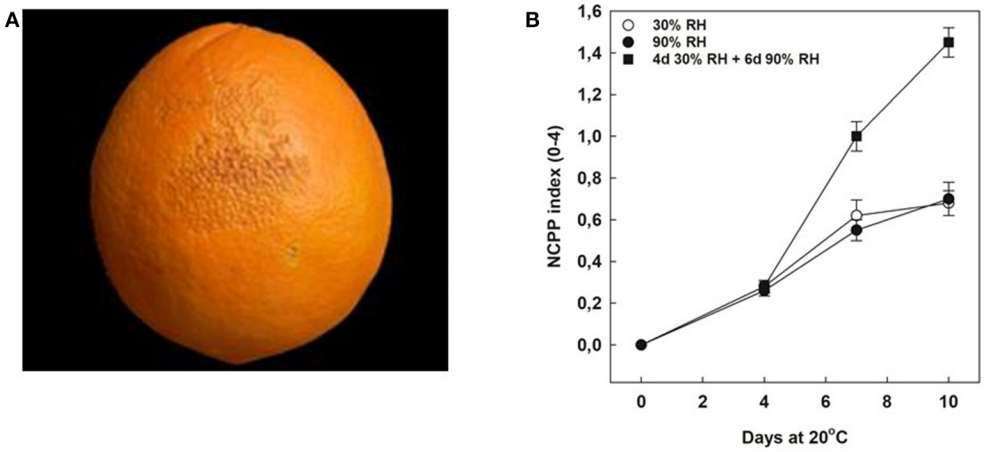

FIGURE 2 | Effect of rehydration stress on peel damage development. **(A)** Typical symptoms of non-chilling peel pitting (NCPP) in mature Navelate oranges. **(B)** NCPP index in Navelate fruit stored for up to 10 days at 20°C and exposed continuously to 30% RH (white circles), or 90% RH (black circles), or for 4 days at 30% RH and then transferred to additional 6 days at 90% RH (squares). Values are means of three biological replicates of 10 fruit samples each per condition. Asterisks indicate statistical differences according to Tukey's test ($P \leq 0.05$).

dehydration (10 days 30%, 407+60 DEG), followed by the short-term response to dehydration stress (4 days 30%, 85+172 DEG); this number was minimum when compared with the fruit stored under constant high RH (10 days 90%, 64+36 DEG). This analysis also revealed a set of genes commonly regulated by all the conditions (353+162 DEG) (**Figure 3A**).

The multivariate analyses (PCA and HCA) were performed to validate the repeatability of the data across replications and to the cluster samples according to their transcriptomic profiles. Under all conditions, the gene expression profiles of the four replicate samples were tightly clustered together (**Figure 3B**). Principal component analysis also revealed marked differences in gene regulation among the FH fruit and those following different storage conditions. The distance among samples stored at different RH was high (X-axis explaining the 26.90% of the total variation), but the distance caused by the time of exposure to dehydration stress, or the rehydration stress *per se* was also significant (y- and z-axes explaining a 30.01% of the total variation) (**Figure 3B**). Hierarchical clustering analysis clustered the samples in two major branches, splitting the samples of the experimental design in those fruit samples stored under high RH and those subjected at some point to severe dehydration. Furthermore, the fruit samples exposed to rehydration stress were allocated closer to the samples stored for a short (4 days) than for a long (10 days) period under low RH (**Figure 3C**).

The functional categorization analyses on the DEGs represented in the Venn diagrams identified BP, MF, CC, and KEGG metabolic pathways significantly ($P < 0.01$) under- or over-represented in the different storage conditions with respect to FH fruit. Gene ontology analyses revealed that the molecular mechanisms underlying severe dehydration and rehydration stresses were widely diverse (**Supplementary Tables 2**–**5**). To better understand the differential responses to these stresses and their relation to the development of NCPP, these GO categories were grouped by the regulation patterns. Pattern 1 includes those GO terms that were induced or repressed specifically by rehydration stress and, therefore, putatively involved in the NCPP development. The results showed high diversity among these BP and MF (**Supplementary Tables 2**, **3**). Among them, it is worth noticing the induction of the "response to desiccation" and the "calcium-mediated signaling," as well as the repression of the "regulation of ethylene biosynthesis" BP (**Supplementary Table 2**). These terms relate to the regulation of the "inositol-polyphosphate 5-phosphatase activity" and the "water channel activity" MF (**Supplementary Table 3**) and the "integral to plasma membrane" CC (**Supplementary Table 4**) and "inositol phosphate metabolism" metabolic pathway (**Supplementary Table 5**). Other interesting responses in relation to the NCPP development and peel damage were the induction of oxidoreductase and oxidase activities and the repression of the cellulase activity MF (**Supplementary Table 3**). Within the context of this study, it should be also pointed out those GO categories commonly regulated by short-term exposure to severe dehydration and by the rehydration stress (4 days at 30% RH and 4 days 30% RH + 6 days 90% RH, respectively) but not by the long-term storage, independently on the RH. These responses cannot be ruled out as related to NCPP development and are included in pattern 2. Among them, the transmembrane ions transport, the salicylic acid, jasmonate and auxins metabolism, the catabolism of terpene, the calcium-dependent phospholipid binding, and the response to sugar stimulus merit to be mentioned (**Supplementary Tables 2**–**5**). The rest of the patterns are not related to NCPP development but to a common regulation between severe dehydration and rehydration stresses (pattern 3), to the early responses to low RH that can be reversed by high RH exposure (pattern 4), to short- and long-term response to dehydration (pattern

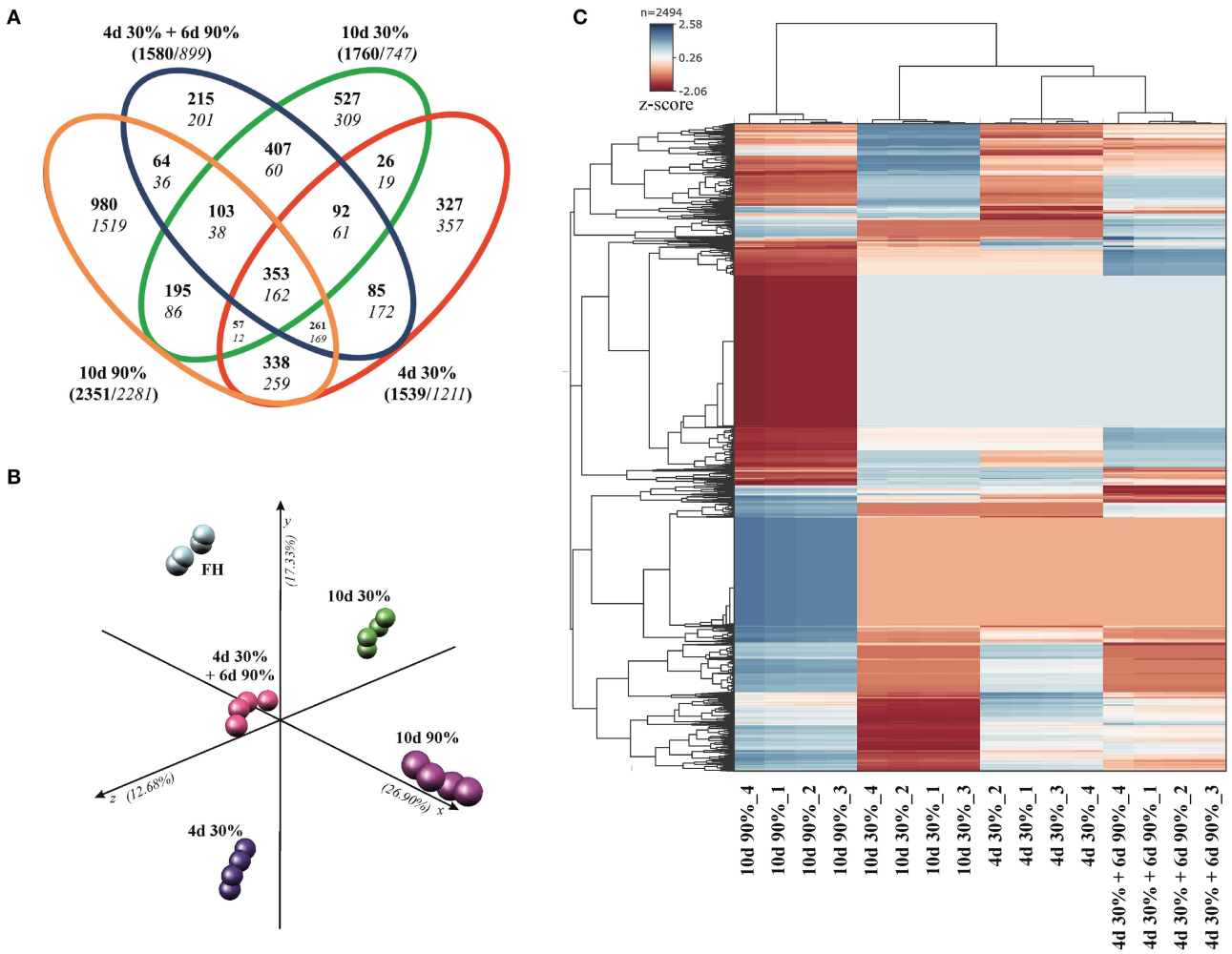

FIGURE 3 | The differential expression and multivariate analysis in response to dehydration/rehydration stress. **(A)** Venn diagrams of Navelate fruit showing the distribution of differentially expressed genes (DEG, $\alpha = 0.05$) satisfying a cutoff of Log_2 FoldChange ≥ 1 for the comparisons between the fruit stored for 4 days at 30% RH, 10 days at 30% RH, 10 days at 90% RH, and 4 days at 30% RH + 6 days at 90% RH respect to the freshly harvested (FH) fruit. Inductions and repression are indicated in bold and italics, respectively, and the total number of induced and repressed DEGs for each conditions are indicated in brackets. **(B)** Principal component analysis (PCA), based on the DEG satisfying an ANOVA analysis ($P < 0.01$) for all conditions represented in the Venn diagrams. The three axes in PCA account for 56.91% of the total variance among conditions. **(C)** Hierarchical cluster analysis (HCA) and heatmap large-scale transcriptional profiles on the genes used for the PCA. Heatmap colors vary from dark blue (induction) to red (repression). Four biological replicates from each condition were used for all the analyses.

5), and to the detachment or senescence stresses (pattern 6) (**Supplementary Tables 2–5**).

To find a more specific response associated with the occurrence of peel damage after rehydration stress, we plotted the large-scale transcriptional profiles of all DEG between the storage conditions and the FH fruit (**Figure 3C**). This analysis provided a high number of expression patterns, which we then narrowed down to those showing a gene regulation specifically related to the rehydration stress condition. The patterns selected in this way then showed an opposite gene regulation between the fruit transferred from low to high RH (rehydration-stressed fruit) and the fruit stored under the rest of constant RH conditions. Within the expression pattern showing genes specifically repressed in response to rehydration stress, we found only 31 genes encoding for very diverse proteins (**Figure 4**). Among them, it is noticing the repression of genes related to photosynthesis and cellular energetics, cell wall proteins, and wax biosynthesis. However, no specific categories were obtained when a functional analysis was performed on this set of genes. The complementary expression pattern, however, included 195 genes that were induced only in response to rehydration stress. Gene Ontology analysis on this set of genes highlighted, among others, BP related to the response to biotic and abiotic stresses, the response to ABA and lipids, and the regulation of jasmonic acid signaling; in addition to the calcium ion binding MF, different stresses, such as osmotic stress, hypoxia, and the cell periphery CC (**Table 1**). To better visualize how the transcriptomic changes were distributed into a general overview and concrete metabolic pathways and how they are similar with

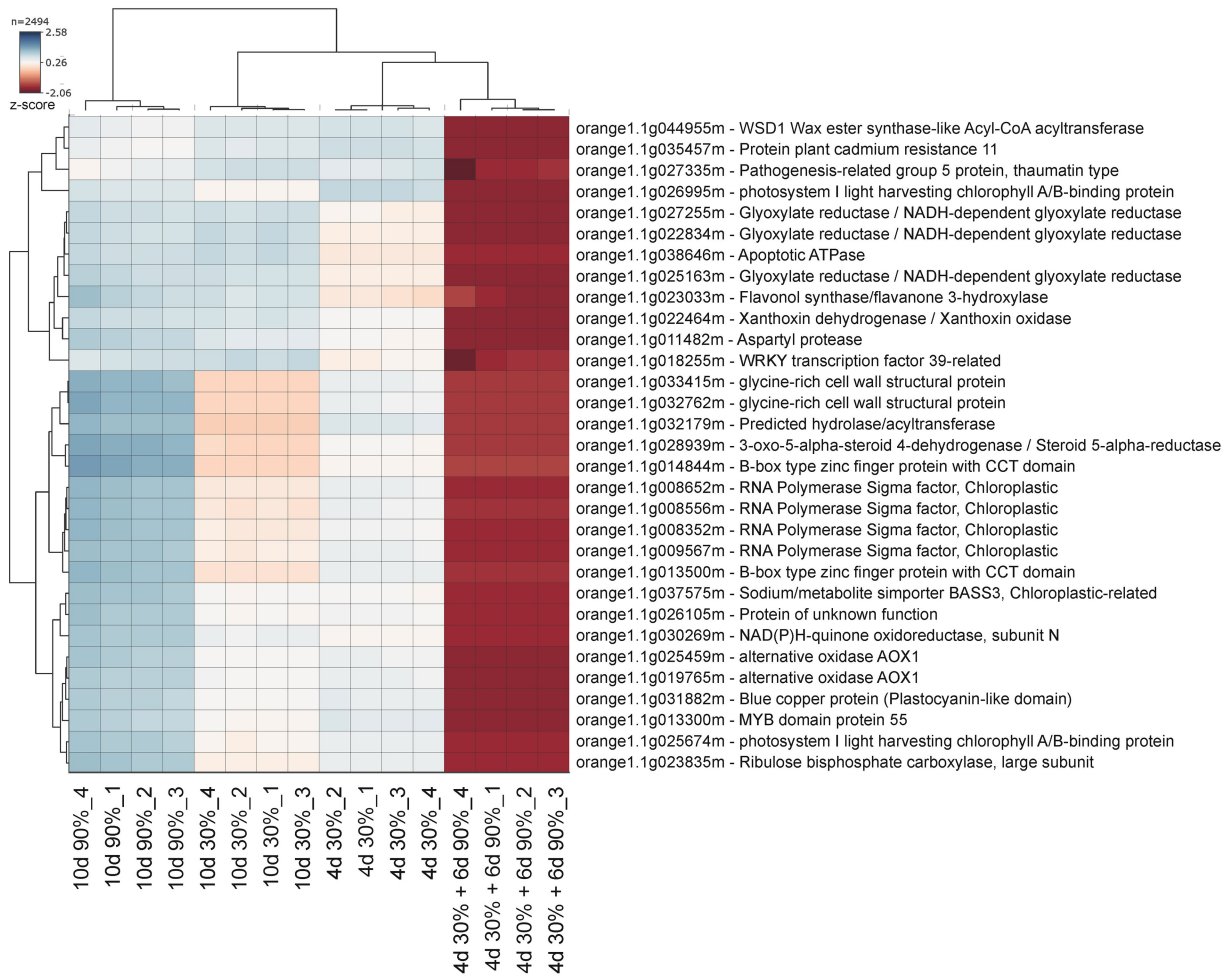

FIGURE 4 | Gene clusters specifically repressed by rehydration stress. The genes included in the selected cluster from the heatmap large-scale transcriptional profiles are represented in **Figure 3**. Colors vary from dark blue (induction) to red (repression). Four biological replicates from each sampling condition were used for the analysis.

the GO analysis, we performed a MapMan analysis (**Figure 5**). It is noteworthy that the group of unidentified proteins is highly upregulated, which may indicate processes related to NCPP development are still to unravel.

DISCUSSION

In this study, we have used a customized microarray covering the whole genome from *C. sinensis* to study fruit flavedo responses to the rehydration stress during post-harvest. The abrupt changes in flavedo and albedo water potential and its components have been previously documented in response to the rehydration stress leading to NCPP. Even though weight gain in fruit was not recorded in response to an increase in RH storage conditions (environmental rehydration), fruit weight loss was immediately arrested following a change in RH, and water potential changed abruptly (data not shown), as reported elsewhere (Alférez et al., 2003, 2010; Cronje et al., 2017). The transcriptomic analysis indicates that changes in RH leading to severe NCPP during post-harvest manipulation of citrus fruit pose differentiated rehydration stress in contrast with the response to constant RH storage conditions. This study fills the gap of knowledge about the molecular mechanisms underlying abrupt changes in storage RH, which ends in the development of NCPP, a well-documented phenomenon in different citrus cultivars (Alférez et al., 2003; Alferez et al., 2005; Alférez et al., 2010; Cronje et al., 2017).

In the study, a storage experiment is performed in the conditions favoring the development of NCPP (Alférez et al., 2003) for 10 days. To gain insight into the molecular mechanisms specific to the NCPP development in response to this RH change, we analyzed the global transcriptomic response and compared it to non-stressed FH fruit (**Table 1**, **Supplementary Tables 2**–**5**).

We found sets of genes commonly regulated in all three conditions assayed (constant low RH, constant high RH, and change from low to high RH) when compared with FH fruit.

TABLE 1 | Gene ontology (GO) categories related to NCPP development, specifically induced by rehydration stress according to the expression patterns shown in **Figure 3**.

GO	Term	Number of genes	Fold enrichment	FDR
Biological Process				
	Regulation of tryptophan metabolic process	2	200	0.025
	Response to chitin	9	19.68	0.000
	Jasmonic acid mediated signaling pathway	4	17.00	0.021
	Response to wounding	10	12.79	0.000
	Cellular response to hypoxia	6	7.74	0.026
	Response to lipid	15	5.58	0.000
	Response to abscisic acid	9	5.45	0.011
	Response to oxidative stress	8	5.27	0.025
	Response to other organism	17	4.69	0.000
	Response to osmotic stress	8	4.57	0.048
	Regulation of response to stimulus	10	4.04	0.029
	Defense response	12	3.81	0.015
	Regulation of transcription, DNA-templated	18	2.51	0.036
Molecular Function				
	Calcium ion binding	8	9.32	0.010
	Sequence-specific DNA binding	16	3.83	0.006
	DNA-binding transcription factor activity	18	3.30	0.008
Cellular Component				
	Cell periphery	28	2.11	0.041

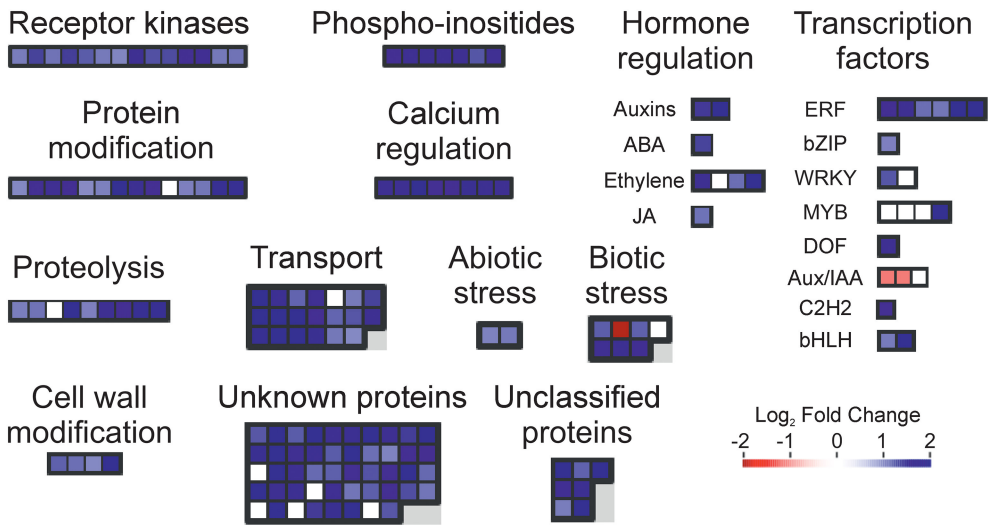

FIGURE 5 | Metabolic overview changes caused by rehydration stress. Transcript accumulation comparison (Log_2 FoldChange) in the flavedo of the fruit stored for 4 days at 30% RH + 6 days at 90% RH (rehydration-stressed fruit) with respect to the freshly harvested (FH) fruit. Red and blue squares represent the genes with decreasing and increasing transcript levels, respectively, in the stored fruit vs. the FH samples. The color scale is indicated in the figure.

These genes may be related to citrus fruit response to starvation stress caused by detachment, which has been related to NCPP in citrus fruit held at 90% RH (Cajuste et al., 2011; Establés-Ortiz et al., 2016; Romero et al., 2020a) or senescence, enhanced by keeping citrus fruit at low RH (Albrigo, 1972; Romero et al., 2013b). Among these common responses, sulfur metabolism appeared downregulated in all the conditions assayed. Sulfur metabolism occurs in the chloroplast, and both assimilation and metabolism are crucial for plant survival during stress (Rausch and Wachter, 2005). Also, the compounds involved in protein synthesis and defense contain sulfur (Lee et al., 2016), and thiol-containing compounds may be modulators of the stress response including oxidative stress (Khan et al., 2009; Szalai et al., 2009). Finally, the phenylpropanoid pathway, a well-known protective

mechanism against diverse post-harvest stresses in citrus fruit aiming to content cell damage propagation (Lafuente et al., 2003; Cajuste and Lafuente, 2007) was activated in all three conditions.

An important finding of this study is that some molecular responses to short-term (4 days) dehydration were similar to those developed at long-term (10 days) dehydration but more similar to responses triggered by the change in RH. It could be possible that the similarity in these responses was due to a priming effect of the original dehydration conditions before changing RH, so no new expression patterns were developed upon provoking rehydration stress by changing RH storage conditions and/or that changing RH conditions resulted in only an aggravation of damage due to prolonged dehydration (**Figure 1**; **Table 1**). However, we ruled out the latter by comparing all the three stress conditions to FH fruit (**Supplementary Tables 2–5**). The nature of the responses to both short-term low RH and rehydration stress involved specifically transmembrane ions transport, salicylic acid, metabolism of jasmonate and auxins, catabolism of terpenes, calcium-dependent phospholipid binding, the response to osmotic stress, hypoxia, and the response to sugar stimulus (**Supplementary Tables 2–5**; **Figure 5**). Together, these responses can be related to loss of membrane integrity leading to NCPP, indicating a complex and orchestrated response to rehydration that ultimately leads to peel damage by energy metabolism and plasma membrane disorganization. The specific responses to rehydration stress also included an oxidative stress response, such as the activation of different oxidoreductase activities. Interestingly, some of these responses to rehydration stress that were also common to short-term dehydration seem to be related to cellular damage contention and hormonal regulation during rehydration and rewatering. The former includes a response to wounding, cell wall (downregulation of cellulase activity), and tryptophan metabolism. Some of these responses have been shown in citrus plants after a cycle of water stress and rehydration (Agusti et al., 2012). In other plants such as papaya, drought stress followed by rewatering induced changes in hormonal levels, specifically jasmonic acid (Mahouachi et al., 2007). In other plants, the role of salicylic acid in alleviating water stress and inducing antioxidant enzymes has been shown (Antonic et al., 2020; Wakchaure et al., 2020). In this system, rehydration stress following dehydration also involved the induction of gene expression related to jasmonic acid, salicylic acid, and antioxidative systems (**Supplementary Table 2**). All these findings, together, point out that common mechanism respond to this combined stress in different plants and support our interpretation of the present results. In addition, rehydration stress dramatically induced proteolysis-related processes (**Figure 5**), as well as inhibition of ethylene BP that are related in tolerance to starvation and cellular damage, supporting the notion that rehydration stress leads to NCPP in a similar way as other stresses, such as those triggered by the uncoupling treatments or high energy demands (Establés-Ortiz et al., 2016).

The responses to osmotic stress and ABA were induced during rehydration (**Table 1**; **Figure 5**). Deficiency in ABA has been related to increased susceptibility to NCPP (Alferez et al., 2005; Romero et al., 2012). In addition, the previous study has shown that abrupt changes from low to high RH induce sharp changes in water potential and its components, both osmotic and turgor potentials in citrus fruit (Alférez et al., 2010), and this has been related to the induction of PL activities (Cronje et al., 2017) and the interplay between PLs and ABA (Romero et al., 2013a, 2014). In this context, it is noteworthy that we found significantly induced BP of calcium-dependent phospholipid binding during rehydration stress. Many plant phospholipase D (PLDs) contain a Ca^{2+}-dependent phospholipid-binding C2 domain (protein kinase C-conserved 2 domain), require Ca^{2+} for activity (Wang, 2000), and have broad substrate specificity, hydrolyzing several common membrane phospholipids, and playing a critical role in many cellular processes, such as signal transduction, membrane trafficking, cytoskeletal rearrangements, and membrane degradation (Qin and Wang, 2002). We also found activation of PLD downstream responses, such as jasmonic acid signaling and cellular periphery (membrane), which together, reinforce the notion of NCPP due to rehydration stress is a result of membrane disorganization *via* phospholipid catabolism. Interestingly, activation of different genes encoding PLD isoforms has been also found to be an early defense response against starvation in citrus fruit; however, prolonged stress may result in higher and constant activation of PLD genes that are also involved in NCPP damage development (Romero et al., 2020b).

A significant number of genes related to response to hypoxia were specifically induced by changing RH conditions (**Table 1**; **Figure 5**). The hypoxia conditions triggered by energy failure due to uncoupling and subsequent drop in ATP levels (Alférez et al., 2007) or high energy demand in fruits held at high RH (Establés-Ortiz et al., 2016) have been related to increased NCPP and peel damage in citrus flavedo comparable to NCPP, as stated above. This notion relates tightly with the previous findings by our groups (Establés-Ortiz et al., 2016; Romero et al., 2020a) and others (Rawyler et al., 1999, 2002) describing energy shortage as a mechanism of membrane integrity loss in plants, that in the case of citrus originates NCPP during post-harvest as well (Alférez et al., 2007; Cajuste et al., 2011). In other plants, resistant to water stress exist compensatory mechanisms for membrane integrity upon rehydration tightly regulated by hormones (Dong et al., 2019), but prolonged stress can reduce the ability of the plant to compensate stress, leading to membrane damage. A similar mechanism appears to be operating during NCPP after rehydration in citrus fruit.

A central dogma in citrus post-harvest is that disparate conditions lead to similar peel disorders, as the fruit can only develop a limited number of phenological responses (Grierson, 1986). In this sense, both this study and results from Establés-Ortiz et al. (2016) and Romero et al. (2020a) support that not only response to hypoxia, but also a response to other conditions, such as wounding, oxidative stress, and salicylic acid, or the repression of the regulation of ethylene biosynthesis, among others, were upregulated in response to both energy shortage and rehydration stress, ultimately leading to undistinguishable NCPP symptoms.

CONCLUSIONS

In a nutshell, global transcriptomic responses to rehydration leading to NCPP during post-harvest can be considered as a palimpsest, since the build-up of specific responses to this stress occurs upon ongoing common responses to dehydration, resulting in a complex expression pattern in the fruit. This expression pattern shares many common features with responses to the other stresses. The fact that peel disorders developed in response to these disparate abiotic stresses are similar in morphology, has blurred for years a correct understanding of the causes and has often led to confusion. This study illustrates the way global molecular analysis can help in discriminating between common and unique causes of post-harvest disorders in citrus.

DATA AVAILABILITY STATEMENT

The datasets presented in this study can be found in online repositories. The names of the repository/repositories and accession number(s) can be found in the https://zenodo.org/record/5171732#.YRDdJkDtZdg.

AUTHOR CONTRIBUTIONS

ML and FA conceived the project. PR and FA performed the research and analyzed the data. FA wrote the original draft with contributions by PR and ML. All authors accepted the final manuscript.

FUNDING

This study was supported by the Spanish Ministry of Economy and Competitiveness, Spain (Research Grant AGL2009-11969-R), and the Generalitat Valenciana, Spain (Grant PROMETEOII/2014/027). FA's Program on citrus fruit quality at UF/IFAS is funded by competitive grants from USDA NIFA (grant #2019-70016-29096), Citrus Research and Development Foundation (CRDF grant #18-032C), and Early Career Seed Grant Fund from UF/IFAS.

ACKNOWLEDGMENTS

The technical assistance of M. Pérez is gratefully acknowledged. The FA's Ramón y Cajal Contract (Spanish Government and Fondo Social Europeo) is acknowledged.

SUPPLEMENTARY MATERIAL

The Supplementary Material for this article can be found online at: https://www.frontiersin.org/articles/10.3389/fpls.2021.732821/full#supplementary-material

Supplementary Table 1 | List of differentially expressed genes (DEG, FDR < 0.01, cutoff $Log_2FC \geq \pm 1$) when compared the different RH storage conditions vs. the freshly harvested (FH) fruit.

Supplementary Table 2 | Biological processes related to NCPP development, rehydration, and dehydration stresses, and fruit detachment and storage, overrepresented in the set of induced (up arrow), and repressed (down arrow) DEG when comparing the indicated storage conditions with respect to freshly harvested (FH) fruit.

Supplementary Table 3 | Molecular functions related to NCPP development, rehydration, and dehydration stresses, and fruit detachment and storage, overrepresented in the set of induced (up arrow), and repressed (down arrow) DEG when comparing the indicated storage conditions with respect to freshly harvested (FH) fruit.

Supplementary Table 4 | Cellular components related to NCPP development, rehydration, and dehydration stresses, and fruit detachment and storage, overrepresented in the set of induced (up arrow), and repressed (down arrow) DEG when comparing the indicated storage conditions with respect to freshly harvested (FH) fruit.

Supplementary Table 5 | Metabolic pathways related to NCPP development, rehydration, and dehydration stresses, and fruit detachment and storage, overrepresented in the set of induced (up arrow), and repressed (down arrow) DEG when comparing the indicated storage conditions with respect to freshly harvested (FH) fruit.

REFERENCES

Agusti, J., Gimeno, J., Merelo, P., Serrano, R., Cercos, J., Conesa, A., et al. (2012). Early gene expression events in the laminar abscission zone of abscission-promoted citrus leaves after a cycle of water stress/rehydration: involvement of CitbHLH1. *J. Exp. Bot.* 63, 6079–6091. doi: 10.1093/jxb/ers270

Agusti, M., Almela, V., Juan, M., Alferez, F., Tadeo, F. R., and Zacarias, L. (2001). Histological and physiological characterization of rind breakdown of Navelate orange. *Ann. Bot.* 88, 415–422. doi: 10.1006/anbo.2001.1482

Albrigo, G. (1972). Distribution of stomata and epicuticular wax on oranges as related to stem end rind breakdown and water loss. *J. Amer. Soc. Horticult. Sci.* 97, 220–223.

Alférez, F., Agustí, M., and Zacarías, L. (2003). Postharvest rind staining in Navel oranges is aggravated by changes in storage relative humidity: effect on respiration, ethylene production and water potential. *Postharvest Biol. Technol.* 28, 143–152. doi: 10.1016/S0925-5214(02)00120-5

Alférez, F., Alquézar, B., Burns, J. K., and Zacarías, L. (2010). Variation in water, osmotic and turgor potentials during development of postharvest peel pitting in 'Marsh' grapefruit. *Postharvest Biol. Technol.* 56, 44–49. doi: 10.1016/j.postharvbio.2009.12.007

Alférez, F., Lluch, Y., and Burns, J. K. (2008). Phospholipase A2 and postharvest peel pitting in Citrus fruit. *Postharvest Biol. Technol.* 49, 69–76. doi: 10.1016/j.postharvbio.2008.01.010

Alferez, F., Singh, S., Umbach, A., Hockema, B., and Burns, J. K. (2005). Citrus abscission and Arabidopsis plant decline in response to 5-chloro-3methyl-4-nitro-1H-pyrazole are mediated by reduction in ATP and activation of lipid signaling. *Plant Cell Environ.* 28, 1436–1449. doi: 10.1111/j.1365-3040.2005.01381.x

Alferez, F., Wu, J., and Graham, J. (2020). Phospholipase D (PLD) response to water stress in citrus roots and leaves. *Agronomy* 10:45. doi: 10.3390/agronomy10010045

Alférez, F., Zhong, G. Y., and Burns, J. K. (2007). A citrus abscission agent induces anoxia-and senescence-related gene expression and plant decline in Arabidopsis. *J. Exp. Bot.* 58, 2451–2462. doi: 10.1093/jxb/erm111

Antonic, D. D., Subotic, A. R., Dragicevic, M. B., Pantelic, D., Milosevic, S. M., Simonovic, A. D., et al. (2020). Effects of exogenous salicylic acid on drought response and characterization of dehydrins in *Impatiens walleriana*. *Plants* 9, 1–22. doi: 10.3390/plants9111589

Benadjaoud, A., Benhassaine-Kesri, G., Zachovski, A., and Aid, F. (2013). Effects of dehydration and rehydration on the leaf lipids and lipid metabolism in *Parkinsonia aculeata* (Caesalpiniaceae). *Botany* 91, 1–9. doi: 10.1139/cjb-2013-0028

Bohnert, H. J., and Sheveleva, E. (1998). Plant stress adaptations - making metabolism move. *Curr. Opin. Plant Biol.* 1, 267–274. doi: 10.1016/S1369-5266(98)80115-5

Boyer, J. S. (1982). Plant productivity and environment. *Science* 218, 443–448. doi: 10.1126/science.218.4571.443

Bray, E. A. (1997). Plant responses to water deficit. *Trends Plant Sci.* 2, 48–54. doi: 10.1016/S1360-1385(97)82562-9

Cajuste, J. F., García-Breijo, F. J., Reig-Armiñana, J., and Lafuente, M. T. (2011). Ultrastructural and histochemical analysis reveals ethylene-induced responses underlying reduced peel collapse in detached citrus fruit. *Microsc. Res. Tech.* 74, 970–979. doi: 10.1002/jemt.20983

Cajuste, J. F., and Lafuente, M. T. (2007). Ethylene-induced tolerance to non-chilling peel pitting asrelated to phenolic metabolism and lignincontent in 'Navelate' fruit. *Postharvest Biol. Technol.* 45, 193–203. doi: 10.1016/j.postharvbio.2007.01.019

Chen, P., Jung, N. U., Giarola, V., and Bartels, D. (2020). The dynamic responses of cell walls in resurrecition plants during dehydration and rehydration. *Front. Plant Sci.* 10:1698. doi: 10.3389/fpls.2019.01698

Cronje, P. J. R., Zacarias, L., and Alferez, F. (2017). Susceptibility to postharvest peel pitting in Citrus fruits as related to albedo thickness, water status, and phospholipase activity. *Postharvest Biol. Technol.* 123, 77–82. doi: 10.1016/j.postharvbio.2016.08.012

Deluc, L., Quilici, D., Decendit, A., Grimplet, J., Wheatley, M., Schlauch, K., et al. (2009). Water deficit alters differentially metabolic pathways affecting important flavor and quality traits in grape berries of Cabernet Sauvignon and Chardonnay. *BMC Genom.* 10:212. doi: 10.1186/1471-2164-10-212

Dong, S., Jiang, Y., Dong, Y., Wang, L., Wang, W., Ma, Z., et al. (2019). A study on soybean responses to drought stress and rehydration. *Saudi, J. Biol. Sci* 26, 2006–2017. doi: 10.1016/j.sjbs.2019.08.005

Establés-Ortiz, B., Romero, P., Ballester, A. R., González-Candelas, L., and Lafuente, M. T. (2016). Inhibiting ethylene perception with 1-methylcyclopropene triggers molecular responses aimed to cope with cell toxicity and increased respiration in citrus fruits. *Plant Physiol. Biochem.* 103, 154–166. doi: 10.1016/j.plaphy.2016.02.036

Falcon, S., and Gentleman, R. (2006). Using GOstats to test gene lists for GO term association. *Bioinformatics* 23, 257–258. doi: 10.1093/bioinformatics/btl567

Gimeno, J., Gadea, J., Forment, J., Perez-Valle, J., Santiago, J., Martinez-Godoy, M. A., et al. (2009). Shared and novel molecular responses of mandarin to drought. *Plant Mol. Biol.* 70, 403–420. doi: 10.1007/s11103-009-9481-2

Gomez-Cadenas, A., Tadeo, F. R., Talon, M., and Primo-Millo, E. (1996). Leaf abscission lnduced by ethylene in water-stressed lntact seedlings of cleopatra mandaand requires previous abscisic acid accumulation in roots. *Plant Phys.* 112, 401–408. doi: 10.1104/pp.112.1.401

Grierson, W. (1986). "Fresh citrus fruits," in Fresh Citrus Fruits, eds W.F. Wardowsky and W. Grierson (Westport, CN: AVI Publishing Company, Inc.), p. 571. doi: 10.1007/978-1-4684-8792-3_20

Iglesias, D. J., Cercós, M., Colmenero-Flores, J. M., Naranjo, M. A., Ríos, G., Carrera, E., et al. (2007). Physiology of citrus fruiting. *Braz. J. Plant. Physiol.* 19, 333–362. doi: 10.1590/S1677-04202007000400006

Khan, N. A., Anjum, N. A., Nazar, R., and Iqbal, N. (2009). Increased activity of ATP sulfurylase and increased contents of cysteine and glutathione reduce high cadmium-induced oxidative stress in mustard cultivar with high photosynthetic potential. *Russ. J. Plant Physiol.* 56, 670–677. doi: 10.1134/S1021443709050136

Lafuente, M. T., Martínez-Téllez, M. A., and Zacarías, L. (1997). Abscisic acid in the response of 'Fortune' mandarins to chilling. Effect of maturity and high-temperature conditioning. *J. Sci. Food Agric.* 73, 494–502. doi: 10.1002/(SICI)1097-0010(199704)73:4<494::AID-JSFA761>3.0.CO;2-B

Lafuente, M. T., Zacarias, L., Martinex-Tellez, M. A., Sanchez-Ballesta, M. T., and Granell, A. (2003). Phenylalanine ammonia-lyase and ethylene in relation to chilling injury as affected by fruit age in citrus. *Postharvest Biol. Technol.* 29, 309–318. doi: 10.1016/S0925-5214(03)00047-4

Lee, B.-K., Zaman, R., Avice, J.-C., Ourry, A., and Kim, T.-H. (2016). Sulfur use efficiency is a significant determinant of drought stress tolerance in relation to photosynthetic activity in *Brassica napus* cultivars. *Front. Plant Sci.* 7:459. doi: 10.3389/fpls.2016.00459

MacCrackken, M. C. (2008). Prospects for future climatic change and the reasons for early action. *J. Air Waste Manage. Assoc.* 58, 735–7886. doi: 10.3155/1047-3289.58.6.735

Mahouachi, J., Arbona, V., and Gomez-Cadenas, A. (2007). Hormonal changes in papaya seedlings subjected to progressive water stress and re-watering. *Plant Growth Reg.* 53, 43–51. doi: 10.1007/s10725-007-9202-2

Mancosu, N., Snyder, R. L., Kyriakakis, G., and Spano, D. (2015). Water scarcity and future challenges for food production. *Water* 7, 975–992. doi: 10.3390/w7030975

Navari-Izzo, F., Quartacci, M. F., Pinzino, C., Rascio, N., Vazzana, C., and Sgherri, C. L. M. (2000). Protein dynamics in thylakoids of the desiccation-tolerant plant *Boea hygroscopica* during dehydration and rehydration. *Plant Phys* 124, 1427–1436. doi: 10.1104/pp.124.3.1427

Nolte, H., MacVicar, T. D., Tellkamp, F., and Kruger, M. (2018). Instant Clue: a software suite for interactive data visualization and analysis. *Sci. Rep.* 8:12648. doi: 10.1038/s41598-018-31154-6

Oliver, M. J., Farrant, J. M., Hilhorst, H. W. M., Mundree, S., Williams, B., and Bewley, J. D. (2020). Dessication tolerance: avoiding cellular damage during drying and rehydration. *Ann. Rev. Plant Biol.* 71, 435–460. doi: 10.1146/annurev-arplant-071219-105542

Qin, C., and Wang, X. (2002). The arabidopsis phospholipase D family. characterization of a calcium-independent and phosphatidylcholine-selective PLDζ1 with distinct regulatory domains. *Plant Phys.* 128, 1057–1068. doi: 10.1104/pp.010928

Quartacci, M. F., Forli, M., Rascio, N., Dalla Vecchia, F., Bochicchio, A., and Navari-Izzo, F. (2002). Desiccation-tolerant *Sporobolus stapfianus:* lipid composition and cellular ultrastructure during dehydration and rehydration. *J. Exp. Bot.* 311, 1269–1279. doi: 10.1093/jxb/48.6.1269

Rausch, T., and Wachter, A. (2005). Sulfur metabolism: a versatile platform for launching defense operations. *Trends Plant Sci.* 10, 503–509. doi: 10.1016/j.tplants.2005.08.006

Rawyler, A., Arpagaus, S., and Braendle, R. (2002). Impact of oxygen stress and energy availability on membrane stability of plant cells. *Ann. Bot.* 90, 499–507. doi: 10.1093/aob/mcf126

Rawyler, A., Pavelic, D., Gianinazzi, C., Oberson, J., and Braendle, R. (1999). Membrane lipid integrity relies on a threshold of ATP production rate in potato cell cultures submitted to anoxia. *Plant Physiol.* 120, 293–300. doi: 10.1104/pp.120.1.293

Rizzini, F. M., Bonghi, C., and Tonutti, P. (2009). Postharvest water loss induces marked changes in transcript profiling in skins of wine grape berries. *Postharvest Biol. Technol.* 52, 247–253. doi: 10.1016/j.postharvbio.2008.12.004

Romero, P., Alferez, F., Estables, B., and Lafuente, M. T. (2020a). Insights into the regulation of molecular mechanisms involved in energy shortage in detached citrus fruits. *Sci. Rep.* 10:1109. doi: 10.1038/s41598-019-57012-7

Romero, P., Alférez, F., and Lafuente, M. T. (2020b). Involvement of phospholipases and sucrose in carbon starvation-induced nonchilling peel pitting in citrus fruit. *Postharvest Biol. Technol.* 169:111295. doi: 10.1016/j.postharvbio.2020.11129

Romero, P., Gandía, M., and Alférez, F. (2013a). Interplay between ABA and phospholipases A2 and D in the response of citrus fruit to postharvest dehydration. *Plant Physiol. Biochem.* 70, 287–294. doi: 10.1016/j.plaphy.2013.06.002

Romero, P., Lafuente, M. T., and Alférez, F. (2014). A transcriptional approach to unravel the connection between phospholipases A2 and D and ABA signal in water stressed citrus fruit and leaves using a fruit specific ABA-deficient mutant. *Plant Physiol. Biochem.* 80, 23–32. doi: 10.1016/j.plaphy.2014.03.014

Romero, P., Lafuente, M. T., and Rodrigo, M. J. (2019). A sweet orange mutant impaired in carotenoid biosynthesis and reduced ABA levels results in altered molecular responses along peel ripening. *Sci. Rep.* 9:9813. doi: 10.1038/s41598-019-46365-8

Romero, P., Rodrigo, M. J., Alférez, F., Ballester, A. R., González-Candelas, L., Zacarías, L., et al. (2012). Unravelling molecular responses to moderate dehydration in harvested fruit of sweet orange (*Citrus sinensis* L. Osbeck)

using a fruit-specific ABA-deficient mutant. *J. Exp. Bot*. 63, 2753–2767. doi: 10.1093/jxb/err461

Romero, P., Rodrigo, M. J., and Lafuente, M. T. (2013b). Differential expression of the *Citrus sinensis* ABA perception system genes during postharvest fruit dehydration. *Postharvest Biol. Technol*. 76, 65–73. doi: 10.1016/j.postharvbio.2012.09.010

Seki, M., Umezawa, T., Urano, K., and Shinozaki, K. (2007). Regulatory metabolic networks in drought stress responses. *Curr. Opin. Plant Biol.* 10, 296–302. doi: 10.1016/j.pbi.2007.04.014

Szalai, G., Kellos, T., Galiba, G., and Kocsy, G. (2009). Glutathione as an antioxidant and regulatory molecule in plants under abiotic stress conditions. *J. Plant Growth Regul*. 28, 66–80. doi: 10.1007/s00344-008-9075-2

Thimm, O., Bläsing, O., Gibon, Y., Nagel, A., Meyer, S., Krüger, P., et al. (2004). MAPMAN: a user-driven tool to display genomics data sets onto diagrams of metabolic pathways and other biological processes. *Plant J*. 37, 914–939. doi: 10.1111/j.1365-313X.2004.02016.x

Wakchaure, G. C., Minhas, P. S., Meena, K. K., Kumar, S., and Rane, J. (2020). Effect of plant growth regulators and deficit irrigation on canopy traits, yield, water productivity and fruit quality of eggplant (*Solanum melongena* L.) grown in the water scarce environment. *J. Environ. Manage*. 262:110320. doi: 10.1016/j.jenvman.2020.110320

Wang, X. (2000). Multiple forms of phospholipase D in plants: the gene family, catalytic and regulatory properties, and cellular functions. *Prog Lipid Res.* 39, 109–149. doi: 10.1016/S0163-7827(00)00002-3

Yamaguchi-Shinozaki, K., and Shinozaki, K. (2006). Transcriptional regulatory networks in cellular responses and tolerance to dehydration and cold stress. *Annu. Rev. Plant Biol.* 57, 781–803. doi: 10.1146/annurev.arplant.57.032905.105444

Yuqing, L., Xiaoshuang, L., Jing, Z., Lu, Z., Xiaojie, L., Ruirui, Y., et al. (2021). Dehydration rates impact physiological, biochemical and molecular responses in desert moss *Bryum argenteum*. *Environ. Exp. Bot*. 183:104346. doi: 10.1016/j.envexpbot.2020.104346

Conflict of Interest: The authors declare that the research was conducted in the absence of any commercial or financial relationships that could be construed as a potential conflict of interest.

Publisher's Note: All claims expressed in this article are solely those of the authors and do not necessarily represent those of their affiliated organizations, or those of the publisher, the editors and the reviewers. Any product that may be evaluated in this article, or claim that may be made by its manufacturer, is not guaranteed or endorsed by the publisher.

frontiers in Plant Science

ORIGINAL RESEARCH
published: 23 September 2021
doi: 10.3389/fpls.2021.738726

Accumulation of Abnormal Amyloplasts in Pulp Cells Induces Bitter Pit in *Malus domestica*

Lina Qiu, Shanshan Hu, Yongzhang Wang and Haiyong Qu**

College of Horticulture, Qingdao Agricultural University, Qingdao, China

OPEN ACCESS

Edited by:
Natalia Marina Villarreal, CONICET, Instituto Tecnológico de Chascomús (INTECH), Argentina

Reviewed by:
Miroslawa Chwil, University of Life Sciences of Lublin, Poland
Sergio Tonetto Freitas, Brazilian Agricultural Research Corporation (EMBRAPA), Brazil
Nicholas Reitz, University of California, Davis, United States

***Correspondence:**
Yongzhang Wang
qauwyz@163.com
Haiyong Qu
haiyongqu@hotmail.com

Specialty section:
This article was submitted to Crop and Product Physiology, a section of the journal Frontiers in Plant Science

Received: *09 July 2021*
Accepted: *30 August 2021*
Published: *23 September 2021*

Citation:
Qiu L, Hu S, Wang Y and Qu H (2021) Accumulation of Abnormal Amyloplasts in Pulp Cells Induces Bitter Pit in Malus domestica. Front. Plant Sci. 12:738726. doi: 10.3389/fpls.2021.738726

Apple bitter pit primarily occurs during fruit ripening and storage; however, its formation mechanism remains unclear. Although it is considered that Ca^{2+} deficiency causes metabolic disorders in apples, there have been few studies on the mechanism of the bitter pit from the perspective of cell structure. At the fruit ripening stage, the fruit with a bitter pit on the tree was taken as the research material. In this study, the microscopic observation revealed numerous amyloplasts in the pulp cells of apples affected with bitter pit, but not in the healthy pulp. Furthermore, the results of fluorescence staining and transmission electron microscopy (TEM) revealed that the bitter pit pulp cells undergo programmed cell death (PCD), their nuclear chromosomes condense, and amyloplast forms autophagy. The cytoplasmic Ca^{2+} concentration in the healthy fruits was lowest near the peduncle, followed by that in the calyx, whereas it was highest at the equator. In contrast, the cytoplasmic Ca^{2+} concentration in apple fruits showing bitter pit disorder was lowest near the peduncle and highest in the calyx. Moreover, the cytosolic Ca^{2+} concentration in the flesh cells of apples with the bitter pit was much lower than that in the healthy apple flesh cells; however, the concentration of Ca^{2+} in the vacuoles of fruits with the bitter pit was higher than that in the vacuoles of healthy fruits. In summary, bitter pit pulp cells contain a large number of amyloplasts, which disrupts the distribution of Ca^{2+} in the pulp cells and causes PCD. These two processes lead to an imbalance in cell metabolism and induce the formation of a bitter pit.

Keywords: programmed cell death, vacuole, calcium, domestic apple, mitochondria, transmission electron microscope

INTRODUCTION

An apple (*Malus domestica*), belonging to the family Rosaceae, is a deciduous tree with the second largest global harvest area after citrus. However, an apple bitter pit is a major physiological disorder that affects the economic characteristics of apples worldwide. For example, in 2016, 74% of "Honeycrisp" apples in orchards of Pennsylvania (American) developed bitter pit (Baugher et al., 2017). Apple bitter pit should be referred to as a disorder rather than a disease (Parbery, 2015), as

it is not associated with fungi, bacteria, or viruses. Bitter pit involves complicated developmental processes (Ferguson and Watkins, 1989). It has been the most studied apple disorder since its discovery over a century ago. However, its formation mechanism has not yet been thoroughly studied. There is a significant correlation between Ca^{2+} concentration and fruit quality, as Ca^{2+} regulates fruit firmness, color, and soluble solid content, among other characteristics. There are 35 types of physiological disorders related to Ca^{2+} concentration in fruits (Freitas and Mitcham, 2012). Several studies have shown that the incidence of a bitter pit is primarily related to the absorption and distribution of calcium in fruits (Neilsen et al., 2005; Sharma et al., 2014), which mainly occurs near the calyx of the apple. During agricultural production, foliar calcium spraying, soil calcium application, and fruit postharvest calcium soaking are employed to reduce the incidence of bitter pit (Blanco et al., 2010; Falchi et al., 2017); however, the incidence of bitter pit in apple fruit has not yet been effectively controlled. For instance, Ernani et al. (2008) carried out spraying experiments on the apples for several years in succession. The period of calcium spraying included the time from flowering to 1 week before harvest, but the incidence of bitter pit remained extremely high (Ferguson and Watkins, 1989; Ernani et al., 2008). The results from various studies on the regulation of Ca^{2+} in the apples with bitter pit are contradictory (Ernani et al., 2008). Although some researchers believe that bitter pit is positively correlated with high [K + Mg]/Ca, Mg/Ca, and K/Ca ratios (do Amarante et al., 2013; Miqueloto et al., 2014; Liu et al., 2021), changes occurring in the structure of flesh cells of apples with bitter pit remain largely unknown, and the role of Ca^{2+} in the formation of bitter pit remains unclear (Torres et al., 2015).

Wilson and Bacic (2012) suggested that researchers should return to the cellular level and study the mechanisms of cellular behavior. Based on the ultrastructure of the cells, changes in the plasmids of three different types of apple pulp cells were analyzed. It is important to understand the complex biological changes in plasmid functions (Schaeffer et al., 2017). The distribution of Ca^{2+} in various cell compartments is affected by various types of stimulation (Meldolesi and Grohovaz, 2001). In a previous study, the ultra-microscopic observation of apple apoplasmic phloem revealed the unloading mechanism of sorbitol during apple development (Zhang et al., 2004). The apple was treated with $Ca(NO_3)_2$, $CaCl_2$, and Ca chelated with EDTA, and the structure of epidermal and hypodermal cells of the fruit was observed ultramicroscopically. Ca^{2+} contributes to the stability of cell structure (Kowalik et al., 2020). The distribution of Ca^{2+} in various cell compartments is affected by various types of stimulation; however, these changes can only be observed at the ultrastructural level (Sedmíková et al., 2003; Kowalik et al., 2020). In another study, the ultramicroscopic analysis of the pulp cells of apples with bitter pit revealed plasmolysis and cell membrane rupture (de Freitas et al., 2010); however, the type and mechanism of cell death remain unclear.

Currently, the "Fuji" apple is an economically important apple cultivar worldwide and is commercially grown in Japan, China, United States, Australia, and South Africa (Chigwaya et al., 2021). In China, 'Fuji' is the main planting variety, and its yield and cultivated area account for more than 70% of the total apple production and total cultivated area (Zhang et al., 2018). However, "Fuji" apples are prone to bitter pit (do Amarante et al., 2013). This study aimed to analyze the microstructure of pulp cells and the distribution of calcium ions in "Fuji" apples with bitter pit, and explore the formation mechanism of apple bitter pit.

MATERIALS AND METHODS

Materials

"Fuji" apples were obtained from the Laixi seedling breeding farm (Qingdao city, China, 120°28E, 36°51N). During the ripening season in autumn, the fruits suffering from the bitter pit were selected and removed from the tree. Healthy and undamaged fruits were used as controls.

Methods

Cell Microscopic Observation

The bitter pit-affected and healthy fruits were washed and dried; then, the bitter pit and healthy tissues were sectioned by hand slicing under a stereo microscope, and structural differences were observed under an optical microscope (Model: DM2500, LEICA, Germany).

Annexin V-FITC/PI Dying

Apoptotic cells were assessed using the Annexin V-FITC Detection Kit (Vazyme, China) according to the protocols of the manufacturer. After pre-cooling, 2–3 mm of flesh under the exocarp was cut into 2 mm × 2 mm × 3 mm cuboids on ice, embedded in optimal cutting temperature (OCT), and placed on a quick-freezing rack. A 25 μm-thick sheet was cut using a freezing microtome (Model: HM525, LEICA, Germany). The cells were washed two times with cold PBS and suspended in the binding buffer. The samples were stained with 10 μl of Annexin V-FITC and 10 μl of PI for 20 min at room temperature (25°C) in the dark. The apoptotic index was immediately determined using a confocal laser scanning microscope (TCS SP5 II, Leica, Germany).

Ultrastructural Observation

The fixation and embedding of apple pulp samples refer to the methods of de Freitas et al. (2010), which are slightly changed according to the characteristics of the samples. Approximately, 2–3 mm of flesh under the exocarp was cut into 1 mm × 1 mm × 2 mm cuboids. The cuboids were fixed with 3% glutaraldehyde in 10 mmol/L PBS (pH 7.2) for 2 h at room temperature, then embedded in 2% agar, and fixed in fresh fixatives under vacuum for 3 h at 4°C. After rinsing with distilled water, the sections were incubated in a 0.5% aqueous uranyl acetate solution at room temperature for 2 h. After another two washes with distilled water, the plant material was dehydrated in a series of acetone at successive concentrations of 30% (10 min), 50% (10 min), 70% (10 min), 90% (10 min), 95% (30 min), and 100% (30 min, two times). The dehydrated plant samples were embedded in Eponate 12 resin (Ted Pella

Inc., Redding, CA, United States) and polymerized at 45°C for 12 h and 60°C for 48 h. The fixed and dehydrated pulp cells were prepared for TEM observation. Ultrathin sections (60 nm) were cut with an ultramicrotome (Model: UC7, Leica, Germany) and stained with uranyl acetate/lead citrate. The sections were examined using a Hitachi TEM system (Model: HT7700) at 80 kV.

The potassium pyroantimonate method was used to determine free Ca^{2+} in the cells. The fixation and embedding of apple pulp samples were performed as described by de Freitas et al. (2010). To verify that the black particles observed *via* electron microscopy were Ca^{2+}, the ultrathin slices of the pulp tissue with bitter pit disorder were chelated with 0.2 mol/L EGTA (Qin et al., 2005).

Nuclear 4′,6-Diamidino-2-Phenylindole Staining

First, 2 g of the sample was weighed and ground to a powder using liquid nitrogen; then, nuclei were extracted using the Plant Cell Nuclear Extraction Kit (Product Number: NXTRACT, Sigma-Aldrich, MO, United States) according to the instruction of the manufacturer. The extracted nuclei were stained with DAPI and observed under a fluorescence microscope (EVOS FL Auto 2, Thermo Fisher Scientific, MA, United States).

Optical Microscope Observation of Amyloplasts

To observe the amyloplasts in bitter pit cells, the pulp was soaked in a fixative (5% (v/v) formaldehyde, 5% (v/v) acetic acid, and 45% (v/v) ethanol) at 4°C for 48 h. The fixed pulp was stained with an I_2-KI solution (0.15% (w/v) I_2 and 0.45% (w/v) KI) for 5 min. Then, the fruit pulp was observed under a light microscope (EVOS Auto 2, Thermo Fisher Scientific, MA, United States) (Takahashi et al., 2003).

Apoplastic Water-Soluble Ca^{2+} Determination

The extraction and determination of water-soluble mineral elements in the apoplast were conducted according to the methods described by de Freitas et al. (2012). Briefly, the outer skin of the healthy and bitter pit fruits was removed with a stainless-steel knife, pulp with a diameter of 1.5 cm was retrieved with a punch perpendicular to the projection position, about 3 mm of the flesh of the surface layer was cut, and a pulp disc with a diameter of 1.5 cm, the thickness of about 3 mm, and weight of 0.40–0.45 g was obtained. The pulp disc was added to ddH_2O for 10 s, the water was sucked up with paper, and the disc was placed into a funnel to extract the mineral elements of the apoplasts; finally, the Whatman filter paper was placed into the funnel and used for filtering 200 μl isotonic mannitol (0.31 mol/L). The funnel samples were eluted with 700 μl of isotonic mannitol under a 25 mm Hg vacuum (70 μl each time). Three discs were obtained from three fruits each, providing a total of nine pulp discs. The extraction liquid volume of each sample was approximately 6.3 ml. The apoplastic Ca^{2+} content was measured using inductively coupled plasma mass spectroscopy (Agilent 7700, Agilent Technologies Inc., Santa Clara, CA, United States).

Transcriptome Analysis

The calyx end pulp of healthy fruit, the calyx end healthy pulp of bitter pit fruit, and the pulp of bitter pit were selected for the transcriptomic analysis. RNAs from the samples were extracted using TRIzol Reagent (Life Technologies, Carlsbad, CA, United States) in three biological replicates as per the instructions from the manufacturer. RNA quality and concentration were verified using the Agilent 2100 Bioanalyzer (Agilent Technologies, Inc., Santa Clara, CA, United States). RNA reverse transcription into cDNA (TIANGEN Biotech, Beijing Co., Ltd, China). The transcribed cDNA was used to construct cDNA libraries using the NEBNext Ultra RNA Library Prep Kit from Illumina (NEB, E7530, MA, United States). The cDNA library was sequenced on a paired-end (PE) flow cell using Illumina HiSeq 2500 sequencing platform (Illumina Inc., San Diego, CA, United States). Beijing Biomarker Technologies[1] provided the commercially available experimental procedures. The transcriptomic data that support the findings of this article are accessible under NCBI's BioProject with accession number PRJNA733599 and SRA accession numbers SRR14684876, SRR14684877, and SRR14684878.

Fluo-4/AM Staining

The fruits were consistently light, and the fruit size was uniform. The apples were cut into four parts on average, and each portion of pulp was taken from near the peduncle to near the calyx. Seven healthy apples and six apples showing bitter pit symptoms were used to isolate the protoplasts from the pulp cells, which were then fluorescently stained with fluo-4/AM (Qiu et al., 2020). The final concentration of fluo-4/AM (Dojindo Laboratories, Kumamoto, Japan) was 5 μmol/L. Since the excitation wavelength of fluo-4/AM is 490 nm, GFP was selected as the light cube. The viability of cells was then determined under a fluorescent microscope (EVOS Auto 2, Thermo Fisher Scientific, United States). The fluorescence results were analyzed using Image-Pro Plus 6.0 software (Media Cybernetics, Inc., MD, United States), according to our published methods (Qu et al., 2016).

Transformation by *in vivo* Fruit Injection

The target gene was transformed into Agrobacterium and propagated in LB medium, then centrifuged, collected sedimentation, and put into MES medium for activation. Immature tomatoes (green ripened) were selected for *in vivo* injection. Injection methods refer to Yasmeen et al. (2009). All tomatoes were injected two times on two consecutive days. Ten fruits were used for each treatment, and both experiments were carried out three times. Fruits injected with agrobacterium without target gene were used as a negative control. The tomatoes were harvested a week after injection.

Statistical Analyses

Microsoft Office 365 was used for data processing. Statistical analysis was performed using GraphPad Prism 7.0 software (GraphPad Software, Inc., La Jolla, CA, United States). The student's *t*-test was used to analyze the differences among the experimental groups.

[1] http://www.biomarker.com.cn

RESULTS

Microscopic Observation of the Pulp Cells of Apples With Bitter Pit

At the fruit ripening stage, the apples growing on the tree were affected with bitter pit (**Supplementary Figure 1A**). The symptoms included small dark depressions near the calyx end of the fruit caused by the collapse of flesh cells just below the peel (**Supplementary Figures 1B–D**). After sections of the fruit were picked from the tree, no organelles were observed in the healthy pulp cells *via* optical microscopy (**Figure 1A**). However, there was abundant granular material in the pulp cells of apples with bitter pit (**Figure 1B**). This granular material showed black and purple color after I_2-IK staining (**Figures 1C,D**), indicating that it contained starch. Upon observing the healthy fruit cells *via* transmission electron microscopy (TEM), the cell membrane surface was found to be smooth without protrusions, and the vacuole had no obvious inclusion and did not undergo plasmolysis (**Figures 2A–C**). However, the protoplasts of the flesh cells of apples with bitter pit extended into vacuoles (**Figures 2D,E**), showed plasmolysis (**Figures 2D,E**), and contained numerous amyloplasts (**Figures 2D–F**). These observations indicated the accumulation of amyloplasts in the flesh cells of apples with bitter pit.

Ultrastructural Detection of Intracellular Free Calcium

As the vacuole occupied the center of the flesh cell of the healthy fruit and the cytoplasm was squeezed around the cell, it was difficult to observe Ca^{2+} precipitation (**Figure 3A**). In the fruit with a bitter pit, the healthy pulp cells near the bitter pit location showed plasmolysis. Extensive Ca^{2+} precipitation was observed in the cytoplasm, but not in the vacuole (**Figure 3B**). The pulp cells of apples with bitter pit showed Ca^{2+} precipitation not only in the cytoplasm but also in the vacuole and mitochondria (**Figure 3C**). These results indicate that the concentration of free Ca^{2+} in the vacuoles of fruits with the bitter pit was higher than that of healthy pulp cells. No black precipitate was

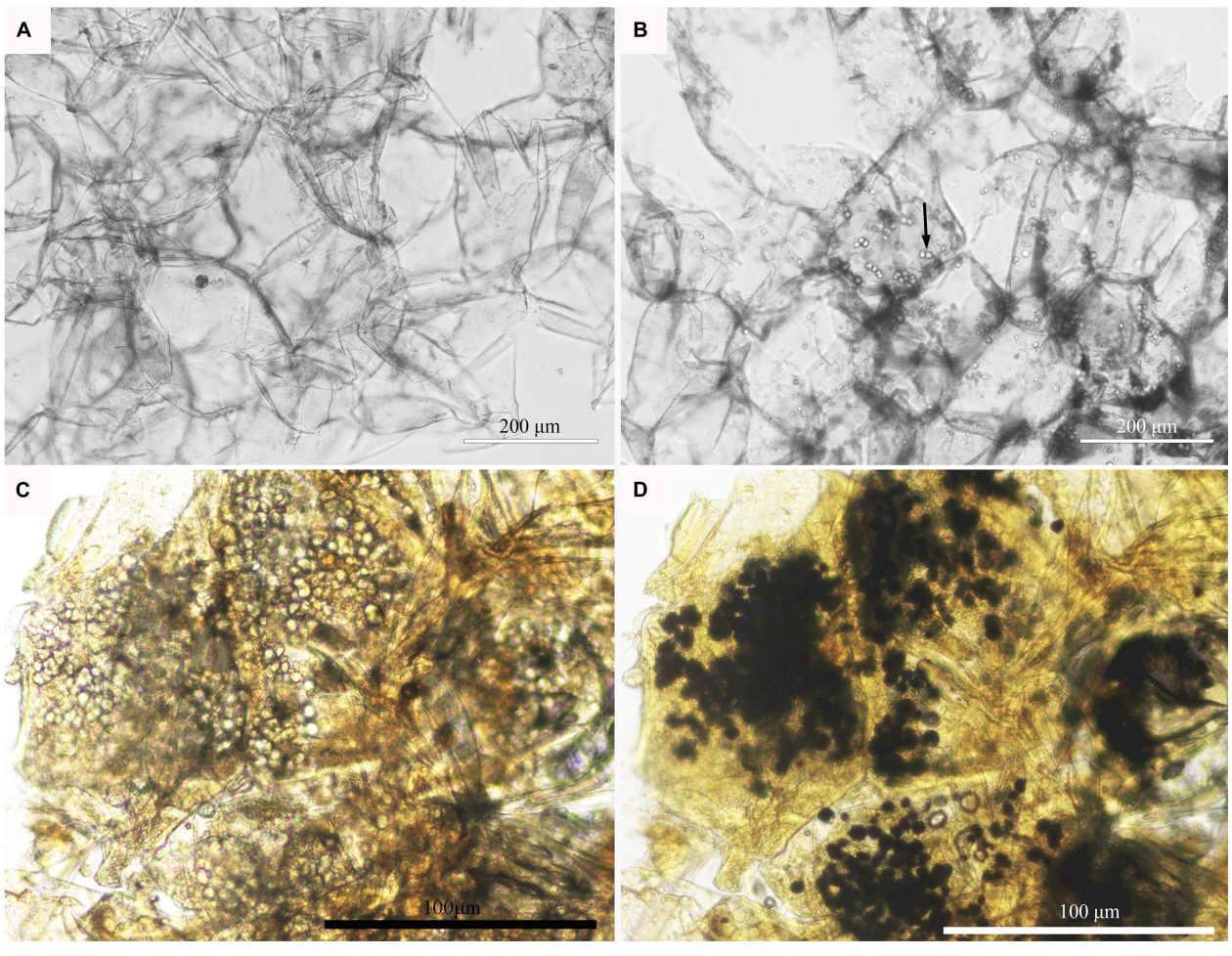

FIGURE 1 | Microscopic observation of amyloplasts in the flesh cells of apples with bitter pit. **(A)** The flesh of healthy fruit. **(B)** The bitter pit flesh; the cells contain granular substances. **(C)** Pulp cells from bitter pit-affected fruits without I_2-IK staining. **(D)** Pulp cells from bitter pit-affected fruits stained with I-IK. Granular material is shown in black and purple. The magnification of the objective of the microscope is 20 times.

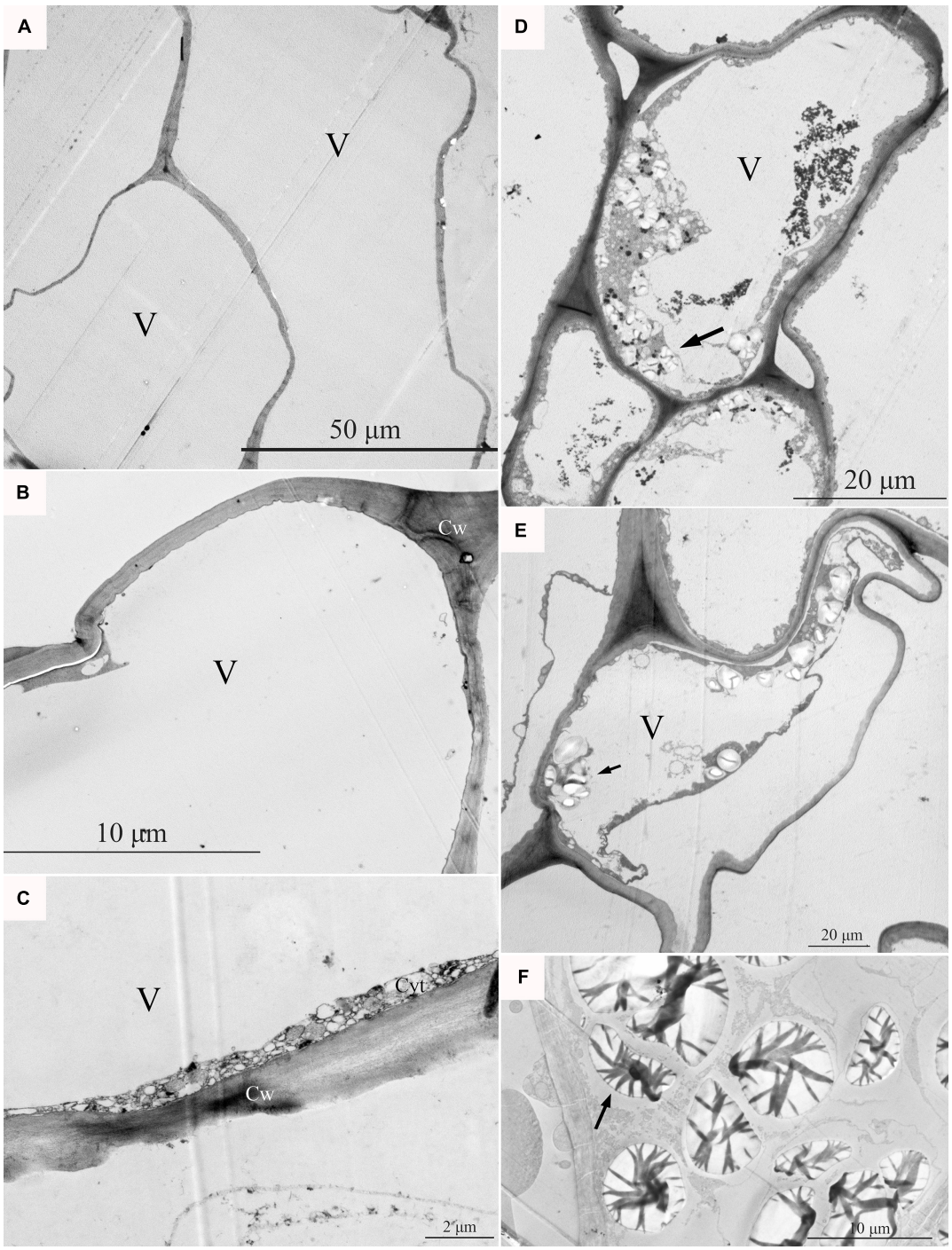

FIGURE 2 | The pulp cells were observed *via* transmission electron microscopy (TEM). **(A–C)** Pulp cells of a healthy fruit; healthy pulp cells gradually enlarge. **(D)** The ultramicroscopic observation of amyloplasts in bitter pit flesh cells. **(E)** Analysis of the flesh cells of bitter pit in apples revealed plasmolysis and abundant amyloplasts. **(F)** Amyloplasts further enlarged. Black arrows indicate amyloplasts. V, vacuole; Cw, cell wall.

observed in the vacuoles of the ultrathin slices of the fruit with bitter pit treated with 0.2 mol/L EGTA, which indicated that the black precipitate observed was due to the precipitation of free Ca^{2+} (**Figure 3D**). In addition, the granular precipitation of Ca^{2+} on the tonoplast of the pulp cells of apples with bitter pit (**Supplementary Figures 2A,B**) was similar to that in the bean hypocotyl cells (*Phaseolus vulgaris* L) (Hanchey, 1982) and the shape of the Ca^{2+} flocculent precipitates (**Supplementary Figures 2C,D**) in the vacuoles were similar to that in rice (*Oryza sativa* L.) lodicules (Qin et al., 2005). The pulp cells from

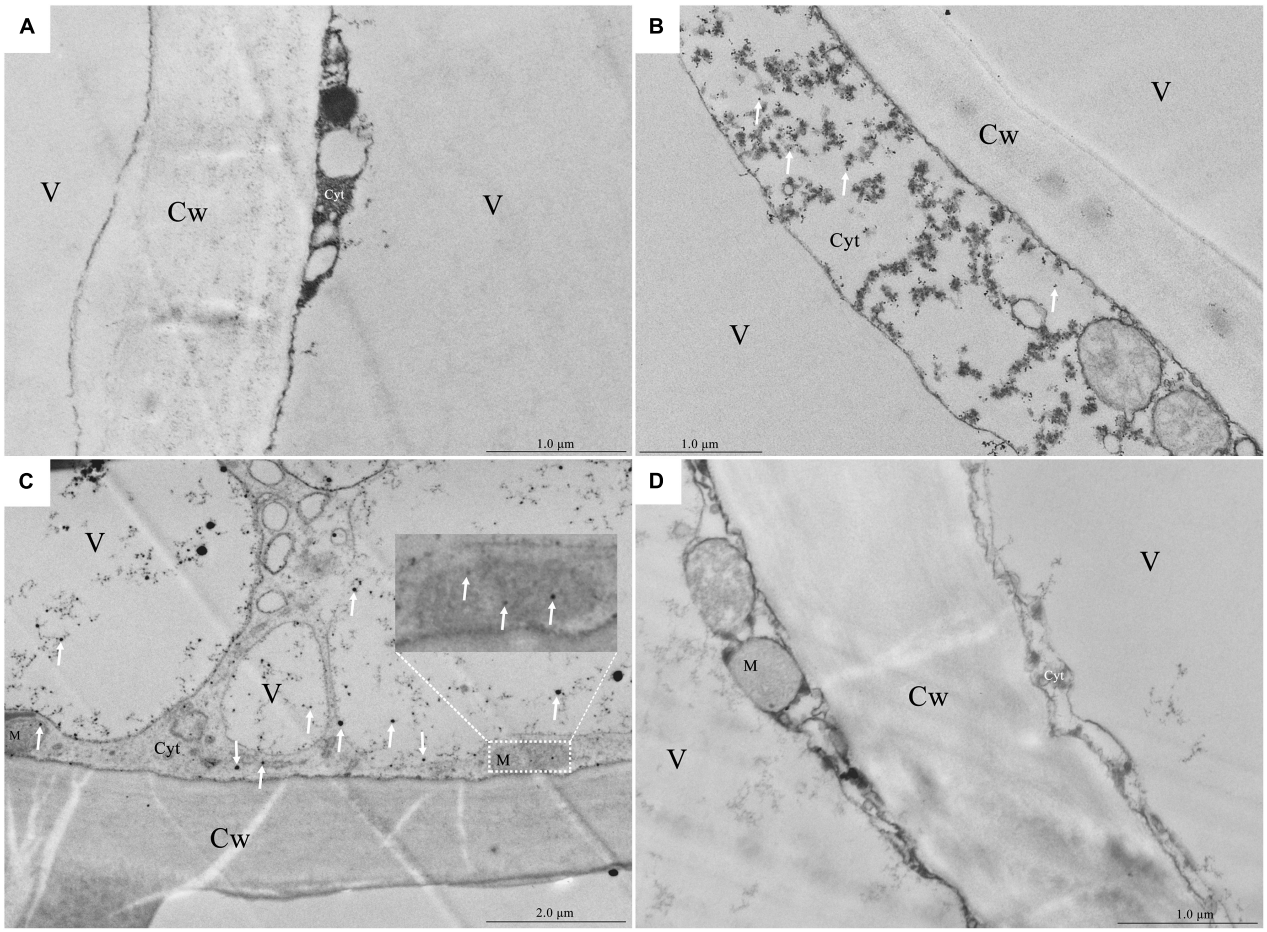

FIGURE 3 | Localization of calcium in the pulp cells *via* potassium pyroantimonate precipitation. **(A)** Healthy fruit pulp cell fragments. **(B)** Pulp cell fragments of the healthy part of the fruit with bitter pit taken from an area close to the bitter pit spot part. **(C)** Fragments of pulp cells with bitter pit. **(D)** The ultrathin section of the fragments of pulp cells from apples with the bitter pit was treated with 0.2 mol/L EGTA. The white arrow points to Ca^{2+} precipitation. Cw, cell wall; M, mitochondria; Cyt, cytoplasm; V, vacuole.

healthy and bitter pit parts of the fruit were observed under a microscope. No amyloplasts were observed in the healthy pulp cells of apples with bitter pit. Contrastingly, the pulp cells close to the bitter pit location contained small amounts of amyloplasts, while pulp cells from the bitter pit part contained numerous amyloplasts (**Supplementary Figures 3A–C**). This is consistent with the results of ultrastructural observations of the distribution of Ca^{2+} (**Figures 3A–D**). These findings suggest that the increase in Ca^{2+} concentration in the pulp cells is consistent with the accumulation of amyloplasts.

Comparison of Apoplastic Water-Soluble Ca^{2+} Concentration and Distribution of Cytoplasmic Ca^{2+} in Fruits

We measured the apoplastic water-soluble Ca^{2+} concentration at the calyx end of the fruit. The Ca^{2+} content of the fruit with the bitter pit was higher than that of healthy fruit, and the Ca^{2+} content of the healthy part of the fruit with the bitter pit was lower than that of healthy fruit, but the difference was not significant (**Figure 4A**). The fruit was divided into four parts (**Figure 4B**). Protoplasts were extracted from each part from the peduncle to the calyx and stained with fluo-4/AM (**Figure 4C**). In healthy fruit, the cytoplasmic Ca^{2+} concentration was lowest in the peduncle and calyx and highest in the equatorial part of the fruit. In the fruit with bitter pit, the cytoplasmic Ca^{2+} concentration was lowest in the peduncle end and inside the equator and highest in the calyx (**Figure 4D**). Thus, the distribution of cytoplasmic Ca^{2+} in fruits with the bitter pit was not consistent with that in the healthy fruits. Transcriptomic analysis revealed 431 common differential genes in the healthy fruit pulp cells, healthy pulp cells of fruits with bitter pit, and bitter pit pulp cells. Upon differential gene analysis using the BMKCloud platform[2], six genes were found to be associated with Ca^{2+} concentration. The six genes were upregulated in the pulp of fruits with bitter pit (**Supplementary Figure 4**). This can explain why Ca^{2+} concentration in the pulp cells of fruits with the bitter pit was higher than that in other parts of the cells.

[2]www.biocloud.net

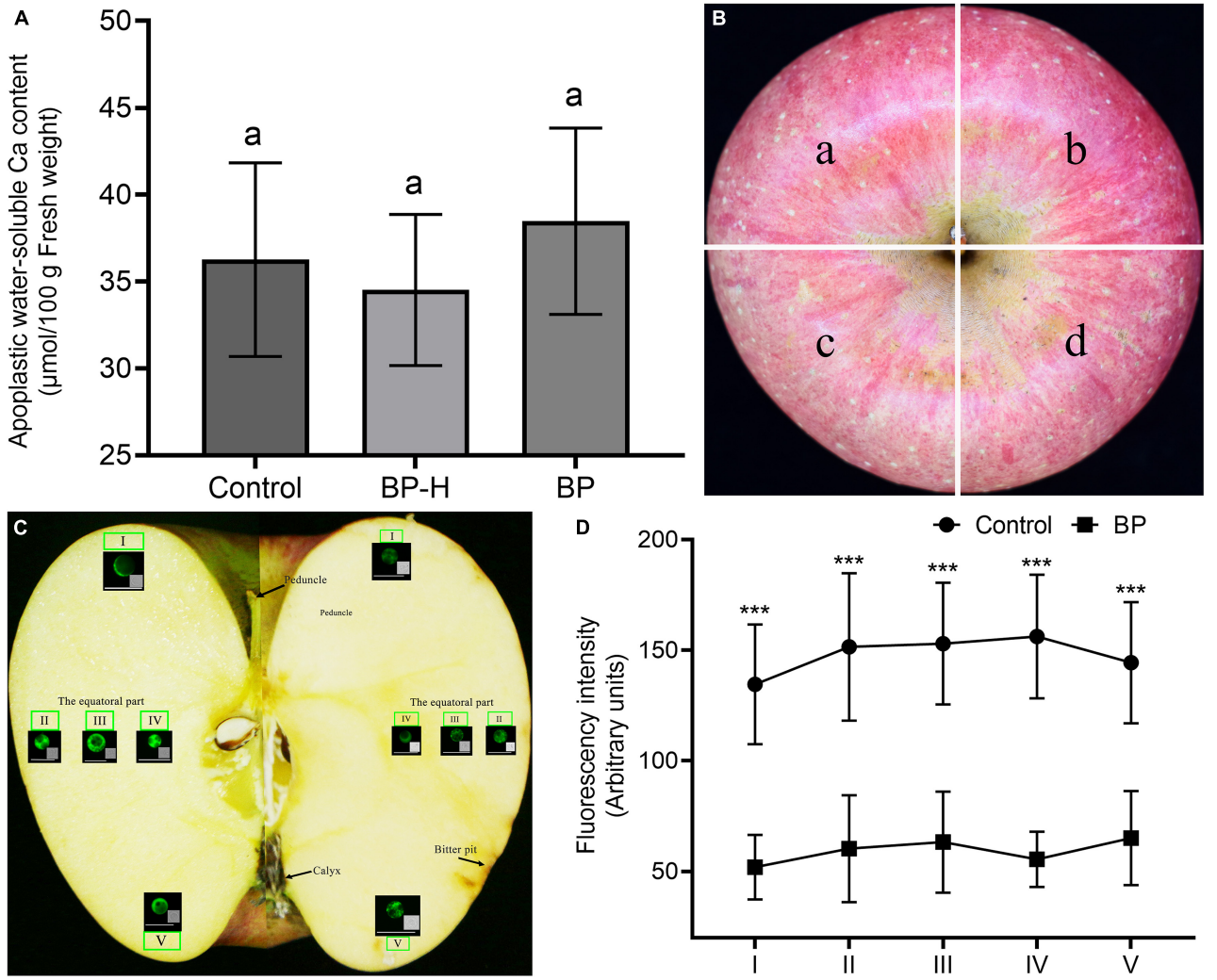

FIGURE 4 | Apoplastic water soluble and cytoplasmic Ca^{2+}. **(A)** The concentrations of water-soluble Ca^{2+} in different pulps near the calyx of fruit were compared. Data are represented as mean ± SE. The same letters indicate no significant difference (α = 0.05). Control, healthy fruit; BP-H, healthy pulp of bitter pit fruit; and BP, bitter pit fruit. **(B)** The image on the left shows a healthy fruit and that on the right shows a fruit with bitter pit disorder. The apple was divided into four sections on average. **(C)** Five pulp portions from each fruit section from near the peduncle to the calyx were sampled, and the pulp cell protoplasts were isolated, as shown in panels I, II, III, IV, and V. Fluorescent staining of cytoplasmic Ca^{2+} in apple fruit tissues from near the peduncle to near the calyx. Panels I–V show representative fluorescence images of protoplasts. **(D)** Ca^{2+} distribution in healthy fruit and bitter pit fruit. Seven healthy and bitter pit fruits were analyzed each. The number of healthy fruit protoplasts analyzed in each fruit section was as follows: I, n = 105; II, n = 92; III, n = 133; IV, n = 136; V, and n = 124. The number of bitter pit fruit protoplasts analyzed in each fruit section was as follows: I, n = 131; II, n = 142; III, n = 165; IV, n = 129; and V, n = 103. Values are presented as mean ± SE. ***Significant difference ($P < 0.001$). Control, healthy fruit; BP, bitter pit fruit. The magnification of the objective of the microscope is 20 times.

In addition, the cytoplasmic Ca^{2+} concentration in each part of the pulp of healthy fruits was significantly ($P < 0.001$) higher than that in the corresponding portions of fruits with bitter pit symptoms (**Figure 4D**). These results suggest that cytoplasmic Ca^{2+} is associated with the occurrence of a bitter pit.

Fluorescence-Based Detection of Programmed Death of Flesh Cells in Apples With Bitter Pit

The results of Annexin V-FITC/PI staining revealed that the healthy flesh cells did not emit fluorescent signals in either green fluorescent protein (GFP) or red fluorescent protein (RFP) channels (**Figure 5A**). This indicated that the cell membranes of healthy and mature pulp cells were intact without losing the selection permeability. However, the pulp cells of apples with bitter pit emitted green fluorescence in the cell membrane in the GFP channel, and the cell nucleus emitted red fluorescence in the RFP channel (**Figure 5B**). This indicated that the cells exhibited apoptotic characteristics, such as phosphatidylserine eversion and loss of selective permeability of the cell membrane. When the cell membrane loses its selective permeability, propidium iodide (PI) can enter the cell and bind with chromatin in the nucleus to emit red fluorescence. We used dexamethasone, which

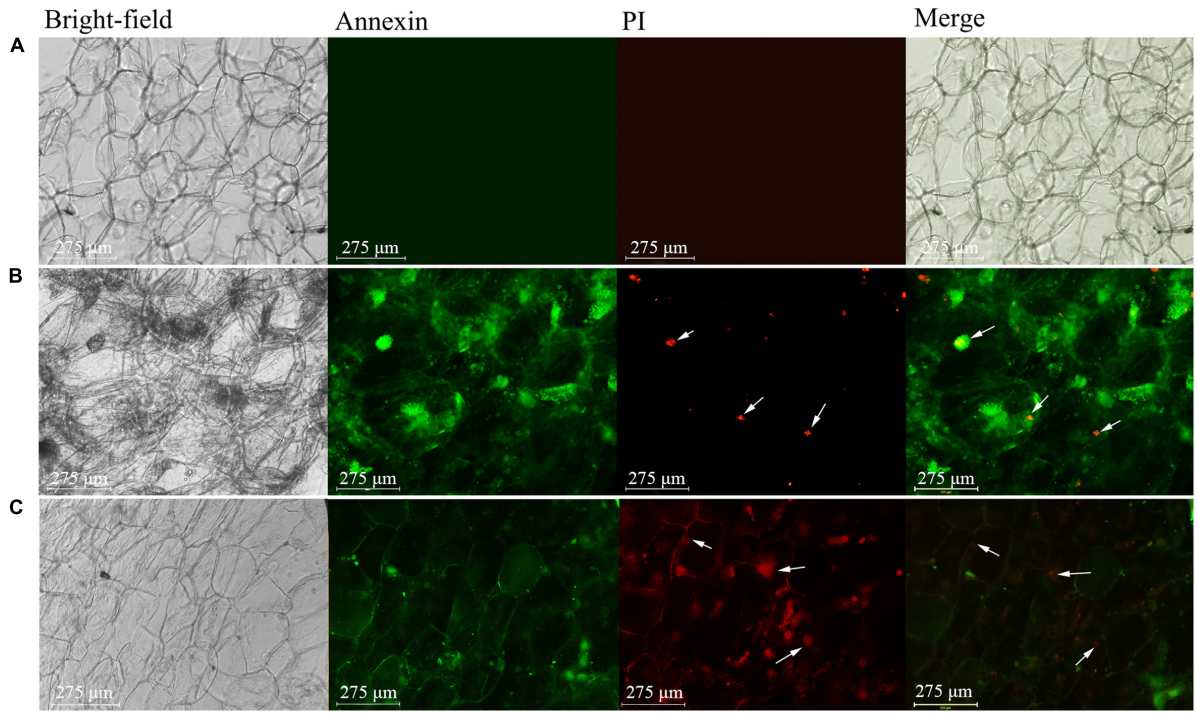

FIGURE 5 | Fluorescence microscopic analysis of apple pulp cells. The cells were double-stained with Annexin V-FITC (green) and PI (red). **(A)** Healthy pulp cell. **(B)** Pulp cells of an apple with bitter pit. **(C)** Pulp cells of an apple treated with dexamethasone. The arrow indicates the nucleus. Bright field, optical photos without fluorescence. Annexin, green fluorescent channel. Green fluorescence indicates that the cell membrane could be stained. PI, red fluorescent channel. Red fluorescence indicates that the chromatin in the nucleus could be stained. Merge, the overlaying of the first three photos is used to illustrate the corresponding structure of the stained fluorescent cells. The magnification of the objective of the microscope is 20 times.

is a programmed cell death (PCD) inducer, to treat flesh cells (Bonapace et al., 2010). The fluorescence staining results of dexamethasone-treated flesh cells were similar to those of flesh cells of apples with bitter pit (**Figure 5C**). These findings indicate that the flesh cells of apples with bitter pit undergo PCD.

Nuclear Pathological Examination

To determine DNA concentration, the extracted nuclei were simultaneously stained with PI and 4′,6-diamidino-2-phenylindole (DAPI). The nuclei of the cells of healthy pulp showed no fluorescence (**Figure 6A**), while those of apples with bitter pit showed red fluorescence (**Figure 6B**). These results indicated that the nuclear membranes of the cells of healthy pulp remained intact, while the nuclear membranes of the pulp cells of apples with bitter pit lost selective permeability. The nuclei of cells of normal pulp and those of apples with bitter pit could be stained by DAPI, but the fluorescence density of healthy flesh cells was low and uniform (**Figure 6A**), while that of the pulp cells of apples with the bitter pit was high and uneven (**Figure 6B**). There was a greater number of high-intensity fluorescent spots, which indicated that the chromosomes in nuclei of the cells of fruits with bitter pit were highly concentrated. Similar to that in the animal cells, extensive chromatin condensation is the most conspicuous feature of plant cells undergoing PCD (Latrasse et al., 2016). The fluorescence of the nuclei, extracted from dexamethasone-treated flesh cells, stained with PI and DAPI was similar to that of the flesh cells of apples with bitter pit (**Figure 6C**). These findings demonstrated that the flesh cells of apples with bitter pit undergo PCD.

Ultramicroscopic Observations of Amyloplasts in the Cells of Apples With Bitter Pit

There were two kinds of amyloplasts in the pulp cells of apples with bitter pit. The first kind of amyloplasts was those containing large starch granules with an average size of 6.81 μm, (**Supplementary Figure 5**) some of which were located in the cytoplasm (**Figure 7A**) and some were lying freely in vacuoles (**Figure 7B**). The other kind contained small starch granules with an average size of 0.31 μm (**Supplementary Figure 5**). The amyloplasts containing small starch granules play a similar role as that of microautophagy (**Figure 7C**) in the programmed death of animal cells. This kind of amyloplasts can divide and proliferate (**Figure 7D**) and then move into the vacuole (**Figure 7E**). These results indicate that autophagy is involved in the apoptosis of flesh cells in apples with bitter pit.

DISCUSSION

The "Fuji" variety is one of the most common types of planted apples in the world, but it is susceptible to bitter pit

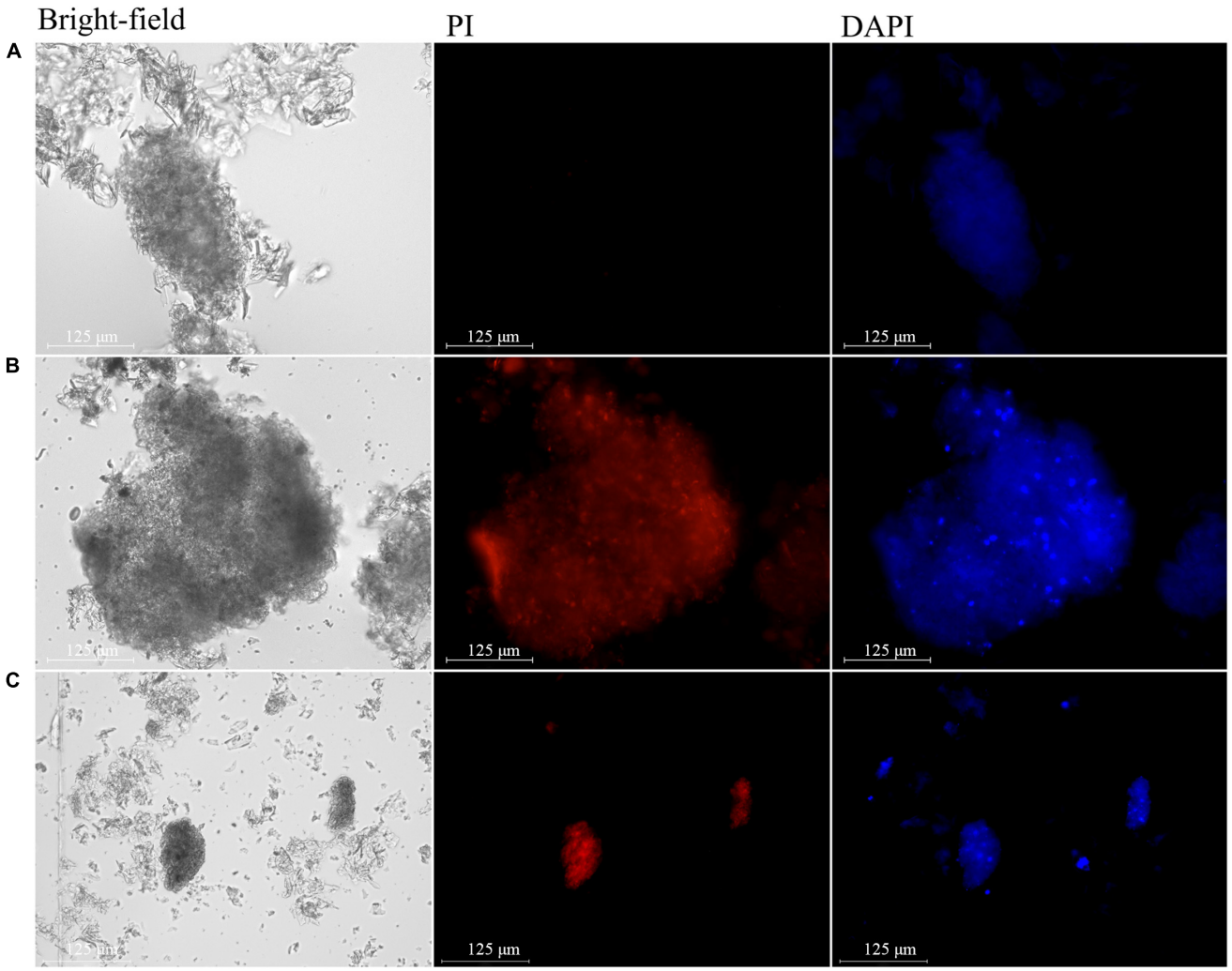

FIGURE 6 | Changes in the nucleus during programmed cell death (PCD). **(A)** Nucleus extracted from healthy pulp cells. Propidium iodide (PI) and 4′,6-diamidino-2-phenylindole (DAPI) positively stained the nucleus. **(B)** Nucleus extracted from the flesh cells of apple with bitter pit. **(C)** Nucleus extracted from dexamethasone-treated flesh cells. The magnification of the objective of the microscope is 20 times.

(Bonomelli et al., 2020). A bitter pit can occur during both the fruit ripening and storage stages (Ferguson and Watkins, 1989), but we chose to study the fruit with a bitter pit in the ripening period. Although the storage temperature was approximately 0°C, the bitter pit spots of apples often developed a fungal infection, which affected the results of the experiment. It was relatively difficult to select an apple whose lesion spots were solely due to bitter pit during the storage stage. A bitter pit at the ripening stage of the fruit is characterized by the presence of sunken, water-soaked lesion spots (**Supplementary Figures 1B,D**) in the outer layers of the fruit. The cells of apples with bitter pit were observed under an optical microscope and were found to contain numerous amyloplasts; however, there were no amyloplasts in the healthy pulp cells, which were consistent with the results of a previous study (Simons and Chu, 1980). Blossom-end rot (BER) in pepper fruits is known as a physiological disorder, and the healthy part of BER fruits had higher concentrations of symplastic starch (Turhan et al., 2006). The amyloplasts are organelles found in plant cells that are responsible for starch synthesis and accumulation in plants. An amyloplast accumulation in the root cap occurs due to an increase in the cytoplasmic Ca^{2+} concentration (Chandra et al., 1982; Kolesnikov et al., 2016; Nakano et al., 2021). As assessed from the *A. thaliana* cell suspension, the amyloplasts are involved in a transient increase in Ca^{2+} concentration *via* several environmental stimuli, which suggests that the amyloplasts can balance Ca^{2+} concentrations (Sello et al., 2016) and that Ca^{2+} is closely related to the amyloplasts. The distribution of Ca^{2+} precipitated by potassium pyroantimonate in the cells of apples with the bitter pit was observed ultramicroscopically. It was found that a large amount of Ca^{2+} precipitated in the vacuoles and mitochondria. The area of Ca^{2+} precipitates represented the Ca^{2+} concentration (Otulak and Garbaczewska, 2011; Yin et al., 2015). In the fruit with bitter pit, the Ca^{2+} concentration

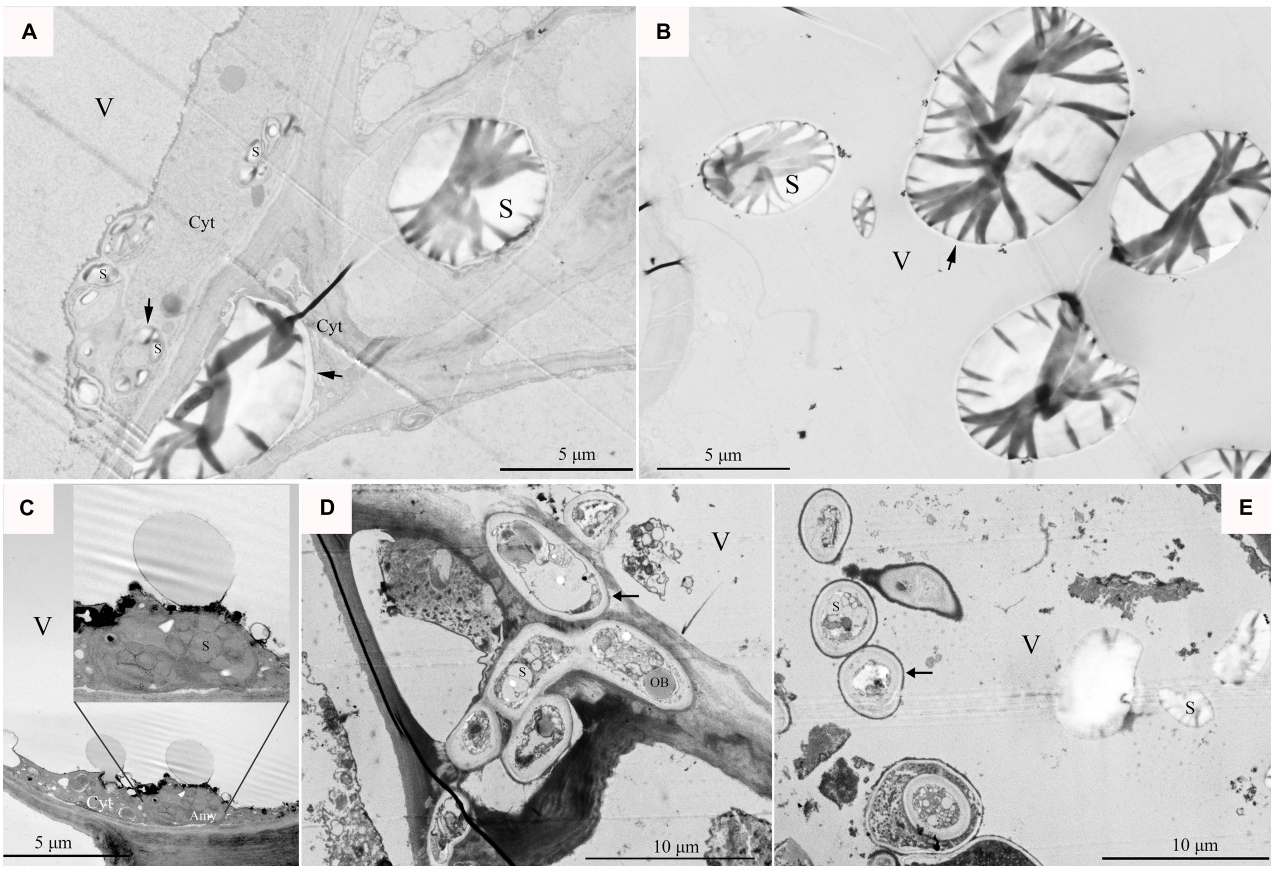

FIGURE 7 | The state of amyloplasts in cells. **(A)** Flesh cell fragments of an apple with bitter pit, with a large amyloplast located in the cytoplasm. **(B)** Starch granules were freely lying in the vacuoles in the pulp cells of apples with bitter pit. **(C)** The amyloplasts contained starch granules and vesicles protruding into vacuoles. The inner image shows an enlarged amyloplast. **(D)** The amyloplast number increased *via* division, and the starch contained small starch granules and osmiophilic bodies. The red box shows amyloplast dividing in the protoplast and dissociating in the vacuole. **(E)** The amyloplasts were freely lying in the vacuoles. V, vacuoles; S, starch granule; OB, osmiophilic body. The arrow indicates the amyloplast similar to autophagy.

in the cells in the bitter pit site was significantly higher than that in the cells close to the bitter pit site (**Supplementary Figure 6**). This finding indicates that there is a relationship between the amyloplasts and Ca^{2+} concentration in the pulp of apples with bitter pit.

Some studies have suggested that the bitter pit in fruits is caused by a decrease in free Ca^{2+} concentration in the apoplasts, which destroys the cell membrane and causes cell death (Miqueloto et al., 2014; DeBrouwer et al., 2020). Apoplastic water-soluble Ca^{2+} is closely related to physiological disorders, which are not affected by the season or harvest date. Pavicic et al. (2004) suggested that the deficiency of water-soluble Ca^{2+} is the most significant factor related to the development of bitter pit in "Idared" apples. However, according to our results, water-soluble calcium in the apoplast is not associated with the bitter pit. Furthermore, Liu et al. (2021) also found that the extracellular water-soluble Ca^{2+} in "Honeycrisp" apples is not associated with bitter pit. This is consistent with the results of the present study. We further investigated which kind of death of the cells of apples with bitter pit. In the present study, the flesh cells of apples with bitter pit were observed using Annexin V-FITC/PI staining. In addition, we used ultra-thin sections and cell nucleus extraction methods to determine the concentration of chromatin. The results were similar to those of oxidative stress-induced apoptosis in the diabetic islet cells (Srivastava et al., 2016) and suggested that the pulp cells of bitter pit undergo PCD. PCD is a physiological activity that regulates the body through active cell death (Hautegem et al., 2015). The process is carried out under the tight regulation of genes (Latrasse et al., 2016). Transcriptomic analysis revealed that the expression of genes that negatively regulate PCD in the flesh cells of apples with the bitter pit was higher than that in the healthy pulp cells (**Supplementary Table 1**). Furthermore, we transferred one of the different genes (*Md12g1174700*) to young tomato fruits using the transient method, which in turn induced PCD in tomatoes (**Supplementary Figure 7**). This further illustrated the PCD of the flesh cells of apples with bitter pit.

In animal cells, when the cell is programmed to die, the cell membrane can fold to form apoptotic bodies and phagosomes, but plant cells are surrounded by rigid cell walls and have no phagocytes; therefore, the system for degrading and recycling dying cells in plants is considered to be different to that in

animals. In the starchy endosperm cells of rice or pericarp cells of wheat, the degradation of cell inclusions involves their digestion and absorption *via* the development of amyloplasts during PCD (Lan, 2004; Zhou et al., 2009). *Arabidopsis thaliana* genotypes grown under anthocyanin inductive conditions, and cotyledons can form autophagy containing anthocyanin deposits (Chanoca et al., 2015). Accordingly, we suggest that the amyloplasts formed in the pulp cells of apples with bitter pit also absorb degraded cell inclusions. In this case, the amyloplasts are involved in microautophagy. The amyloplasts contain small vesicles, starch granules, and an osmiophilic body (**Supplementary Figure 8A**). In *Arabidopsis* cotyledon cells, the microphages are formed when the tonoplast surrounds anthocyanin vacuolar inclusions and then enters the vacuole (Chanoca et al., 2015). However, in the flesh of apples with bitter pit, many cytoplasmic vesicles in the cells extend into the vacuole (**Supplementary Figures 8B,C**), which indicates that the amyloplasts enter the vacuoles by division.

In wheat endosperm cells, PCD can reduce the number of amyloids under waterlogged conditions (Fan et al., 1995; Herzog et al., 2016). During storage, the potato tubers degrade starch in the amyloplasts *via* PCD and destroy the amyloplast membranes (Sowokinos et al., 1987), but this type of degradation is not uniform across the tuber (Carvalho, 2017). During apple ripening, the starch in the cells of healthy fruits gradually transforms into soluble carbohydrates (Fan et al., 1995). Some fruits have low cytoplasmic Ca^{2+} concentrations, which leads to the destruction of amyloplast membranes, accelerates the degradation of starch, and increases the growth rate of the fruit and the concentration of soluble carbohydrates. This can also explain why the soluble carbohydrate content of the healthy pulp cells of fruits with the bitter pit was higher than that of healthy fruits, along with the weight of a single fruit, which was also higher than that of a healthy fruit (**Supplementary Table 2**). However, when soluble carbohydrate content increased, the number of amyloplasts increased. The amyloplasts may regulate cells to increase the Ca^{2+} concentration and maintain the integrity of the amyloplast membranes but disrupt Ca^{2+} distribution in fruit cells. In addition, the genes related to Ca^{2+} were highly expressed in the pulp of the fruit with bitter pit. Some studies have suggested that the reversal of the membrane damage in amyloplasts can help maintain their integrity and the accumulation of starch (Kumar and Knowles, 1993; Hepler, 2005).

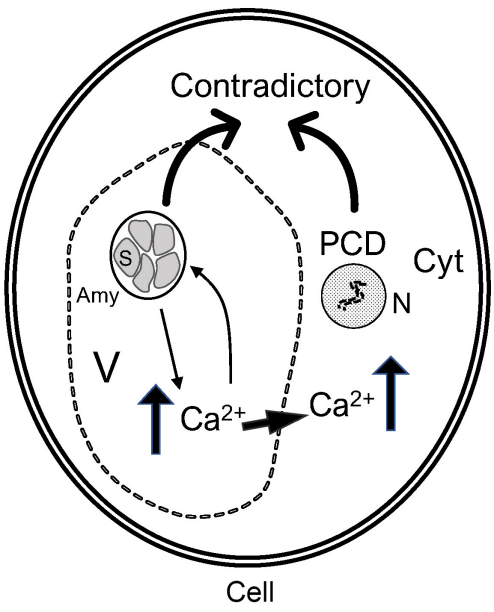

FIGURE 8 | Patterns of interaction between the amyloplasts and Ca^{2+} inducing bitter pit in fruits. The low cytoplasmic Ca^{2+} concentration of fruits affects the degradation of amyloplasts, and amyloplasts disrupt the distribution of Ca^{2+} in cells, thereby causing metabolic disorders. Amy, amyloplast; S, starch granule; V, vacuole; Cyt, cytoplasm; N, nucleus.

The amyloplasts in bitter pit flesh cells can increase in number in a manner similar to that in rice endosperm cells. Moreover, when the number of amyloplast splits increases, the synthesis of starch also increases significantly (Kawagoe, 2009). PCD involves the degradation of starch in the amyloplasts. When the wheat suspension cell culture is cultured under sugar starvation, PCD is induced and begins to degrade the starch amyloplasts. However, the accumulation of starch in the pericarp cells of *Triticum aestivum* L. is accompanied by PCD. Interestingly, there are two contradictory processes in pericarp cells that occur simultaneously (Zhou et al., 2009). In this study, there was a large number of amyloplasts in the pulp cells of apples with bitter pit undergoing PCD at the same time. Ca^{2+} concentration increases in the early stage of post-harvest physiological deterioration of cassava storage roots, thereby causing PCD (Ren et al., 2021).

In conclusion, the amyloplasts and Ca^{2+} regulate each other in pulp cells. Excessively large fruits were found to be highly susceptible to bitter pit. During fruit development, the concentration of Ca^{2+} in fruits showing rapid growth is lower (Saure, 2005). During fruit ripening, these types of fast-growing fruits can degrade the starch faster. Contrastingly, some pulp cells undergo the opposite process to that observed in amyloplasts, and the damaged amyloplasts can be restored. In cold-induced sweet potato, the integrity of amyloplasts can be restored because this process is reversible (Murphy et al., 2005). Intact amyloplasts can affect the distribution of Ca^{2+} in the fruit and increase the concentration of Ca^{2+} in cells. A high Ca^{2+} concentration could maintain the integrity of amyloplasts while inducing PCD. Thus, there are two contradictory processes in cells, the accumulation of amyloplasts and programmed death, that cause the metabolic disorder of the pulp cells, thereby leading to the formation of a bitter pit (**Figure 8**).

DATA AVAILABILITY STATEMENT

The datasets presented in this study can be found in online repositories. The names of the repository/repositories and accession number(s) can be found below: NCBI's BioProject with accession number PRJNA733599 and SRA accession numbers SRR14684876, SRR14684877, and SRR14684878.

AUTHOR CONTRIBUTIONS

HQ and YW conceived and designed the experiments. LQ and SH performed the experiments. HQ analyzed the data. All authors contributed to the article and approved the submitted version.

FUNDING

This work was supported by the Agricultural Variety Improvement Project of Shandong Province (2019LZGC007), China.

SUPPLEMENTARY MATERIAL

The Supplementary Material for this article can be found online at: https://www.frontiersin.org/articles/10.3389/fpls.2021.738726/full#supplementary-material

Supplementary Figure 1 | Comparison of healthy and bitter pit "Fuji" apples. **(A)** At maturity, fruit with a bitter pit on the tree, **(B)** healthy fruit, **(C)** fruit with bitter pit, **(D)** and the cut site of fruit with bitter pit. In general, there were no spots on the outer epidermis of the healthy fruits **(B)**, but fruits with bitter pit had several lesions in the outer peel **(C)**. Most of the lesions occurred near the calyx end and rarely occurred near the fruit stalk **(C)**. In the diseased part, the pulp under the peel developed brown lesions initially, and then, the symptoms spread to the outer skin. During the late stage of the disease, the flesh shrinks, and the epidermis becomes necrotic. The dark brown spots are 2–3 mm deep and the fruit has a bitter taste **(D)**.

Supplementary Figure 2 | The free Ca^{2+} levels in pulp cells in apples with bitter pit were detected using the potassium pyroantimonate precipitation method. There was abundant Ca^{2+} granular precipitation on the vacuole membrane **(A,B)** and flocculent Ca^{2+} precipitation in the vacuole **(C,D)**. The white arrow indicates Ca^{2+} precipitation. Cw, cell wall; M, mitochondria; Cyt, cytoplasm; V, vacuole.

Supplementary Figure 3 | Amyloplasts in the cells of apples with bitter pit. **(A)** Cells of the healthy pulp of the fruit with bitter pit. **(B)** Pulp cells near the site of the bitter pit. The red circle indicates an amyloplast. **(C)** Bitter pit pulp cells. The red arrow indicates an amyloplast.

Supplementary Figure 4 | The expression of 6 genes was associated with Ca^{2+} concentration in pulp cells, as assessed *via* quantitative PCR. Control, healthy fruit; BP-H, healthy pulp of bitter pit fruit; BP, bitter pit fruit. Data are presented as mean ± SE. **Highly significant data ($P < 0.01$).

Supplementary Figure 5 | We counted three bitter pit cells and measured six large starch granules and six small starch granules in each cell. Each starch granule was cross-measured two times, and the average value was taken as the size of a starch granule. Data are means ± SE. LSG, large starch granule; SSG, small starch granule.

Supplementary Figure 6 | Comparison of the area of Ca^{2+} precipitation between the bitter pit pulp and the pulp close to the bitter pit spots. Three cells were randomly selected from a different region, and 10 Ca^{2+} precipitation particles were counted in each region. Data are presented as mean ± sSE (***difference at $P < 0.001$). BP-C, the pulp close to a bitter pit spot; BP, bitter pit pulp.

Supplementary Figure 7 | Through the transcriptomic analysis, five genes were found to be related to programmed cell death (PCD) (**Supplementary Table 1**). These genes were further confirmed *via* quantitative PCR. As *Md12g1174700* was the most differentially expressed gene (DEG) in the bitter pit and healthy tissues, it was transferred to young tomato fruits using the transient method. Seven days later, the tomatoes were picked, and the flesh was stained with Annexin V-FITC (red) and PI (green). The results of fluorescence observation suggested that the gene could induce PCD in tomatoes. **(A)** Cells of healthy tomato fruits, **(B)** cells of tomato fruits treated with dexamethasone, and **(C)** cells of tomato fruits after transient expression treatment. The arrow indicates the nucleus.

Supplementary Figure 8 | Ultramicroscopic observation of amyloplasts and vesicles in the pulp cells of apples with bitter pit. **(A)** Amyloplasts are similar to autophagy. The amyloplasts contain small starch granules and osmiophilic bodies. The amyloid extends into the vacuole *via* division. The arrow indicates the amyloplast. S, starch granules; OB, osmiophilic bodies. **(B,C)** The protoplast had a large number of vesicles extending into the vacuole. The arrow indicates the vesicle.

Supplementary Table 1 | The pulp tissue of healthy fruits, the flesh of the healthy part of the bitter pit fruit, and the flesh of the bitter pit-affected parts. RNA was extracted and transcriptomic analysis was performed. We identified five genes involved in PCD. The results showed that these genes were highly expressed in the bitter pit-affected parts of the fruits. This further illustrated the PCD of the flesh cells of apples with bitter pits.

Supplementary Table 2 | The effect of the bitter pit on "Fuji" apple quality. Comparison of fruit solid content, single fruit weight, and fruit firmness between the bitter pit-affected fruit and healthy fruit. Three repetitions were performed with 10 fruits per repetition.

REFERENCES

Baugher, T. A., Marini, R., Schupp, J. R., and Watkins, C. B. (2017). Prediction of bitter pit in 'honeycrisp' apples and best management implications. *Hortscience* 52, 1368–1374. doi: 10.21273/hortsci12266-17

Blanco, A., Fernández, V., and Val, J. (2010). Improving the performance of calcium-containing spray formulations to limit the incidence of bitter pit in apple (malus x domestica borkh.). *Sci. Hortic.* 127, 23–28. doi: 10.1016/j.scienta.2010.09.005

Bonapace, L., Bornhauser, B. C., Schmitz, M., Cario, G., Ziegler, U., Niggli, F. K., et al. (2010). Induction of autophagy-dependent necroptosis is required for childhood acute lymphoblastic leukemia cells to overcome glucocorticoid resistance. *J. Clin. Investig.* 120, 1310–1323. doi: 10.1172/jci39987

Bonomelli, C., Mogollón, R., Tonetto, De Freitas, S., Zoffoli, J. P., and Contreras, C. (2020). Nutritional relationships in bitter pit-affected fruit and the feasibility of vis-nir models to determine calcium concentration in 'fuji' apples. *Agronomy* 10:1476. doi: 10.3390/agronomy10101476

Carvalho, C. (2017). *Understanding Mechanisms and Identifying Markers for the Onset of Senescent Sweetening of Potato (Solanum tuberosum)*. Ph.D. thesis. England: University of Greenwich.

Chandra, S., Chabot, J. F., Morrison, G. H., and Leopold, A. C. (1982). Localization of calcium in amyloplasts of root-cap cells using ion microscopy. *Science* 216, 1221–1223. doi: 10.1126/science.216.4551.1221

Chanoca, A., Kovinich, N., Burkel, B., Stecha, S., Bohorquez-Restrepo, A., Ueda, T., et al. (2015). Anthocyanin vacuolar inclusions form by a microautophagy mechanism. *Plant Cell* 27, 2545–2559. doi: 10.1105/tpc.15.00589

Chigwaya, K., Plessis, A. D., Viljoen, D. W., Crouch, I. J., and Crouch, E. M. (2021). Use of X-Ray Computed Tomography and 3D Image Analysis to Characterize Internal Browning in 'Fuji' Apples after Exposure to CO2 Stress. *Sci. Hortic.* 277:109840. doi: 10.1016/j.scienta.2020.109840

de Freitas, S. T., Handa, A. K., Wu, Q., Park, S., and Mitcham, E. J. (2012). Role of pectin methylesterases in cellular calcium distribution and blossom-end rot development in tomato fruit. *Plant J.* 71, 824–835. doi: 10.1111/j.1365-313x.2012.05034.x

de Freitas, S., Amarante, C., Labavitch, J. M., and Mitcham, E. J. (2010). Cellular approach to understand bitter pit development in apple fruit. *Postharvest Biol. Technol.* 57, 6–13. doi: 10.1016/j.postharvbio.2010.02.006

DeBrouwer, E. J., Sriskantharajah, K., El Kayal, W., Sullivan, J. A., Paliyath, G., and Subramanian, J. (2020). Pre-Harvest hexanal spray reduces bitter pit and

enhances post-harvest quality in 'honeycrisp' apples (malus domestica borkh.). *Sci. Hortic.* 273:109610. doi: 10.1016/j.scienta.2020.109610

do Amarante, C. V. T., Miqueloto, A., Freitas, S. T. D., Steffens, C. A., Silveira, J. P. G., and Corrêa, T. R. (2013). Fruit sampling methods to quantify calcium and magnesium contents to predict bitter pit development in 'fuji' apple: a multivariate approach. *Sci. Hortic.* 157, 19–23. doi: 10.1016/j.scienta.2013.03.021

Ernani, P. R., Dias, J., Amarante, C. V. T. D., Ribeiro, D. C., and Rogeri, D. A. (2008). Preharvest calcium sprays were not always needed to improve quality of 'gala' apples in Brazil. *Rev. Bras. Frutic.* 30, 892–896. doi: 10.1590/s0100-29452008000400009

Falchi, R., D'agostin, E., Mattiello, A., Coronica, L., Spinelli, F., Costa, G., et al. (2017). ABA regulation of calcium-related genes and bitter pit in apple. *Postharvest Biol. Technol.* 132, 1–6. doi: 10.1016/j.postharvbio.2017.05.017

Fan, X., Mattheis, J. P., Patterson, M. E., and Fellman, J. K. (1995). Changes in amylose and total starch content in 'fuji' apples during maturation. *Hortscience* 30, 104–105. doi: 10.21273/hortsci.30.1.104

Ferguson, I. B., and Watkins, C. B. (1989). "Bitter Pit in Apple Fruit," in *Horticultural Reviews* eds J. Janick (New York: Timber Press), 289–355. doi: 10.1002/9781118060841.ch8

Freitas, S. T. D., and Mitcham, E. J. (2012). "Factors involved in fruit calcium deficiency disorders," in *Horticultural Reviews*, ed. J. Janick (Hoboken: John Wiley & Sons, Inc), 107–146. doi: 10.1002/9781118351871.ch3

Hanchey, S. P. (1982). Cytohistochemical techniques for calcium localization and their application to diseased plants. *Plant Physiol.* 70, 244–251. doi: 10.1104/pp.70.1.244

Hautegem, V. T., Waters, A. J., Goodrich, J., Nowack, M. K. (2015). Only in dying, life: programmed cell death during plant development. *Trends Plant Sci.* 20, 102–113. doi: 10.1016/j.tplants.2014.10.003

Hepler, P. K. (2005). Calcium: a central regulator of plant growth and development. *Plant Cell* 17, 2142–2155. doi: 10.1105/tpc.105.032508

Herzog, M., Striker, G. G., Colmer, T. D., and Pedersen, O. (2016). Mechanisms of waterlogging tolerance in wheat – a review of root and shoot physiology. *Plant Cell Environ.* 39, 1068–1086. doi: 10.1111/pce.12676

Kawagoe, Y. Y. (2009). Amyloplast division progresses simultaneously at multiple sites in the endosperm of rice. *Plant Cell Physiol.* 50, 1617–1626. doi: 10.1093/pcp/pcp104

Kolesnikov, Y. S., Kretynin, S. V., Volotovsky, I. D., Kordyum, E. L., Ruelland, E., and Kravets, V. S. (2016). Molecular mechanisms of gravity perception and signal transduction in plants. *Protoplasma* 253, 1–18.

Kowalik, P., Lipa, T., Michaoj, Z., and Chwil, M. (2020). Ultrastructure of cells and microanalysis in malus domestica borkh. 'szampion' fruit in relation to varied calcium foliar feeding. *Molecules* 25:4622. doi: 10.3390/molecules25204622

Kumar, G., and Knowles, N. R. (1993). Age of potato seed-tubers influences protein synthesis during sprouting. *Physiol. Plant.* 89, 262–270. doi: 10.1034/j.1399-3054.1993.890203.x

Lan, S. (2004). The Starchy endosperm denucleation by a process of programmed cell death during rice grain development. *J. Mol. Cell Biol.* 37, 34–44.

Latrasse, D., Benhamed, M., Bergounioux, C., Raynaud, C., and Delarue, M. (2016). Plant programmed cell death from a chromatin point of view. *J. Exp. Bot.* 67, 5887–5900.

Liu, J., Jiang, Z., Qi, Y., Liu, Y., Ding, Y., Tian, X., et al. (2021). MdCAX affects the development of the 'honeycrisp' bitter pit by influencing abnormal Ca distribution. *Postharvest Biol. Technol.* 171:111341. doi: 10.1016/j.postharvbio.2020.111341

Meldolesi, J., and Grohovaz, F. (2001). Total calcium ultrastructure: advances in excitable cells. *Cell Calcium* 30, 1–8. doi: 10.1054/ceca.2001.0216

Miqueloto, A., Amarante, C., Steffens, C. A., Santos, A. D., and Mitcham, E. (2014). Relationship between xylem functionality, calcium content and the incidence of bitter pit in apple fruit. *Sci. Hortic.* 165, 319–323. doi: 10.1016/j.scienta.2013.11.029

Murphy, A. S., Bandyopadhyay, A., Holstein, S. E., and Peer, W. A. (2005). Endocytotic cycling of pm proteins. *Ann. Rev. Plant Biol.* 56, 221–251. doi: 10.1146/annurev.arplant.56.032604.144150

Nakano, M., Furuichi, T., Sokabe, M., Iida, H., and Tatsumi, H. (2021). The Gravistimulation-Induced very Slow Ca2+ increase in arabidopsis seedlings requires mca1, a ca2+-permeable mechanosensitive channel. *Sci. Rep.* 11:227.

Neilsen, G., Neilsen, D., Dong, S., Toivonen, P., and Peryea, F. (2005). Application of CaCl2 sprays earlier in the season may reduce bitter pit incidence in 'Braeburn' apple. *Hortscience* 40, 1850–1853. doi: 10.21273/hortsci.40.6.1850

Otulak, K., and Garbaczewska, G. (2011). Cellular localisation of calcium ions during potato hypersensitive response to potato virus Y. *Micron* 42, 381–391. doi: 10.1016/j.micron.2010.11.001

Parbery, D. G. (2015). *Daniel McAlpine and The Bitter Pit*. Switzerland: Springer International Publishing.

Pavicic, N., Jemric, T., Kurtanjek, Z., Osj, T., Pavlovic, I., and Blbakovj, D. E. (2004). Relationship between water soluble Ca and other elements and bitter pit occurrence in 'idare' apples: a multivariate approach. *Ann. Appl. Biol.* 145, 193–196. doi: 10.1111/j.1744-7348.2004.tb00375.x

Qin, Y., Yang, J., and Zhao, J. (2005). Calcium changes and the response to methyl jasmonate in rice lodicules during anthesis. *Protoplasma* 225, 103–112. doi: 10.1007/s00709-005-0086-6

Qiu, L., Wang, Y., and Qu, H. (2020). Loading calcium fluorescent probes into protoplasts to detect calcium in the flesh tissue cells of malus domestica. *Hortic. Res.* 7:91.

Qu, H., Xing, W., Wu, F., Wang, Y., and Agustín, G. (2016). Rapid and inexpensive method of loading fluorescent dye into pollen tubes and root hairs. *PLoS One* 11:e0152320. doi: 10.1371/journal.pone.0152320

Ren, H., Zhao, X., Li, W., Hussain, J., Qi, G., and Liu, S. (2021). Calcium signaling in plant programmed cell death. *Cells* 10:1089. doi: 10.3390/cells10051089

Saure, M. C. (2005). Calcium translocation to fleshy fruit: its mechanism and endogenous control. *Sci. Hortic.* 105, 65–89. doi: 10.1016/j.scienta.2004.10.003

Schaeffer, S. M., Christian, R., Castro-Velasquez, N., Hyden, B., and Dhingra, A. (2017). Comparative ultrastructure of fruit plastids in three genetically diverse genotypes of apple (malus × domestica borkh.) during development. *Plant Cell Rep.* 36, 1627–1640.

Sedmíková, M., Rajmon, R., Petr, J., Vanková, M., and Jílek, F. (2003). Ultrastructural localisation of calcium deposits in the mouse ovary. *Reprod. Fertil. Dev.* 15, 415–421. doi: 10.1071/rd03040

Sello, S., Perotto, J., Carraretto, L., Szabò, I., Vothknecht, U. C., and Navazi, L. (2016). Dissecting Stimulus-specific Ca2+ signals in amyloplasts and chloroplasts of arabidopsis thalianacell suspension cultures. *J. Exp. Bot.* 67, 3965–3974. doi: 10.1093/jxb/erw038

Sharma, R. R., Pal, R. K., Sagar, V. R., Parmanick, K. K., Paul, V., Gupta, V. K., et al. (2014). Impact of pre-harvest fruit-bagging with different coloured bags on peel colour and the incidence of insect pests, disease and storage disorders in 'royal delicious' apple. *J. Pomol. Hortic. Sci.* 89, 613–618. doi: 10.1080/14620316.2014.11513128

Simons, R. K., and Chu, M. C. (1980). Scanning electron microscopy and electron microprobe studies of bitter pit in apples. *Mineral Nutr. Fruit Trees* 92, 57–69. doi: 10.1016/b978-0-408-10662-7.50012-0

Sowokinos, J. R., Orr, P. H., Knoper, J. A., and Varns, J. L. (1987). Influence of potato storage and handling stress on sugars, chip quality and integrity of the starch (amyloplast) membrane. *Am. Potato J.* 64, 213–226. doi: 10.1007/bf02853559

Srivastava, A., Bhatt, N. M., Patel, T. P., Dadheech, N., Singh, A., and Gupta, S. (2016). Anti-apoptotic and cytoprotective effect of enicostemma littorale against oxidative stress in islets of langerhans. *Pharm. Biol.* 54, 1–12.

Takahashi, N., Yamazaki, Y., Kobayashi, A., Higashitani, A., and Takahashi, H. (2003). Hydrotropism interacts with gravitropism by degrading amyloplasts in seedling roots of arabidopsis and radish. *Plant Physiol.* 132, 805–810. doi: 10.1104/pp.102.018853

Torres, E., Recasens, I., Peris, J. M., and Alegre, S. (2015). Induction of symptoms pre-harvest using the 'passive method': an easy way to predict bitter pit. *Postharvest Biol. Technol.* 101, 66–72. doi: 10.1016/j.postharvbio.2014.11.002

Turhan, E., Aktas, H., Deventurero, G., Karni, L., Bar-Tal, A., and Aloni, B. (2006). Blossom-end rot is associated with impairment of sugar metabolism and growth of pepper (Capsicum annuum L.) fruits. *J. Hortic. Sci. Biotechnol.* 81, 921–927. doi: 10.1080/14620316.2006.11512160

Wilson, S. M., and Bacic, A. (2012). Preparation of plant cells for transmission electron microscopy to optimize immunogold labeling of carbohydrate and protein epitopes. *Nat. Protocols* 7, 1716–1727. doi: 10.1038/nprot.2012.096

Yasmeen, A., Mirza, B., Inayatullah, S., Safdar, N., Jamil, M., Ali, S., et al. (2009). In Planta transformation of tomato. *Plant Mol. Biol. Rep.* 27, 20–28. doi: 10.1007/s11105-008-0044-5

Yin, S., Wang, C., Jiao, M., Li, F., Han, Q., Huang, L., et al. (2015). Subcellular localization of calcium in the incompatible and compatible interactions of wheat and puccinia striiformis f. sp. tritici. *Protoplasma* 252, 103–116. doi: 10.1007/s00709-014-0659-3

Zhang, L. Y., Peng, Y. B., Pelleschi-Travie, R. S., Fan, Y., Lu, Y. F., Lu, Y. M., et al. (2004). Evidence for apoplasmic phloem unloading in developing apple fruit. *Plant Physiol.* 135, 574–586. doi: 10.1104/pp.103.036632

Zhang, Q., Zhou, B. B., Min-Ji, L. I., Wei, Q. P., and Han, Z. H. (2018). Multivariate analysis between meteorological factor and fruit quality of fuji apple at different locations in china. *J. Integr. Agric.* 17, 1338–1347. doi: 10.1016/s2095-3119(17)61826-4

Zhou, Z., Wang, L., Li, J., Song, X., and Yang, C. (2009). Study on programmed cell death and dynamic changes of starch accumulation in pericarp cells of *Triticum aestivum* L. *Protoplasma* 236, 49–58. doi: 10.1007/s00709-009-0046-7

Conflict of Interest: The authors declare that the research was conducted in the absence of any commercial or financial relationships that could be construed as a potential conflict of interest.

Publisher's Note: All claims expressed in this article are solely those of the authors and do not necessarily represent those of their affiliated organizations, or those of the publisher, the editors and the reviewers. Any product that may be evaluated in this article, or claim that may be made by its manufacturer, is not guaranteed or endorsed by the publisher.

frontiers in Plant Science

ORIGINAL RESEARCH
published: 05 November 2021
doi: 10.3389/fpls.2021.726797

RhWRKY33 Positively Regulates Onset of Floral Senescence by Responding to Wounding- and Ethylene-Signaling in Rose Plants

Weikun Jing[1,2†], Qingcui Zhao[1,2†], Shuai Zhang[1,2], Daxing Zeng[3], Jiehua Xu[3], Hougao Zhou[4], Fenglan Wang[4], Yang Liu[3] and Yonghong Li[1*]*

[1] School of Food and Drug, Shenzhen Polytechnic, Shenzhen, China, [2] Postdoctoral Innovation Practice Base, Shenzhen Polytechnic, Shenzhen, China, [3] School of Construction Engineering, Shenzhen Polytechnic, Shenzhen, China, [4] College of Horticulture and Landscape Architecture, Zhongkai University of Agriculture and Engineering, Guangzhou, China

OPEN ACCESS

Edited by:
Isabel Lara,
Universitat de Lleida, Spain

Reviewed by:
Paul Larsen,
University of California, Riverside, United States
Antonio Chalfun-Junior,
Universidade Federal de Lavras, Brazil

***Correspondence:**
Yonghong Li
liuyang@szpt.edu.cn
Yang Liu
liyongh@szpt.edu.cn

[†] These authors have contributed equally to this work

Specialty section:
This article was submitted to Plant Abiotic Stress, a section of the journal Frontiers in Plant Science

Received: 17 June 2021
Accepted: 06 September 2021
Published: 05 November 2021

Citation:
Jing W, Zhao Q, Zhang S, Zeng D, Xu J, Zhou H, Wang F, Liu Y and Li Y (2021) RhWRKY33 Positively Regulates Onset of Floral Senescence by Responding to Wounding- and Ethylene-Signaling in Rose Plants. Front. Plant Sci. 12:726797. doi: 10.3389/fpls.2021.726797

Rose plants are one of the most important horticultural crops, whose commercial value mainly depends on long-distance transportation, and wounding and ethylene are the main factors leading to their quality decline and accelerated senescence in the process. However, underlying molecular mechanisms of crosstalk between wounding and ethylene in the regulation of flower senescence remain poorly understood. In relation to this, transcriptome analysis was performed on rose flowers subjected to various treatments, including control, wounding, ethylene, and wounding- and ethylene- (EW) dual treatment. A large number of differentially expressed genes (DEGs) were identified, ranging from 2,442 between the ethylene- and control-treated groups to 4,055 between the EW- and control-treated groups. Using weighted gene co-expression network analysis (WGCNA), we identified a hub gene *RhWRKY33* (rchiobhmchr5g0071811), accumulated in the nucleus, where it may function as a transcription factor. Moreover, quantitative reverse transcription PCR (RT-qPCR) results showed that the expression of *RhWRKY33* was higher in the wounding-, ethylene, and EW-treated petals than in the control-treated petals. We also functionally characterized the *RhWRKY33* gene through virus-induced gene silencing (VIGS). The silencing of *RhWRKY33* significantly delayed the senescence process in the different treatments (control, wounding, ethylene, and EW). Meanwhile, we found that the effect of *RhWRKY33*-silenced petals under ethylene and EW dual-treatment were stronger than those under wounding treatment in delaying the petal senescence process, implying that *RhWRKY33* is closely involved with ethylene and wounding mediated petal senescence. Overall, the results indicate that *RhWRKY33* positively regulates the onset of floral senescence mediated by both ethylene and wounding signaling, but relies heavily on ethylene signaling.

Keywords: rose, senescence, wound, ethylene, *RhWRKY33*

INTRODUCTION

Rose plants are one of the most important horticultural crops worldwide; their ornamental and economic value mainly depends on the full expansion and slow senescence of their petals (Lu et al., 2014). Most cut flowers are produced in developing countries, whereas their sales are mainly concentrated in developed countries. Therefore, long-distance transportation from the production region to the point of sale is the mainstream channel for cut rose trade. However, long-distance transportation, usually in darkness under, low temperature, and without water, can easily trigger a massive burst of exogenous ethylene production (Faragher et al., 1987; Mor et al., 1989; Reid et al., 1989; Noodén and Schneider, 2004). Furthermore, stress-induced exogenous ethylene accelerates flower opening and senescence and decreases the vase life of cut rose by coupling with the mechanical damage during postharvest treatment (Müller et al., 2000). Therefore, avoiding and reducing the negative effects of long-distance transportation is crucial in maintaining the postharvest quality of cut roses.

As sessile organisms, plants have developed intricate mechanisms to defend themselves against external adversities, including wounding and hormones, and other biotic, and abiotic stresses. Plants are also able to sense injured tissues and protect themselves by regulating defense system-related genes. The endogenous signals released from wounded tissues may act to activate the plant defense system, and wounding-induced responses are distributed in both the site of damage (local response) and systemically (systemic response), mediated by hormone signaling, including jasmonic acid (JA), ethylene (Eth), brassinolide (BRs), salicylic acid (SA), and abscisic acid (ABA).

Previous studies revealed that mechanical damage results in a large increase in the content (∼25-fold) of endogenous JA and JA-isoleucine (JA-Ile) within 5 min of tissue injury (Chung et al., 2008; Glauser et al., 2008; Koo et al., 2009). The phytohormone, JA, is a well-characterized signaling molecule for its role in protection against wounding damage (Leon et al., 2001); it also plays a central role in activating the systemic defense in many vital processes, including flower development and senescence (Wasternack, 2007). The transcript levels of several JA biosynthesis-related genes, including *LIPOXYGENASE 2* (*LOX2*), *LIPOXYGENASE 3* (*LOX3*), and *ALLENE OXIDE SYNTHASE* (*AOS*), are upregulated together with the JA acceleration (Bell et al., 1995). Arabidopsis genes such as *LOX2*, *AOS*, and *VEGETATIVE STORAGE PROTEIN* (*VSP*) were found to be induced by IAA (Indoleacetic Acid), and endogenous auxin content also showed a decline after wounding, showing a significant cross-talk between the two hormone-dependent signaling pathways (Devoto and Turner, 2003). The *rea1* (RAP2.6 expresser in shoot apex) mutants show a constitutive cell death phenotype, and early wounding response requires an intact JA signaling pathway (Zou et al., 2016); however, the application of methyl jasmonate (MeJA) has been shown to provide significant protection against cell death (Overmyer et al., 2000).

Ethylene is another essential systemic signal of protection of plants against wounding damage. Ethylene released from wounded plant tissues and its participation in wounding response signaling has been extensively studied for decades. Upon wounding at harvest, ethylene was rapidly synthesized in the damaged stem tissue as a result of the marked increase in 1-aminocyclopropane-1-carboxylic acid (ACC) synthase activity and the increased abundance of its transcripts. In melons, the ACC oxidase gene (*CmACO1*), the encoding enzyme controlling the last step of ethylene biosynthesis in plants, was rapidly induced (within 10 min) by ethylene treatment or upon wounding in leaves. 1-methylcyclopropene (1-MCP), a powerful inhibitor of ethylene action, significantly inhibited the accumulation of ethylene-induced *CmACO1* messenger RNA (mRNA) transcripts, while the findings did not apply to wounding-induced *CmACO1* expression (Bouquin et al., 1997). Previous pieces of evidence indicated that the transcripts of several genes encoding ACC oxidase (ACO) and ACC synthase (ACS) were rapidly and transiently accumulated after mechanical injury (Kato et al., 2002). In some cases, the enrichment of *ACS* transcripts was detected within a few hours, even as quickly as 10 min after touching or mechanical wounding in mung bean or soybean plants, respectively (Liu et al., 1993; Botella et al., 1995). Similarly, 1-aminocyclopropane-1-carboxylic acid oxidase (ACO*)* mRNA levels were also induced within several hours, while some were generally induced at a shorter period (20 or 30 min) (Balague et al., 1993; Kim and Yang, 1994; Jones and Woodson, 1999).

An increasing number of studies have shown that many members of the WRKY family are involved in multiple plant processes, such as stress defense responses, plant senescence, wounding, seed dormancy, and seed germination (Rushton et al., 2010; Birkenbihl et al., 2012; Rinerson et al., 2015; Zhao M. et al., 2020). Moreover, functional studies have shown that WRKY transcription factors (TFs) are involved in regulating senescence by interacting with JA, ABA, auxin, gibberellins (GAs), and SA-mediated signaling. In wheat, TaWRKY40-D positively regulated leaf senescence following JA and ABA treatment (Zhao L. et al., 2020). Another WRKY TF, TaWRKY42-B, interacted with and promoted the JA biosynthesis gene (*AtLOX3*, and its ortholog-*TaLOX3*), resulting in an increased JA content and an initiation of leaf senescence in Arabidopsis and wheat (Zhao M. et al., 2020). In Arabidopsis, *AtWRKY54* and *AtWRKY70* functioned redundantly in regulating leaf senescence, as revealed by single and double mutant studies (Besseau et al., 2012). Concerning the diverse roles of WRKY TFs, *AtWRKY57* functioned as a repressor in the JA-induced senescence, which was downregulated by JA and upregulated by auxin (Jiang et al., 2014). *AtWRKY45* played a positive role in the regulation of leaf senescence via GA-mediated signaling (Chen et al., 2017). Genetic analysis revealed that the crosstalk of *AtWRKY75*- SA/ROS functions correlatively in age-dependent leaf senescence (Guo et al., 2017). Finally, eight SlER-WRKYs-SlWRKY16, 17, 22, 25, 31, 33, 53, and 54 were reported to be responsive to ethylene during tomato fruit ripening (Wang et al., 2017). Taken together, WRKY proteins play critical roles in regulating plant senescence.

Ethylene is required for the signal transduction pathway in injury. However, the components involved in the initial wounding signal perception and transmission leading to ethylene synthesis are not clear. In addition, the detailed molecular

mechanisms of the action between ethylene and wounding to regulate the onset of floral senescence remain poorly understood. In relation to this, identifying the initial signal of wounding and signal crosstalk between wounding and the ethylene pathway are crucial steps in understanding the early onset of floral senescence. Here, we monitored the status of the flower opening and senescence after the wounding, ethylene gas, or dual treatment daily. Furthermore, we employed RNA-sequencing (RNA-seq) and weighted gene co-expression network analysis (WGCNA) assays to investigate the signal crosstalk involvement of wounding and the ethylene pathway in the senescence process of rose flowers, and screened a WRKY transcription factor, RhWRKY33, which closely responds to wounding- and ethylene signaling. A biological analysis revealed that *RhWRKY33* plays a positive role in regulating petal senescence. In summary, our findings highlight that *RhWRKY33* mediates petal senescence by integrating wounding and ethylene signaling (a leading role).

MATERIALS AND METHODS

Plant Materials

Cut roses (*Rosa hybrida* cv. Samantha) were grown in a greenhouse at the China Agricultural University (Beijing, China) and harvested at the second stage of a flower opening. The pretreatment methods and user definitions of flower opening stages were performed based on a previous description (Ma et al., 2006).

For the ethylene treatment, the cut roses and petal discs were exposed to gaseous ethylene (10 ppm) in an airtight growth container for 24 h (Ma et al., 2006). An aqueous solution of sodium hydroxide (NaOH) (1 M) was also placed into the sealed container to absorb the accumulated carbon dioxide (CO_2) as previously described (Ma et al., 2005; Wu et al., 2017). For the wounding treatment, the outermost layer petals of the cut rose were wounded with a dissecting needle across its surface, and the petal discs were wounded and slightly squeezed. Then, the gas-treated and wounded cut rose or discs were incubated under the following conditions: $22 \pm 1°C$, 16 h/8 h photoperiod, and ∼60% relative humidity. Three whole outermost layer petals of the cut rose and petal discs were harvested for RNA extraction.

Total RNA Extraction and RNA-Seq Library Preparation

Total RNA was extracted from the rose petals as previously described (Tian et al., 2014; Wu et al., 2017), and removed from genomic DNA contamination using RNase-free DNase I (Promega); the quality and quantity were evaluated using a NanoPhotometer® spectrophotometer (Implen, California, USA) and an Agilent 2100 Bioanalyzer (Agilent Technologies, California, USA). The RNA integrity number (RIN) of all the samples (>8.0) was used for RNA-seq. The RNA-seq was performed by Beijing Novogene Bioinformatics Technology Co., Ltd. (Beijing, China). Three micrograms of the total RNA per sample were used as the input material for cDNA library construction and Illumina sequencing, and the RNA-seq data were processed, assembled, and annotated as previously described (Yang et al., 2015). Briefly, the clean RNA-seq reads were aligned to the reference genome (*Rosa chinensis* cv. Old Blush, GenBank ID 8255808) and analysis was performed using HISAT2 (version 2.0.4) (Acosta et al., 2005) for the reads derived from mRNA fragments using default parameters. The mapped reads of each sample were assembled using Stringtie (v2.1.5) (Pertea et al., 2015), and functional annotations were accomplished by searching against the National Center for Biotechnology Information (NCBI) non-redundant protein (Nr) database using the Basic Local Alignment Search Tool (BLAST)x with an E-value threshold of $\leq 10^{-5}$.

Differential Expression Analysis

Differentially expressed genes between mock and other treatment conditions were performed using the DESeq R package (version 1.10.1) (Anders and Huber, 2010). The DESeq provides statistical routines for determining differential expressions in digital gene expression data using a model based on a negative binomial distribution. The resulting *p* values were adjusted using Benjamini and Hochberg's approach to control the false discovery rate. The differentially expressed genes (DEGs) were identified by DESeq, with fold changes ≥ 2 and adjusted *p*-value ≤ 0.05. All raw data were deposited in the NCBI BioProject database under the accession number PRJNA550484 (https://www.ncbi.nlm.nih.gov/bioproject/?term=PRJNA550484).

Gene Ontology (GO) and Kyoto Encyclopedia of Genes and Genomes (KEGG) Enrichment Analysis of DEGs

The Blast2GOsoftware package was used to identify the GO enriched terms (Conesa et al., 2005). The GO terms with a corrected FDR < 0.05 were considered significantly enriched in DEGs (Conesa et al., 2005). The KEGG Orthology-Based Annotation System (KOBAS) software was used to test the statistical pathway enrichment of DEGs among the KEGG pathways (http://www.genome.jp/kegg/) (Mao et al., 2005).

MapMan Visualization

To identify the gene functions that may play essential roles in regulating the onset of floral senescence, a MapMan visualization was performed as described previously (Thimm et al., 2004). Based on the Mercator with a blast cutoff of 50, contigs were classified into a set of hierarchical functional categories (BINs) (Lohse et al., 2014). Facing classification problems with one unigene that might have multiple contigs, the functional term of unigene was determined by the highest bit score (Nham et al., 2015). Enrichment analysis was performed using Fisher's test and Mefisto (http://www.usadellab.org/cms/index.php?page$=$mefisto) with Bonferroni correction. Gene expression changes were assessed using MapMan 3.5.1 R2.

Ethylene Production Measurements

The petals of each flower were collected and placed in an airtight container (13 ml). The containers were capped and incubated for 1 h at 25°C. Then, a gas sample of 1 ml was withdrawn, using a gas-tight hypodermic syringe, and injected into a gas chromatograph (GC 17A, Shimadzu, Kyoto, Japan) for

the ethylene concentration measurement (Ma et al., 2006). All measurements were performed with three replicates.

Co-expression Analysis of Protein-Coding Genes With RNA-Seq Data

The WGCNA R software package (Langfelder and Horvath, 2008) was used to test whether the expression of protein-coding genes correlated with the senescence degree of rose flowers under the different treatments.

Virus-Induced Gene Silencing (VIGS)

The virus-induced gene silencing of *RhWRKY33* in rose petal discs was performed as previously described (Zhang et al., 2019a). A specific fragment of *RhWRKY33* (417 bp in length) was cloned and inserted into the pTRV2 vector using X*baI* and K*pnI* sites. The recombined-TRV2 vector, pTRV2, and pTRV1 were transformed into *Agrobacterium tumefaciens* strain GV3101, and the transformed *A. tumefaciens* cells were cultured in an LB medium (supplemented with 50 μg/ml kanamycin and 50 μg/ml rifampicin) on a rocking platform (200 rpm) at 28°C for 18 h. Cells were harvested and resuspended in an infiltration buffer (10mM $MgCl_2$, 200 mM acetosyringone, 10 mM MES, pH 5.6) to a final OD 600 of ∼1.0. The culture mixtures contained pTRV1- and pTRV2-*RhWRKY33* at a ratio of 1:1 (v/v) or pTRV1 and pTRV2 (negative control). The culture mixtures were incubated in the dark at room temperature for 3–4 h before infiltration. Discs (1 cm diameter) were submerged in the infiltration buffer and were exposed to a vacuum (−25 kPa) two times (each for 5 min), washed with deionized water, and then incubated in the dark at 8°C for 3 days. The phenotypes of the discs were observed and counted.

RT-qPCR

The genomic DNA of the total RNA samples was removed using RNase-free DNase I (Promega). Reverse transcription was performed with 1 μg of the total RNA using HiScript II Q Select RT SuperMix for qPCR (+gDNA wiper) (Vazyme, Nanjing, China). Together with 2 μl [20ng] cDNA used as a template, RT-qPCR was performed using a StepOne Real-Time PCR System (Applied Biosystems, California, USA) with a Kapa SYBR Fast Universal qPCR Kit (Kapa Biosystems, Boston, Massachusetts, USA). Rose *RhUBI2* and *RhActin5* were used as reference genes (Bustin et al., 2009; Meng et al., 2013; Pei et al., 2013; Gao et al., 2016; Wu et al., 2017; Zhang et al., 2019b, 2021), and the mean of reference genes was used in the following analysis to avoid discrepancies; Relative quantification of the transcript abundance of each gene was performed using the $2^{-\Delta\Delta Ct}$ method (Livak and Schmittgen, 2001). All primers are listed in **Supplementary Table 6**.

Statistical Analyses

GraphPad Prism 8.0.2 software (http://www.graphpad.com/) was used to analyze the statistical differences in the data. Two groups of data were compared by using two-sided Student's *t*-tests ($^{*}p$ <0.05, $^{**}p$ <0.01, $^{***}p$ <0.001, $^{****}p$ <0.0001). The means of the multiple groups of data were compared *via* one-way ANOVA and Bonferroni's *post-hoc* test, with p <0.05 considered significant.

RESULTS

Wounding Accelerates Rose Floral Senescence Dependent on Ethylene Signaling

The role of ethylene in the acceleration of floral senescence has been reported (Ma et al., 2018), but limited research has been conducted on the function of wounding in petal senescence. To determine the effects and signaling crosstalk between wounding and ethylene during floral senescence, we studied the lifespan of cut rose flowers under different treatments. Results showed that the wounded cut roses displayed a slight wilting until 7 days after treatment (DATs); their lifespan was 6.6 ± 0.6 days and there existed significant differences compared with the controls (7.4 ± 0.7 days) (**Figures 1A,B**). The rose flower that underwent ethylene treatment showed severe wilting after 6 days, and after the dual treatment with wounding and ethylene, the wilting started at 4 DAT, and nearly all flowers displayed complete wilting after 6 DAT. The life cycle of the cut rose that underwent the dual-treatment by wounding and ethylene was 4.7 ± 0.7 days, which showed more severe wilting than those that dealt with single treatments (**Figures 1A,B**). Furthermore, the expression level of senescence-associated gene *RhSAG12*, a molecular marker of rose floral senescence progression, was significantly higher in the dual-treated flowers compared with the control-treated flowers at 1, 3, and 6 DAT (**Figure 1C**). Moreover, we measured the ethylene production under different treatments, and we found that the ethylene production in the wound-treated petals (4.2 ± 0.7 C_2H_4 g^{-1} FW h^{-1}) was higher than that in the control (2.2 ± 0.6 C_2H_4 g^{-1} FW h^{-1}) but lower than that in the ethylene (4.5 ± 0.8 C_2H_4 g^{-1} FW h^{-1}) or wounding- and ethylene- (EW) dual treatment (6.9 ± 0.9 C_2H_4 g^{-1} FW h^{-1}) at 6 DAT (**Supplementary Figure 1**). Briefly, these results indicate that the single wounding or ethylene treatment could significantly accelerate the senescence process of rose flowers to some content; however, the role of the wounding was of a senescence-facilitating factor in ethylene signaling.

Global Analysis of Transcriptome Data

To determine the alteration in gene expression during the onset of flower senescence under the dual treatment with wounding and ethylene, we extracted RNA samples from the four different treatments with three biological replicates. The RNA sequencing produced 48,033,008; 55,887,823; 57,773,772; and 58,588,791 clean reads from the four different treatments, respectively. Sequences were mapped to the reference genome (*Rosa chinensis* cv. Old Blush, GenBank ID 8255808) for annotation, and the mapping rate reached over 83% for the samples from each treatment (**Supplementary Table 1**). Differentially expressed genes were screened by comparing three different treatments with the control treatment, and 6,771 unigenes that were differentially expressed across these treatments were generated (fold changes ≥ 2, p ≤0.05). The number of DEGs was counted as 274 from Group 1 (wounding vs. control), 2,442 from group 2 (ethylene vs. control), and 4,055 from group 3 (EW vs. control) (**Supplementary Figure 2A**).

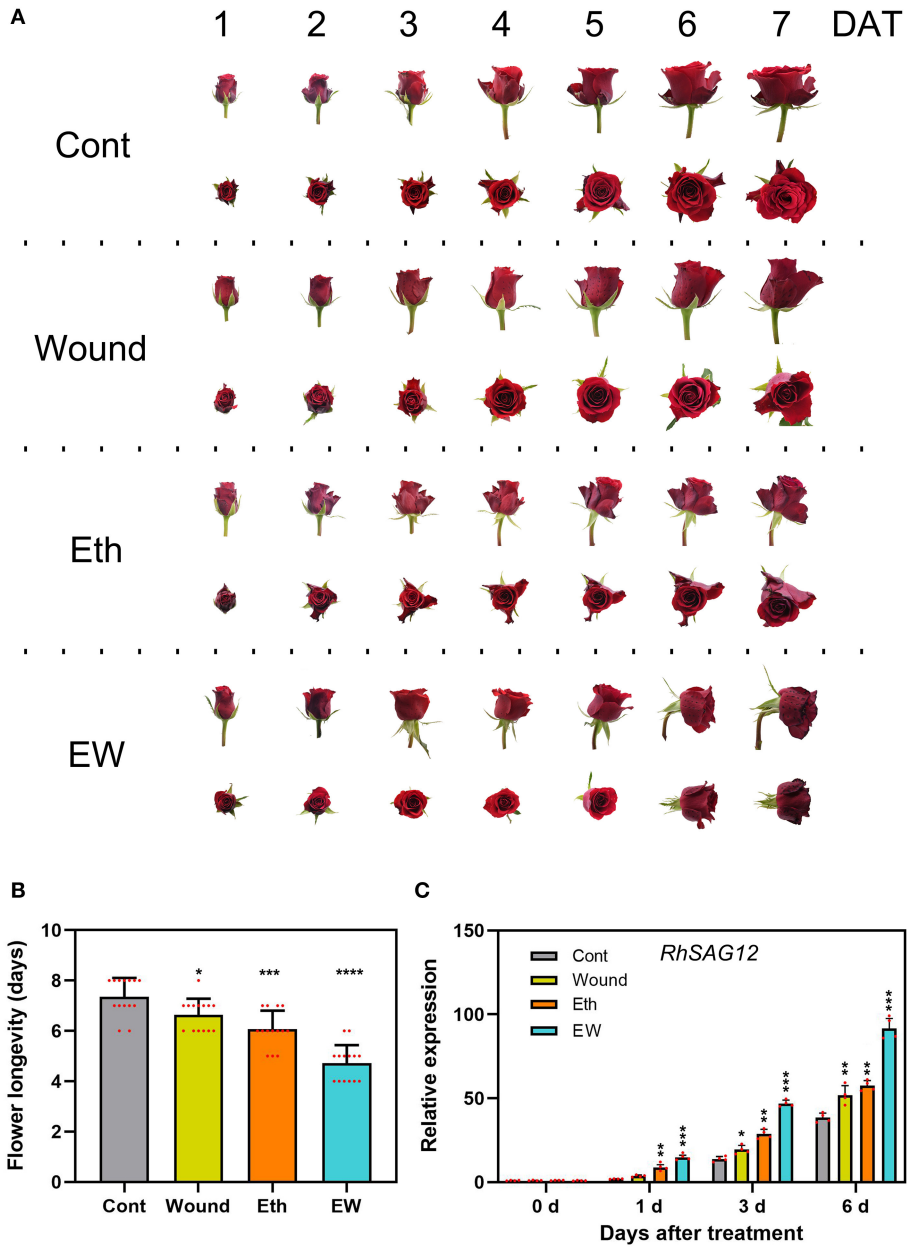

FIGURE 1 | Effects of wound and ethylene on the senescence of rose flowers. **(A)** The phenotypes of flowers were recorded and photographed every day after wound and ethylene treatment. **(B,C)** The flower longevity and relative expression of *RhSAG12* by reverse transcription PCR (RT-qPCR) were determined. Values are means ± SD, *RhUBI2* and *RhActin5* were used as reference genes, and asterisks indicate statistically significant differences (*$p < 0.05$, **$p < 0.01$, ***$p < 0.001$, Student's *t*-test).

Results showed that the three groups that shared 96 DEGs attributed to the wounding, drawing few gene expression changes, which was consistent with the single wounding not accelerating the floral senescence process. In addition, Groups 2 and 3 shared 2,093 DEGs, and Group 3 specifically induced 1,903 DEGs (**Supplementary Figure 2B**), both of which had enriched functional categories related to protein degradation, hormone metabolism, and transcription regulation.

Complex Hormone Biosynthesis and Signaling Pathways Involved in Wounding and Ethylene Signaling

To further understand the detailed regulatory network during the onset of rose floral senescence under wounding and ethylene treatments, all DEGs related to hormone biosynthesis and signaling pathways across the three groups were analyzed using the MapMan software. The largest numbers of DEGs were

related to biosynthesis and signal transduction of auxin and ethylene, followed by DEGs in the cytokinin pathway (**Figure 2**; **Supplementary Table 2**).

For the auxin pathway, the vast majority of DEGs were downregulated after the wounding and ethylene treatments. For example, 76.4% of the DEGs (42/55) were downregulated in Group 2 and 74.3% (55/74) in Group 3. Among these genes, 52 DEGs were co-regulated by the ethylene and wounding- and ethylene- dual treatments, including 35 small auxin upregulated RNA (SAUR) and SAUR-like genes, two PIN-FORMED (PIN) family genes (rchiobhmchr2g0169101 and rchiobhmchr3g0448071), and four auxin-responsive GH3 family proteins (rchiobhmchr2g0107081, rchiobhmchr2g0107091, rchiobhmchr2g0162261, and rchiobhmchr4g0428671). There were 22 DEGs that responded specifically to EW treatment related to auxin biosynthesis and signal transduction. Most DEGs related to the ethylene pathway were upregulated in Groups 2 and 3, with the proportions of 68.2% (15/22) and 77.1% (27/35), respectively. In the ethylene biosynthesis pathway, including ACC oxidase (rchiobhmchr5g0001831 and rchiobhmchr3g0474401), two ethylene receptors (rchiobhmchr4g0391281 and rchiobhmchr6g0294491), and three ERF genes were upregulated, whereas eight ERF genes were downregulated in Groups 2. Among the genes related to the cytokinin signaling pathway, ∼39.3% (11/28) and 51.3% (20/39) of DEGs were increased in groups 2 and 3, respectively. Cytokinin synthase IPT3/5 genes (rchiobhmchr5g0029421 and rchiobhmchr4g0418401) and cytokinin oxidase CKX6/7 genes (rchiobhmchr1g0319331 and rchiobhmchr6g0301781) were identified and upregulated in Groups 2 and 3, whereas the expression of cytokinin oxidase CKX3 was specifically enhanced in Group 3.

Differentially expressed genes related to ABA, BRs, JA, SA, and GA were also identified. For the ABA pathway, a total of 11 genes, including the biosynthesis genes AAO3 (rchiobhmchr5g0049511), NCED (rchiobhmchr4g0397001 and rchiobhmchr5g0027901), and signal transduction genes PP2C (rchiobhmchr2g0094051), were regulated by the ethylene or EW treatments. A total of 27 DEGs were found in Group 3, referred to as brassinosteroid biosynthetic and signaling pathways, these included biosynthetic genes DEF4 (rchiobhmchr2g0101791), CYP90D1 (rchiobhmchr2g0142901), CAS1 (novel00019), and signaling transduction genes BEH4 (rchiobhmchr5g0011971) and BRH1 (rchiobhmchr7g0197001). Among the JA-related genes, the upregulated DEGs, including AOS2 (rchiobhmchr6g0261031, rchiobhmchr6g0261011, and rchiobhmchr6g0300221), OPR2 (rchiobhmchr2g0167371), and LOX1 (rchiobhmchr3g0455111), were related to biosynthesis and detected in Group 3. In the SA pathway, the expression of UDP-glucosyltransferase gene UGT74E2 (rchiobhmchr6g0248381, rchiobhmchr6g0248411, rchiobhmchr7g0179611, and rchiobhmchr6g0248381) was enhanced, whereas SABATH methyltransferase expression (novel01210 and rchiobhmchr6g0265391) was decreased in Group 3. The expression of eight GA biosynthetic and four signal transduction genes showed changes in Groups 2 and 3. Among those DEGs, the biosynthetic genes were GA2 (rchiobhmchr5g0023471), GA20ox1

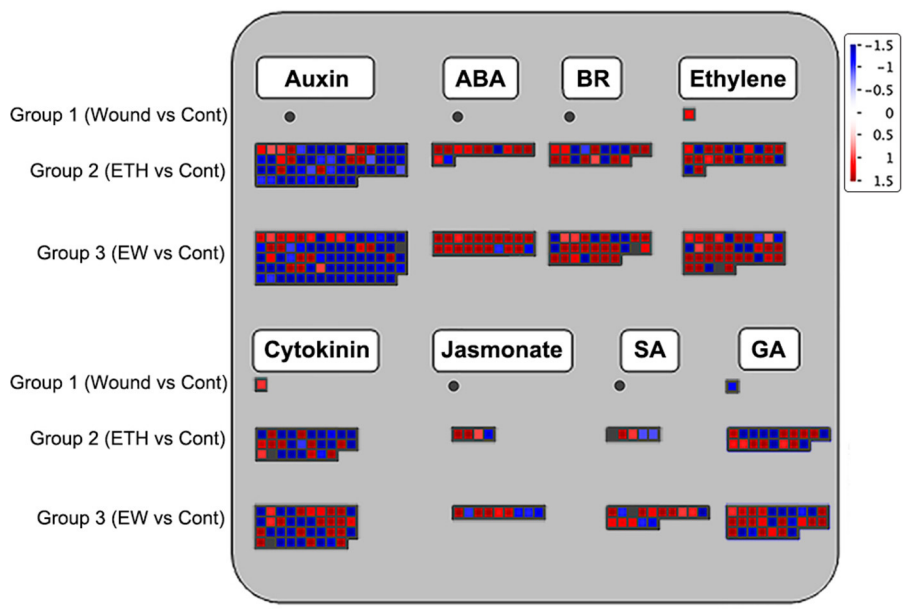

FIGURE 2 | Display of differentially expressed genes (DEGs) involved in hormone biosynthesis and signaling transduction pathway. Significant DEGs (fold changes ≥ 2 and adjusted *p*-value ≤0.05) were organized into functional categories (BINs) (Thimm et al., 2004) and visualized using the MapMan software (version 1.0). The color set scale was placed on the top right, and the gene expression increased is indicated in red and decreased in blue. Detailed information on gene expression is listed in **Supplementary Table 2**.

(rchiobhmchr1g0351591 and rchiobhmchr1g0376161), GA3ox1/2 (rchiobhmchr7g0236321 and rchiobhmchr2g 0137231), GA2ox1/2/6 (rchiobhmchr5g0027981, rchiob hmchr5g0014211, and rchiobhmchr4g0426161), and signaling pathway genes, including GAI (rchiobhmchr2g0089571), GID1B (rchiobhmchr6g0292241), and GASA6 (rchiobhmchr7g0181391). Briefly, we speculated that different hormone biosynthesis and signaling pathways may be involved in the senescence process induced by wounding and ethylene.

Differential Gene Expression Related to Transcription Factors, Protein Modification, and Degradation

In terms of transcription factors, a total of 1,123, and 222 DEGs encoding TFs were observed in Groups 1, 2, and 3, respectively (**Figure 3**; **Supplementary Table 3**). Major differentially expressed TF families included WRKY, MYB, bHLH, HB, bZIP, AP2-EREBP, and C2H2. The predominant family was AP2-EREBP TF, with 14/16 DEGs, including 11/13 upregulated genes in Groups 2 and 3, respectively, followed by MYB (12/12), C2H2 type-zinc finger protein (9/10), bHLH (8/10), WRKY (7/10), HB (7/8), and bZIP (3/5) families. These data suggest that the TFs above may be involved in EW signaling during flower senescence.

Screening of Candidate Genes Based on Co-expression Network

To further identify the major groups, we performed a WGCNA and obtained 13 distinct modules (**Figure 4A**). Focused on the rose senescence degree, we found that the "Yellow" module was the most significantly associated with rose senescence (**Figure 4B**). Moreover, we analyzed the expression profile of hub genes in the "Yellow" module and found that *RchiOBHmChr5g0071811* was the most significantly upregulated gene when compared with control (**Figure 4C**).

Phylogenetic and protein sequence analyses were performed (**Supplementary Figures 3**, **4**), and RchiOBHmChr5g0071811 was closely related to AtWRKY33, which contains two WRKY domains. Furthermore, it was located in the nucleus by subcellular localization in *Nicotiana benthamiana* (**Supplementary Figure 4B**). Based on these results, *RchiOBHmChr5g0071811* was named *RhWRKY33*. RhWRKY33 accumulates in the nucleus, where it may function as a transcription factor.

To better understand its expression characteristics, the transcription level of *RhWRKY33* was measured in different organs and petal stages through RT-qPCR. As shown in **Supplementary Figure 4C**, the expression level of *RhWRKY33* was higher in the sepals, petals, and stamens, and lower in young leaves, receptacles, and pistils, whereas it significantly increased from stage 1 to stage 5 (**Supplementary Figure 4D**), implying that *RhWRKY33* may function in rose petal senescence.

RhWRKY33 Accelerates the Petal Senescence Depended on Wounding and Ethylene Signaling

To evaluate whether *RhWRKY33* was involved in regulating the senescence of rose petals, we silenced the *RhWRKY33* transcripts in petal discs by VIGS and found that the color

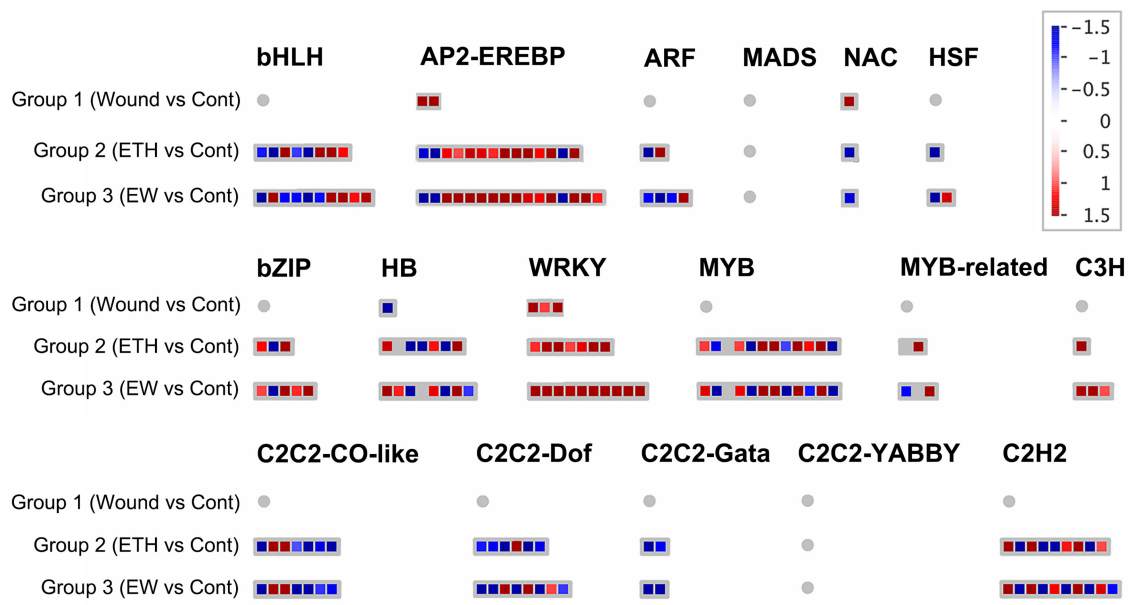

FIGURE 3 | Display of differentially expressed genes related to transcription factors. Significant DEGs (fold changes ≥ 2 and adjusted *p*-value ≤ 0.05) were organized into functional categories (BINs) (Thimm et al., 2004) and visualized by MapMan software (version 1.0). The color set scale was placed on the top right, and the gene expression increased is indicated in red and decreased in blue. Detailed information on gene expression is listed in **Supplementary Table 3**.

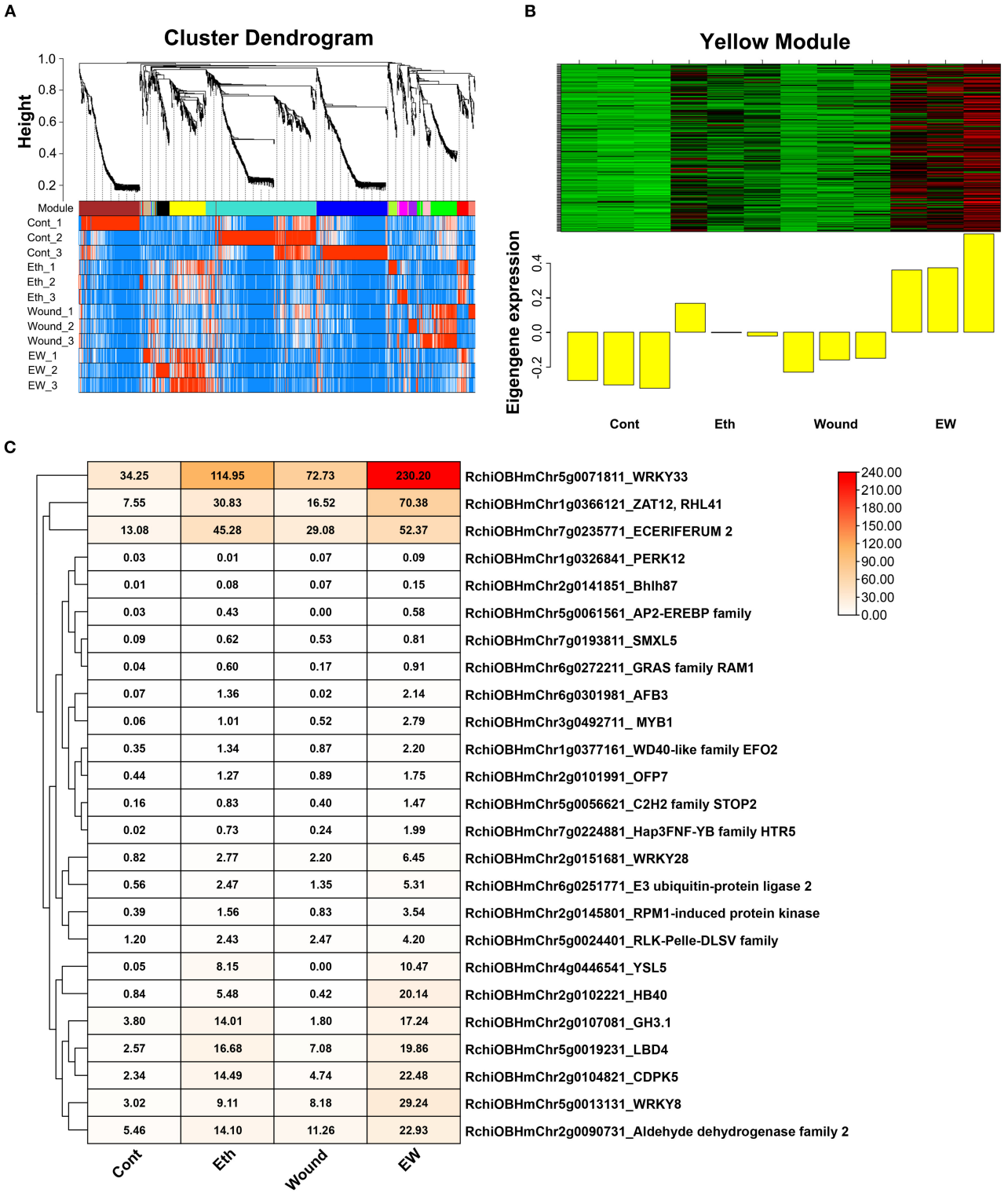

FIGURE 4 | Co-expression network analysis of DEGs involved in wound and ethylene signaling. **(A)** Clustering dendrogram of genes across all samples, with dissimilarity based on the topological overlap, together with assigned merged colors and original module colors. **(B)** Heatmap of the eigengene expression in the "yellow" module in response to wound and ethylene signaling. **(C)** Expression profile of screened hub genes in different treatments.

fading of TRV discs began after 6 days, whereas the TRV-*WRKY33* discs, with *WRKY33* silenced, did not display any significant color fading (**Figure 5A**); in contrast, the degree of the TRV disc fading was more serious after 9 and 12 days compared with the TRV-*WRKY33* discs (**Figure 5D**). The expression of *RhWRKY33* was significantly lower in the TRV-*WRKY33* discs than in the TRV control discs (**Figure 5B**); Concurrently, we measured the expression of *RhSAG12* and ion leakage in TRV and TRV-*WRKY33* discs at 0, 6, 9, 12 days. Consistent with this, the *WRKY33*-silenced discs presented lower expression of *RhSAG12* and less ion leakage than TRV control (**Figures 5C,E**). These data provide evidence that *RhWRKY33* plays a positive regulatory role during rose petal senescence.

further investigate whether *RhWRKY33* was involved in EW signaling, we also performed ethylene, wounding, and EW treatments through the VIGS assay. As shown in **Figures 6A–G**, the fading color and ion leakage were significantly increased in the ethyne and EW treatment compared with wounding-treatment at 6, 9, and 12 DAT, either in TRV or in TRV-*RhWRKY33*, suggesting the stronger role of ethylene than wounding on petal senescence. Irrespective of the wounding, ethylene, or EW treatment, all *RhWRKY33*-silenced discs exhibited longer floral longevity, lower color fading rate, and ion leakage when compared with the TRV. In addition, the expression of *RhSAG12* was significantly lower in *RhWRKY33*-silenced discs at 6 DAT than in TRV discs under the above treatments

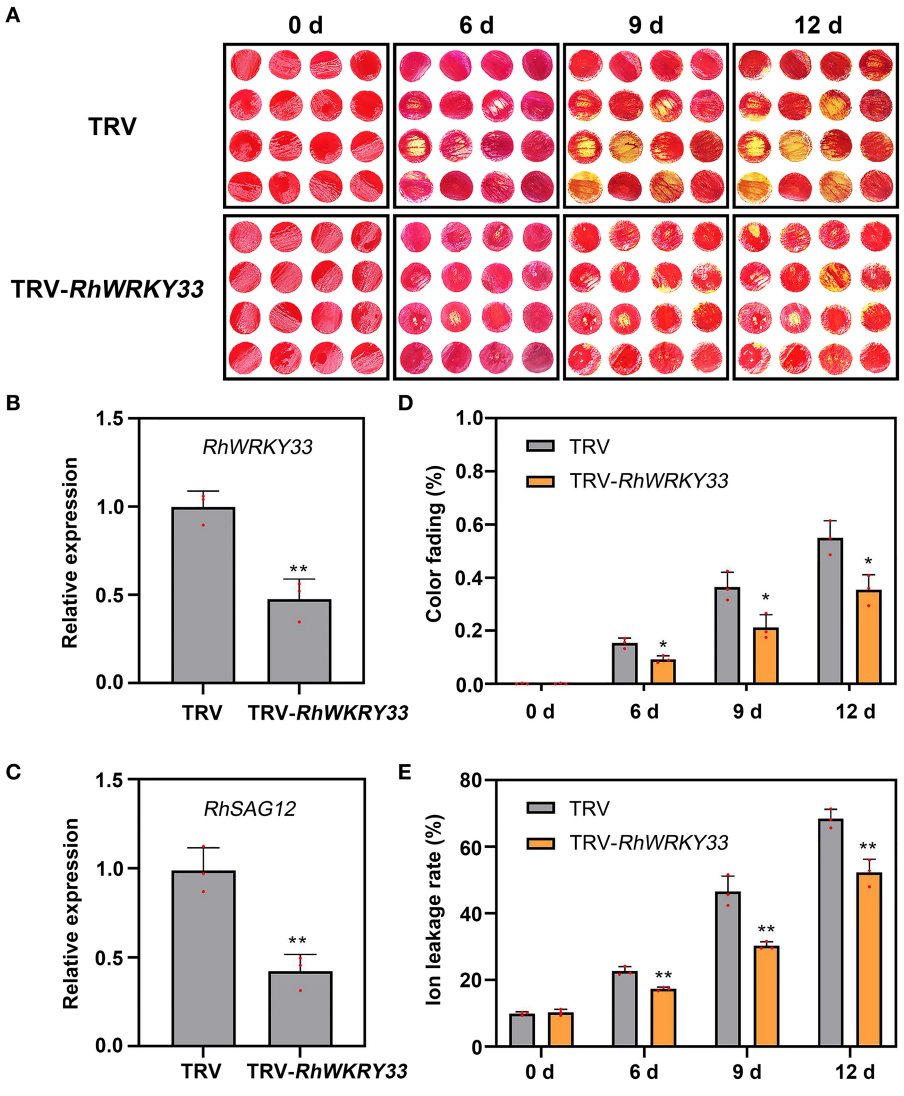

FIGURE 5 | Effect of TRV-*RhWRKY33* on the senescence of rose petal discs. **(A)** Color fading phenotypes of TRV and TRV-*RhWRKY33* petal discs. **(B)** RT-qPCR validation of expression level of *RhWRKY33* in TRV and TRV-*RhWRKY33* petal discs. **(C)** *RhSAG12* expression levels were analyzed in *RhWRKY33*-silenced and TRV control petal discs. **(D)** Color fading rate. **(E)** Ion leakage rate. The error bars represent the means of three biological replicates ± SDs, *RhUBI2,* and *RhActin5* were used as reference genes, and the asterisks indicate significant differences based on Student's *t*-test (*$p < 0.05$; **$p < 0.01$).

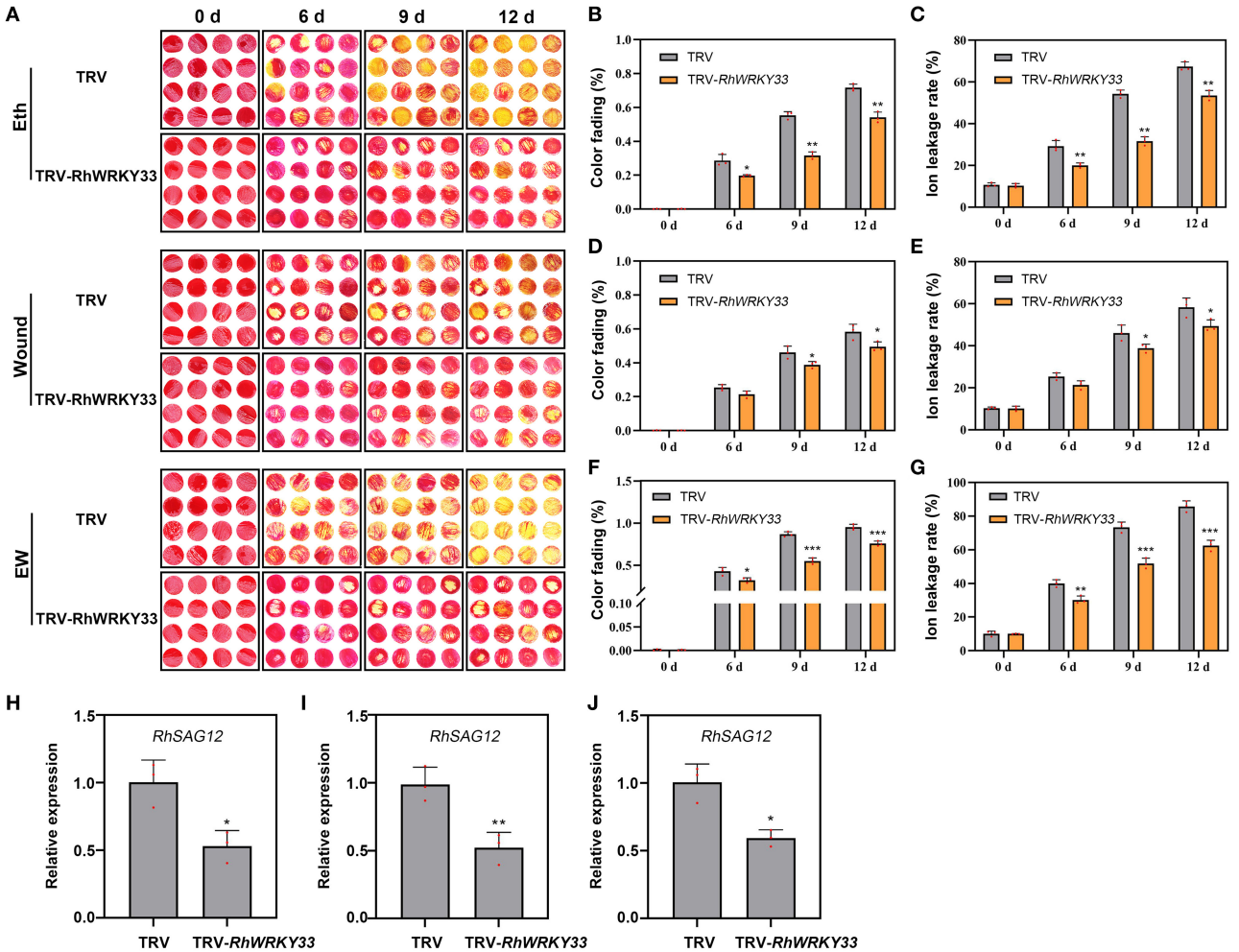

FIGURE 6 | Effect of wounding-, ethylene- and EW-treatment on the senescence of *RhWRKY33*-silenced rose petal discs. **(A)** The phenotypes of rose petal discs treated with 10 μl/L ethylene, wound, or EW. **(B,D,F)** Color fading rate. **(C,E,G)** Ion leakage rate. **(H,I,J)** Expression levels of *RhSAG12* were analyzed in *RhWRKY33*-silenced and TRV control petal discs under different treatments. The error bars represent the means of three biological replicates ± SDs, *RhUBI2,* and *RhActin5* were used as reference genes, and the asterisks indicate significant differences based on Student's *t*-test (*$p < 0.05$; **$p < 0.01$; ***$p < 0.001$).

(**Figure 6**). These results indicate that *RhWRKY33* can accelerate the senescence process of rose petals depending on the wounding and ethylene signaling, but mainly on ethylene signaling.

We previously found that JA and ethylene could promote senescence in rose flowers (Zhang et al., 2019b), and JA levels increased significantly in plants subjected to wounding (Chung et al., 2008; Glauser et al., 2008; Koo et al., 2009); whether *RhWRKY33* was induced by JA remains unknown. To examine the relationship between JA and *RhWRKY33*, we measured the expression of *RhWRKY33* in JA- and ethylene-induced petals and found that *RhWRKY33* was upregulated by JA and ethylene treatment (**Supplementary Figure 5**). These results further indicate that *RhWRKY33* accelerates the petal senescence process mediated by both ethylene and wounding signaling, but relies heavily on ethylene signaling.

DISCUSSION

Ethylene Is a Senescence-Promoter Hormone in Rose Petals

Phytohormones possess pivotal roles in initiating and modulating floral senescence programs and finally influence the quality and long vase life of fully open petals. Among those hormones, ethylene and ABA function as the senescence-accelerating factors, while auxin, CTKs, SA, and GA act the inhibited function in floral senescence (Lu et al., 2014; Trivellini et al., 2015; Wu et al., 2017; Shabanian et al., 2018). Particularly, ethylene has been considered as a major endogenous regulator of fruit ripening, leaf- and petal-senescence, and floral organ abscission (Li et al., 2013; Han et al., 2016; Shabanian et al., 2018). Once the senescence process of leaves and flowers was initiated, the expression of ethylene biosynthesis genes *ACS1/2* was strongly increased,

accompanied by a massive burst of ethylene production (Ma et al., 2005). In this study, two ethylene biosynthesis genes, *ACS* (rchiobhmchr6g0310191) and *ACO* (rchiobhmchr3g0474401, rchiobhmchr5g0001831), had higher levels of expression in all the ethylene treatment flowers (group 2 and 3) (**Figure 2**; **Supplementary Table 2**). Meanwhile, we also found that the expression of eight *ERF* genes (rchiobhmchr4g0392451, rchiobhmchr4g0392501, rchiobhmchr5g0008991, rchiobhmchr 5g0009711, rchiobhmchr5g0032721, rchiobhmchr6g0288231, rchiobhmchr6g0299771, and rchiobhmchr7g0204641) were increased, and three *ERF* genes (rchiobhmchr2g0135921, rchiobhmchr6g0298011, and rchiobhmchr7g0230931) were decreased in response to the ethylene signal, and *RhERF1* (rchiobhmchr2g0135921) and *RhERF4* (rchiobhmchr6g0298011) have been proved to function in petal abscission mediated by ethylene pathway (Gao et al., 2019).

The exogenous application of ethylene also triggers the gene expression change related to the biosynthesis and signaling pathway of other hormones. During the leaf senescence and abscission process, the massive production of ethylene could inhibit auxin synthesis and transport, enhance auxin degradation, and lower diffusible auxin levels (Burg, 1968). Here, up to 55 DEGs associated with the auxin pathway were induced and 76.4% of those genes (42/55) were downregulated by exogenous ethylene applying, including auxin polar transport PIN family genes (*PIN5*, rchiobhmchr3g0448071; *PIN8*, rchiobhmchr2g0169101), auxin-responsive SAUR, and the genes of GH3 family (**Figure 2**; **Supplementary Table 2**). We speculate that ethylene may directly or indirectly regulate the expression of auxin-related genes to affect flower senescence. Meanwhile, the exogenous application of ethylene further enhanced senescence-promoting hormone responses, such as ABA, and while declined the genes expression associated with synthesis and signaling transduction of cytokinin, which functions in delaying senescence.

Wounding Function in Acceleration Floral Senescence Depend on Ethylene Signaling

Numerous studies have revealed that wounding is implicated in multiple signaling pathways, such as JA, auxin, and ethylene. Wounding is considered one of the early triggers of plant regeneration (Chen et al., 2016), and the content of JA and auxin accumulates within seconds to minutes after wounding, making them candidates for early wounding signal. Further analysis indicated that cell damage leads to JA accumulation, and tissue integrity loss leads to local auxin accumulation by impeding polar auxin transport (Glauser et al., 2009; Larrieu et al., 2015; Zhou et al., 2019). Endogenous JA levels acceleration in response to mechanical wounding and herbivore damage have been extensively reported (Creelman and Mullet, 1997; Rao et al., 2000). JA signal marker genes, namely, *LOX2*, *AOS*, and *VSP,* were found to be induced, whereas endogenous levels of auxins were also shown to decline after wounding, showing a significant cross-talk between the hormone and damage signaling pathways (Devoto and Turner, 2003; Zou et al., 2016). Previous studies confirmed that the damage signal is one of the primary factors in the induction of the senescence phenotype in detached leaves or petals, whereas ethylene is implicated as a regulator of the rate of the process (Philosophhadas et al., 1991). Additional evidence has revealed that ethylene content is generally induced by various environmental stresses, such as damage signaling, exposure to low temperatures, and water stress, in plants (Hyodo et al., 1991).

Our previous study revealed that *RhMYB108* could accelerate rose petal senescence by mediating JA and ethylene signaling (Zhang et al., 2019b; Fan et al., 2020). In this study, we found that the rate of petal senescence was not significantly accelerated or delayed in the single wounding treatment. However, the senescence rate of EW-treated petals was faster than those treated by wounding or ethylene, which suggested that wounding could strengthen ethylene signaling, which was consistent with those of a study by Hyodo (Hyodo et al., 1991). In conclusion, further research is needed to reveal the mechanisms underlying the wound-ethylene crosstalk in petal senescence. In addition, our study suggested that RhWRKY33 could accelerate the floral senescence process of cut roses by mediating EW-signaling (**Figures 1**, **6**).

RhWRKY33 Mediates Ethylene and Wounding Signaling During Senescence

A complex network of transcription factors is involved in senescence. In terms of transcription factors, a total of 1,123, and 222 DEGs encoding TFs were observed in Groups 1, 2, and 3, respectively (**Figure 3**; **Supplementary Table 3**). Among the differentially expressed TFs, 119 DEGs responded to both Groups 2 and 3 (**Supplementary Table 4**), whereas 102 genes were expressed in response to Group 3 (**Supplementary Table 5**). Major differentially expressed TF families included WRKY, MYB, bHLH, HB, bZIP, AP2-EREBP, and C2H2. Here, AP2-EREBP TF was the predominant family with 14/16 DEGs, including 11/13 upregulated genes in Groups 2 and 3, respectively, followed by MYB (12/12), C2H2 type-zinc finger protein (9/10), bHLH (8/10), WRKY (7/10), HB (7/8), and bZIP (3/5) families.

Up to date, increasing studies have shown that many WRKY family members are involved in stress-defense responses, plant senescence, wounding, seed dormancy, and seed germination (Rushton et al., 2010; Rinerson et al., 2015; Zhao M. et al., 2020). In addition, a complex regulatory network consisting of WRKY TFs and plant hormone functions is involved in plant senescence. In our study, the expression of *RhWRKY33* was significantly upregulated more than 9 and 6 times, when induced by JA and ethylene, respectively. However, it was significantly repressed by 1-MCP (**Supplementary Figure 5**). We speculate that *RhWRKY33* may be induced by wounds by increasing the JA content. However, in this study, we discovered that the expression of *RhWRKY33* was upregulated more than two times under wounding treatment, and less than nine times under JA treatment. Whether there are other factors involved in the regulation of rose petal senescence requires further study.

Overall, using RNA-seq analysis and WGCNA, we identified the RhWRKY33, which is closely related to AtWRKY33 from *Arabidopsis thaliana* and is located in the nucleus. The silencing of *RhWRKY33* (TRV-*RhWRKY33*) significantly delayed the rose petal senescence process either on the control or on other treatments (ethylene, wounding, and EW). Ethylene plays a major role in petal senescence. From the above results, we conclude that RhWRKY33 is involved in regulating rose petal senescence by mediating wound- and ethylene-signaling.

DATA AVAILABILITY STATEMENT

The original contributions presented in the study are publicly available. This data can be found here: National Center for Biotechnology Information (NCBI) BioProject database under accession number PRJNA550484 (https://www.ncbi.nlm.nih.gov/bioproject/?term=PRJNA550484).

AUTHOR CONTRIBUTIONS

WJ and QZ performed the experiments and analyzed the data. YLi and YLiu designed the study. SZ, DZ, JX, HZ, and FW provided technical support and conceptual advice. WJ, QZ, SZ, and YLi wrote the manuscript. All authors read and approved the final manuscript.

FUNDING

This study was supported by the General Project of Shenzhen Science and Technology and Innovation Commission (21K270360620) and the National Natural Science Foundation of China (Grant No. 31902054).

ACKNOWLEDGMENTS

We thank Editage (https://app.editage.com/) for the careful editing of this article.

SUPPLEMENTARY MATERIAL

The Supplementary Material for this article can be found online at: https://www.frontiersin.org/articles/10.3389/fpls.2021.726797/full#supplementary-material

Supplementary Figure 1 | The ethylene production of different treatments was determined at 0, 1, 3, and 6 days. Values are means ± SD, and asterisks indicate statistically significant differences (*$p < 0.05$, **$p < 0.01$, Student's *t*-test).

Supplementary Figure 2 | Identification of differentially expressed genes among all treatments during the onset of floral senescence.

Supplementary Figure 3 | Biochemical characteristics and spatiotemporal expression analysis of RhWRKY33.

Supplementary Figure 4 | Display of DEGs relating to transcription factors, protein modification, protein degradation **(A)**, and hormone signaling **(B)** was specifically regulated by Group 3.

Supplementary Figure 5 | Effects of different hormone treatments on the expression of *RhWRKY33*.

Supplementary Table 1 | Statistics of annotation results for rose unigenes.

Supplementary Table 2 | Detailed information of DEGs involved in hormone biosynthesis and signaling transduction pathway.

Supplementary Table 3 | Detailed information of DEGs related to transcription factors.

Supplementary Table 4 | Detailed information of DEGs relating to transcription factors, protein modification, protein degradation **(A)**, and hormone signaling **(B)** was co-regulated between Groups 2 and 3.

Supplementary Table 5 | Detailed information of DEGs relating to transcription factors, protein modification, protein degradation **(A)**, and hormone signaling **(B)** was specifically regulated by group 3.

Supplementary Table 6 | List of primers used.

REFERENCES

Acosta, M. B. R., Ferreira, R. C. C., Ferreira, L. C. S., and Costa, S. O. P. (2005). Intracellular polyamine pools, oligopeptide-binding protein A expression, and resistance to aminoglycosides in Escherichia coli. *Mem I Oswaldo Cruz.* 100, 789–793. doi: 10.1590/S0074-02762005000700020

Anders, S., and Huber, W. (2010). Differential expression analysis for sequence count data. *Genome Biol.* 11:R106. doi: 10.1186/gb-2010-11-10-r106

Balague, C., Watson, C. F., Turner, A. J., Rouge, P., Picton, S., Pech, J. C., et al. (1993). Isolation of a Ripening and wound-induced cdna from cucumis-melo l encoding a protein with homology to the ethylene-forming enzyme. *Eur. J. Biochem.* 212, 27–34. doi: 10.1111/j.1432-1033.1993.tb17628.x

Bell, E., Creelman, R. A., and Mullet, J. E. (1995). A chloroplast lipoxygenase is required for wound-induced jasmonic acid accumulation in arabidopsis. *P Natl. Acad. Sci. USA.* 92, 8675–8679. doi: 10.1073/pnas.92.19.8675

Besseau, S., Li, J., and Palva, E. T. (2012). WRKY54 and WRKY70 co-operate as negative regulators of leaf senescence in Arabidopsis thaliana. *J. Exp. Bot.* 63, 2667–2679. doi: 10.1093/jxb/err450

Birkenbihl, R. P., Diezel, C., and Somssich, I. E. (2012). Arabidopsis WRKY33 is a key transcriptional regulator of hormonal and metabolic responses toward botrytis cinerea infection. *Plant Physiol.* 159, 266–285, doi: 10.1104/pp.111.192641

Botella, J. R., Arteca, R. N., and Frangos, J. A. (1995). A mechanical strain-induced 1-aminocyclopropane-1-carboxylic acid synthase gene. *P Natl. Acad. Sci. USA* 92, 1595–1598. doi: 10.1073/pnas.92.5.1595

Bouquin, T., Lasserre, E., Pradier, J., Pech, J. C., and Balague, C. (1997). Wound and ethylene induction of the ACC oxidase melon gene CM-ACO1 occurs via two direct and independent transduction pathways. *Plant Mol. Biol.* 35, 1029–1035. doi: 10.1023/A:1005902226054

Burg, S. P. (1968). Ethylene, plant senescence and abscission. *Plant Physiol.* 43, 1503–1511.

Bustin, S. A., Benes, V., Garson, J. A., Hellemans, J., Huggett, J., Kubista, M., et al. (2009). The MIQE guidelines: minimum information for publication of quantitative real-time PCR experiments. *Clin. Chem.* 55, 611–622. doi: 10.1373/clinchem.2008.112797

Chen, L., Sun, B., Xu, L., and Liu, W. (2016). Wound signaling: the missing link in plant regeneration. *Plant Signal. Behav.* 11:e1238548. doi: 10.1080/15592324.2016.1238548

Chen, L. G., Xiang, S. Y., Chen, Y. L., Li, D. B., and Yu, D. Q. (2017). Arabidopsis WRKY45 interacts with the DELLA protein RGL1 to positively regulate age-triggered leaf senescence. *Mol. Plant.* 10, 1174–1189. doi: 10.1016/j.molp.2017.07.008

Chung, H. S., Koo, A. J., Gao, X., Jayanty, S., Thines, B., Jones, A. D., et al. (2008). Regulation and function of Arabidopsis JASMONATE ZIM-domain genes in response to wounding and herbivory. *Plant Physiol.* 146, 952–964. doi: 10.1104/pp.107.115691

Conesa, A., Götz, S., García-Gómez, J. M., Terol, J., Talón, M., and Robles, M. (2005). Blast2GO: a universal tool for annotation, visualization and analysis in functional genomics research. *Bioinformatics* 21, 3674–3676. doi: 10.1093/bioinformatics/bti610

Creelman, R. A., and Mullet, J. E. (1997). Biosynthesis and action of jasmonates in plants. *Annu. Rev. Plant Physiol. Plant Mol. Biol.* 48, 355–381. doi: 10.1146/annurev.arplant.48.1.355

Devoto, A., and Turner, J. G. (2003). Regulation of jasmonate-mediated plant responses in arabidopsis. *Ann. Bot.* 92, 329–337. doi: 10.1093/aob/mcg151

Fan, Y., Liu, J. T., Zou, J., Zhang, X. Y., Liu, K., Lv, P. T., et al. (2020). The RhHB1/RhLOX4 module affects the dehydration tolerance of rose flowers (Rosa hybrida) by fine-tuning jasmonic acid levels. *Hortic Res.* 7, 74–87. doi: 10.1038/s41438-020-0299-z

Faragher, J. D., Mor, Y., and Johnson, F. (1987). Role of 1-aminocyclopropane-1-carboxylic acid (ACC) in control of ethylene production in fresh and cold-stored rose flowers. *J. Exp. Bot.* 38, 1839–1847. doi: 10.1093/oxfordjournals.aob.a086774

Gao, Y., Liu, C., Li, X., Xu, H., Liang, Y., and Ma, N. (2016). Transcriptome profiling of petal abscission zone and functional analysis of an Aux/IAA family gene RhIAA16 involved in petal shedding in rose. *Front. Plant Sci.* 7, 1375–1388. doi: 10.3389/fpls.2016.01375

Gao, Y., Liu, Y., Liang, Y., Lu, J., Jiang, C., Fei, Z., et al. (2019). Rosa hybrida RhERF1 and RhERF4 mediate ethylene- and auxin-regulated petal abscission by influencing pectin degradation. *Plant J.* 99, 1159–1171. doi: 10.1111/tpj.14412

Glauser, G., Dubugnon, L., Mousavi, S. A., Rudaz, S., Wolfender, J. L., and Farmer, E. E. (2009). Velocity estimates for signal propagation leading to systemic jasmonic acid accumulation in wounded Arabidopsis. *J. Biol. Chem.* 284, 34506–34513. doi: 10.1074/jbc.M109.061432

Glauser, G., Grata, E., Dubugnon, L., Rudaz, S., Farmer, E. E., and Wolfender, J. L. (2008). Spatial and temporal dynamics of jasmonate synthesis and accumulation in Arabidopsis in response to wounding. *J. Biol. Chem.* 283, 16400–16407. doi: 10.1074/jbc.M801760200

Guo, P. R., Li, Z. H., Huang, P. X., Li, B. S., Fang, S., Chu, J. F., et al. (2017). A tripartite amplification loop involving the transcription factor wrky75, salicylic acid, and reactive oxygen species accelerates leaf senescence. *Plant Cell.* 29, 2854–2870. doi: 10.1105/tpc.17.00438

Han, Y. C., Kuang, J. F., Chen, J. Y., Liu, X. C., Xiao, Y. Y., Fu, C. C., et al. (2016). Banana transcription factor MaERF11 recruits histone deacetylase MaHDA1 and represses the expression of *MaACO1* and expansins during fruit ripening. *Plant Physiol.* 171, 1070–1084. doi: 10.1104/pp.16.00301

Hyodo, H., Tanaka, K., and Suzuki, T. (1991). Wound-induced ethylene synthesis and its involvement in enzyme induction in mesocarp tissue of Cucurbita maxima. *Postharvest Biol Tec.* 1, 127–136. doi: 10.1016/0925-5214(91)90004-U

Jiang, Y. J., Liang, G., Yang, S. Z., and Yu, D. Q. (2014). Arabidopsis WRKY57 Functions as a Node of Convergence for Jasmonic Acid- and Auxin-Mediated Signaling in Jasmonic Acid-Induced Leaf Senescence. *Plant Cell* 26, 230–245. doi: 10.1105/tpc.113.117838

Jones, M. L., and Woodson, W. R. (1999). Differential expression of three members of the 1-aminocyclopropane-1-carboxylate synthase gene family in carnation. *Plant Physiol.* 119, 755–764. doi: 10.1104/pp.119.2.755

Kato, M., Kamo, T., Wang, R., Nishikawa, F., Hyodo, H., Ikoma, Y., et al. (2002). Wound-induced ethylene synthesis in stem tissue of harvested broccoli and its effect on senescence and ethylene synthesis in broccoli florets. *Postharvest Biol. Technol.* 24, 69–78. doi: 10.1016/S0925-5214(01)00111-9

Kim, W. T., and Yang, S. F. (1994). Structure and expression of cdnas encoding 1-aminocyclopropane-1-carboxylate oxidase homologs isolated from excised mung bean hypocotyls. *Planta* 194, 223–229. doi: 10.1007/BF011 01681

Koo, A. J. K., Gao, X. L., Jones, A. D., and Howe, G. A. (2009). A rapid wound signal activates the systemic synthesis of bioactive jasmonates in Arabidopsis. *Plant J.* 59, 974–986. doi: 10.1111/j.1365-313X.2009.03924.x

Langfelder, P., and Horvath, S. (2008). WGCNA: an R package for weighted correlation network analysis. *BMC Bioinform.* 9, 559–572. doi: 10.1186/1471-2105-9-559

Larrieu, A., Champion, A., Legrand, J., Lavenus, J., Mast, D., Brunoud, G., et al. (2015). A fluorescent hormone biosensor reveals the dynamics of jasmonate signalling in plants. *Nat. Commun.* 6:6043. doi: 10.1038/ncomms7043

Leon, J., Rojo, E., and Sanchez-Serrano, J. J. (2001). Wound signalling in plants. *J. Exp. Bot.* 52, 1–9. doi: 10.1093/jexbot/52.354.1

Li, Z. H., Peng, J. Y., Wen, X., and Guo, H. W. (2013). ETHYLENE-INSENSITIVE3 is a senescence-associated gene that accelerates age-dependent leaf senescence by directly repressing miR164 transcription in arabidopsis. *Plant Cell.* 25, 3311–3328. doi: 10.1105/tpc.113.113340

Liu, D. R., Li, N., Dube, S., Kalinski, A., Herman, E., and Mattoo, A. K. (1993). Molecular characterization of a rapidly and transiently wound-induced soybean (Glycine-Max L) gene encoding 1-Aminocyclopropane-1-Carboxylate synthase. *Plant Cell Physiol.* 34, 1151–1157.

Livak, K. J., and Schmittgen, T. D. (2001). Analysis of relative gene expression data using real-time quantitative PCR and the 2(-Delta Delta C(T)). *Methods* 25, 402–408. doi: 10.1006/meth.2001.1262

Lohse, M., Nagel, A., Herter, T., May, P., Schroda, M., Zrenner, R., et al. (2014). Mercator: a fast and simple web server for genome scale functional annotation of plant sequence data. *Plant Cell Environ.* 37, 1250–1258. doi: 10.1111/pce.12231

Lu, P. T., Zhang, C. Q., Liu, J. T., Liu, X. W., Jiang, G. M., Jiang, X. Q., et al. (2014). RhHB1 mediates the antagonism of gibberellins to ABA and ethylene during rose (*Rosa hybrida*) petal senescence. *Plant J.* 78, 578–590. doi: 10.1111/tpj.12494

Ma, N., Cai, L., Lu, W. J., Tan, H., and Gao, J. P. (2005). Exogenous ethylene influences flower opening of cut roses (*Rosa hybrida*) by regulating the genes encoding ethylene biosynthesis enzymes. *Sci. China Ser. C.* 48, 434. doi: 10.1360/062004-37

Ma, N., Ma, C., Liu, Y., Shahid, M. O., Wang, C. P., and Gao, J. P. (2018). Petal senescence: a hormone view. *J. Exp. Bot.* 69, 719–732. doi: 10.1093/jxb/ery009

Ma, N., Tan, H., Xue, J. H., Li, Y. Q., and Gao, J. P. (2006). Transcriptional regulation of ethylene receptor and *CTR* genes involved in ethylene-induced flower opening in cut rose (*Rosa hybrida*) cv. *Samantha. J. Exp. Bot.* 57, 2763–2773. doi: 10.1093/jxb/erl033

Mao, X., Cai, T., Olyarchuk, J. G., and Wei, L. (2005). Automated genome annotation and pathway identification using the KEGG Orthology (KO) as a controlled vocabulary. *Bioinformatics* 21, 3787–3793. doi: 10.1093/bioinformatics/bti430

Meng, Y. L., Li, N., Tian, J., Gao, J. P., and Zhang, C. (2013). Identification and validation of reference genes for gene expression studies in postharvest rose flower (Rosa hybrida). *Sci. Hortic.* 158, 16–21. doi: 10.1016/j.scienta.2013.04.019

Mor, Y., Johnsen, F., and Faragher, J. D. (1989). Preserving the quality of cold-stored rose flowers with ethylene antagonists. *HortScience* 24, 436–440.

Müller, R., Sisler, E. C., and Serek, M. (2000). Stress induced ethylene production, ethylene binding, and the response to the ethylene action inhibitor 1-MCP in miniature roses. *Sci. Hortic.* 83: 51–59. doi: 10.1016/S0304-4238(99)00 099-0

Nham, N. T., de Freitas, S. T., Macnish, A. J., Carr, K. M., Kietikul, T., Guilatco, A. J., et al. (2015). A transcriptome approach towards understanding the development of ripening capacity in 'Bartlett' pears (Pyrus communis L.). *BMC Genomics* 16:762. doi: 10.1186/s12864-015-1939-9

Noodén, L. D., and Schneider, M. J. (2004). 26—light control of senescence. *Plant cell Death Process.* 1, 375–383. doi: 10.1016/B978-012520915-1/50029-1

Overmyer, K., Tuominen, H., Kettunen, R., Betz, C., Langebartels, C., Sandermann, H., et al. (2000). Ozone-sensitive Arabidopsis *rcd1* mutant reveals opposite roles for ethylene and jasmonate signaling pathways in regulating superoxide-dependent cell death. *Plant Cell* 12, 1849–1862. doi: 10.1105/tpc.12.10.1849

Pei, H., Ma, N., Tian, J., Luo, J., Chen, J., Li, J., et al. (2013). An NAC transcription factor controls ethylene-regulated cell expansion in flower petals. *Plant Physiol.* 163, 775–791. doi: 10.1104/pp.113.223388

Pertea, M., Pertea, G. M., Antonescu, C. M., Chang, T. C., Mendell, J. T., and Salzberg, S. L. (2015). StringTie enables improved reconstruction of a transcriptome from RNAseq reads. *Nat Biotechnol.* 33, 290–295. doi: 10.1038/nbt.3122

Philosophhadas, S., Meir, S., and Aharoni, N. (1991). Effect of wounding on ethylene biosynthesis and senescence of detached spinach leaves. *Physiol. Plant.* 83, 241–246. doi: 10.1111/j.1399-3054.1991.tb02148.x

Rao, M. V., Lee, H., Creelman, R. A., Mullet, J. E., and Davis, K. R. (2000). Jasmonic acid signaling modulates ozone-induced hypersensitive cell death. *Plant Cell.* 12, 1633–1646. doi: 10.1105/tpc.12.9.1633

Reid, M. S., Evans, R. Y., Dodge, L. L., and Mor, Y. (1989). Ethylene and silver thiosulfate influence opening of cut rose flowers. *J. Amer. Soc. Hort Sci.* 114, 436–440.

Rinerson, C. I., Scully, E. D., Palmer, N. A., Donze-Reiner, T., Rabara, R. C., Tripathi, P., et al. (2015). The WRKY transcription factor family and senescence in switchgrass. *BMC Genomics* 16, 912–928. doi: 10.1186/s12864-015-2057-4

Rushton, P. J., Somssich, I. E., Ringler, P., and Shen, Q. J. (2010). WRKY transcription factors. *Trends Plant Sci.* 15, 247–258. doi: 10.1016/j.tplants.2010.02.006

Shabanian, S., Nasr, E. M., Karamian, R., and Tran L. S. (2018). Salicylic acid modulates cutting-induced physiological and biochemical responses to delay senescence in two gerbera cultivars. *Plant Growth Regul.* 87, 245–256. doi: 10.1007/s10725-018-0466-5

Thimm, O., Blasing, O., Gibon, Y., Nagel, A., Meyer, S., Kruger, P., et al. (2004). MAPMAN: a user-driven tool to display genomics data sets onto diagrams of metabolic pathways and other biological processes. *Plant J.* 37, 914–939. doi: 10.1111/j.1365-313X.2004.02016.x

Tian, J., Pei, H. X., Zhang, S., Chen, J. W., Chen, W., Yang, R. Y., et al. (2014). TRVGFP: a modified Tobacco rattle virus vector for efficient and visualizable analysis of gene function. *J. Exp. Bot.* 65, 311–322. doi: 10.1093/jxb/ert381

Trivellini, A., Cocetta, G., Vernieri, P., Mensuali-Sodi, A., and Ferrante, A. (2015). Effect of cytokinins on delaying petunia flower senescence: a transcriptome study approach. *Plant Mol. Bio.* 87, 169–180. doi: 10.1007/s11103-014-0268-8

Wang, L., Zhang, X. L., Wang, L., Tian, Y. A., Jia, N., Chen, S. Z., et al. (2017). Regulation of ethylene-responsive SlWRKYs involved in color change during tomato fruit ripening. *Sci. Res.* 7:16674. doi: 10.1038/s41598-017-16851-y

Wasternack, C. (2007). Jasmonates: An update on biosynthesis, signal transduction and action in plant stress response, growth and development. *Ann. Bot.* 100, 681–697. doi: 10.1093/aob/mcm079

Wu, L., Ma, N., Jia, Y. C., Zhang, Y., Feng, M., Jiang, C. Z., et al. (2017). An ethylene-induced regulatory module delays flower senescence by regulating cytokinin content. *Plant Physiol.* 173, 853–862. doi: 10.1104/pp.16.01064

Yang, M., Zhu, L. P., Pan, C., Xu, L. M., Liu, Y. L., Ke, W. D., et al. (2015). Transcriptomic analysis of the regulation of rhizome formation in temperate and tropical lotus (*Nelumbo nucifera*). *Sci. Res.* 5:13059. doi: 10.1038/srep13059

Zhang, S., Feng, M., Chen, W., Zhou, X. F., Lu, J. Y., Wang, Y. R., et al. (2019a). In rose, transcription factor PTM balances growth and drought survival via PIP2;1 aquaporin. *Nat. Plants.* 5, 290–299. doi: 10.1038/s41477-019-0376-1

Zhang, S., Zhao, Q. C., Zeng, D. X., Xu, J. H., Zhou, H. G., Wang, F. L., et al. (2019b). RhMYB108, an R2R3-MYB transcription factor, is involved in ethylene- and JA-induced petal senescence in rose plants. *Horti Res.* 6, 131–143. doi: 10.1038/s41438-019-0221-8

Zhang, Y., Wu, Z. C., Feng, M., Chen, J., Qin, M., Wang, W., et al. (2021). The circadian-controlled PIF8-BBX28 module regulates petal senescence in rose flowers by governing mitochondrial ROS homeostasis at night. *Plant cell* 11:152. doi: 10.1093/plcell/koab152

Zhao, L., Zhang, W., Song, Q., Xuan, Y., Li, K., Cheng, L., et al. (2020). A WRKY transcription factor, TaWRKY40-D, promotes leaf senescence associated with jasmonic acid and abscisic acid pathways in wheat. *Plant Biol.* 22, 1072–1085. doi: 10.1111/plb.13155

Zhao, M. M., Zhang, X. W., Liu, Y. W., Li, K., Tan, Q., Zhou, S., et al. (2020). A WRKY transcription factor, TaWRKY42-B, facilitates initiation of leaf senescence by promoting jasmonic acid biosynthesis. *BMC Plant Biol.* 20:444. doi: 10.1186/s12870-020-02650-7

Zhou, W. K., Lozano-Torres, J. L., Blilou, I., Zhang, X. Y., Zhai, Q. Z., Smant, G., et al. (2019). A jasmonate signaling network activates root stem cells and promotes regeneration. *Cell* 177, 942–956. doi: 10.1016/j.cell.2019.03.006

Zou, Y., Chintamanani, S., He, P., Fukushige, H., Yu, L. P., Shao, M. Y., et al. (2016). A gain-of-function mutation in Msl10 triggers cell death and wound-induced hyperaccumulation of jasmonic acid in Arabidopsis. *J. Integr. Plant Biol.* 58, 600–609. doi: 10.1111/jipb.12427

Conflict of Interest: The authors declare that the research was conducted in the absence of any commercial or financial relationships that could be construed as a potential conflict of interest.

Publisher's Note: All claims expressed in this article are solely those of the authors and do not necessarily represent those of their affiliated organizations, or those of the publisher, the editors and the reviewers. Any product that may be evaluated in this article, or claim that may be made by its manufacturer, is not guaranteed or endorsed by the publisher.

frontiers in Plant Science

ORIGINAL RESEARCH
published: 10 December 2021
doi: 10.3389/fpls.2021.792384

Changes of Morphology, Chemical Compositions, and the Biosynthesis Regulations of Cuticle in Response to Chilling Injury of Banana Fruit During Storage

Hua Huang[1], Ling Wang[2], Diyang Qiu[1], Nan Zhang[1] and Fangcheng Bi[1]**

[1] Institute of Fruit Tree Research, Guangdong Academy of Agricultural Sciences, Key Laboratory of South Subtropical Fruit Biology and Genetic Resource Utilization, Ministry of Agriculture and Rural Affairs, Guangdong Provincial Key Laboratory of Tropical and Subtropical Fruit Tree Research, Guangzhou, China, [2] Sericultural & Agri-Food Research Institute, Guangdong Academy of Agricultural Sciences, Key Laboratory of Functional Foods, Ministry of Agriculture and Rural Affairs, Guangdong Key Laboratory of Agricultural Products Processing, Guangzhou, China

OPEN ACCESS

Edited by:
Isabel Lara,
Universitat de Lleida, Spain

Reviewed by:
José Alejandro Heredia-Guerrero,
University of Malaga, Spain
Antonio Heredia,
University of Malaga, Spain

***Correspondence:**
Hua Huang
huangw0109@gmail.com
Fangcheng Bi
bifangcheng@gdaas.cn

Specialty section:
This article was submitted to Crop and Product Physiology, a section of the journal Frontiers in Plant Science

Received: *10 October 2021*
Accepted: *12 November 2021*
Published: *10 December 2021*

Citation:
Huang H, Wang L, Qiu D, Zhang N and Bi F (2021) Changes of Morphology, Chemical Compositions, and the Biosynthesis Regulations of Cuticle in Response to Chilling Injury of Banana Fruit During Storage. Front. Plant Sci. 12:792384. doi: 10.3389/fpls.2021.792384

The plant cuticle covers almost all the outermost surface of aerial plant organs, which play a primary function in limiting water loss and responding to the environmental interactions. Banana fruit is susceptible to thermal changes with chilling injury below 13°C and green ripening over 25°C. Herein, the changes of surface morphology, chemical compositions of cuticle, and the relative expression of cuticle biosynthesis genes in banana fruit under low-temperature storage were investigated. Banana fruit exhibited chilling injury rapidly with browned peel appearance stored at 4°C for 6 days. The surface altered apparently from the clear plateau with micro-crystals to smooth appearance. As compared to normal ones, the overall coverage of the main cuticle pattern of waxes and cutin monomers increased about 22% and 35%, respectively, in browned banana stored under low temperature at 6 days. Fatty acids (C_{16}–C_{18}) and ω-OH, mid-chain-epoxy fatty acids (C_{18}) dominated cutin monomers. The monomers of fatty acids, the low abundant ω, mid-chain-diOH fatty acids, and 2-hydroxy fatty acids increased remarkably under low temperature. The cuticular waxes were dominated by fatty acids (> C_{19}), *n*-alkanes, and triterpenoids; and the fatty acids and aldehydes were shifted to increase accompanied by the chilling injury. Furthermore, RNA-seq highlighted 111 cuticle-related genes involved in fatty acid elongation, biosynthesis of very-long-chain (VLC) aliphatics, triterpenoids, and cutin monomers, and lipid-transfer proteins were significantly differentially regulated by low temperature in banana. Results obtained indicate that the cuticle covering on the fruit surface was also involved to respond to the chilling injury of banana fruit after harvest. These findings provide useful insights to link the cuticle on the basis of morphology, chemical composition changes, and their biosynthesis regulations in response to the thermal stress of fruit during storage.

Keywords: banana fruit, chilling injury, surface morphology, cuticle, biosynthesis regulations

INTRODUCTION

Banana is one of the most populated horticultural crops planted widely in the tropical and subtropical regions including south China. Banana contains abundant bioactive phytochemicals such as carbohydrates, vitamins, minerals, etc., being one of the most consumed fruit worldwide (Sidhu and Zafar, 2018). Low-temperature storage is one of the most efficient methods to preserve the food and crop quality. However, banana fruit is sensitive to temperatures, which exhibits chilling injury below 13°C and softening without normal yellow-colored under high temperature over 25°C (Yang et al., 2009; Hashim et al., 2012). The thermal sensitivity severely affects the fruit quality and their market values after harvest. The chilling injury symptoms of banana fruit mainly exhibit as browning in the vascular tissues and appearance and abnormal flesh softening (Wang et al., 2012). The chilling injury with browning changes is widely reported to be regulated by the reactive oxygen species (ROS), antioxidant activity, ATP level, and ion concentration in banana fruit. The temperature below chilling conditions disturbs the cellular ROS homeostasis, inducing the oxidation of polyphenols, accelerating energy dissipation, and ion flux (Huang et al., 2016; Liu et al., 2019). In addition, the integrity of the plasma membrane, which is pivotal for quality maintenance, is altered or damaged under ROS, temperature, or other stress stimulations during storage (Huang et al., 2019).

The plant cuticle constituted by complex lipids covers almost all aerial plant organs. The plant cuticle consists of soluble lipids as wax mixtures embedded in a cutin matrix. Cutin is prominently composed of C_{16} and C_{18} fatty acid monomers polymerized into the framework that harbors the various waxes (Philippe et al., 2020). The cuticular waxes are very-long-chain (VLC) fatty acids and their derivatives, which are tightly packed and aligned to act as impermeable flake obstacles, together with cyclic triterpenoids and sterols, form less hydrophobic amorphous zones (Jetter et al., 2008). The outermost lipid layer of cuticle plays multiple functions for the interactions between plant cells and environment (Yeats and Rose, 2013). The biosynthesis of cutin and wax compositions is well stated and regulated by a series of key enzyme genes. These genes are mainly within VLC fatty acid elongation, *n*-alkane pathway, alcohol pathway, ester formation, biosynthesis of triterpenoids, and sterols for the wax mixtures (Lewandowska et al., 2020), and also forming mid-chain hydroxyl and epoxy groups and polymerization process (Fich et al., 2016).

The accumulation of cuticular compositions is involved in response to abiotic and biotic stresses. Both the cuticular waxes and cutin were reported to play barrier or signal roles in the interactions between plant surface and the microorganisms (Isaacson et al., 2009; Hansjakob et al., 2010). As the primary function of cuticle is to limit the uncontrolled water loss, the biosynthesis of VLC components in waxes has been found to be significantly accumulated to adapt to the drought or salt stresses in plants (Kosma et al., 2009; Dimopoulos et al., 2020). Moreover, the high temperature or water-deficit environment will induce the accumulation of VLC esters ($\geq C_{36}$) and triterpenoids in desert plant leaves (Schuster et al., 2016; Bueno et al., 2019). These reported results indicate that the surface cuticular components may have an effect on the temperature stress for plant tissues.

Recently, studies have tried to explore the effect of cuticular lipids on postharvest fruit quality changes (Heredia et al., 2019). The deficit biosynthesis of cutin monomers affected the fruit to resistant the microbial infection in tomato fruit after harvest (Isaacson et al., 2009). The triterpenoid fraction in fruit waxes was detected to exhibit a significant correlation with the postharvest behavior in blueberries (Moggia et al., 2016). The accumulation and crystal structure of cuticular waxes in orange fruit were found to be modified during storage under both low and room temperatures (Ding et al., 2018). Furthermore, the peel gloss, which was reported to be largely related to the cuticle changes (Petit et al., 2014), decreased with the ripening of banana fruit (Ward and Nussinovitch, 1996). Therefore, the cuticular lipids and their morphological appearance may play an important role in the ripening of fruit after harvest. The horticultural crops are usually stored under low temperatures to delay the shelf life and maintain their quality. So far, very few studies reported the cuticular waxes in varieties of bananas (Brian and David, 1985; Sampangi-Ramaiah et al., 2016), and the cutin mixtures of bananas have not yet been reported. Therefore, the cuticular lipids, including the cutin monomers and waxes, are necessary to be analyzed in detail as an update. Additionally, banana is a typical thermal-sensitive fruit, and the response of surface cuticular lipids to the chilling injury is also awaiting to be comprehensively investigated.

Banana fruit are usually harvested at green mature stage and turns to be yellow softening over 3 weeks during storage (Huang et al., 2013) but suffers chilling injury with most of browning appearance at 6 days (Huang et al., 2016). There are almost no obvious changes for the green mature banana fruit after 6 days stored under room temperature (Huang et al., 2013). Therefore, in the present study, banana fruit stored at 6 days under 4 and 25°C, respectively, were selected as the comparative samples. The chilling index and color changes of banana peel, surface morphology, and the changes of cuticle compositions including waxes and cutin monomers and the relative expression levels of cuticle-related genes were carried out in detail. The results obtained will broad insights on exploring the chilling injury of banana fruit on basis of the morphology, chemical, and molecular regulations of cuticle.

MATERIALS AND METHODS

Plant Materials and Chemical Reagents

Banana fruits (*Musa* spp., AAA group, cv. Brazil) at physiological mature stage with green were harvested from an orchard in Guangzhou, Guangdong Province, P.R. China (23°30′N, 113°30′E). Harvested fruits were packed with polypropylene plastic bags (film thickness: 32 μm) and immediately transported to the laboratory within 2 h. Fruits were selected for uniformity of shape, color, and size, and rinsed the surface gently. Then fruits were placed into two groups randomly and packed in polyethylene bags (200 mm × 50 mm, 0.03 mm thickness, and three fruit per bag) and stored at 4 and 25°C, respectively. Six

bags in total of 18 fingers from each treatment were randomly selected at 0, 2, 4, and 6 days during storage, and the chilling index and hue angle were evaluated. To isolate cuticular membranes, chemical reagents of analytical grade were prepared as previously described (Huang and Jiang, 2019). The peel tissues were sliced, frozen in liquid N_2, and stored at − 80°C for further analysis.

Determination of Chilling Injury Index and Hue Angle

The symptom of chilling injury was estimated by the extent of browning surface with different scales: "1" smooth surface without browning point; "2" slight browning with 1/4 of the fruit surface; "3" 1/4–1/2 browning area; "4" 1/2–3/4 browning area; and "5" > 3/4 browning area. The chilling injury index was calculated as: CI (chilling injury scale × corresponding fruit fingers within each class)/(number of total fruit × the highest scale) × 100.

The peel color degree was determined using a Minolta Chroma Meter CR-400 (Minolta Camera Co., Ltd., Osaka, Japan). Nine fruit fingers from each treatment at each stored stage and three points around the middle of each fruit were measured. Color was recorded as parameters of CIE L*, a*, and b* scales. In which, L indicates the lightness or darkness, a* indicates green to red, and b* donates blue to yellow. The overall color index was indicated by L* or general value of hue angle [$h° = \tan^{-1}(b^*/a^*)$].

Scanning Electronic Microcopy

The surface characteristics of each organ of the two kinds of vegetables were observed using scanning electron microscopy (SEM). Briefly, small pieces (3 mm × 3 mm) of the peel tissues were picked and fixed in 2.5% glutaraldehyde in 0.2 M sodium phosphate buffer, pH 7.2–7.4 at 4°C overnight. The fixed samples were vacuum-infiltrated in the material on ice for 1 h. The samples were washed using sodium phosphate buffer and then dehydrated in a graded alcohol series with 30, 50, 75, 90, and 100% three times. After the samples were dried completely, the small pieces were mounted on aluminum stubs using a conductive double-sided adhesive tape prior to observation. The dried samples were coated with gold:palladium (60:40) at 30 mA using a LEICA EM ACE600 (Leica Microsystems, Wetziar, Germany) sputter coater, depositing an alloy of approximately 10 nm thickness. The characteristics of the sample surfaces were examined under a field emission SEM (JEOL JSM-6360LV, Tokyo, Japan) at 15 kV accelerating voltage.

Isolation of Cuticular Membranes

The cuticles of banana fruit were isolated enzymatically following the protocol described by Huang and Jiang (2019). Fruit samples from each group at each stage were randomly selected. Peel discs were obtained by a puncher 1.2 cm in diameter near the middle position of the fruit. The punched discs were soaked in 10 mM citric acid buffer containing 1% (w/v) pectinase and 1% (w/v) cellulase (Beijing Solarbio Science & Technology Co., Ltd., Beijing, China). The cuticular membranes isolated from peel tissues were then washed by 10 mM sodium tetraborate decahydrate and distilled water in series. After that, cuticles were air-dried for further cuticular chemical analysis.

Cuticular Wax and Cutin Monomer Extraction

The cuticular waxes and cutin monomers of banana fruit were extracted using the isolated cuticular membranes following the reported procedure previously (Huang, 2017). The dry and fine intact cuticular membranes isolated from banana fruit were immersed in chloroform completely. To better release the soluble waxes, the extraction was set with a moderate temperature at 40°C. The extraction for each sample was repeated three times, and each time for 2 min. After combining the extracted solution, *n*-tetracosane (Sigma-Aldrich, Shanghai, China) as an internal standard was added to help detect the accumulation of cuticular waxes. Gentle stream of nitrogen gas was used to dry the extracts for further analysis.

The above matrix membrane after removing waxes was subsequently depolymerized in boron trifluoride with methanol (BF_3-methanol, 10%, ∼1.3 M) overnight at 70°C. Then, *n*-dotriacontane (Sigma-Aldrich, Shanghai, China) was added as an internal standard. Saturated aqueous sodium chloride solution and chloroform were added subsequently to extract the cutin monomers. The organic phase containing cutin monomers was collected and evaporated to dryness under a gentle stream of nitrogen gas for further analysis.

Gas Chromatography-Mass Spectrometry

Prior to the analysis of the chemical composition of cuticular waxes and cutin monomers, the dry extracts prepared in the aforementioned manner were derivatized with pyridine (Shanghai Aladdin Bio-Chem Technology Co., Ltd., Shanghai, China) and N,O-*bis* (trimethylsilyl)trifluoroacetamide (BSTFA; Sigma-Aldrich, Shanghai, China) for 30 min at 70°C. To quantify wax and cutin monomer components, the extracts were analyzed using a capillary gas chromatography instrument equipped with a flame ionization detector (7820A, GC System; Agilent Technologies, Santa Clara, CA, United States), and on-column injection with a capillary column (30 m × 0.32 mm, DB-1 ms, 0.1 μm film; J&W Scientific, Agilent Technologies, Santa Clara, CA, United States). To separate cuticular wax compounds, 10 μL samples were injected at 50°C; after 2 min at 50°C, the temperature was raised to 200°C at 40°C min^{-1}, held for 2 min at 200°C, and then raised to 320°C at 3°C min^{-1} and held for 30 min at 320°C. For separation of the cutin monomers, 10 μl samples were injected at 50°C; following 1 min at 50°C, the temperature was raised to 150°C at 10°C min^{-1}, held for 2 min at 150°C, and then raised to 320°C at 3°C min^{-1} and held for 30 min at 320°C. The area under the peaks was compared with that of the internal standards to obtain the quantity of cuticular wax and cutin monomer components.

The chemical components were analyzed using a temperature-controlled capillary gas chromatography instrument equipped with a mass spectrometric detector (*m/z* 50–750, MSD 5975; Agilent Technologies, Santa Clara, CA, United States). Single compounds were identified based on their electron ionization mass spectra using authentic standards, the Wiley 10^{th}/NIST 2014 mass spectral library (W10N14; John Wiley & Sons), or by interpretation of the spectra according to the retention

times and/or by comparison with data from the literature (Holloway, 1982; Jetter et al., 2008) or online database (LipidWeb)[1]. The coverage was quantified against the amount of the internal standard, and the average chain length of the VLC acyclic compounds was calculated following the method reported by Huang (2017).

RNA-seq Analysis and Reverse Transcription Analysis

Three biological replicates were performed for each sample. Total RNA was extracted and removed the contaminations with DNase I. Then, the purity and concentration of the RNA were checked by multifunction microwell plate detector (Shanghai Dobio Biology Technology Inc., Spark®, Tecan, Shanghai, China) and Agilent 2100 Bioanalyzer (Agilent Technologies, Santa Clara, CA, United States). Then the cDNA was synthesized by mixing with DNA polymerase I and RNase H. The samples were amplified and sequenced on Illumina HiSeq™ 4000 by Gene *Denovo* Co. (Guangzhou, China). The fine data were mapped to the reference genome using published banana data. The gene expression abundance was represented by an RPKM value. Differentially expressed genes (DEGs) were identified by the DESeq2[2], which indicated the change of false discovery rate genes over twofold with statistical significance (false discovery rate, FDR < 0.05). DEGs in the pointed pathways were analyzed in detail.

The total RNA of banana peel tissues using a HiPure Plant RNA Mini Kit (Magen, Guangzhou, China) and cleaned with DNase I (TaKaRa, Otsu, Japan). The DNA-free RNA was used as the template for reverse-transcription PCR (RT-PCR). The first-strand cDNA template of each gene was synthesized using PrimeScript® RT Master Mix (Perfect Real Time) template kit (DRR036A; TaKaRa, Otsu, Japan), and their concentrations were determined using a multifunction microwell plate detector (Shanghai Dobio Biology Technology Inc., Spark®, Tecan, Shanghai, China). Relative expression levels of the sequenced DEGs related to fatty acid elongation (*MaLACS*, *MaKCS*, *MaKCR,* and *MaECR*) and wax biosynthesis (*MaCER1* and *MaFAR*) were carried out by qRT-PCR. The reaction system was SYBR Premix Ex Taq Kit (DRR420A; TaKaRa, Otsu, Japan) where PCR conditions for the primers were 95°C for 30 s, 95°C for 5 s, and 60°C for 34 s, 40 cycles. The Primer Premier 6.0 software (Premier, Canada) was used to design the primers (**Supplementary Table 1**). The qRT-PCR was performed with SYBR® Premix Ex Taq™ II (Takara, Otsu, Japan) in an ABI7500 Real-Time PCR System (Thermo Fisher Scientific, Waltham, MA, United States). Three independent biological replicates were used in the analysis.

Statistical Analysis

Statistical analyses were performed using the IBM SPSS (version 23, IBM Corp., Armonk, NY, United States) and SigmaPlot 12.5 (Systat Software, Inc., San Jose, CA, United States). Comparison analyses were performed by one-way ANOVA, and significant differences were analyzed at a level of 0.05. SigmaPlot 12.5 was used to elaborate the graphs shown in the figures.

[1]https://www.lipidmaps.org/resources/lipidweb/lipidweb_html/index.html
[2]http://www.bioconductor.org/packages/release/bioc/html/DESeq2.html

RESULTS

Changes in Fruit Appearance and Morphology During Storage

Banana fruit exhibited an obvious browning appearance as the chilling injury symptom with an index over 80% of surface-browned at 6 days under 4°C after harvest (**Figures 1A,B**). The hue angle of fruit peel decreased rapidly from 120° to less than 100° following the chilling injury process, inducing the discoloration of green to brown at 4°C during storage (**Figure 1C**). In contrast, banana fruit stored at 25°C as control, the green peel appearance showed no obvious changes with trace of browning pot with most of them for mechanical damages during treatments after harvest (**Figures 1A,B**). The hue angle values of fruit exhibited relatively stable around 120° at 6 days stored at 25°C (**Figure 1C**). The green mature banana fruit changed slowly without ripening changes in the early storage period under room temperature, whereas suffered chilling injury rapidly as browning peel appearance under low-temperature storage (Huang et al., 2016).

The SEM observation showed the morphological changes of banana peel surface stored at 6 days under different temperatures. The epidermis of banana fruit consists of small square-, rectangular-, and gourd-shaped epidermal cells. These epidermal cells were outward forming numerous plateau ridges (**Figure 2A**). Similar to the previous anatomical analysis, the epidermal cells covered a thin layer of cell wall and cuticle on the outer surface of banana fruit (Amnuaysin et al., 2012). The outermost surface accumulated sparse small wax crystals (**Figure 2C**). After 6 days, the green mature banana fruit stored at 25°C showed clear cell shapes with crystals, indicating the well status for the morphological appearance in fruit (**Figures 2A,C**). However, the appearance of morphology was observed to be modified by the chilling injury under low temperature. Followed by the development of chilling-browning symptoms, the protruding epidermal cells collapsed and the surface of the fruit became flat (**Figures 2B,D**).

Cuticular Chemicals Response to the Chilling Injury

The main pattern of cuticular components of cuticular waxes and cutin monomers was detected and quantitated thoroughly. The overall accumulation of cutin monomers was detected as 23.1 $\mu g\ cm^{-2}$ in green mature fruit stored at 25°C, which was shifted to increase significantly ($p < 0.05$) as 31.2 $\mu g\ cm^{-2}$ by chilling injury after 6 days (**Table 1**). Similarly, the total wax coverage was stimulated to increase from 30.0 to 36.6 $\mu g\ cm^{-2}$ at 6 days under 25 and 4°C, respectively (**Table 1**). As a result, the ratio of total wax over cutin monomers showed no significant changes, which were about 1.2–1.3 (**Table 1**).

Changes of Cutin Monomers

The cutin monomers in the series detected were prominently mid-chain epoxy ω-hydroxy fatty acids followed by fatty acids, primary alcohols, ω-mid-dihydroxy fatty acids, and 2-hydroxy fatty acids in banana fruit cuticles (**Figure 3**). The most abundant chain length of monomers was C_{16} and C_{18} fatty acids without

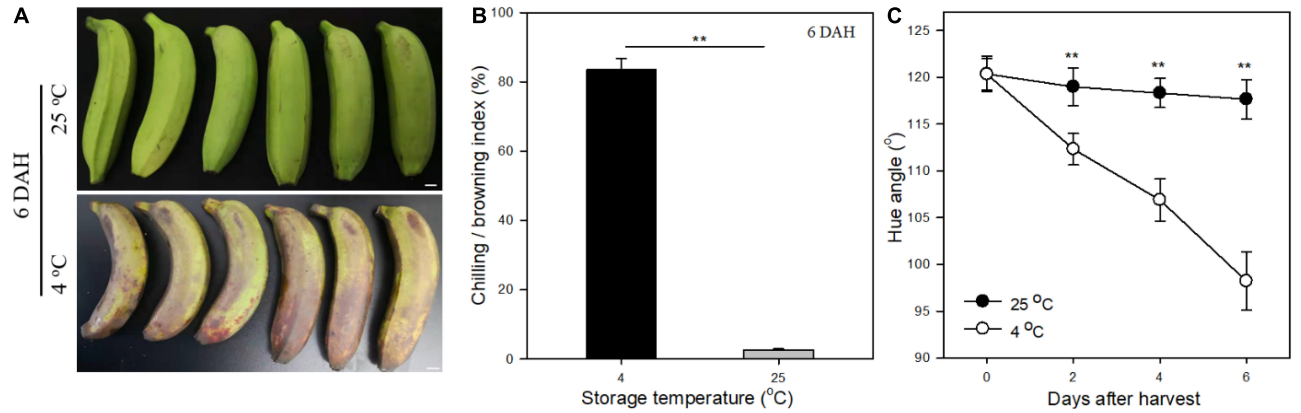

FIGURE 1 | Changes of chilling injury of banana fruit under low temperature. **(A)** Appearance of fruit stored at 4 and 25°C for 6 days, and obvious browning occurred in banana at 4°C. **(B)** Chilling index indicated by browning area of fruit under low and room temperature at 6 days. **(C)** Changes in hue angle values following the storage time under different temperature storage. Data are presented as the mean ± SD. Significant differences detected by the *t*-test are indicated by $^{*}p < 0.05$ and $^{**}p < 0.01$, respectively.

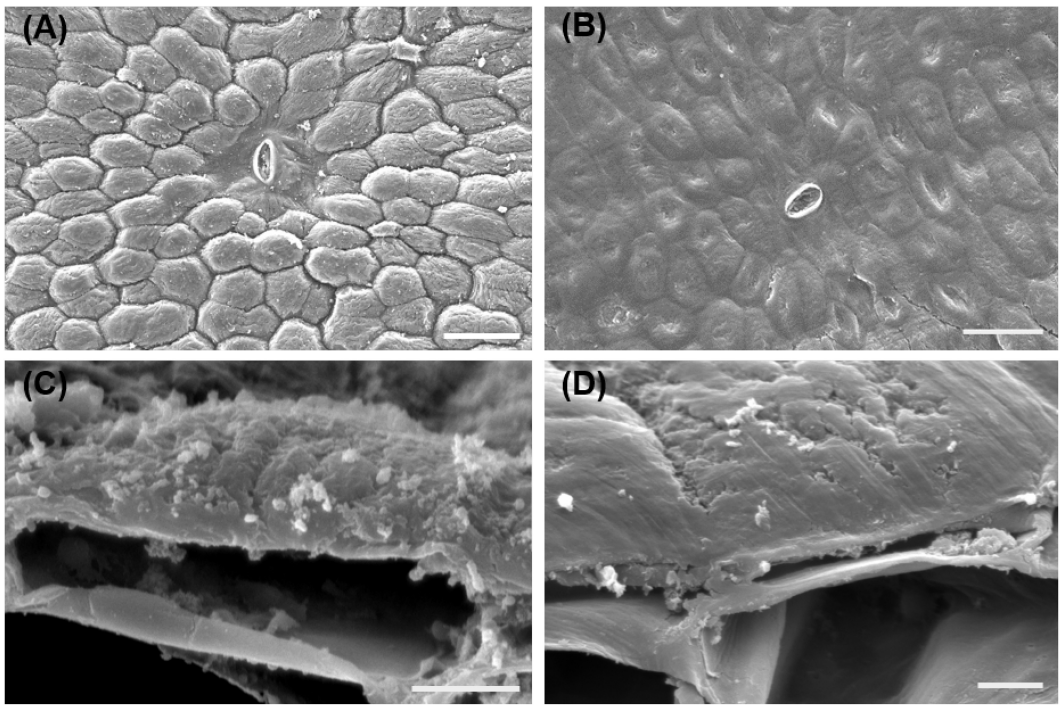

FIGURE 2 | SEM observation of the surface changes of banana fruit during storage. **(A,C)** Surface microstructure changes sored at 25°C for 6 days. **(B,D)** Surface of banana fruit under 4°C at 6 days. Size bars: **(A,B)** 50 μm and **(C,D)** 5 μm.

or with branched hydroxyl or epoxy group. The predominant C_{18} monomer was 9,10-epoxy-18-hydroxyoctadecanoic acid, which showed no significant changes around 10 μg cm^{-2} in banana fruit cuticles under different temperatures (**Figure 3** and **Supplementary Table 2**). Fatty acids without added groups accumulated in a wide range of chain-length distribution from C_{16} to C_{30}, with most abundant of C_{16}, C_{18}, C_{24}, and C_{30}. The chilling stress stimulated the increase of C_{16}- and C_{18}-chain fatty acids remarkably, whereas C_{24} and C_{30} were relatively stable, resulting in the total fatty acids raised from 5.5 to 10.0 μg cm^{-2} (**Figure 3** and **Supplementary Table 1**). The 9(10), 16-dihydroxyhexadecanoic acid was the main dihydroxy fatty acid increased slightly from 0.98 to 1.3 μg cm^{-2} (**Figure 3** and **Supplementary Table 2**). Consequently, the prominent carbon chain of C_{16} over C_{18} in cutin monomers was shifted from 0.21 to 0.35 by chilling stimulation (**Table 1**). Noteworthy, another monomer of 2-hydroxy fatty acids accumulated with a chain length of C_{22}–C_{26} with most abundant of C_{24}, raised from 0.6

to 2.1 μg cm^{-2} after 6 days of low-temperature storage. Primary alcohols ranged from C_{20} to C_{30} with even-numbered carbon chains showed no obvious changes. In addition, cyclic monomers, predominantly coumaric acid and their derivatives, were also detected and increased slightly under low-temperature storage (**Figure 3** and **Supplementary Table 2**).

Changes of Cuticular Waxes

The cuticular waxes in banana fruit cuticles were accumulated with a variety of typical VLC aliphatic and cyclic compounds. The VLC aliphatic pattern contained most abundant of fatty acids followed by *n*-alkanes, primary alcohols, and aldehydes. The cyclic pattern in waxes was dominated by pentacyclic triterpenoids and sterols (**Figure 4** and **Supplementary Table 3**). Generally, the aliphatics accumulated higher than cyclics in banana fruit cuticles. The accumulation of aliphatics increased significantly to 26.8 μg cm^{-2} in banana fruit stored under 4°C compared with that of 19.9 μg cm^{-2} in fruit under room temperature (**Table 1**). The cyclics exhibited no obvious changes (about 8.0 μg cm^{-2}) under both temperature storage. As a result, the ratio of aliphatics over cyclics was shifted from 2.6 to 3.3 (**Table 1**).

The various cuticular wax components accumulated into a homologous series. The VLC aliphatics ($> C_{18}$) were detected within a fairly broad range of carbon chain lengths. Fatty acids as the most abundant aliphatic pattern ranged from C_{20} to C_{30} with most abundant of C_{22} and C_{24}, which raised significantly under low-temperature storage at 6 days compared to that stored under 25°C (**Figure 5A**). Carbon chain ranged between C_{20} and C_{32} was detected for *n*-alkanes, almost no changes for all the *n*-alkane series of components, with an increase for C_{25} at 6 days under 4°C (**Figure 5C**). Aldehydes (C_{26} to C_{30}) and primary alcohols (C_{20} to C_{32}) accumulated with prominent of C_{28} and C_{30}, which increased for C_{30} under low temperature (**Figures 5B,D**).

The pentacyclic triterpenoids dominated the cyclic pattern containing a variety of members with the most abundant being uvaol, followed by α-amyrin, β-amyrin, epi-lupeol, and epi-lupeol acetate. Sterols were comprised of β-sitosterol and stigmasterol (**Figure 6** and **Supplementary Table 3**). After 6 days, besides uvaol, which showed a slight increase, the content of all the other triterpenoids was lower in fruit cuticles under 4°C than that under 25°C. In contrast, both β-sitosterol and stigmasterol were stimulated to increase under chilling temperature (**Figure 6** and **Supplementary Table 3**).

TABLE 1 | The overall chemical composition of cutin monomers and waxes.

	25°C 6 days	4°C 6 days	$p < 0.05$	Unit
Wax yield	30.00 ± 3.24	36.61 ± 0.44	*	μg cm^{-2}
Cutin yield	23.11 ± 3.92	31.21 ± 2.15	*	μg cm^{-2}
Wax/cutin	1.32 ± 0.25	1.18 ± 0.09		Ratio
Aliphatics	19.94 ± 3.54	26.81 ± 1.87	*	μg cm^{-2}
Cyclics	7.76 ± 0.92	8.37 ± 1.27		μg cm^{-2}
Aliphatics/cyclics	2.56 ± 0.34	3.28 ± 0.75	*	Ratio
C_{16}/C_{18} cutin monomer	0.21 ± 0.04	0.35 ± 0.05	*	Ratio
ACL	24.88 ± 0.10	23.76 ± 0.82		Carbons

*The accumulation of total wax coverage and cutin monomers, the very-long-chain aliphatics, and cyclics (μg cm^{-2}); the ratio of total wax versus cutin monomers, aliphatics versus cyclics, cyclics versus cutin, and monomers of C_{16} versus C_{18} in cutin; and weight average chain length (ACL) of aliphatics in waxes are shown. Data are given as mean value with SD (n = 5). *Indicates the significant deference at level of 0.05.*

Response of the Biosynthesis of Cuticle

The gene response to the chilling injury on mRNA level was thoroughly analyzed using RNA-sequencing together with RT-qPCR. The results showed that in total of 16,707 DEGs were annotated with 9,420 DEGs (56%) downregulation and 7,287 DEGs (44%) upregulation in this study. The Gene Ontology (GO) annotation indicated that 7,576 DEGs (47.7% of total GO-annotated DEGs) were identified as "biological process" with 18 functional groups; 4,834 DEGs (30.5%) were annotated as "cellular component" with 14 functional groups; and 3,464 DEGs (21.8%) were involved in "molecular function" with 10 functional groups (**Supplementary Figure 1**). The Kyoto Encyclopedia of Genes and Genomes (KEGG) mapping analysis revealed that the DEGs were mainly involved in seven classes of various metabolism pathways (61.6% of total annotated DEGs), when compared to low temperature with room temperature storage (**Supplementary Figure 2**).

As cuticular constituents were mostly constituted by lipids, a total of 392 DEGs in 15 different pathways involved in lipid metabolism were detected. Fatty acid elongation, ether lipid metabolism, biosynthesis of unsaturated fatty acids, etc., were enriched markedly (rich factor > 0.5, **Figure 7A**). Further analysis revealed that 111 DEGs involved in biosynthesis and formation of cuticle were identified. These DEGs were mainly structural genes in five pathways for the biosynthesis of cuticle, i.e., fatty acid elongation, VLC alcohol and *n*-alkane pathways, cyclic waxes, cutin biosynthesis, and lipid-transfer proteins (**Figure 7B**).

Among these cuticle-related genes, 23 DEGs were involved in fatty acid elongation including *MaLCAS1/2/9*, *MaKCS1/2/3/4/11*, *MaKCR1*, *MaECR*, and *MaCER26/26L* (**Figure 8A** and **Supplementary Table 4**). Besides numerous DEGs in sterol biosynthesis, 22 DEGs were identified as structure genes in wax biosynthesis respond to chilling injury, which were *MaCER1/3/7*, *MaFAR1/4*, *MaWSD1*, *MaDGAT1/2*, *MaSQS1/2*, and *Masqe1/3* (**Figure 8B** and **Supplementary Table 4**). About 26 DEGs in cutin monomer biosynthesis, *MaCYP74A*, *MaCYP74A2*, *MaCYP86A1/2*, *MaCYP86B1*, *MaHHT1*, *MaHHT*, *MaPXG4*, *MaDCR1/2/3*, *MaGPAT1/3/4/5/6/7*, and *MaAGPAT6* were differentially regulated (**Figure 8C** and **Supplementary Table 5**). And 12 DEGs of lipid transporters *MaLTP1/2*, *MaLTPG1/2*, and *MaABCG11*, which were potentially related to the transportation of cutin monomers and waxes were detected (**Figure 8D** and **Supplementary Table 5**).

DISCUSSION

The present study focused on characterizing the response of cuticle to the chilling injury in banana fruit under low

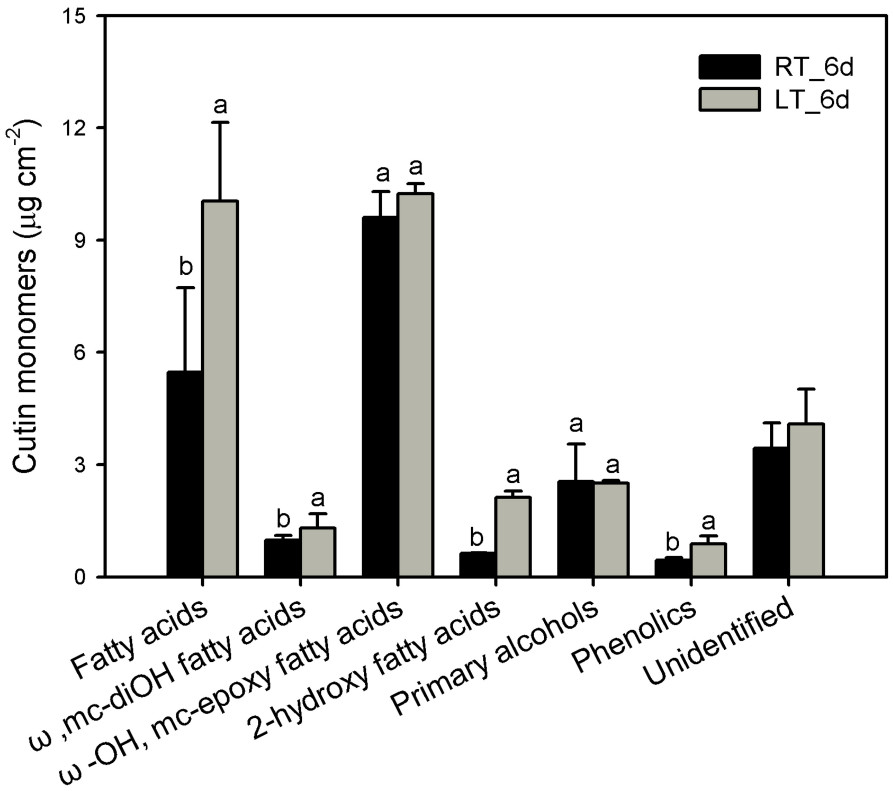

FIGURE 3 | Chemical compositions of cutin monomers in banana fruit cuticle stored under 4°C (low temperature, LT) and 25°C (room temperature, RT) at 6 days. Data are given as mean ± SD (n = 5). Letters indicate the significant differences at the 0.05 level.

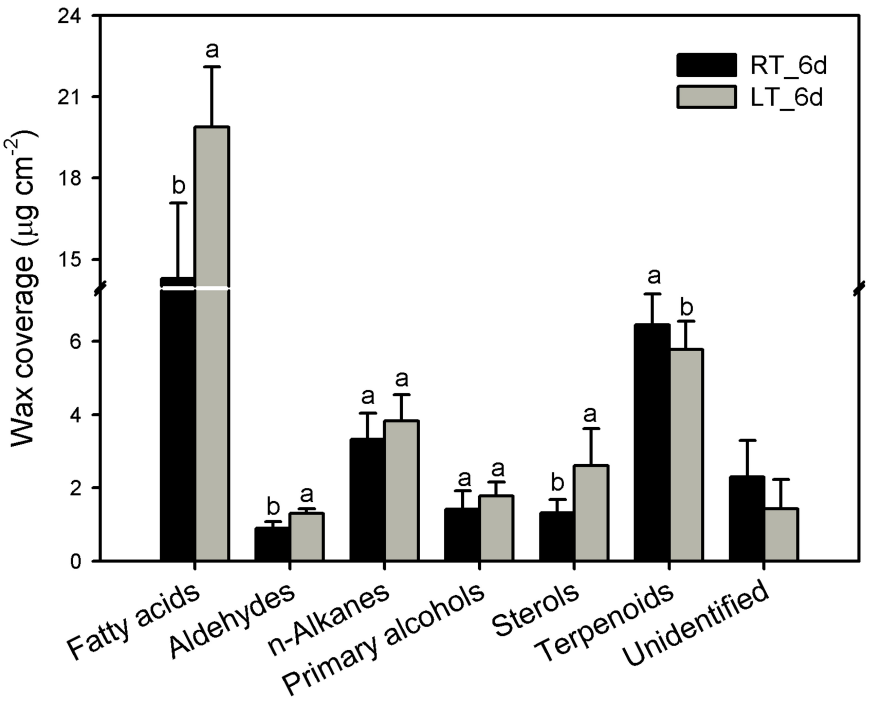

FIGURE 4 | Chemical compositions of cuticular waxes in banana fruit cuticle stored under 4°C and 25°C at 6 days. Data are given as mean ± SD (n = 5). Letters indicate the significant differences at the 0.05 level.

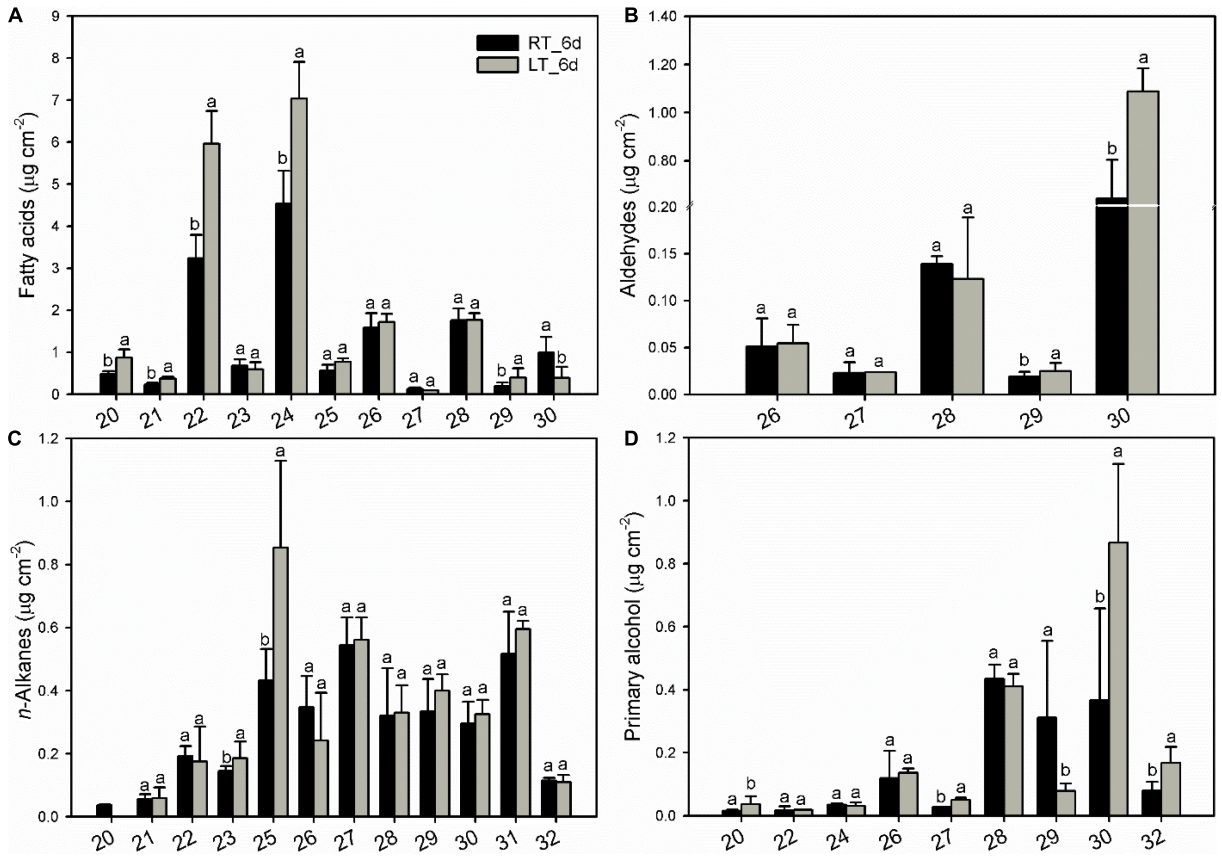

FIGURE 5 | Changes in chain-length distribution and content of variety aliphatics in banana fruit cuticle stored under 4°C (low temperature, LT) and 25°C (room temperature, RT) at 6 days. **(A)** Fatty acids; **(B)** aldehydes; **(C)** *n*-alkanes; and **(D)** primary alcohols. Data are given as means ± SD (n = 5). Letters indicate the significant differences at the 0.05 level.

temperature using room temperature as control. Banana is a typical horticultural crop that is sensitive to temperature changes during growing and postharvest storage. The chilling injury with browning of the peel tissues and discoloration, and informal firmness in banana fruit occurred after harvest. Low temperature disturbed the distribution of oxidation-related enzymes and the polyphenolics in plant cells, inducing the oxidation of polyphenolics in peel tissues (Huang et al., 2016). In addition, researchers proposed that the senescence of horticulture crops, including browning, discoloration, and softening, in banana fruit was also affected by the deficit of energy status. Under low temperature, the energy dissipation was accelerated following the chilling stimulation, thus inducing rapid browning and senescence in banana fruit (Liu et al., 2019). In addition to the subcellular changes, membrane integrity has been reported to be the earlier response to the ripening senescence and temperature injury for horticultural crops (Liang et al., 2020). The membrane lipids have been revealed as a pivotal pattern, especially the unsaturation degree of fatty acids, in adaptation to the temperature alterations (Zheng et al., 2011). The plasma membrane mainly constituted by mobile lipids with most of saturated and unsaturated C_{16} and C_{18} fatty acids. The chilling conditions could shift the ratio of saturated and unsaturated fatty acids in the plasma membrane and induce lipid peroxidation (Liu et al., 2020).

Similarly, besides the membrane lipids, the changes in cuticle, which are prominently lipid compounds, might also be involved in response to the temperature stress in banana fruit. The cuticle strength and stiffness showed largely to be affected by temperature changes (Domínguez et al., 2011). The high-temperature environment improved the accumulation of cyclic triterpenoids and VLC alkyl esters in desert plants (Schuster et al., 2016; Bueno et al., 2019). In addition, the cuticle structures, especially the arrangement of cuticular components, are dynamically modified by temperature changes, thus affecting the cuticle functions (Merk et al., 1997; Riederer, 2006). So far, few studies have reported the postharvest changes of cuticular compositions to affect the storage quality of fruit. The fruit ripening and postharvest cold storage were detected to accompany with alteration of cuticular waxes in blueberries (Moggia et al., 2016; Chu et al., 2018). However, the changes in cuticle of banana fruit in responding to low temperature are still unclear.

In banana fruit, the surface microstructure was apparently disturbed by low temperature after 6 days following the occurrence of chilling injury (**Figure 2**). The structural changes

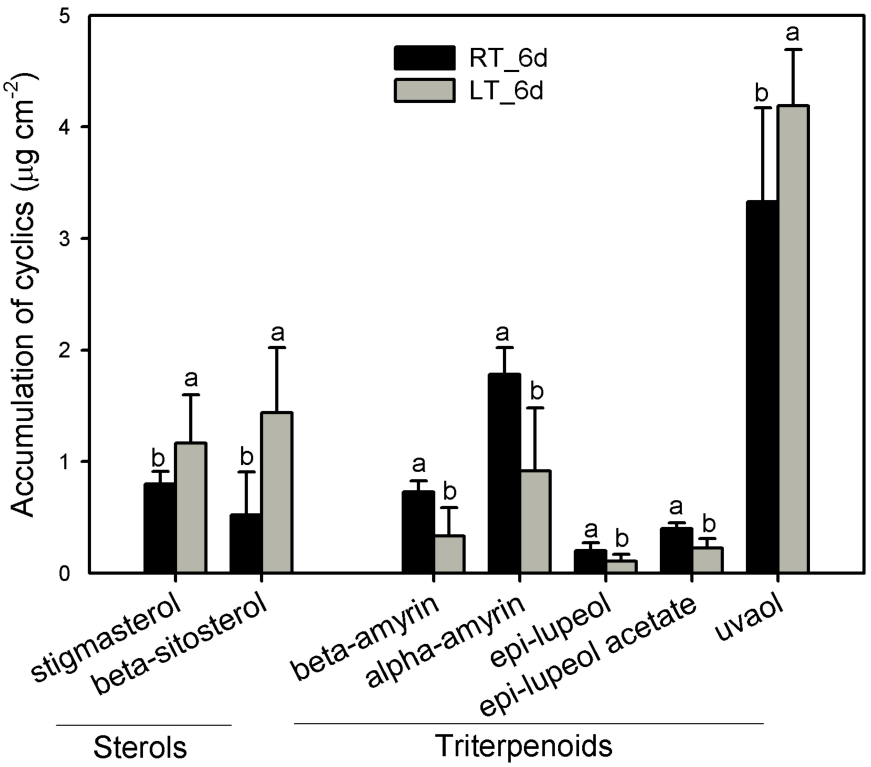

FIGURE 6 | Changes in the components of triterpenoids in wax mixtures of banana fruit cuticle stored under 4°C (low temperature, LT) and 25°C (room temperature, RT) at 6 days. Data are given as mean ± SD (n = 5). Letters indicate the significant differences at the 0.05 level.

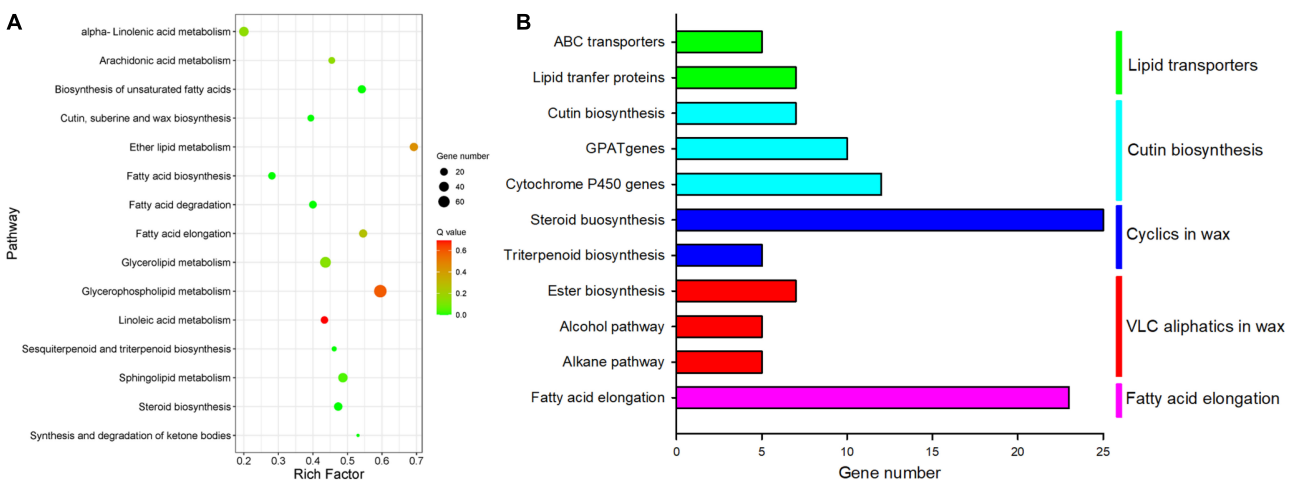

FIGURE 7 | Enriched KEGG pathways involved lipids and cuticle metabolisms. **(A)** Scatter plot of enriched in lipid metabolisms; the rich factor is the ratio of the number of DEGs in each lipid pathway to the total DEGs involved in lipid metabolisms (0–1). **(B)** The number of differential cuticle-related genes in the five main cuticle biosynthesis pathways.

are usually accompanied by the shift of chemical compositions. For instance, the skin greasiness of apple fruit has been reported by the accumulation of liquid wax of propyl-, butyl-, pentyl-, and farnesyl-linoleate and oleate during storage (Yang et al., 2021). Similarly, low temperature induced changes in both cuticular waxes and cutin monomers in banana fruit cuticle followed by appearance changes. After 6 days of storage, low temperature largely downregulated the fatty acid elongation pathway in banana fruit (only five were upregulated out of 23 DEGs, **Figure 8A** and **Supplementary Table 4**). The fatty acid elongation enzymes (FAEs), such as long-chain acyl-CoA synthetases (LACSs), 3-ketoacyl-CoA synthases (KCSs),

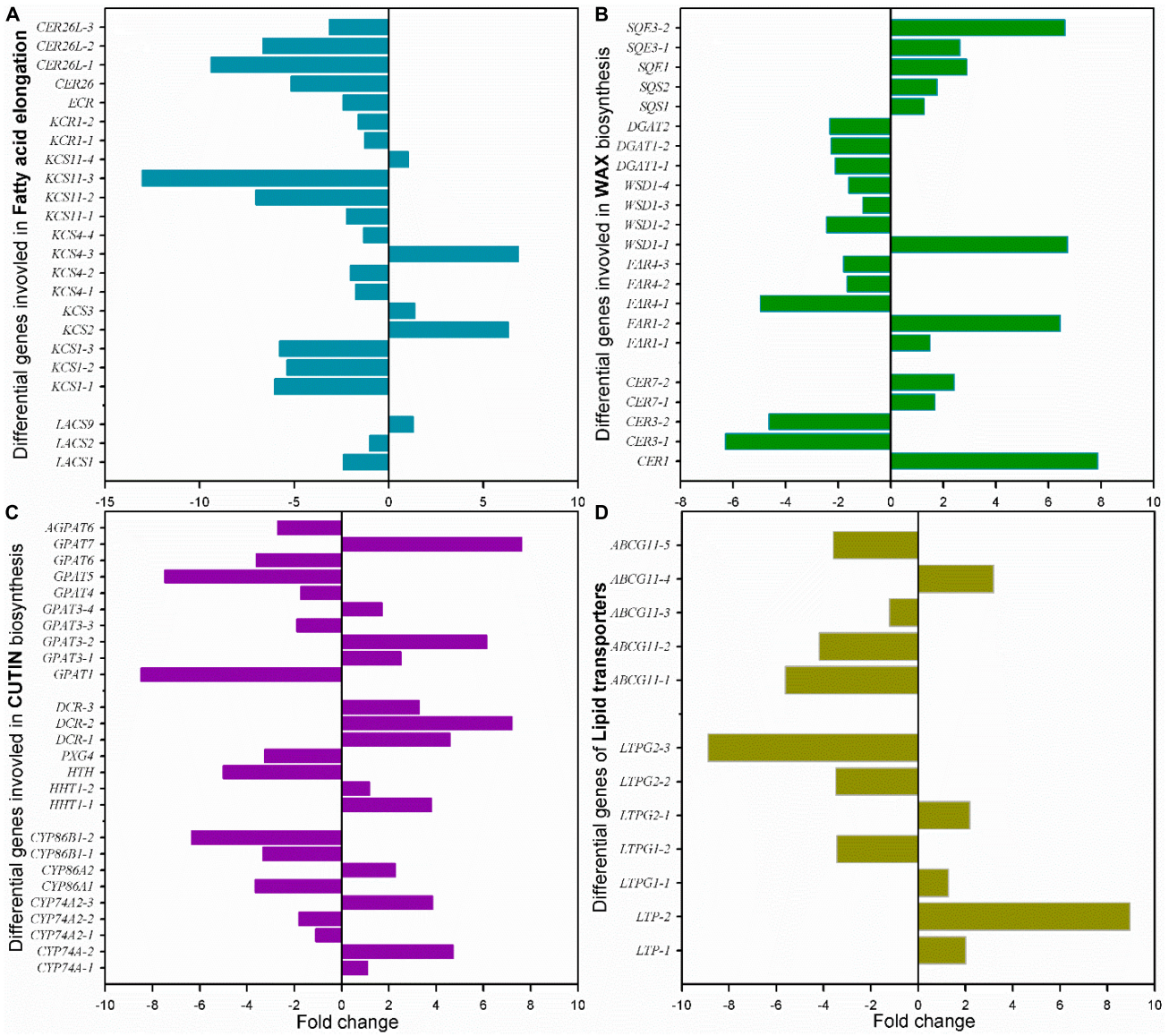

FIGURE 8 | Changes of the main differential genes in cuticle biosynthesis of banana fruit during storage. **(A)** 23 DEGs in fatty acid elongation pathway, **(B)** 22 main DEGs in wax accumulation pathway, **(C)** 26 main DEGs in cutin monomer biosynthesis pathway, and **(D)** 12 DEGs for lipid-transfer proteins involved in cuticle forming were detected.

beta-ketoacyl-CoA reductases (KCRs), (3R)-3-hydroxyacyl-CoA dehydratases (HACDs), and enoyl-CoA reductase (ECR), are limit factors to regulate the elongation of VLC fatty acids (Samuels et al., 2008). In addition, CER26 or CER26L has also been identified to limit the biosynthesis of VLC fatty acids, particularly longer than C_{30} (Pascal et al., 2013). Compared with room temperature storage, most of the FAEs detected in DEGs were downregulated by chilling temperature. The downregulation of FAEs resulted in slowing down the accumulation of VLC fatty acids, particularly the chain length over C_{28}. Accordingly, the accumulation of C_{22} and C_{24} as relatively short carbon chains in the VLC fatty acids in waxes increased in banana under low temperature (**Figures 4**, **5**).

The cuticular waxes are stimulated to accumulate by the environmental stresses, i.e., the drought stress improved the accumulation of VLC *n*-alkanes with C_{29} and C_{31}, or stimulated the increase of VLC alkyl esters in plant leaf or fruit cuticles (Kosma et al., 2009; Patwari et al., 2019; Dimopoulos et al., 2020). In banana fruit, an equal number of five genes were down- and upregulated, respectively, in the *n*-alkane and alcohol forming pathways. It was consistent with the relatively stable coverage of alcohols and *n*-alkanes, which only increased slightly for aldehydes with C_{30} and *n*-alkanes with C_{25} during storage (**Figures 4**, **5**, **8B**). One gene for each step in elongation and wax forming pathways of *MaLACS*, *MaKCS*, *MaKCR*, *MaECR*, *MaCER1*, and *MaFAR* was selected to further perform the

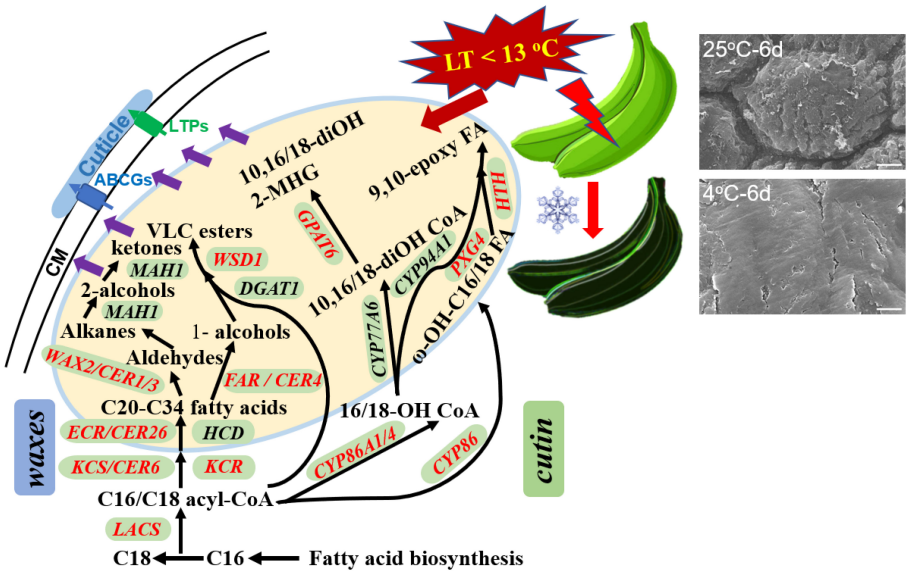

FIGURE 9 | The overall changes in cuticle biosynthesis response to chilling temperature in banana fruit. The structural genes involved in cuticular wax and cutin monomer biosynthesis were differentially regulated (labeled in red) by low temperature in response to the appearance changes during storage.

qPCR analysis. The relative expression level of these genes was stimulated to increase by the low temperature in 4 days, but declined rapidly following the chilling injury (**Supplementary Figure 3**). In addition, changes in cyclic waxes, i.e., triterpenoids have been reported to be related to the postharvest quality of blueberries during storage (Moggia et al., 2016). In banana fruit, the sterols in cuticle of banana fruit increased obviously, whereas a decreasing trend was found for the triterpenoids under low temperature (**Figure 6**). Numerous EDGs were annotated as sterol biosynthesis, but only five candidates as *SQS* and *SQE* members were as the DEGs involved in biosynthesis of triterpenoids (**Figures 6**, **6B** and **Supplementary Table 4**). In contrast to the accumulation of triterpenoids to reinforce the cuticle to adapt to the high-temperature condition in desert plants (Schuster et al., 2016), declined trend of triterpenoids was detected in banana fruit under low temperature. The decrease of triterpenoids might be one of the factors influencing the mechanical support of cuticle, thus inducing the collapsed surface for banana fruit during storage.

The cutin monomers polymerized as matrix is another main part of cuticle besides waxes. Genetic monitoring of the cutin deficiency induced the susceptible infection of microbial in tomato fruit (Isaacson et al., 2009). However, so far, postharvest changes of cutin monomers in fruit have been rarely reported. The cutin monomers of fatty acids without extra groups increased markedly, whereas the monomers with ω-OH mid-chain-OH or epoxy groups exhibited a declined trend under low-temperature storage in cherry fruit (Belge et al., 2014). On the contrary, an increasing trend for fatty acids without added groups or with 2-OH group was detected in banana fruit cuticle under low temperature (**Figure 3**). However, the monomers with ω-OH and mid-chain epoxy group, and abundant monomers as mono-functional fatty acids, exhibited no obvious changes during storage (**Figure 3** and **Supplementary Table 2**). Both the carboxyl and hydroxyl groups in monomers are necessary to form polymers (Philippe et al., 2020). The cutin polymers in banana fruit might be rarely modified since the relatively stable monomers are added with functional groups. In addition, small molecules of phenolics as the aromatic pattern mainly including *p*-coumaric acid and their derivatives, which were common in plant cuticles, were also detected in banana fruit. These small molecules of phenolics are thought to be mainly embedded in the intracuticular layer together with cutin polymers (Fich et al., 2016). It might enhance the mechanical property for the cuticle, while this has been rarely cared and further work should be addressed. As shown in **Figure 8C**, besides the C_{16} and C_{18} fatty acids, the biosynthesis of cutin monomers regulated by *CYP74* and *CYP86* members, *HHT*, *DCR*, and *GPATs* exhibited homeostasis status with an equal number of 13 genes for downregulation and upregulation, respectively (**Figure 8C** and **Supplementary Table 5**). These results were highly consistent with the chemical results, which showed a relatively steady content of cutin monomers in banana cuticle during storage.

In addition, 12 lipid-transfer proteins involved in cutin monomer and wax secretion were also detected to be differentially regulated in banana cuticle under low temperatures (**Figure 8D** and **Supplementary Table 5**). Generally, two LTPs, five LTPG1/2, and five ABCG11 members were detected. LTPs have been widely found in flowering plants and are capable of exchanging lipids between membranes (Yeats and Rose, 2008). LTPGs are glycosylphosphatidylinositol-anchored lipid-transfer proteins, which have been identified as part of the export machinery in secreting cuticular waxes (DeBono et al., 2009; Kim et al., 2012). Under low temperatures, four LTPs and three LTPs were up- or downregulated, respectively, which might result in stable cuticular wax secretion. Accumulation of evidence

indicated that ABCGs [ATP-binding cassette (ABC) subfamily G members] functioned to plant surface protecting against environmental stresses, and most of the reported members are involved in cutin formation (Elejalde-Palmett et al., 2021; Lee et al., 2021). In banana fruit, four of the five differential ABCG11 members were downregulated. The downregulation of ABCG members might slow down the secretion of cutin monomers; thus, the relatively stable cutin monomers, besides C_{16} and C_{18} fatty acids, were detected in banana fruit cuticle.

CONCLUSION

This study in detail reported the changes of appearance morphology, response of chemical compositions, and their biosynthesis regulation genes in banana cuticle under low-temperature storage. Our study demonstrated that the appearance of banana fruit was altered apparently into flat paralleled with changes of cuticular wax and cutin monomers in cuticle stimulated by the chilling injury. Fatty acids of C_{16} and C_{18} as the monomers in cutin, and C_{22} and C_{24} fatty acids and cyclic sterols and triterpenoids in wax mixtures were the most changed cuticular components. To respond the chilling injury, a series of cuticle-related genes, i.e., *MaLACS*, *MaKCS*, *MaKCR*, *MaCER26*, *MaCER1/3*, and *MaFAR* in cuticular wax biosynthesis and *MaCYP86*, *MaCYP86A1/4*, *MaPXG4*, *MaHTH*, and *MaGPAT6* involved in cutin monomer accumulation, were differentially expressed in banana fruit (**Figure 9**). In addition, several lipid-transfer proteins, such as LTPG1/2 and ABCG11 members, were also differentially regulated. To our best knowledge so far, this study provides the initial exploration to link the cuticular response, on the basis of morphology, chemical, and biosynthesis regulation, to chilling stress on postharvest fruit. Further work on how the temperature affects the biosynthesis of cuticle and the potential functions for the response of cuticle to thermal changes and the molecular mechanisms will be comprehensively investigated.

DATA AVAILABILITY STATEMENT

The original contributions presented in the study are included in the article/**Supplementary Material**, further inquiries can be directed to the corresponding author/s.

AUTHOR CONTRIBUTIONS

HH designed and prepared the manuscript, performed most of the experiments, and prepared the draft of the manuscript. LW, DQ, and NZ contributed to part of the experiments and data analyses. FB took part in revising the manuscript and funding acquisition. All authors approved the final version of the manuscript.

FUNDING

This work was supported by the Common Technical Innovation Team of Guangdong Province on Preservation and Logistics of Agricultural Products (2019KJ145), the Guangdong Basic and Applied Basic Research Foundation (2019A1515110611), Funding from the State Key Laboratory for Conservation and Utilization of Subtropical Agro-bioresources (FKLCUSA-b201916), Natural Science Foundation of China (31772289), funding from the Guangxi Key Laboratory of Fruits and Vegetables Storage-Processing Technology (2021-01), the Special Fund for Scientific Innovation Strategy-Construction of High Level Academy of Agriculture Science of Guangdong Academy of Agricultural Sciences (R2019QD-012), and the "Pearl River Talent Plan" Postdoctoral Program of Guangdong Province (2018[2]).

SUPPLEMENTARY MATERIAL

The Supplementary Material for this article can be found online at: https://www.frontiersin.org/articles/10.3389/fpls.2021.792384/full#supplementary-material

REFERENCES

Amnuaysin, N., Seraypheap, K., and Kidyoo, M. (2012). Anatomical Changes in Peel Structure of 'Hom Thong' Banana during Fruit Development and Ripening. *Trop. Nat. Hist.* 12, 127–136.

Belge, B., Llovera, M., Comabella, E., Gatius, F., Guillén, P., Graell, J., et al. (2014). Characterization of Cuticle Composition after Cold Storage of "Celeste" and "Somerset" Sweet Cherry Fruit. *J. Agricult. Food Chem.* 62, 8722–8729. doi: 10.1021/jf502650t

Brian, F. A., and David, W. T. B. (1985). The epicuticular waxes on the organs of different varieties of banana. *Austr. J. Bot.* 33, 393–408. doi: 10.1071/bt9850393

Bueno, A., Alfarhan, A., Arand, K., Burghardt, M., Deininger, A.-C., Hedrich, R., et al. (2019). Temperature effects on the cuticular transpiration barrier of two desert plants with water-spender and water-saver life strategies. *J. Exp. Bot.* 70, 1613–1625. doi: 10.1093/jxb/erz018

Chu, W., Gao, H., Chen, H., Wu, W., and Fang, X. (2018). Changes in cuticular wax composition of two blueberry cultivars during fruit ripening and postharvest cold storage. *J. Agricult. Food Chem.* 66, 2870–2876. doi: 10.1021/acs.jafc.7b05020

DeBono, A., Yeats, T. H., Rose, J. K. C., Bird, D., Jetter, R., Kunst, L., et al. (2009). Arabidopsis LTPG Is a Glycosylphosphatidylinositol-Anchored Lipid Transfer Protein Required for Export of Lipids to the Plant Surface. *Plant Cell* 21, 1230–1238. doi: 10.1105/tpc.108.064451

Dimopoulos, N., Tindjau, R., Wong, D. C., Matzat, T., Haslam, T., Song, C., et al. (2020). Drought stress modulates cuticular wax composition of the grape berry. *J. Exp. Bot.* 71, 3126–3141. doi: 10.1093/jxb/eraa046

Ding, S., Zhang, J., Wang, R., Ou, S., and Shan, Y. (2018). Changes in cuticle compositions and crystal structure of 'Bingtang' sweet orange fruits (*Citrus sinensis*) during storage. *Internat. J. Food Propert.* 21, 2411–2427.

Domínguez, E., Cuartero, J., and Heredia, A. (2011). An overview on plant cuticle biomechanics. *Plant Sci.* 181, 77–84. doi: 10.1016/j.plantsci.2011.04.016

Elejalde-Palmett, C., Martinez San, Segundo, I., Garroum, I., Charrier, L., De Bellis, D., et al. (2021). ABCG transporters export cutin precursors for the formation of the plant cuticle. *Curr. Biol.* 31, 2111.e–2123.e.

Fich, E. A., Segerson, N. A., and Rose, J. K. (2016). The plant polyester cutin: biosynthesis, structure, and biological roles. *Annu. Rev. Plant Biol.* 67, 207–233. doi: 10.1146/annurev-arplant-043015-111929

Hansjakob, A., Bischof, S., Bringmann, G., Riederer, M., and Hildebrandt, U. (2010). Very-long-chain aldehydes promote in vitro prepenetration processes of Blumeria graminis in a dose-and chain length-dependent manner. *New Phytolog.* 188, 1039–1054. doi: 10.1111/j.1469-8137.2010.03419.x

Hashim, N., Janius, R. B., Baranyai, L., Rahman, R. A., Osman, A., and Zude, M. (2012). Kinetic model for colour changes in bananas during the appearance of chilling injury symptoms. *Food Bioproc. Technol.* 5, 2952–2963. doi: 10.1007/s11947-011-0646-z

Heredia, A., Lara, I., and Domínguez, E. (2019). Shelf life potential and the fruit cuticle: the unexpected player. *Front. Sci.* 10:770. doi: 10.3389/fpls.2019.00770

Holloway, P. (1982). "The chemical constitution of plant cutins," in *The Plant Cuticle*, eds D. F. Cutler, K. L. Alvin, and C. E. Price (London: Academic Pres), 45–85.

Huang, H. (2017). *Comparative Investigation of the Chemical Composition and the Water Permeability of Fruit and Leaf Cuticles*. Ph.D. thesis. Würzburg: Opus Bibliothek, Uni-Wuerzburg.

Huang, H., Guo, L., Wang, L., Wang, H., Ma, S., Jiang, Y., et al. (2019). 1-Methylcyclopropene (1-MCP) slows ripening of kiwifruit and affects energy status, membrane fatty acid contents and cell membrane integrity. *Postharv. Biol. Technol.* 156:110941. doi: 10.1016/j.postharvbio.2019.110941

Huang, H., Jian, Q., Jiang, Y., Duan, X., and Qu, H. (2016). Enhanced chilling tolerance of banana fruit treated with malic acid prior to low-temperature storage. *Postharv. Biol. Technol.* 111, 209–213. doi: 10.1016/j.postharvbio.2015.09.008

Huang, H., and Jiang, Y. (2019). Chemical composition of the cuticle membrane of pitaya fruits (*Hylocereus Polyrhizus*). *Agriculture-Basel* 2019:9.

Huang, H., Jing, G., Guo, L., Zhang, D., Yang, B., Duan, X., et al. (2013). Effect of oxalic acid on ripening attributes of banana fruit during storage. *Postharv. Biol. Technol.* 84, 22–27. doi: 10.1016/j.postharvbio.2013.04.002

Isaacson, T., Kosma, D. K., Matas, A. J., Buda, G. J., He, Y., Yu, B., et al. (2009). Cutin deficiency in the tomato fruit cuticle consistently affects resistance to microbial infection and biomechanical properties, but not transpirational water loss. *Plant J.* 60, 363–377. doi: 10.1111/j.1365-313X.2009.03969.x

Jetter, R., Kunst, L., and Samuels, A. L. (2008). Composition of plant cuticular waxes. *Biol. Plant Cut.* 23, 145–181. doi: 10.1002/9781119312994.apr0232

Kim, H., Lee, S. B., Kim, H. J., Min, M. K., Hwang, I., and Suh, M. C. (2012). Characterization of Glycosylphosphatidylinositol-Anchored Lipid Transfer Protein 2 (LTPG2) and Overlapping Function between LTPG/LTPG1 and LTPG2 in Cuticular Wax Export or Accumulation in Arabidopsis thaliana. *Plant Cell Physiol.* 53, 1391–1403.

Kosma, D. K., Bourdenx, B., Bernard, A., Parsons, E. P., Lue, S., Joubes, J., et al. (2009). The Impact of Water Deficiency on Leaf Cuticle Lipids of Arabidopsis. *Plant Physiol.* 151, 1918–1929. doi: 10.1104/pp.109.141911

Lee, E.-J., Kim, K. Y., Zhang, J., Yamaoka, Y., Gao, P., Kim, H., et al. (2021). Arabidopsis seedling establishment under waterlogging requires ABCG5-mediated formation of a dense cuticle layer. *New Phytolog.* 229, 156–172. doi: 10.1111/nph.16816

Lewandowska, M., Keyl, A., and Feussner, I. (2020). Wax biosynthesis in response to danger: its regulation upon abiotic and biotic stress. *New Phytolog.* 227, 698–713. doi: 10.1111/nph.16571

Liang, S.-M., Kuang, J.-F., Ji, S.-J., Chen, Q.-F., Deng, W., Min, T., et al. (2020). The membrane lipid metabolism in horticultural products suffering chilling injury. *Food Qual. Saf.* 4, 9–14.

Liu, J., Li, F., Li, T., Yun, Z., Duan, X., and Jiang, Y. (2019). Fibroin treatment inhibits chilling injury of banana fruit via energy regulation. *Sci. Horticult.* 248, 8–13.

Liu, J., Li, Q., Chen, J., and Jiang, Y. (2020). Revealing Further Insights on Chilling Injury of Postharvest Bananas by Untargeted Lipidomics. *Foods* 9:894. doi: 10.3390/foods9070894

Merk, S., Blume, A., and Riederer, M. (1997). Phase behaviour and crystallinity of plant cuticular waxes studied by Fourier transform infrared spectroscopy. *Planta* 204, 44–53. doi: 10.1007/s004250050228

Moggia, C., Graell, J., Lara, I., Schmeda-Hirschmann, G., Thomas-Valdés, S., and Lobos, G. A. (2016). Fruit characteristics and cuticle triterpenes as related to postharvest quality of highbush blueberries. *Sci. Horticult.* 211, 449–457.

Pascal, S., Bernard, A., Sorel, M., Pervent, M., Vile, D., Haslam, R. P., et al. (2013). The Arabidopsis cer26 mutant, like the cer2 mutant, is specifically affected in the very long chain fatty acid elongation process. *Plant J.* 73, 733–746. doi: 10.1111/tpj.12060

Patwari, P., Salewski, V., Gutbrod, K., Kreszies, T., Peisker, H., Steiner, U., et al. (2019). Surface wax esters contribute to drought tolerance in Arabidopsis. *Plant J.* 98, 727–744. doi: 10.1111/tpj.14269

Petit, J., Bres, C., Just, D., Garcia, V., Mauxion, J. P., Marion, D., et al. (2014). Analyses of tomato fruit brightness mutants uncover both cutin-deficient and cutin-abundant mutants and a new hypomorphic allele of GDSL lipase. *Plant Physiol.* 164, 888–906. doi: 10.1104/pp.113.232645

Philippe, G., Sørensen, I., Jiao, C., Sun, X., Fei, Z., Domozych, D. S., et al. (2020). Cutin and suberin: assembly and origins of specialized lipidic cell wall scaffolds. *Curr. Opin. Plant Biol.* 55, 11–20. doi: 10.1016/j.pbi.2020.01.008

Riederer, M. (2006). Thermodynamics of the water permeability of plant cuticles: characterization of the polar pathway. *J. Exp. Bot.* 57, 2937–2942. doi: 10.1093/jxb/erl053

Sampangi-Ramaiah, M. H., Ravishankar, K. V., Seetharamaiah, S. K., Roy, T. K., Hunashikatti, L. R., Rekha, A., et al. (2016). Barrier against water loss: relationship between epicuticular wax composition, gene expression and leaf water retention capacity in banana. *Funct. Plant Biol.* 43, 492–501. doi: 10.1071/FP15296

Samuels, L., Kunst, L., and Jetter, R. (2008). Sealing Plant Surfaces: Cuticular Wax Formation by Epidermal Cells. *Ann. Rev. Plant Biol.* 59, 683–707. doi: 10.1146/annurev.arplant.59.103006.093219

Schuster, A.-C., Burghardt, M., Alfarhan, A., Bueno, A., Hedrich, R., Leide, J., et al. (2016). Effectiveness of cuticular transpiration barriers in a desert plant at controlling water loss at high temperatures. *Aob Plants* 2016:8. doi: 10.1093/aobpla/plw027

Sidhu, J. S., and Zafar, T. A. (2018). Bioactive compounds in banana fruits and their health benefits. *Food Quality Saf.* 2, 183–188. doi: 10.1093/fqsafe/fyy019

Wang, H., Zhang, Z., Xu, L., Huang, X., and Pang, X. (2012). The effect of delay between heat treatment and cold storage on alleviation of chilling injury in banana fruit. *J. Sci. Food Agricult.* 92, 2624–2629. doi: 10.1002/jsfa.5676

Ward, G., and Nussinovitch, A. (1996). Peel gloss as a potential indicator of banana ripeness. *Lebensm. Wissenschaft Technol.* 29, 289–294.

Yang, X., Pang, X., Xu, L., Fang, R., Huang, X., Guan, P., et al. (2009). Accumulation of soluble sugars in peel at high temperature leads to stay-green ripe banana fruit. *J. Exp. Bot.* 60, 4051–4062. doi: 10.1093/jxb/erp238

Yang, Y., Ren, X., Gong, H., Huang, H., Sun, S., Wang, P., et al. (2021). Skin greasiness in apple is caused by accumulations of liquid waxes: evidence from chemical and thermodynamic analyses. *LWT Food Sci. Technol.* 2021:111639.

Yeats, T. H., and Rose, J. K. (2013). The formation and function of plant cuticles. *Plant Physiol.* 2013:222737.

Yeats, T. H., and Rose, J. K. C. (2008). The biochemistry and biology of extracellular plant lipid-transfer proteins (LTPs). *Protein Sci.* 17, 191–198. doi: 10.1110/ps.073300108

Zheng, G., Tian, B., Zhang, F., Tao, F., and Li, W. (2011). Plant adaptation to frequent alterations between high and low temperatures: remodelling of membrane lipids and maintenance of unsaturation levels. *Plant, Cell Env.* 34, 1431–1442. doi: 10.1111/j.1365-3040.2011.02341.x

Conflict of Interest: The authors declare that the research was conducted in the absence of any commercial or financial relationships that could be construed as a potential conflict of interest.

Publisher's Note: All claims expressed in this article are solely those of the authors and do not necessarily represent those of their affiliated organizations, or those of the publisher, the editors and the reviewers. Any product that may be evaluated in this article, or claim that may be made by its manufacturer, is not guaranteed or endorsed by the publisher.

frontiers in Plant Science

ORIGINAL RESEARCH
published: 09 March 2022
doi: 10.3389/fpls.2022.771094

Antioxidant and Fatty Acid Changes in Pomegranate Peel With Induced Chilling Injury and Browning by Ethylene During Long Storage Times

Mónika Valdenegro[1], Lida Fuentes[2], Maricarmen Bernales[1], Camila Huidobro[3], Liliam Monsalve[2], Ignacia Hernández[1], Maximiliano Schelle[2] and Ricardo Simpson[2,4]*

[1] Escuela de Agronomía, Pontificia Universidad Católica de Valparaíso, Quillota, Chile, [2] Centro Regional de Estudios en Alimentos Saludables (CREAS), CONICYT-Regional GORE Valparaíso Proyecto R17A10001, Valparaíso, Chile, [3] Instituto de Química, Bioquímica, Pontificia Universidad Católica de Valparaíso, Valparaíso, Chile, [4] Departamento de Ingeniería Química y Ambiental, Universidad Técnica Federico Santa María, Valparaíso, Chile

OPEN ACCESS

Edited by:
Natalia Marina Villarreal, CONICET Instituto Tecnológico de Chascomús (INTECH), Argentina

Reviewed by:
Fakhreddin Salehi, Bu-Ali Sina University, Iran
Misael Vega Garcia, Universidad Autónoma de Sinaloa, Mexico

***Correspondence:**
Mónika Valdenegro
monika.valdenegro@pucv.cl

Specialty section:
This article was submitted to Plant Abiotic Stress, a section of the journal Frontiers in Plant Science

Received: *05 September 2021*
Accepted: *17 January 2022*
Published: *09 March 2022*

Citation:
Valdenegro M, Fuentes L, Bernales M, Huidobro C, Monsalve L, Hernández I, Schelle M and Simpson R (2022) Antioxidant and Fatty Acid Changes in Pomegranate Peel With Induced Chilling Injury and Browning by Ethylene During Long Storage Times. Front. Plant Sci. 13:771094. doi: 10.3389/fpls.2022.771094

Pomegranate (*Punica granatum*) is a non-climacteric fruit with a high antioxidant content in arils and peels, of which 92% are anthocyanins and tannins. However, it is susceptible to chilling injury (CI), a physiological disorder concentrated in the peel, which can affect the organoleptic quality of the fruit. To understand the effects of modified atmosphere and ethylene in responses to stress on the antioxidant quality of the fruit and composition of fatty acids in the peel under CI conditions, the exogenous ethylene treatments (0.5, 1.0, and 1.5 $\mu g\ L^{-1}$), 1-methylcyclopropene (1-MCP; 1 $\mu l\ L^{-1}$), modified atmosphere packaging (MAP: XTend^{TM} bags), combined strategy MAP/1-MCP, and package in macroperforated bags (MPB-control treatment) were evaluated. The assay was performed in cold conditions (2 ± 1°C; 85% RH) to stimulate damage and was sampled for 120 days (+3 days at 20°C). During cold storage, CI symptoms began at 20 days in MPB and at 60 days for all treatments with exogenous ethylene; CI symptoms were delayed up to 120 days in MAP, 1-MCP, and the combined MAP/1-MCP treatment. Damage was concentrated in the peel. Ethylene and MPB-control treatments induced significant electrolyte leakage, lipid peroxidation, and oxidative damage. In contrast, MAP alone or in combination with 1-MCP successfully delayed CI symptoms. However, no significant differences were observed between treatments in fatty acid content, e.g., in the peel, oleic acid, linoleic acid, palmitic acid, but a significant loss was noted after 60 days of storage. Cold storage caused an increase in anthocyanin concentration in the peel and arils, increasing up to 12 times in the peel of the fruit treated with ethylene at the final stage of storage (120 days + 3 days at 20°C), with non-significant differences in the tannin content in the peel. During long-term cold storage of pomegranate, MAP and 1-MCP treatments delay and reduce the appearance of CI symptoms. This long cold storage induces an important decrease in the unsaturated/saturated fatty acid ratio, which is not reversed by any postharvest treatment. A higher unsaturated/saturated

fatty acid ratio after 1-MCP treatments showed a protective effect in peel tissues. In addition, it was possible to increase the concentration of anthocyanins in the peel of cold-storage pomegranates treated with ethylene.

Keywords: chilling injury, postharvest pomegranate, cold storage, total polyphenols, anthocyanins, fatty acids

INTRODUCTION

Pomegranate (*Punica granatum*) is a non-climacteric fruit (Kader, 2003) belonging to the family *Punicaceae* (Selcuk and Erkan, 2015) that grows in tropical and subtropical regions. Pomegranate fruit has bioactive molecules such as polyphenols, tannins, anthocyanins, principally ellagitannins, and phenolic acids, which give it health properties (Pirzadeh et al., 2020). However, the short harvest period and long travel times induce significant quality loss, which reduces the storability and affects the consumer acceptance of these fruits (Fawole and Opara, 2013; Matityahu et al., 2013; Pareek et al., 2015; Selcuk and Erkan, 2015). Therefore, within the changes associated with the loss of quality, one can observe shriveling, decay, weight loss, development of superficial scald, chilling injury (CI), and a decrease in flavor acceptability (Gamrasni et al., 2015; Li et al., 2016).

One of the most critical problems during storage is CI, a complex physiological disorder that affects the appearance and organoleptic attributes of the fruit (Sala, 1998). This physiological disorder is mainly observed in fruits and vegetables when storage is below the threshold temperatures for too long a time, resulting in metabolic dysfunction and finally noticeable chilling symptoms (Farneti et al., 2015). In pomegranate, the CI has several undesirable effects on the quality that can be more visible, such as surface pitting, brown discoloration of the peel, husk scald, reduced color and hardness, and susceptibility to fungal development. Additionally, these changes can include internal damage or more subtle changes, such as aroma degradation, arils of pale color, and white separating segments of the arils with brown discoloration from exposure at temperatures below 5°C during 2 months (Artés et al., 2000; Fawole and Opara, 2013).

One of the principal characteristics of CI is the change in the structure and composition of the membrane, with the consequent loss of permeability regulation and metabolic disorders (Sala, 1998; Ben-Amor et al., 1999; Li et al., 2016). It has been suggested that a higher ratio of unsaturated and saturated fatty acids (SFAs) provides major tolerance to cold damage by chilling temperature in fruits such as banana, loquat, mango, and peach, preventing ion leakage, membrane peroxidation, and final tissue damage (Promyou et al., 2008; Jin et al., 2014; Li et al., 2014).

The browning of peel pomegranate is an essential problem at these cold temperatures and can be associated with the accumulation of brown polymeric pigments by enzymatic activity. It has been suggested that tannins are the basic substance of pomegranate peel browning (Zhang et al., 2008). Furthermore, the browning index of the peel has been positively correlated with polyphenol oxidase (PPO), the enzyme responsible for phenolic compound oxidation into quinone compounds, and negatively correlated with catalase (CAT) activity (Zhang et al., 2008). Therefore, an oxidative stress phenomenon associated with decreases in the enzymatic reactive oxygen-scavenging mechanism, i.e., CAT, peroxidase (POX), and superoxide dismutase (SOD) activity has been suggested during cold storage of pomegranate (Pech et al., 2008).

In recent years, the effect of different treatments on reducing CI during cold storage of pomegranate has been studied. Methyl jasmonate and acetylsalicylic acid reduce CI symptoms by decreasing respiration, softening, and ion leakage (Sayyari et al., 2011, 2017; Chen et al., 2021). Furthermore, oxalic acid's reduction in CI symptoms is related to lower losses of total phenolics and increased ascorbic acid content in arils (Sayyari et al., 2011). However, salicyloyl chitosan treatment has been associated with alleviating CI by maintaining membrane integrity resulting from a higher unSFA/SFA ratio and enhancing antioxidant capacity by total phenols, anthocyanins, and ascorbic acid accumulation (Sayyari et al., 2016). The postharvest strategies related to reducing ethylene production and the respiratory rate of the pomegranate can have a positive impact on the quality and consumer acceptance of pomegranate after long cold storage. For example, a modified atmosphere is an effective strategy in reducing CI during the storage of mango fruits at 12°C (Pesis et al., 2000), and treatment with ethylene inhibitor 1-methylcyclopropene (1-MCP) improves the postharvest storage of pomegranate (Defilippi et al., 2006; Gamrasni et al., 2015; Li et al., 2016). Previously, it was reported that endogenous ethylene biosynthesis induced by ethrel application accelerated the appearance of CI symptoms, in contrast to observations made for modified atmosphere and 1-MCP treatments during the long-term cold storage of pomegranate (Valdenegro et al., 2018). Additionally, ethrel at 1 or 1.5 $\mu g\ L^{-1}$ accelerates endogenous ethylene production at 20 days relative to cold-induced ethylene production at 160 days (Valdenegro et al., 2018). However, the mechanisms by which ethylene increases or accelerates CI in pomegranate are unknown. Therefore, this study aimed to evaluate the relationship among antioxidant response, fatty acid composition, and CI under ethrel and 1-MCP applications during cold storage at 2°C of the pomegranate fruit.

MATERIALS AND METHODS

Plant Material

The pomegranate (*Punica granatum*) cv. Wonderful fruits were collected from 6-year-old trees from an orchard in Curacaví (–33.318S, –71.123W, 224 m.a.s.l.), Chile. The drip irrigation system and pomegranate tree culture were made at approximately 5,388 $m^3\ ha^{-1}\ year^{-1}$ (Holland et al., 2009; Franck et al., 2015), and the fertilization used was 350, 165, and

TABLE 1 | Treatment tested for the study of chilling injury in pomegranate fruit.

Treatment	Details
Macroperforated bags control (MPB-control)	No treatment, stored in air
Passive modified atmosphere (MAP)	Commercial bag MAP XTend™ film (StePac, São Paulo, Brazil), stored in the air
1-MCP	1-MCP (SmartFresh™), 1 μg L^{-1}, stored in air
Combined MAP/1-MCP	Combinated MAP/1-MCP, stored in air
E1	0.5 μg L^{-1} Ethrel™, dipping 3 min, stored in air
E2	Ethrel™ (1.0 μg L^{-1}), dipping 3 min, stored in air
E3	Ethrel™ (1.5 μg L^{-1}), dipping 3 min, stored in air

85 kg ha^{-1} $year^{-1}$ for potassium, nitrogen, and phosphorus, respectively (Franck et al., 2015).

The fruits were harvested and selected on the basis of maturity, considering size, weight, color, and other quality parameters according to Valdenegro et al. (2018), before experimental treatments.

Experimental Strategy

The pomegranates were randomly divided into eight groups of 180 fruits as described in Valdenegro et al. (2018). The experimental unit was formed by ten fruits, selected by sanity and size, in the mature stage (16°Brix). The treatments were performed as follows (details in **Table 1**): The first group consisted of packing in macroperforated bags (MPB-control) like control groups without treatment or modification of atmosphere around the fruit, according to previous studies of the modified atmosphere (Hussein et al., 2015). In the second group, ten fruits per bag were packed in commercial conditions under a passive modified atmosphere (MAP: commercial bag MAP XTend™ film (StePac, São Paulo, Brazil), according to details described in Valdenegro et al. (2018). Bag-sealed films were dimensioned as follows: 80 × 56 cm^2 with a 0.002% perforated area, according to previous studies (Porat et al., 2009). The third group was treated with 1-MCP (SmartFresh™) according to the specifications of the manufacturer (1 μg L^{-1}) and Valdenegro et al. (2018). The fourth group was subjected to combined treatment with MAP and 1-MCP. Finally, the three treatments at different levels of increasing exogenous application of analogous ethylene (E), E1, E2, and E3, were performed by dipping the fruit in 0.5, 1, or 1.5 μg L^{-1} Ethrel™ solution for 3 min followed by drying (Valdenegro et al., 2012). After all these treatments, the fruits were stored at 2 ± 1°C to stimulate chilling symptoms and sampled at 0, 20, 60, and 120 days, followed by storage for 3 days at 20°C to simulate shelf life conditions. Each sample unit was composed of ten fruits per treatment and the sampling date was evaluated in triplicate. The quality parameters (color, acidity, and total soluble solids) and physiological parameters were evaluated as described by Valdenegro et al. (2018). After fruit quality assessments, the peel and arils were separated for further analysis. The fruit peel was cut into small pieces, and both tissues were frozen under liquid nitrogen and stored at −80°C until fatty acid profile and antioxidant and non-antioxidant enzymatic systems evaluation.

Determination of Chilling Injury Indicators

The visual estimation of CI was determined in peel and aril tissues by rating the extent of surface pitting and browning using a grading scale ranging from non-symptomatic (0) to 4 (severe symptoms 100%) according to Sayyari et al. (2009) as described by Valdenegro et al. (2018). Additionally, the symptom severity was evaluated according to the percent (0–100%) of damage in the fruit surfaces.

Determination of Membrane Damage: Peel Electrolyte Leakage and Lipid Peroxidation by Malondialdehyde Determination

The cell membrane damage in pomegranate peels was measured as the percentage of electrolyte leakage according to Ben-Amor et al. (1999) and modified by Valdenegro et al. (2018). Briefly, ten disks of 1 cm in diameter were cut from different areas of the peel of each sample. The samples were incubated in 40 ml of 0.4 mol L^{-1} mannitol for 2 h at 25°C. Then, the samples were frozen for 12 h, autoclaved at 120°C for 35 min, and finally cooled at ambient temperature (20°C). The percentage of electrolyte leakage was calculated as the ratio of initial to total conductivity of the samples.

The level of lipid peroxidation in cell membranes was measured using 2-thiobarbituric acid-reactive substances, mainly malondialdehyde (MDA), following the method of Vendruscolo et al. (2007), with the modification described in Valdenegro et al. (2018). Ten grams of peel sample was ground in liquid nitrogen and extracted in 40 ml of 10% trichloroacetic acid. A 2-ml aliquot of the supernatant obtained by centrifugation at 8,000 × *g* for 10 min was mixed with 2 ml of 10% trichloroacetic acid containing 0.6% thiobarbituric acid. The mixture was heated at 95°C for 30 min and then quickly cooled in an ice bath. After the tube was centrifuged at 8,000 × *g* for 10 min, the absorbance at 532 nm was read. The MDA concentration was calculated using its molar extinction coefficient (155 mM cm^{-1}). The results are expressed as μmol of MDA per g of fresh weight (FW).

Determination of Fatty Acid Methyl Ester Methods

The pomegranate oil was extracted according to Hernández et al. (2017). The fatty acids in the pomegranate peel oil were determined using the method described by Chirinos et al. (2013), with modifications. The pomegranate fatty acid methyl esters (FAMEs) were analyzed using external standards in an Agilent 7890B gas chromatograph equipped with a flame ionization detector (GC-FID) with a phenylalanine ammonia-lyase (PAL)3 autosampler (Agilent Technologies, Santa Clara, CA, United States) and an SPTM-2560 fused silica capillary (100 m × 0.25 mm × 0.2 μm) column (Sigma Chemical Co., St. Louis, MO, United States). One microliter was injected in split

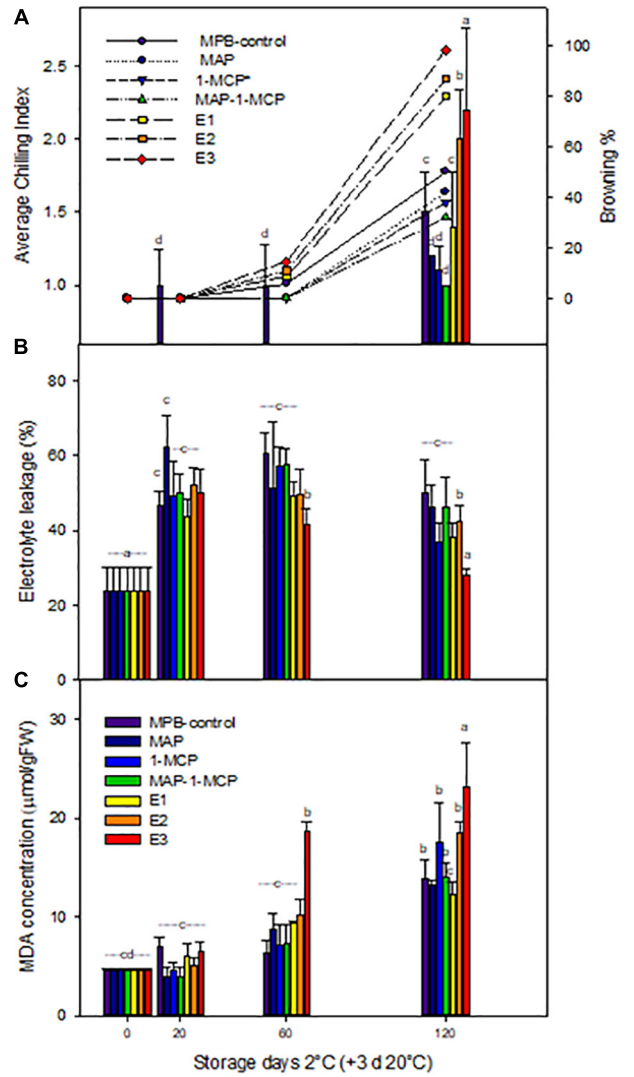

FIGURE 1 | Chilling injury on 'Wonderful' pomegranate fruits. Pomegranates were stored at 2°C for up to 120 days and rewarmed for an additional 3 days at 20°C. Average chilling index and browning percent **(A)** and effects on electrolyte leakage percent **(B)** and lipid peroxidation (MDA concentration, mmol/gFW^{-1}) **(C)** on the peel. The fruit was stored in macroperforated bags like control treatment (MPB-control), under a modified atmosphere (MAP), treated with ethylene inhibitor (1-MCP), (1 μg L^{-1}), under combined treatment (MAP/1-MCP), and treated with increasing exogenous ethylene application (E1, E2, and E3; 0.5–1.5 μg L^{-1}). Samples were taken at 0, 20, 60, and 120 days. In addition, a group maintained at room temperature (20°C) was used as a control (C). The results of chemical analysis are presented as the mean values ± SE considering five independent extractions and five technical replicates. Values followed by a different lowercase case letter are significantly different ($p < 0.05$).

mode (1:50) at 220°C. The oven temperature was programmed to start at 80°C, increase to 175°C at 25°C min^{-1}, hold at 175°C for 25 min, increase to 205°C at 10°C min^{-1}, hold at 205°C for 4 min, increase to 225°C at 10°C min^{-1}, hold at 225°C for 20 min, and finally, decrease to 80°C at 20°C min^{-1}. The detector temperature was set at 225°C. Helium (Indura, Santiago, Chile) was used as a carrier gas at a constant flow of 1.6 ml min^{-1}. The results were expressed as mg of fatty acid per g of pomegranate dried weight (DW).

Browning in Peel and Aril Tissues: Phenylalanine Ammonia-Lyase (EC 4.3.1.24) and Polyphenol Oxidase (EC 1.10.3.2) Activity Determination

The *phenylalanine ammonia-lyase activity* was measured on the basis of the conversion of L-phenylalanine to *trans*-cinnamic acid, according to the method described by Peltonen and Karjalainen (1995). Briefly, 50 mg of polyvinylpyrrolidone (PVP) and 4 ml of 0.1 M Tris–HCl buffer (pH 8.9) including 10 mM β-mercaptoethanol were added to 500 mg of ground pomegranate tissue, peel, and arils. The extracts were centrifuged at 10,000 × *g* for 20 min at 4°C. Five hundred microliters of tissue extract, 1,000 μl of 80 mM borate buffer (pH 8.9), and 30 mM phenylalanine were mixed and incubated for 1 h in a water bath at 30°C, and then 1.5 ml of 2 M HCl was added. Finally, the concentration of trans-cinnamic acid was determined at 290 nm, and the PAL activity was expressed as nmol of cinnamic acid/min mg of protein.

The *polyphenol oxidase activity* was evaluated by UV/Vis spectrophotometry using Agilent 845X equipment (Santiago, Chile) according to the methodology set forth by Espin et al. (1995). For this, the crude extract was prepared, homogenizing 50 g of pomegranate peel with 100 ml of 0.2 M sodium phosphate buffer at pH = 7 in an ultra-Turrax T-18 (IKA, Scaufen, Germany). The homogenate was centrifuged at 18,000 × *g* at 4°C for 30 min in a Solvall RC-5B centrifuge (Germany), and the supernatant was separated with a Whatman #1 filter (Whatman, Great Britain). The enzyme extract was kept frozen at −80°C until analysis. The PPO activity is expressed as delta activity/min/mg of protein.

Enzymatic Antioxidant Activity in Peel Tissue: Catalase (EC.1.11.1.6), Guaiacol Peroxidase (EC.1.11.1.7), and Superoxide Dismutase (EC.1.15.1.1)

The *catalase* (EC.1.11.1.6) activity was determined according to Aebi (1984). Then, 1.5 ml of 100 mM sodium phosphate buffer (pH 7.0) containing 2% polyvinyl pyrrolidone (PVPP) and 1.4 mM of ethylenediaminetetraacetic acid (EDTA) was added to 350 mg of ground peel. After centrifugation at 20,000 *g* for 15 min at 4°C, the supernatant was used for the enzymatic assay. The reaction mixture contained 30 mM H_2O_2 in 50 mM phosphate buffer (pH 7.0) and 100 μl peel extract in a total volume of 1 ml. The CAT activity was estimated by a decrease in absorbance of H_2O_2 at 240 nm and was expressed as units/mg protein.

The *guaiacol peroxidase activity* (EC.1.11.1.7) was determined as the oxidation of guaiacol by the rate of tetraguaiacol formation at 470 nm (ε = 26,600 mM^{-1} cm^{-1}) (Rao et al., 1998). The assay mixture (195 μl) contained 16 mM guaiacol, 16.2 μl 88 mM H_2O_2, 60 μl 500 mM potassium phosphate buffer (pH 7.0), and 2.5 μl 10 mM EDTA (pH 7.0). The reaction was initiated by

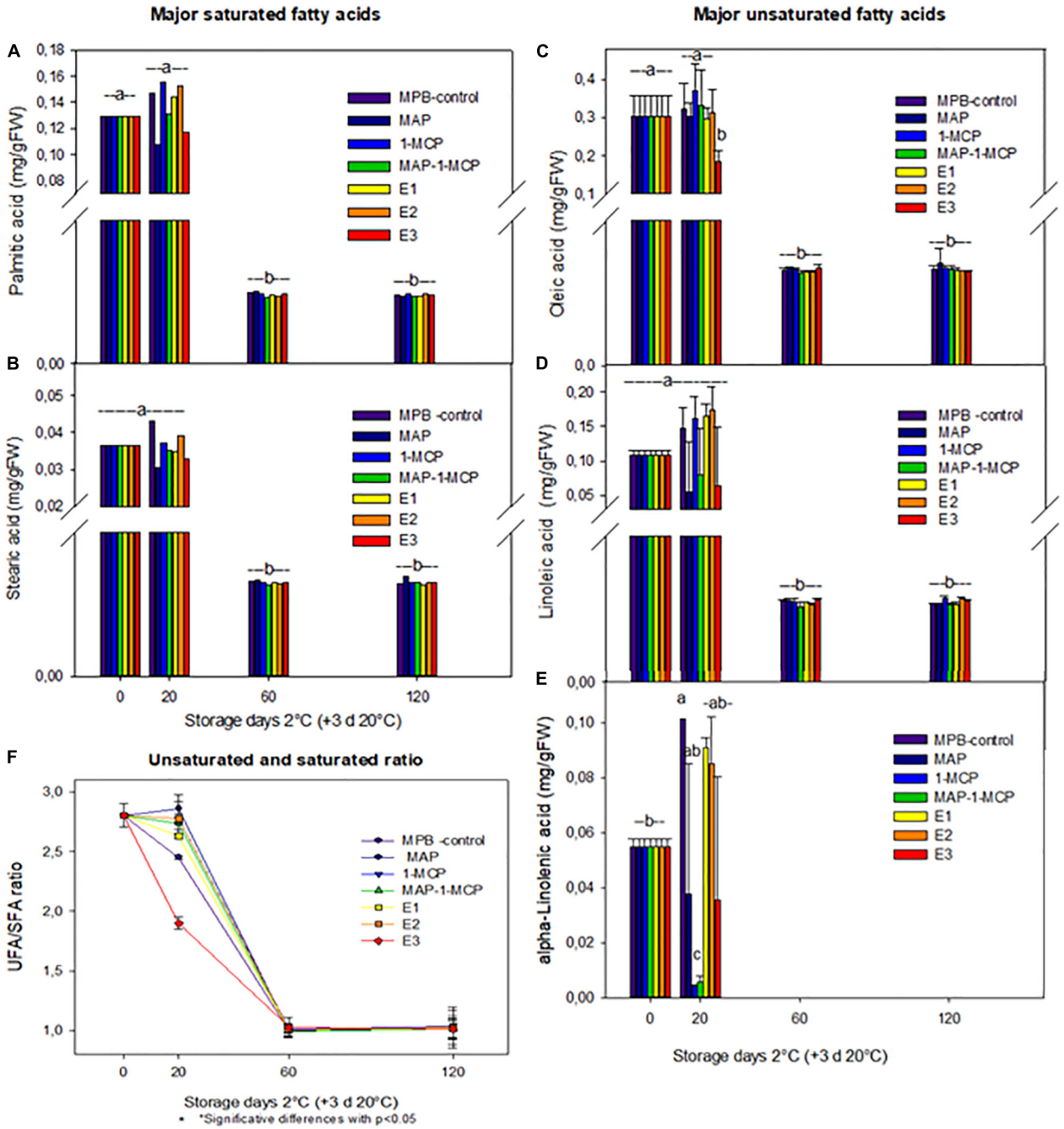

FIGURE 2 | Fatty acids in the peel of 'Wonderful' pomegranate during cold storage. Effects of low-temperature storage at 2°C and rewarmed for an additional 3 days at 20°C on the content of principal fatty acids (mg/g FW): palmitic acid **(A)**, stearic acid **(B)**, oleic acid **(C)**, linoleic acid **(D)**, and alpha-linolenic acid **(E)** in the peel. Unsaturated and saturated ratio **(F)**. The fruit was stored in macroperforated bags like MPB-control, under a MAP, treated with 1-MCP, under combined treatment (PMA/1-MCP) and treated with increasing exogenous ethylene applications (E1, E2, and E3). Samples were taken at 0, 20, 60, and 120 days. The results of chemical analysis are presented as the mean values ± SE considering five independent extractions and five technical replicates. Values followed by a different lowercase case letter are significantly different ($p < 0.05$).

adding 105 μl of peel protein extract. The results were expressed as Unit/mg protein.

The *superoxide dismutase activity* (EC.1.15.1.1) was determined through a spectrophotometric assay based on the reduction of highly water-soluble tetrazolium salts by xanthine-xanthine oxidase (Ukeda et al., 1999). The results were expressed as Unit/mg protein. The protein content was measured for all enzymatic activities according to Bradford (1976).

Non-enzymatic Antioxidant Activity: Trolox Equivalent Antioxidant Capacity and (1,1-diphenyl-2-picrylhydrazyl) free radical (DPPH)

The antioxidant activity by (1,1-diphenyl-2-picrylhydrazyl) free radical (DPPH) assay (Brand-Williams et al., 1995) was determined using Trolox as the standard. Briefly, 100 μl of methanol extract dilution of peel was mixed with 3.9 ml of 103.5 μM solution of DPPH radical in methanol and incubated at room temperature for 60 min in the dark. The reduction of the DPPH radical was measured at 517 nm in a UV/Vis spectrophotometer (model Lambda 25, Perkin Elmer). The standard curve was generated with 0.1–0.7 mM 6-hydroxy-2,5,7,8-tetramethylchroman-2-carboxylic acid (Trolox, #238813, Sigma Chemicals) in methanol. The results are expressed as% inhibition and IC_{50} (μ g/ml).

The Trolox equivalent antioxidant capacity (TEAC) assay (van den Berg et al., 1999) was performed with modifications (Valdenegro et al., 2012) using Trolox as the standard. The methanol extract from peel was diluted in phosphate-buffered saline (PBS) solution (pH 7.4), and 40 μl was mixed with 1.96 ml of the radical solution. The decrease in the optical density (OD) at 734 nm in a UV/Vis spectrophotometer (model Lambda 25, Perkin Elmer) was recorded for 6 min. The results were expressed as mg Trolox equivalents (TE)/g FW.

Polyphenol, Anthocyanin, and Hydrolyzable Tannin Contents

The total polyphenols were determined according to Folin-Ciocalteu's method. Forty milliliters of methanol/HCl (99:1 v/v) was added to 9 g frozen tissue (peel or arils). Each sample was homogenized for 10 min using an ultra-Turrax T-18 (IKA, Scaufen, Germany) and centrifuged for 20 min at 16,000 × *g*. The supernatant solution was filtered using 0.22 μm cellulose filters. The extraction procedure was repeated two times for each sample. The spectrophotometric measurements were carried out using a UV/Vis spectrophotometer (model Lambda 25, Perkin Elmer). The sample extract (5 ml) was introduced in a 20 ml volumetric flask; 5 ml of Folin Ciocalteu's reagent and 10 ml of saturated sodium carbonate solution (75 g/L) were added and mixed. The solution was brought to 100 ml with water. After incubation at room temperature for 2 h, the absorption at 750 nm was measured. The results were expressed as mg of gallic acid per 100 g of fresh tissue.

The hydrolyzable tannins were determined by the method of Bossu et al. (2006) with slight modifications. Ground aril or peel tissue (0.25 g) was extracted with 50 ml of methanol (80%) with agitation at room temperature for 6 h. After centrifugation (10 min, 2,000 rpm), the fruit extract was diluted three times with water; then, 1 ml of the diluted sample was added to 5 ml of KIO_3 aqueous solution (2.5% w/v) tempered at 30°C, and the absorbance was measured at 550 nm. The standard curve was obtained using tannic acid solution (5,000 mg/L). The results were expressed as mg tannic acid equivalent (TAE) per g of dry weight (DW).

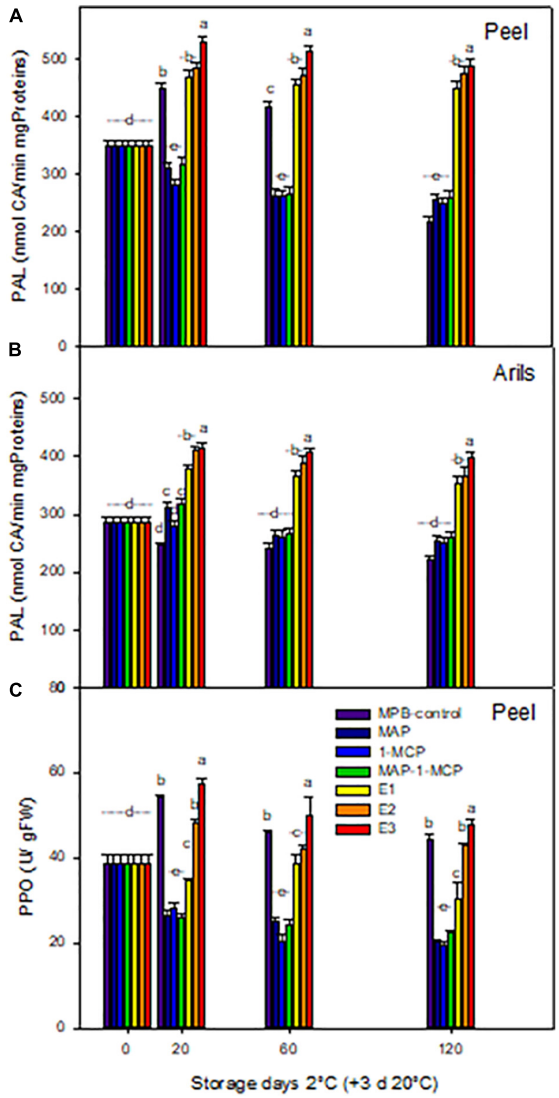

FIGURE 3 | Enzymatic activities related to browning in 'Wonderful' pomegranate fruits. Pomegranate was stored at 2°C for up to 120 days and 3 at 20°C. Effect of storage on phenylalanine ammonia lyase (PAL) activity (nmols of cinnamic acid/min × g proteins) in peel **(A)** and arils **(B)** and polyphenol oxidase (PPO) activity (units of activity/g FW) in the peel **(C)**. The fruit was stored in macroperforated bags like MPB-control, under a MAP, treated with 1-MCP, under combined treatment (PMA/1-MCP), and treated with increasing exogenous ethylene applications (E1, E2, and E3). Samples were taken at 0, 20, 60, and 120 days. The results of chemical analysis are presented as the mean values ± SE considering five independent extractions and five technical replicates. Values followed by a different lowercase case letter are significantly different ($p < 0.05$).

The total anthocyanins were calculated as cyanidin-3-glucoside and were determined by means of the pH differential method (Giusti and Wrolstad, 2001) using two buffer systems: potassium chloride buffer, pH 1.0 (0.025 M), and sodium acetate buffer, pH 4.5 (0.4 M). An aliquot of the fruit extract anthocyanin solution was adjusted to pH 1.0, and another aliquot was adjusted to pH 4.5. Each 0.2 ml aliquot (two replicates) of the

fruit extract was diluted with 1.8 ml of pH 1.0 buffer or with pH 4.5 buffer. Each solution was allowed to stand at room temperature for 20 min. The absorption was measured using a UV/Vis spectrophotometer (model Lambda 25, Perkin Elmer) at 510 and 700 nm.

The total anthocyanin content was calculated based on the Lambert–Beer law using the coefficient of molar extinction for cyanidin-3-glucoside (26,900 M^{-1} cm^{-1}). The results of four extractions from each treatment at each postharvest time point were expressed as mg of cyanidin-3-glucoside equivalent per 100 g of FW.

Sensory Determinations

Ten trained panelists evaluated the pomegranate sensory quality for sweetness, color and luminosity, aroma, and sourness after 20, 60, and 120 days of storage at 2°C (+3 days at 20°C). The evaluation was performed on a scale of 1–10 (1 = weakest and 10 = excellent). The average of scores was used for evaluation (Ehteshami et al., 2020).

Statistical Analysis

The experimental design was two-factorial, and the sources of variation were postharvest treatment and the date of sampling. Statistical analyses were performed using SPSS v.14. A two-way ANOVA was performed. Mean comparisons were performed using the Honestly Significant-Difference (HSD) test at $P \leq 0.05$. The results of the chemical analysis are presented as the mean values ± SE considering five independent extractions and five technical replicates.

RESULTS AND DISCUSSION

Average Chilling Injury Index

The chilling injury in pomegranate is characterized by the browning of the peel surface. In this study, the CI appeared in 'Wonderful' pomegranates at 120 days of cold storage (3 days at 20°C), and it increased rapidly throughout the remaining shelf life. 1-MCP treatment delayed and reduced the CI index of pomegranate storage at cold temperatures (**Figure 1**). The average CI was 79.87 and 62.32% lower in 1-MCP-treated fruit than in the control fruit on the 120th and 160th days of storage, respectively.

Our previous studies showed that scalding on the blossom end of pomegranates was observed in MPB-control-stored fruits starting at 20 days and in E1-, E2-, and E3-treated fruits at 60 days of storage (Valdenegro et al., 2018), with an increase in the severity of chilling (>50%) from 100 days of cold storage, potentially related to senescence, decay, and deterioration (Defilippi et al., 2006). However, in this study, MAP and MAP/1-MCP treatments showed a CI symptom severity of 50% at 120 days of cold storage, indicating a delay of CI symptoms. Our previous studies showed an increase in ethylene production in E2- and E3-treated fruits at 20 days (Valdenegro et al., 2018), without a correlation between CO_2 levels and visual symptoms during cold storage of pomegranate.

The modified atmosphere, e.g., the use of Xtend™ films, has been suggested as a good alternative to reduce dehydration, humidity, decay, and CI, preserving the hardness and shriveling of pomegranate (Porat et al., 2009; Valdenegro et al., 2018) and other fruits (Pesis et al., 2000; Aharoni et al., 2008), compared with another bag packaging. In this study, the average CI index (ACII) was observed from 20 days in MPB-control fruits and was highest in E2 and E3 at 120 days (+3 days at 20°C) (**Figure 1**). The severity of CI symptoms (**Figure 1**) increased on MPB-control fruits, E2 (11%), and E3 (14%) fruit from 60 days at 2°C (+3 days at 20°C), with a severity major of 40% from 120 days for all treatments, being higher for MPB-control and E3 (greater than 100%). In contrast, under the 1-MCP and MAP/1-MCP treatments, high CI symptom severity tended to show only after 120 days. In cherry fruits, the application of 1-MCP (0.3 and 1 ml L^{-1}) reduced decay, pitting rot development, and respiration depending on cultivar during cold storage (Caleb et al., 2012; Piazzolla et al., 2015; Li et al., 2016). Contrary to 1-MCP treatment, it has been reported that controlled atmosphere storage conditions meaningfully reduced the incidence and severity of scald in pomegranate storage at 7°C (Defilippi et al., 2006). However, the delay of CI symptoms in pomegranate at temperatures below 5°C for 60 days can be associated with ethylene signaling (Valdenegro et al., 2018). Concerning the quality parameters, we previously showed that the peel color, TSS, and acidity of pomegranate arils were affected only by cold storage, with no significant differences between treatments, similar to Artés et al. (2000) and Casares et al. (2019).

Relations Between Membrane Integrity and Ethylene Application During Cold Storage

Loss of membrane permeability is the first effect of cold damage in cold-sensitive species (McCollum and McDonald, 1991; Sala et al., 1998; Ben-Amor et al., 1999). In non-climacteric fruits such as grapes, electrolyte leakage is not previous to CI symptoms (Bellincontro et al., 2006). In the same way, this study showed an increase in the appearance of visual symptoms of CI parallel to electrolyte leakage in pomegranate peel (Casares et al., 2019). 1-MCP alone and MAP/1-MCP combination treatments decreased significant membrane damage compared to MBP and ethylene treatment at 20 days (**Figure 1C**), suggesting solute leakage, oxidative damage, and chilling membrane damage in pomegranate peel as a function of exogenous ethylene dose and O_2 levels during the first days of storage, as reported by Valdenegro et al. (2018).

Changes in Fatty Acids in the Peel

The decompartmentalization and ion leakage are products of changes in lipid constituents during damage to membrane structures (Casares et al., 2019). The decrease in unSFA content might affect the phase transition of membrane lipids. In loquat fruit, high levels of CI have been associated with a decrease in lipid unsaturation (Cao et al., 2011). Additionally, in pear fruit, some authors showed that preserved unsaturated lipid content and membrane fluidity enhance tolerance to chilling

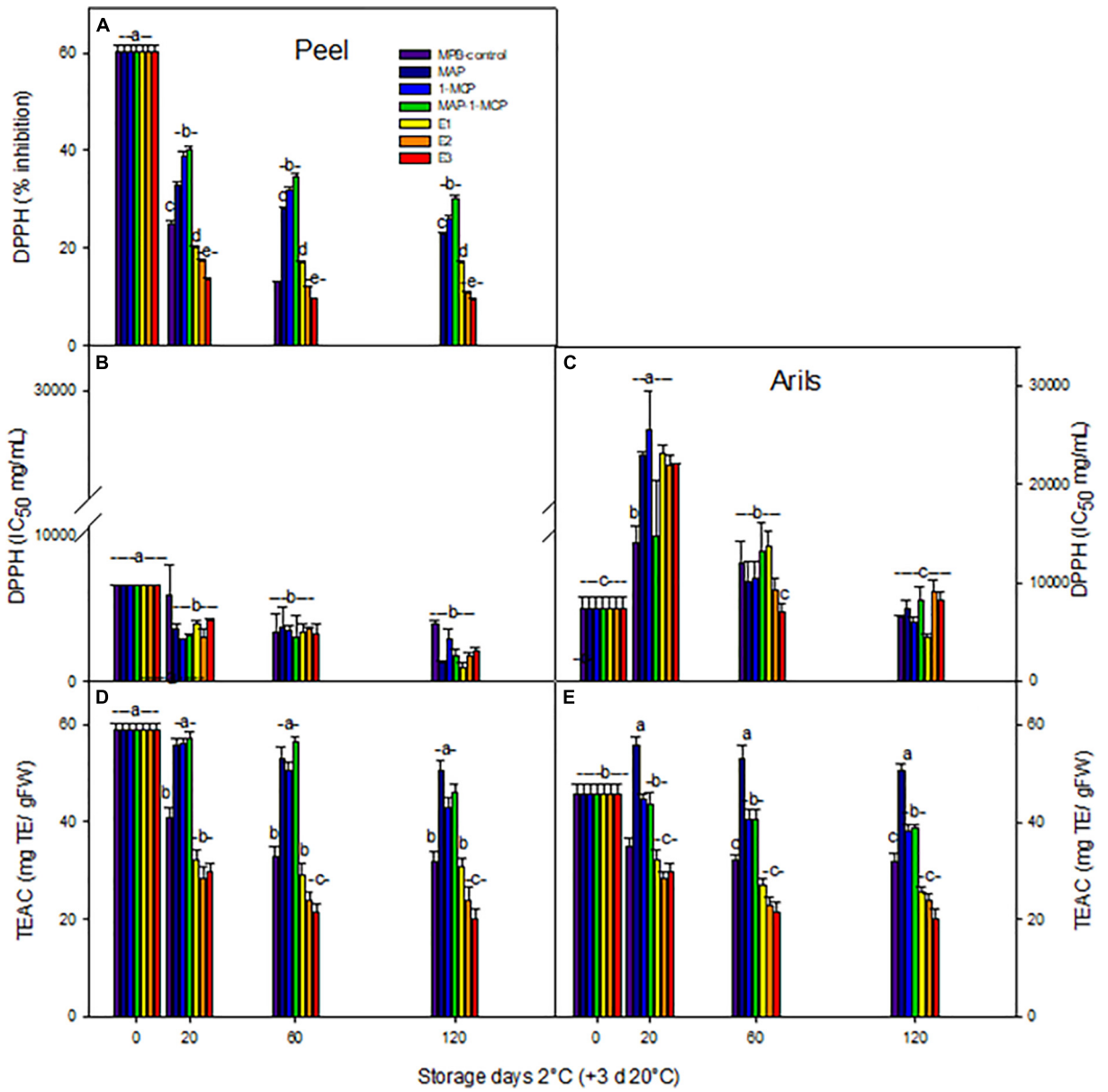

FIGURE 4 | Total antioxidant capacity of 'Wonderful' pomegranate during cold storage. Effects of low-temperature storage at 2°C and rewarmed for an additional 3 days at 20°C on DPPH activity:% inhibition in peel **(A)**, IC_{50} (mg/ml) in peel **(B)**, arils **(C)**, TEAC (mgTE/gFW) in peel **(D)**, and arils **(E)** of pomegranate. The fruit was stored in macroperforated bags like MPB-control, under a MAP, treated with 1-MCP, under combined treatment (PMA/1-MCP), and treated with increasing exogenous ethylene applications (E1, E2, and E3). Samples were taken at 0, 20, 60, and 120 days. The results of chemical analysis are presented as the mean values ± SE considering five independent extractions and five technical replicates. TE: Trolox equivalent. Values followed by a different lowercase case letter are significantly different ($p < 0.05$).

stress (Zheng et al., 2008; Cao et al., 2011; Jin et al., 2014). In this study, five major fatty acids (FAs) of membrane lipids were identified, including three unsaturated FAs, linoleic acid (18:2), linolenic acid (18:3), and alpha-linolenic acid (18:3), and two saturated FAs, palmitic acid (16:0) and stearic acid (18:0). Other authors found that linoleic acid, palmitic acid, and oleic acid are present in the peel and aril juice (Bar-Ya'akov et al., 2019). Additionally, the relative composition of individual FA components (**Figure 2**) and the unsaturated/saturated FA ratio (uns/sat FA ratio) were calculated to provide further insights into FA metabolism patterns under cold storage (**Figure 2F**). From 60 days, the contents of fatty acids were reduced during all treatments (**Figure 2**). However, when analyzing the unSFA and saturated acid rates, treatments with 1-MCP showed higher values. The most abundant fatty acids, such as linoleic acid and linolenic acid, and the ratio of unSFA to SFAs were

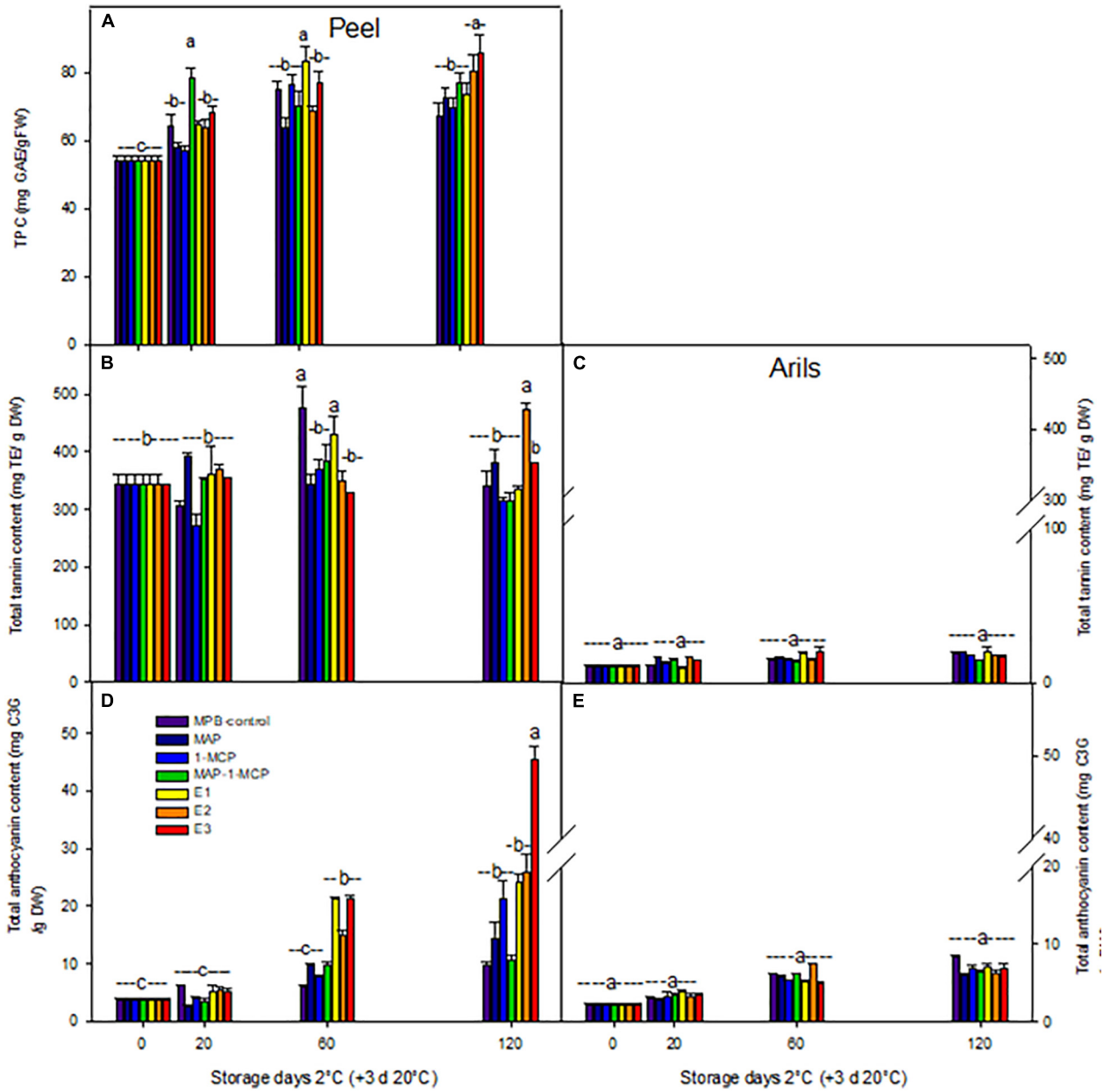

FIGURE 5 | Effect of cold storage on the antioxidant molecules of 'Wonderful' pomegranate. Effects of low-temperature storage at 2°C and rewarmed for an additional 3 days at 20°C on total polyphenol content (TPC; mg GAE/gFW) in the peel **(A)**, total tannin content (mg TE/DW) in the peel **(B)**, arils **(C)**, total anthocyanin content [mg cyanidin-3-glucoside (C3G)/g DW] in the peel **(D)**, and arils **(E)** of pomegranate. The fruit was stored in macroperforated bags like MPB-control, under a MAP, treated with 1-MCP, under combined treatment (PMA/1-MCP), and treated with increasing exogenous ethylene application (E1, E2, and E3). Samples were taken at 0, 20, 60, and 120 days. The results of the chemical analysis are presented as the mean values ± SE considering five independent extractions and five technical replicates. Values followed by a different lowercase case letter are significantly different ($p < 0.05$).

higher in 1-MCP treatments (only and combined with MAP) than in MPB-control-treated fruits (**Figure 2**). These results suggest that 1-MCP might help to maintain the normal function of membranes and reduce CI in pomegranate fruit during cold storage. Our results may be aligned with Cheng et al. (2015), who previously established a relief mechanism of CI by regulating the metabolism of fatty acids and energy in pears. A high ratio of unSFA to SFAs in cell membranes could prevent leakage and MDA content increase, thereby preventing membrane peroxidation and damage. In addition, the change in membrane unsaturation was reflected by the alteration of the unsaturated/saturated FA ratio. During the first 20 days, a significantly higher unsaturated/saturated FA ratio was found in all 1-MCP treatments than in MPB-control fruits. Previous

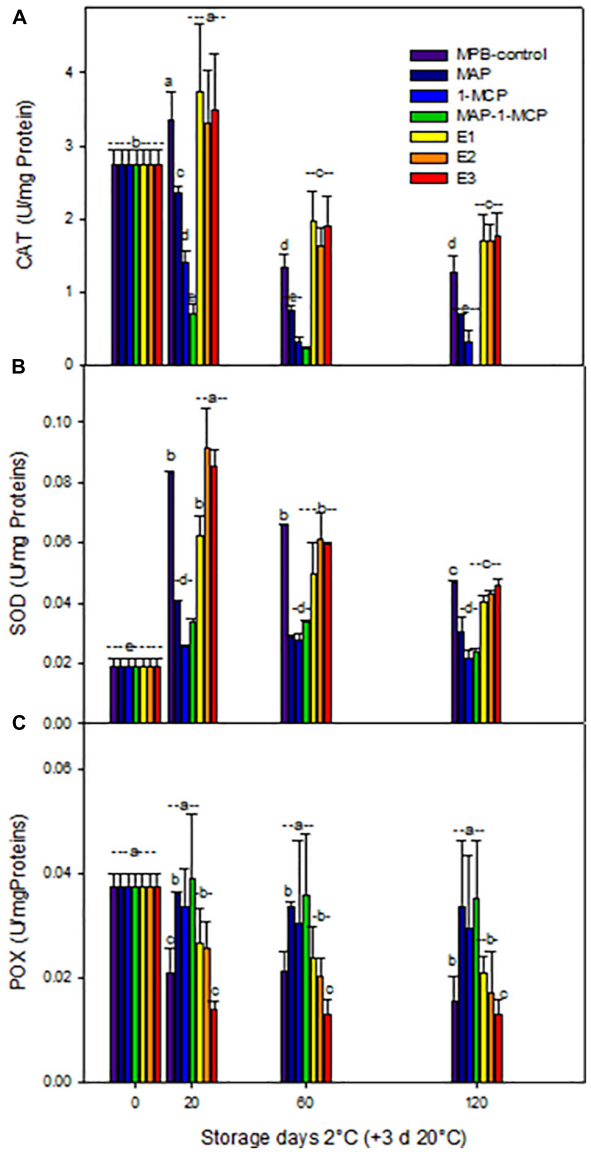

FIGURE 6 | Antioxidant enzymatic response during cold storage of 'Wonderful' pomegranate. Effects of low-temperature storage at 2°C and rewarming for an additional 3 days at 20°C on the activities (U/mg Proteins) of catalase (CAT) **(A)**, superoxide dismutase (SOD) **(B)**, and guaiacol peroxidase (POX) **(C)** in the peel of a pomegranate. The fruit was stored in macroperforated bags like MPB-control, under a MAP, treated with 1-MCP, under combined treatment (PMA/1-MCP), and treated with increasing exogenous ethylene application (E1, E2, and E3). Samples were taken at 0, 20, 60, and 120 days. The results of the chemical analysis are presented as the mean values ± SE considering five independent extractions and five technical replicates. Values followed by a different lowercase case letter are significantly different ($p < 0.05$).

studies have shown that the cell membranes adapt, changing their lipid composition and ion channel transport and receptor protein activity by the effect of environmental temperature changes (Welti et al., 2002; Holthuis and Menon, 2014; Bustamante et al., 2018; Baghel et al., 2021).

Enzymatic Activities Related to Browning in 'Wonderful' Pomegranate Fruits: Phenylalanine Ammonia-Lyase and Polyphenol Oxidase Activities

An increase in PAL activity is a cold-induced response that could be stimulated in fruit showing chilling damage, and that response may occur concomitantly with the development of chilling symptoms (Lafuente et al., 2003). The fruits of MAP, 1-MC, and combined treatments presented less PAL activity than MBP and ethylene treatment at 20 and 60 days in the peel (**Figure 3A**), while a significant increase of PAL was observed in all concentrations of ethrel treatment in the arils compared to other treatments (**Figure 3B**). **Figure 3C** shows the effect of the treatments and the storage time on PPO activity expressed as a variation in absorbance at 420 nm per min and gram of tissue. In the control treatment (MPB-control), the enzymatic activity values remained practically constant during the storage period tested, being higher in the first 20 days of evaluation. For the treatments with atmospheric modification or 1-MCP treatment, the activity was reduced by 50%, while a great increase in activity was observed from 20 days for all levels of exogenous ethylene treatments in a dose-dependent manner. The harvest time to chilling tolerance is very important for 'Wonderful' pomegranate, so full ripeness shows a greater capacity to withstand cold stress conditions (Kashash et al., 2016). At this stage, the enzymatic and non-enzymatic antioxidant systems have a greater capacity to delay the appearance of symptoms of damage caused by exposure to cold (Ben-Arie and Or, 1986; Marangoni et al., 1996; Matityahu et al., 2013; Jin et al., 2014). However, it is not enough to counteract stress, destabilizing cell membranes. In prolonged periods of exposure to cold, the modification of the surrounding atmosphere can offer protection by delaying and reducing the level of damage (Pareek et al., 2015; Li et al., 2016).

Total Antioxidant Capacity and Antioxidant Molecules

The antioxidant activity by DPPH activity (**Figures 4A–C**) and TEAC (**Figures 4D,E**) decreased considerably during storage in all treatments in the peel. The IC_{50} value achieved significantly lower values in the peel (**Figure 4B**) than in arils (**Figure 4C**). In arils, an increased TEAC value product by exposure to cold stress was present, being higher in modified atmosphere and 1-MCP treatments (**Figures 4D,E**). However, the rate of decrease was lower in peel and arils treated with MAP or combined treatment MAP-1-MCP, compared to MPB-control treatment.

The ethylene treatments showed higher browning in the peel, while the decrease in the total polyphenol content (TPC) in pomegranate peel (data not shown) may be due to the decomposition of TPC as a result of enzymatic activity during storage (Elfalleh et al., 2012); it could also be due to the oxidation or polymerization of TPC or the breakdown of the cell structure throughout product aging (Xie et al., 2019). One of the main causes of fruit browning is related to PPO activity, which reduces TPC. Increasing the activity of the PPO enzyme in browned peel causes a relative decrease in the phenol levels.

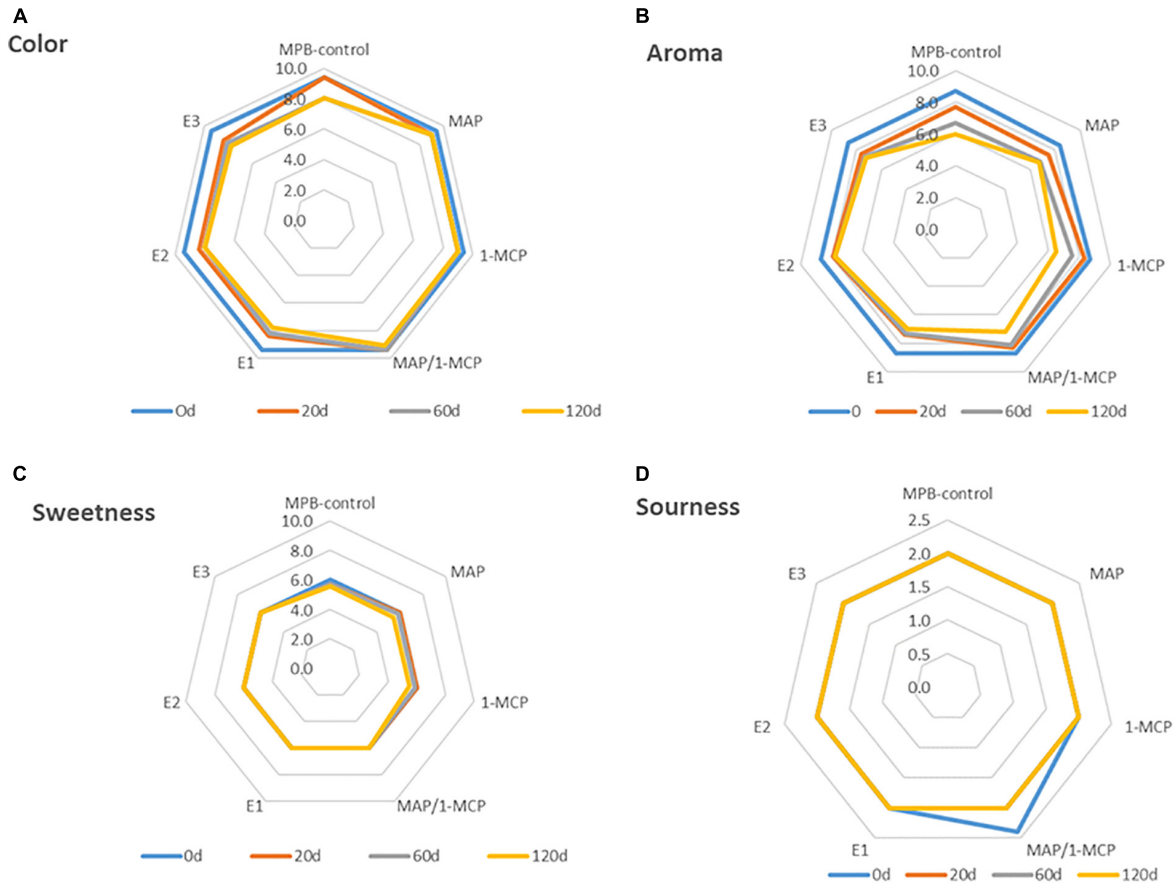

FIGURE 7 | Sensory evaluation of 'Wonderful' pomegranate storage at low temperature. Effects of low-temperature storage at 2°C and rewarmed for an additional 3 days at 20°C on color, sweetness aroma, and sourness perception. The fruit was stored in macroperforated bags like MPB-control, under a MAP, treated with 1-MCP, under combined treatment (PMA/1-MCP), and treated with increasing exogenous ethylene application (E1, E2, and E3). Samples were taken at 0 **(A)**, 20 **(B)**, 60 **(C)**, and 120 days **(D)**. The evaluation was made using a hedonic scale of 10 points, with 4 as the minimum score for an acceptable attribute.

Enzymatic oxidation of TPC, leading to browning of the peel in ethylene treatments, is probably conducted by the PPO enzyme, which is due to the highly reactive o-quinones forming brown colored polymers, leading to fruit browning (Shivashankar et al., 2012). In arils, the color is related to anthocyanin content, which contains cyanidin, pelargonidin, and delphinidin; color can be beneficial to health due to its antioxidant properties (Miguel et al., 2004; Naing and Kim, 2021). (**Figures 5A–C**) an increased concentration of anthocyanins in the peel (200, 5%) with a maximum value of 120 days was detected in ethylene treatments. However, its rate was lower in the 1-MCP or MAP-1-MCP treatments compared to the MPB-control treatment (**Figure 5D**). The lowest anthocyanin content was related to the MPB-control in arils and peel (**Figures 5D,E**). The tannin content remained stable over time in the peel in all treatments, without significant differences between treatments, slightly increasing its aril content from 20 days. It is important to note that the results presented in the current research are related to the 'Wonderful' cultivar, and the changes in tannins and anthocyanins could be different during cold temperatures in other varieties (Miguel et al., 2004; Alighourchi et al., 2008). Several authors point out the differences in varieties with respect to the abundance of anthocyanins in arils and skin (Zhao and Yuan, 2021). The most abundant arils are usually delphinidin 3,5-diglucoside, delphinidin 3-glucoside, cyanidin 3,5-diglucoside, cyanidin 3-glucoside, pelargonidin 3,5-diglucoside, and pelargonidin 3-glucoside (Alighourchi et al., 2008; Zhao et al., 2013). Zhao et al. (2013) studied Chinese varieties and found high variability in anthocyanins in the peel, presenting only pelargonidin and cyanidin derivatives. Naing and Kim (2021) point out that under cold stress conditions, reactive oxygen species are overproduced and cause oxidative damage to plants, and plants can produce anthocyanins, such as antioxidant responses, by neutralizing radicals with their hydroxyl groups to maintain normal cellular redox homeostasis.

The modifications in the non-enzymatic antioxidant content of pomegranate fruits were related to the capacity of 1-MCP (alone or MAP combined) to increase their storability. With respect to enzymatic antioxidant systems, the CAT activity was increased in response to cold stress in ethylene treatments at 20 days at 2°C + 3 days 20°C, while MAP, 1-MCP, and combined treatment decreased activity by more than half of the ethrel

treatments until the end of the assay (**Figure 6A**). The SOD activity (**Figure 6B**) had a similar trend with increased levels in ethylene treatments, while 1-MCP treatments (only and combined with MAP) remained stable. The POX activity (**Figure 6C**) showed the lowest levels in ethylene treatments. The lower browning of peel in pomegranate treated with 1-MCP can be due to higher antioxidant enzymes in the tissue, SOD, and CAT activities leading to a lower peel H_2O_2 accumulation and higher membrane integrity in agreement with lower electrolyte leakage and MDA accumulation observed in the treatment with major enzymatic antioxidant activity. These results are in concordance with Baghel et al. (2021), who studied the expression of these enzymatic activities. Additionally, the lower peel browning in pomegranate fruit of the combined MAP/1-MCP treatment resulted from a higher peel PAL/PPO enzyme activity ratio.

However, interestingly, the highest contents of anthocyanins and hydrolyzed tannins were detected when exogenous ethylene was applied to the fruits like a response to stress condition by cold temperature, with an increase in functional molecules. The treatment of exogenous ethylene E3 reduced TEAC antioxidant activity by 50% in the peel (**Figure 4D**) and 33% in arils (**Figure 4E**). In the peel, the refrigerated storage reduced the non-enzymatic antioxidant capacity, while in the arils, this parameter was increased, in accordance with the increase in the anthocyanin level. The treatments with the inhibitor of the action of ethylene 1-MCP had a clear effect on the maintenance of the antioxidant capacity, so it seems that ethylene is involved in the non-enzymatic mechanisms of detoxification in this fruit. 1-MCP and modified atmosphere packaging could preserve the functional quality of fruit tissues. Our results coincide with Naing and Kim (2021), since other non-climatic fruits showed increases in non-enzymatic antioxidant activity as a product of exposure to cold storage, which reduced CI symptoms.

Sensory Aspects

According to the evaluations of the panelists, few changes were perceived from 60 days (**Figure 7**). Less sweetness, color (luminosity), and aroma were recorded in MPB-control arils compared with other treatments (**Figures 7C,D**). Among the treatments used, the MAP and combined MAP-1-MCP had better sensory properties than the other treatments during cold storage. The MAP and the combined MAP-1-MCP treatment had no negative effect on the color, luminosity, or aroma of the arils. The ethylene exogenous treatments showed less color and luminosity and reduced appreciations of the aroma of arils. The results showed a significant acceptance of color and aroma for the storage pomegranate and a minor acceptance of sourness.

CONCLUSION

This study found that during long-term cold storage of pomegranate fruits, the protective effect of MAP/1-MCP or MAP treatments delays the appearance of CI symptoms and reduces the oxidation of tissues. The antioxidant response was higher in these treatments. This long storage induces an important decrease in fatty acids, which is not reverted by any postharvest treatment. However, it was slowest in 1-MCP treatments. Furthermore, our results also showed that the metabolism of membrane lipid FAs was involved in the responses associated with CI. A higher unSFA/SFA ratio after 1-MCP treatments showed a protective effect in peel tissues. In addition, it is possible to increase the concentration of anthocyanins in the peel of cold-storage pomegranates treated with ethylene, similar to a tolerance mechanism to cold stress.

DATA AVAILABILITY STATEMENT

The raw data supporting the conclusions of this article will be made available by the authors, without undue reservation.

AUTHOR CONTRIBUTIONS

MV, MB, CH, LF, MS, LM, and IH contributed to the structure and focus of the manuscript. MV, MB, LF, MS, LM, IH, and RS performed the physical-chemical analysis. MV, MB, LF, and IH conducted an investigation. LF and MV contributed to the preparation, wrote the original draft of the manuscript, review and editing, supervision, and project administration. MV, LF, MS, LM, MB, CH, IF, and RS contributed to funding acquisition. All authors have agreed to the published version of the manuscript.

FUNDING

This research was supported by FONDECYT Project 1140817 and DI Regular project PUCV 039.437/2017.

ACKNOWLEDGMENTS

We wish to thank Agrofresh (Curicó, Chile) for supplying 1-MCP.

REFERENCES

Aebi, H. (1984). Catalase in vitro. *Methods Enzymol.* 105, 121–126. doi: 10.1016/S0076-6879(84)05016-3

Aharoni, N., Rodov, V., Fallik, E., Porat, R., Pesis, E., and Lurie, S. (2008). Controlling humidity improves the efficacy of modified atmosphere packaging of fruits and vegetables. *Acta Hortic.* 804, 121–128. doi: 10.17660/ActaHortic.2008.804.14

Alighourchi, H., Barzegar, M., and Abbasi, S. (2008). Anthocyanins characterization of 15 Iranian pomegranate (*Punica granatum* L.) varieties and their variation after cold storage and pasteurization. *Eur. Food Res. Technol.* 227, 881–887. doi: 10.1007/s00217-007-0799-1

Artés, F., Villaescusa, R., and Tudela, J. A. (2000). Modified atmosphere packaging of pomegranates. *J. Food Sci.* 65, 1112–1116. doi: 10.1111/j.1365-2621.2000.tb10248.x

Baghel, R., Keren-Keiserman, A., and Ginzberg, I. (2021). Metabolic changes in pomegranate fruit skin following cold storage promote chilling injury of the peel. *Sci. Rep.* 11:9141. doi: 10.1038/s41598-021-88457-4

Bar-Ya'akov, I., Tian, L., Amir, R., and Holland, D. (2019). Primary metabolites, anthocyanins, and hydrolyzable tannins in the pomegranate fruit. *Front. Plant Sci.* 10:620. doi: 10.3389/fpls.2019.00620

Bellincontro, A., Fardelli, A., De Santis, D., Botondi, R., and Mencarelli, F. (2006). Postharvest ethylene and 1-MCP treatments both affect phenols, anthocyanins, and aromatic quality of Aleatico grapes and wine. *Austr. J. Grape Wine Res.* 12, 141–149. doi: 10.1111/j.1755-0238.2006.tb00054.x

Ben-Amor, M., Flores, B., Latché, A., Bouzayen, M., Pech, J. C., and Romojaro, F. (1999). Inhibition of ethylene biosynthesis by antisense ACC oxidase RNA prevents chilling injury in Charentais cantaloupe melons. *Plant Cell Environ.* 22, 1579–1586. doi: 10.1046/j.1365-3040.1999.00509.x

Ben-Arie, R., and Or, E. (1986). The development and control of husk scald on Wonderful pomegranate fruit during storage. *J. Am. Soc. Hortic. Sci.* 111, 395–399. doi: 10.1016/j.postharvbio.2006.04.006

Bossu, C., Ferreira, E., Chaves, F., Menezes, E., and Nogueira, A. (2006). Flow injection system for hydrolysable tannin determination. *Microchem. J.* 84, 88–92. doi: 10.1016/j.microc.2006.04.022

Bradford, M. M. (1976). A rapid and sensitive method for the quantification of microgram quantities of protein utilizing the principle of protein-dye binding. *Anal. Biochem.* 72, 248–254. doi: 10.1006/abio.1976.9999

Brand-Williams, W., Cuvelier, M., and Berset, C. (1995). Use of a free radical method to evaluate antioxidant activity. *LWT Food Sci. Technol.* 28, 25–30. doi: 10.1016/S0023-6438(95)80008-5

Bustamante, C. A., Brotman, Y., Monti, L. L., Gabilondo, J., Budde, C. O., Lara, M. V., et al. (2018). Differential lipidome remodeling during postharvest of peach varieties with different susceptibility to chilling injury. *Physiol. Plant.* 163, 2–17. doi: 10.1111/ppl.12665

Caleb, O. J., Mahajan, P. V., Opara, U. L., and Witthuhn, C. R. (2012). Modeling the effect of time and temperature on respiration rate of pomegranate arils (cv. "Acco" and "Herskawitz"). *J. Food Sci.* 77, E80–E87. doi: 10.1111/j.1750-3841.2012.02623.x

Cao, S. F., Zhenfeng, Y., Cai, Y., and Zheng, Y. (2011). Fatty acid composition and antioxidant system in relation to susceptibility of loquat fruit to chilling injury. *Food Chem.* 127, 1777–1783. doi: 10.1016/j.foodchem.2011.02.059

Casares, A., Escribá, P., and Roselló, A. (2019). Review. Membrane lipid composition: effect on membrane and organelle structure, function and compartmentalization and therapeutic avenues. *Int. J. Mol. Sci.* 20:2167. doi: 10.3390/ijms20092167

Chen, L., Pan, Y., and Li, H. (2021). Methyl jasmonate alleviates chilling injury and keeps intact pericarp structure of pomegranate during low temperature storage. *Food Sci. Technol. Int.* 27, 22–31. doi: 10.1177/1082013220921597

Cheng, S., Wei, B., Tan, D., and Ji, S. (2015). 1-Methylcyclopropene alleviates chilling injury by regulating energy metabolism and fatty acid content in 'Nanguo' pears year. *Postharvest Biol. Technol.* 109, 130–136. doi: 10.1016/j.postharvbio.2015.05.012

Chirinos, R., Zuloeta, G., Pedreschi, R., Mignolet, E., Larondelle, Y., and Campos, D. (2013). Sacha inchi (*Plukenetia volubilis*): a seed source of polyunsaturated fatty acids, tocopherols, phytosterols, phenolic compounds and antioxidant capacity. *Food Chem.* 141, 1732–1739. doi: 10.1016/j.foodchem.2013.04.078

Defilippi, B. G., Whitaker, B. D., Hess-Pierce, B. M., and Kader, A. A. (2006). Development and control of scald on wonderful pomegranates during long-term storage. *Postharvest Biol. Technol.* 41, 234–243.

Ehteshami, S., Abdollahi, F., Ramezanian, A., Rahimzadeh, M., and Mirzaalian, A. (2020). Maintenance of quality and bioactive compounds of cold stored pomegranate (*Punica granatum* L.) fruit by organic acids treatment. *Food Sci. Technol. Int.* 27, 151–163. doi: 10.1177/1082013220940466

Elfalleh, W., Hannachi, H., Tlili, N., Yahia, Y., Nasri, N., and Ferchichi, A. (2012). Total phenolic contents and antioxidant activities of pomegranate peel, seed, leaf and flower. *J. Med. Plant Res.* 6, 4724–4730. doi: 10.5897/JMPR11.995

Espin, J. C., Morales, M., Varon, M., Tudela, J., and García-Casanovas, F. (1995). A continuous spectrophotometric method for determining the monophenolase and diphenolase activities of apple polyphenoloxidase. *Anal. Biochem.* 43, 2807–2812. doi: 10.1006/abio.1995.1526

Farneti, B., Alarcón, A. A., Papasotiriou, F. G., Samudrala, D., Cristescu, S. M., Costa, G., et al. (2015). Chilling-Induced changes in aroma volatile profiles in tomato. *Food Bioprocess Technol.* 8, 1442–1454. doi: 10.1016/0304-4238(84)90113-4

Fawole, O. A., and Opara, U. L. (2013). Developmental changes in maturity indices of pomegranate fruit: a descriptive review. *Sci. Hortic.* 159, 152–161. doi: 10.1016/j.scienta.2013.05.016

Franck, N., Alfaro, L., and Zamorano, D. (2015). "Manejo del huerto," in *Bases Para el Cultivo Del Granado En Chile,Serie Ciencias Agronómicas N° 25*, eds J. L. Henríquez and N. Franck (Santiago: Universidad de Chile), 105–158.

Gamrasni, D., Gadban, H., Tsvilling, E., Goldberg, T., Neria, O., Ben-Arie, R., et al. (2015). 1-MCP improves the quality of stored 'wonderful' pomegranates. *Acta Hortic.* 1079, 229–234. doi: 10.17660/ActaHortic.2015.1079.26

Giusti, M., and Wrolstad, R. E. (2001). Characterization and measurement of anthocyanins by UV-visible spectroscopy. *Curr. Prot. Food Anal. Chem.* 00, F1.2.1–F1.2.13. doi: 10.1002/0471142913.faf0102s00

Hernández, I., Fuentealba, C., Olaeta, J., Poblete-Echeverría, C., Defilippi, B., González-Agüero, M., et al. (2017). Effects of heat shock and nitrogen shock pre-treatments on ripening heterogeneity of Hass avocados stored in controlled atmosphere. *Sci. Hortic.* 225, 408–415. doi: 10.1016/j.scienta.2017.07.025

Holland, D., Hatib, K., and Bar-Yàakov, I. (2009). Pomegranate: botany, horticulture and breeding. *Hortic. Rev.* 35, 127–191. doi: 10.1002/9780470593776.ch2

Holthuis, J., and Menon, A. (2014). Lipid landscapes and pipelines in membrane homeostasis. *Nature* 510, 48–57 . doi: 10.1038/nature13474

Naing, A. K., and Kim, C. K. (2021). Abiotic stress-induced anthocyanins in plants: their role in tolerance to abiotic stresses. *Physiol. Plantarum* 172, 1711–1723. doi: 10.1111/ppl.13373

Hussein, Z., Caleb, O., Jacobs, K., Manley, M., and Opara, U. (2015). Effect of perforation-mediated modified atmosphere packaging and storage duration on physicochemical properties and microbial quality of fresh minimally processed 'Acco' pomegranate arils. *LWT Food Sci. Technol.* 64, 911–918. doi: 10.1016/j.lwt.2015.06.040

Jin, P., Zhu, H., Wang, L., Shan, T., and Zheng, Y. (2014). Oxalic acid alleviates chilling injury in peach fruit by regulating energy metabolism and fatty acid contents. *Food Chem.* 161, 87–93. doi: 10.1016/j.foodchem.2014.03.103

Kader, A. A. (ed.) (2003). *Postharvest Technology of Horticultural Crops*, 3rd Edn. St, Davis, CA: University of California, Agricultural and Natural Resources.

Kashash, Y., Mayuoni-Kirshenbaum, L., Goldenberg, L., Choi, H. J., and Porat, R. (2016). Effects of harvest date and low-temperature conditioning on chilling tolerance of 'Wonderful' pomegranate fruit. *Sci. Hortic.* 209, 286–292.

Lafuente, M. T., Zacarías, L., Martínez-Téllez, M., Sánchez-Ballesta, M., and Granell, A. (2003). Phenylalanine ammonia-lyase and ethylene in relation to chilling injury as affected by fruit age citrus. *Postharvest Biol. Technol.* 29, 309–318. doi: 10.1016/S0925-5214(03)00047-4

Li, L., Lichter, A., Chalupowicz, D., Gamrasni, D., Goldberg, T., Nerya, O., et al. (2016). Effects of the ethylene-action inhibitor 1-methylcyclopropene on postharvest quality of non-climacteric fruit crops. Review. *Postharvest Biol. Technol.* 111, 322–329. doi: 10.1016/j.postharvbio.2015.09.031

Li, P., Zheng, X., Liu, Y., and Zhu, Y. (2014). Pre-storage application of oxalic acid alleviates chilling injury in mango fruit by modulating proline metabolism and energy status under chilling stress. *Food Chem.* 142, 72–78. doi: 10.1016/j.foodchem.2013.06.132

Marangoni, A. G., Palma, T., and Stanley, D. W. (1996). Membrane effects in postharvest physiology. *Postharvest Biol. Technol.* 7, 193–217. doi: 10.1016/0925-5214(95)00042-9

Matityahu, I., Glazer, I., Holland, D., Bar-Ya'akov, I., Ben-Arie, R., and Amir, R. (2013). Total antioxidative capacity and total phenolic levels in pomegranate husks correlate to several postharvest fruit quality parameters. *Food Bioprocess Tech.* 7, 1938–1949. doi: 10.1007/s11947-013-1184-7

McCollum, T. G., and McDonald, R. E. (1991). Electrolyte leakage, respiration and ethylene production as indices of chilling injury in grapefruit. *Hortic. Sci.* 26, 1191–1192. doi: 10.21273/HORTSCI.26.9.1191

Miguel, G., Fontes, M., Antunes, D., Neves, A., and Martins, D. (2004). Anthocyanin concentration of 'Assaria' pomegranate fruits during different cold storage conditions. *J. Biomed. Biotechnol.* 5, 338–342. doi: 10.1155/S1110724304403076

Pareek, S., Valero, D., and Serrano, M. (2015). Postharvest biology and technology of pomegranate. Review. *J. Sci. Food Agric.* 95, 2360–2379. doi: 10.1002/jsfa.7069

Pech, J. C., Bouzayen, M., and Latché, A. (2008). Climacteric fruit ripening: ethylene-dependent and independent regulation of ripening pathways in melon fruit. *Plant Sci.* 175, 114–120. doi: 10.1016/j.plantsci.2008.01.003

Peltonen, S., and Karjalainen, R. (1995). Phenylalanine ammonia-lyase activity in barley after infection with *Bipolaris sorokiniana* or treatment with its purified xylanase. *J. Phytopathol.* 143, 239–245.

Pesis, E., Aharoni, D., Aharon, Z., Ben-Arie, R., Aharoni, N., and Fuchs, Y. (2000). Modified atmosphere and modified humidity packaging alleviates chilling injury symptoms in mango fruit. *Postharvest Biol. Technol.* 19, 93–101. doi: 10.1016/S0925-5214(00)00080-6

Piazzolla, F., Amodio, M. L., Colantuono, F., and Colelli, G. (2015). Effects of 1-methylcyclopropene (1-MCP) on quality of sweet cherry *(Prunus avium* L. 'Ferrovia') during storage. *Acta Hortic.* 1071, 551–557. doi: 10.17660/ActaHortic.2015.1071.71

Pirzadeh, M., Caporaso, N., Rauf, A., Shariati, M. A., Yessimbekov, Z., Khan, M. U., et al. (2020). Pomegranate as a source of bioactive constituents: a review on their characterization, properties and applications. *Crit. Rev. Food Sci. Nutr.* 1–18. doi: 10.1080/10408398.2020.1749825

Porat, R., Weiss, B., Fuchs, Y., Sandman, A., Ward, G., Kosto, I., et al. (2009). Modified atmosphere/modified humidity packaging for preserving pomegranate fruit during prolonged storage and transport. *Acta Hortic.* 818, 299–304. doi: 10.17660/ActaHortic.2009.818.44

Promyou, S., Kesta, S., and Van Doorn, W. (2008). Hot water treatments delay cold induced banana peel blackening. *Postharvest Biol. Technol.* 48, 132–138. doi: 10.1016/j.postharvbio.2007.09.006

Rao, M. V., Watkins, C. B., Brown, S. K., and Weeden, N. F. (1998). Active oxygen species metabolism in 'White Angel' × 'Rome Beauty' apple selections resistant and susceptible to superficial scald. *J. Am. Soc. Hortic. Sci.* 123, 299–304. doi: 10.21273/jashs.123.2.299

Sala, J. M. (1998). Involvement of oxidative stress in chilling injury in cold-stored mandarin fruits. *Postharvest Biol. Technol.* 13, 255–261. doi: 10.1016/S0925-5214(98)00011-8

Sayyari, M., Babalar, M., Kalantarie, S., Serrano, M., and Valero, D. (2009). Effect of salicylic acid treatment on reducing chilling injury in stored pomegranates. *Postharvest Biol. Technol.* 53, 152–154. doi: 10.1016/j.postharvbio.2009.03.005

Sayyari, M., Castillo, S., Valero, D., Díaz-Mula, H. M., and Serrano, M. (2011). Acetyl salicylic acid alleviates chilling injury and maintains nutritive and bioactive compounds and antioxidant activity during postharvest storage of pomegranates. *Postharvest Biol. Technol.* 60, 136–142. doi: 10.1016/j.postharvbio.2010.12.012

Sayyari, M., Salehi, F., and Valero, D. (2017). New approaches to modeling methyl jasmonate effects on pomegranate quality during postharvest storage. *Int. J. Fruit Sci.* 17, 374–390. doi: 10.1080/15538362.2017.1329051

Sayyari, M., Soleimani Aghdam, M., Salehi, F., and Ghanbari, F. (2016). Salicyloyl chitosan alleviates chilling injury and maintains antioxidant capacity of pomegranate fruits during cold storage. *Sci. Hortic.* 211, 110–117. doi: 10.1016/j.scienta.2016.08.015

Selcuk, N., and Erkan, M. (2015). Changes in phenolic compounds and antioxidant activity of sour–sweet pomegranates cv. 'Hicaznar' during long-term storage under modified atmosphere packaging. *Postharvest Biol. Technol.* 109, 30–39. doi: 10.1016/j.postharvbio.2015.05.018

Shivashankar, S., Singh, H., and Sumathi, M. (2012). Aril browning in pomegranate (*Punica granatum* L.) is caused by the seed. *Curr. Sci.* 103, 26–28.

Ukeda, H., Kawana, D., Maeda, S., and Sawamura, M. (1999). Spectrophotometric assay for superoxide dismutase based on the reduction of highly water-soluble tetrazolium salts by xanthine-xanthine oxidase. *Biosci. Biotechnol. Biochem.* 63, 485–488. doi: 10.1271/bbb.63.485

Valdenegro, M., Fuentes, L., Herrera, R., and Moya-León, M. A. (2012). Changes in antioxidant capacity during development and ripening of goldenberry (*Physalis peruviana* L.) fruit and in response to 1-methylcyclopropene treatment. *Postharvest Biol. Technol.* 67, 110–117. doi: 10.1016/j.postharvbio.2011.12.021

Valdenegro, M., Huidobro, C., Monsalve, L., Bernales, M., Fuentes, L., and Simpson, R. (2018). Effects of ethrel, 1-MCP and modified atmosphere packaging on the quality of 'wonderful' pomegranates during cold storage. *J. Sci. Food Agric.* 98, 4854–4865. doi: 10.1002/jsfa.9015

van den Berg, R., Haenen, G. R. M. M., and Bast, A. (1999). Applicability of an improved trolox equivalent antioxidant capacity (TEAC) assay for evaluation of antioxidant capacity measurements of mixtures. *Food Chem.* 66, 511–517. doi: 10.1016/s0308-8146(99)00089-8

Vendruscolo, E. C. G., Schuster, I., Pileggi, M., Scapim, C. A., Correa, H. B., Jamil, C., et al. (2007). Stress-induced synthesis of proline confers tolerance to water deficit in transgenic wheat. *J. Plant Physiol.* 164, 1367–1376. doi: 10.1016/j.jplph.2007.05.001

Welti, R., Li, W., Li, M., Sang, Y., Biesiada, H., Zhou, H. E., et al. (2002). Profiling membrane lipids in plant stress responses. Role of phospholipase Dα in freezing-induced lipid changes in *Arabidopsis*. *J. Biol. Chem.* 277, 31994–32002. doi: 10.1074/jbc.M205375200

Xie, Z., Li, X., Tang, R., Wang, G., Lu, Y., Li, X., et al. (2019). Reactions of polyphenols in pomegranate peel with nitrite under simulated stomach conditions. *Food Sci. Nutr.* 7, 3103–3109. doi: 10.1002/fsn3.1173

Zhang, L. H., Zhang, Y. H., Li, L. L., and Li, Y. X. (2008). Effect of 1-MCP on peel browning of pomegranates. *Acta Hortic.* 774, 275–282. doi: 10.17660/ActaHortic.2008.774.36

Zhao, X., and Yuan, Z. (2021). Anthocyanins from pomegranate (*Punica granatum* L.) and their role in antioxidant capacities in vitro. *Chem. Biodivers.* 18:e2100399. doi: 10.1002/cbdv.202100399

Zhao, Z., Yuan, Z., Fang, Y., Yin, Y., and Feng, L. (2013). Characterization and evaluation of major anthocyanins in pomegranate (*Punica granatum* L.) peel of different cultivars and their development phases. *Eur. Food Res. Technol.* 236, 109–117. doi: 10.1007/s00217-012-1869-6

Zheng, Y. H., Fung, R. W. M., Wang, S. Y., and Wang, C. Y. (2008). Transcript levels of antioxidative genes and oxygen radical scavenging enzyme activities in chilled zucchini squash in response to superatmospheric oxygen. *Postharvest Biol. Technol.* 47, 151–158. doi: 10.1016/j.postharvbio.2007.06.016

Conflict of Interest: The authors declare that the research was conducted in the absence of any commercial or financial relationships that could be construed as a potential conflict of interest.

Publisher's Note: All claims expressed in this article are solely those of the authors and do not necessarily represent those of their affiliated organizations, or those of the publisher, the editors and the reviewers. Any product that may be evaluated in this article, or claim that may be made by its manufacturer, is not guaranteed or endorsed by the publisher.

Advantages of publishing in Frontiers

OPEN ACCESS
Articles are free to read for greatest visibility and readership

FAST PUBLICATION
Around 90 days from submission to decision

HIGH QUALITY PEER-REVIEW
Rigorous, collaborative, and constructive peer-review

TRANSPARENT PEER-REVIEW
Editors and reviewers acknowledged by name on published articles

Frontiers
Avenue du Tribunal-Fédéral 34
1005 Lausanne | Switzerland

Visit us: www.frontiersin.org
Contact us: frontiersin.org/about/contact

REPRODUCIBILITY OF RESEARCH
Support open data and methods to enhance research reproducibility

DIGITAL PUBLISHING
Articles designed for optimal readership across devices

FOLLOW US
@frontiersin

IMPACT METRICS
Advanced article metrics track visibility across digital media

EXTENSIVE PROMOTION
Marketing and promotion of impactful research

LOOP RESEARCH NETWORK
Our network increases your article's readership